Universitat Autònoma de Barcelona

TESI DOCTORAL

SÍNTESI i FUNCIONALITZACIÓ d'*o*-CARBORANS i METAL·LOCARBORANS COM A NUCLIS DE DENDRONS I DENDRÍMERS. APLICACIONS EN MEDICINA.

Ariadna Pepiol i Martí

2011

Directora: Prof. Clara Viñas Teixidor

Programa de Doctorat en Química

Departament de Química. Facultat de Ciències

ICMAB

CSIC

3.- Conclusions

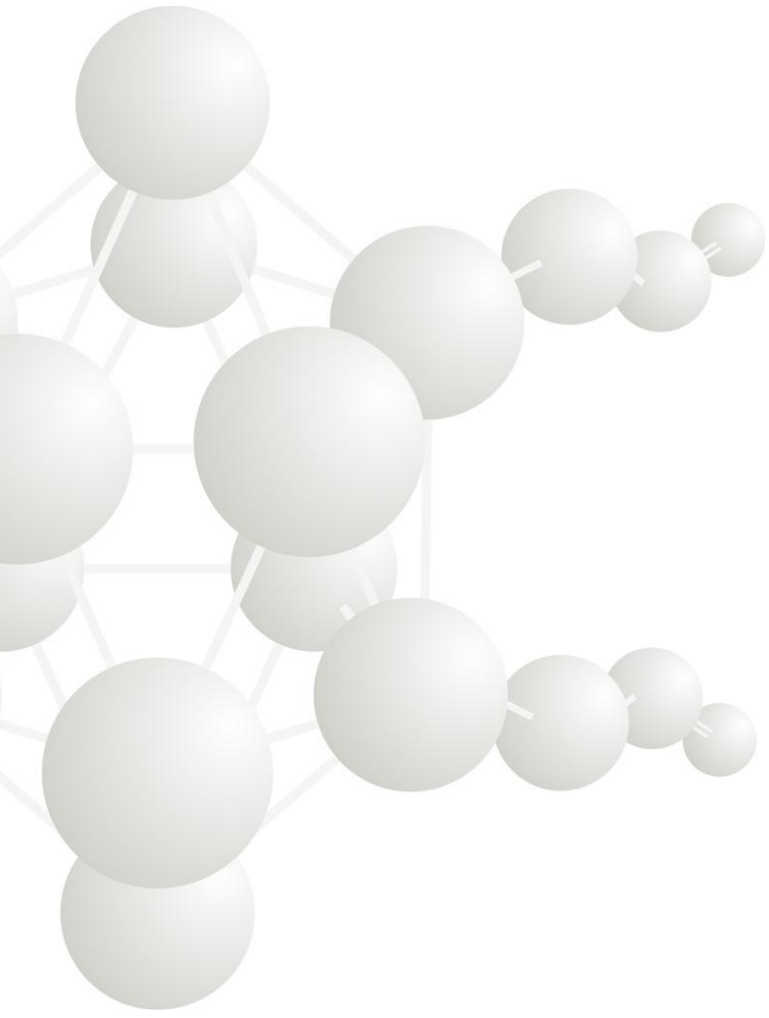

3. CONCLUSIONS OF THE THESIS

The *ortho*-carborane cluster can be the core of multibranched dendrimeric molecules or arborols. A first approach to the synthesis of these unimolecular nanoparticles has been done by Kumada cross-coupling reaction of 9,12-I_2-*closo*-1,2-$C_2B_{10}H_{10}$ **(2)** and 8,9,10,12-I_4-*closo*-1,2-$C_2B_{10}H_8$ **(3)** with several Grignard reagents, generating B-C bonds from the corresponding B-I bonds. Allylmagensium chloride, phenylmagnesium chloride and phenylethynylmagnesium chloride have been used as a source of organic moieties. Using allylmagensium chloride, 9,12-$(CH_2{=}CHCH_2)_2$-*closo*-1,2-$C_2B_{10}H_{10}$ **(4)** and 8,9,10,12-$(CH_2{=}CHCH_2)_4$-*closo*-1,2-$C_2B_{10}H_8$ **(6)** were produced providing ‘‘free’’ ends for further functionalization reactions.

The four-fold phenylation of **(3)** with phenylmagnesium chloride under Kumada conditions have not been achieved, only two iodine atoms were readily exchanged, but the coupling of a third phenyl ring into the cage was extremely slow, producing 8,10-Ph_2-9,12-I_2-*closo*-1,2-$C_2B_{10}H_8$ **(8)**. The design of a new synthetic strategy to get 8,9,10,12-Ph_4-1,2-*closo*-$C_2B_{10}H_8$ has been performed, first reacting **(2)** with phenylmagnesium chloride to display phenyl groups into the neighboring vertexes B(9,12), second, inducing an electrophilic iodination over the unsubstituted boron vertexes B(8) and B(10) by a solvent free reaction with I_2 in a sealed tub to obtain the corresponding geometrical isomer 9,12-Ph_2-8,10-I_2-*closo*-1,2-$C_2B_{10}H_8$ **(11)**. Unfortunately, the cross coupling reaction of **(11)** with PhMgCl did not lead to the expected four-fold phenylation of the *o*-carborane.

Reaction of **(2)** with phenylethynylmagnesium chloride proceeded completely to give 9,12-$(PhC{\equiv}C)_2$-1,2-*closo*-$C_2B_{10}H_{10}$ **(5)**, in contrast, the same reaction of **(3)** leads to the exchange of three of the four iodine atoms to give 8,9,10,12-$(PhC{\equiv}C)_3$I-1,2-*closo*-$C_2B_{10}H_8$ **(7)**.

Subsequent functionalization of 9,12-$(CH_2{=}CHCH_2)_2$-*closo*-1,2-$C_2B_{10}H_{10}$ **(4)** and 8,9,10,12 $(CH_2{=}CHCH_2)_4$-*closo*-1,2-$C_2B_{10}H_8$ **(6)** were performed either by Heck cross coupling reactions with phenyl iodide, thus obtaining **(12)** and **(13)** with a highly regioselective and stereospecific introduction of aryl groups into double bonds, or by hydro-boration/oxidation reaction of the corresponding olefinic moieties to regioselectively achieve terminal OH groups in **(14)** and **(15)**, ready for further derivatization.

Derivatization of terminal hydroxyl groups of 9,12-$(HOCH_2CH_2CH_2)_2$-1,2-*closo*-$C_2B_{10}H_{10}$ **(14)** and 8,9,10,12-$(HOCH_2CH_2CH_2)_4$-1,2-*closo*-$C_2B_{10}H_8$ **(15)** by exchanging OH unites for better leaving groups,

such as chloride, bromide or tosil group have been accomplished. Moreover, oxidation reaction to the corresponding carboxylic acid and Steglich esterification reaction with benzoic acid have also been successfully performed.

The basic degradation process of *closo B*-iodinated derivatives **(2)** and **(3)** afforded the expected *nido* anions [5,6-I_2-*nido*-7,8-$C_2B_9H_{10}]^-$ **([26]$^-$)** and [1,5,6,10-I_4-*nido*-7,8-$C_2B_9H_8]^-$ **([28]$^-$)**. The acidity of the B-H-B bridging hydrogen of the latter anion, located over the C_2B_3 open face, has been estimated by means of NMR experiments (pK_a near 5.5). It is noticeable that, as for the *closo* species, *B*-iodine substitution is responsible for the high acidity of the related *nido* anions. Furthermore, basic degradation process of several *closo B*-alkylated derivatives has been achieved, obtaining the corresponding *nido* species **(30)**, **(32)**, **(33)** and **(34)**.

Subsequent complexation reaction with Co (II) over the *B*-iodined *nido* counterparts afforded the expected cobaltabisdicarbollide polyiodinated derivatives: $[N(CH_3)_4]$[3,3'-Co-(9,12-I_2-1,2-*closo*-$C_2B_9H_9)_2$] **(27)** and $[N(CH_3)_4]$[3,3'-Co-(8,9,10,12-I_4-1,2-*closo*-$C_2B_9H_7)_2$] **(29)**. The octaiodinated cobaltabisdicarbollide **(29)** is the highest iodinated derivative reported so far. Electrochemical studies have shown an additive behaviour in respect to their redox potential $E_{1/2}(Co^{III}/Co^{II})$, experimentally determined by cyclic voltammetry. In other words, each generated B-I bond causes an anodic shift of the cobaltabisdicarbollide framework of 0.133V, producing a stepwise tunable redox potential system. Electrochemical growth of PPy doped with polyiodinated cobaltabisdicarbollide frameworks have been performed showing that any differences in the growth of PPy will depend little on the number of iodine substituents and largely on their $E_{1/2}(Co^{III}/Co^{II})$.

,

Synthesized *B*-substituted molecules keep their $C_{cluster}$-H vertexes intact and able to introduce different substituents, therefore electrophilic substitution on carbon cluster vertexes of **(4)** and **(6)** have been carried out using allyl bromide, thus obtaining tetra- and hexa-branched molecules. Subsequent derivatization reaction over all olefinic groups of **(35)** and **(36)** to hydroxyl, chloride and bromide unites have been successfully afforded. Substitution of both carbon cluster hydrogen atoms by thiol groups have been performed on 8,9,10,12-I_4-*closo*-1,2-$C_2B_{10}H_8$ **(3)** isolating the corresponding dithiol by acidification of the dithiolate to give 1,2-$(SH)_2$-8,9,10,12-I_4-1,2-*closo*-$C_2B_{10}H_6$ **(42).** Nevertheless, a certain tendency to oxidation was observed giving the corresponding dimer **(43)** where the carborane units are linked through disulfide bridges.

Polyanionic water-soluble molecules have been obtained by the ring-opening reaction of the zwitterionic compound 3,3'-Co(8-$(OCH_2CH_2)_2$-1,2-$C_2B_9H_{10}$)(1',2'-C_2B_9-H_{11}). This molecule has a positively charged oxygen atom connected to the B(8) vertex of cobaltabisdicabollide which is susceptible to nucleophilic substitution by hydroxyl groups of **(14)**, **(15)** and **(39)**. These ring-opening reactions lead to the formation of polyanionic high-boron-content compounds such as, the dianion [9,12-{3',3''-Co(8'-$((OCH_2CH_2)_2O(CH_2)_3$-1',2'-$C_2B_9H_{10}$)(1'',2''-$C_2B_9H_{11}$)}$_2$-1,2-$C_2B_{10}H_{10}]^{2-}$ **([24]$^{2-}$)**, the tetra-anion [8,9,10,12-{3',3''-Co(8'-$((OCH_2CH_2)_2O(CH_2)_3$-1',2'-$C_2B_9H_{10}$)(1'',2''-$C_2B_9H_{11}$)}$_4$-1,2-$C_2B_{10}H_8]^{4-}$ **([25]$^{4-}$)** and the hexa-anion [1,2,8,9,10,12-{3',3''-Co(8'-$((OCH_2CH_2)_2O(CH_2)_3$-1',2'-$C_2B_9H_{10}$)(1'',2''-$C_2B_9H_{11}$)}$_6$-1,2-$C_2B_{10}H_6]^{4-}$ **([41]$^{6-}$)**.

Electrophilic iodination on carbon cluster vertexes of *o*-carborane and *C*-monosubstituted *o*-carborane derivatives: 1,2-*closo*-$C_2B_{10}H_{12}$ **(1)**, 1-Me-*closo*-1,2-$C_2B_{10}H_{11}$ **(47)** and 1-Ph-*closo*-1,2-$C_2B_{10}H_{11}$ **(49)** have been performed to obtain 1,2-I_2-*closo*-$C_2B_{10}H_{10}$ **(1)**1-Me-2-I-*closo*-1,2-$C_2B_{10}H_{10}$ **(48)** and 1-Ph-2-I-*closo*-1,2-$C_2B_{10}H_{10}$ **(50)**.

Highly *B*-iodinated *o*-carborane derivatives, 4,5,7,8,9,10,11,12-I_8-1,2-*closo*-$C_2B_{10}H_4$ and 8,9,10,12-I_4-*closo*-1,2-$C_2B_{10}H_8$ **(3)** have been tested as X-ray contrast agents in acrylic bone cements for Vertebroplasty purpose. Polymeric microspheres and subsequent bone cement containing 8,9,10,12-I_4-*closo*-1,2-$C_2B_{10}H_8$ **(3)** have been successfully prepared. Main chemical and physical properties of the prepared bone cement have been evaluated and compared with the commercial $BaSO_4$ cement. The cement containing 8,9,10,12-I_4-*closo*-1,2-$C_2B_{10}H_8$ **(3)** featured less viscous dough phase, excellent cell-compatibility *in vitro*, as well as sufficient radiopacity in a realistic experimental set-up

4.- ARTICLES PUBLICATS

(Comissió de Doctorat del setembre de 2011)

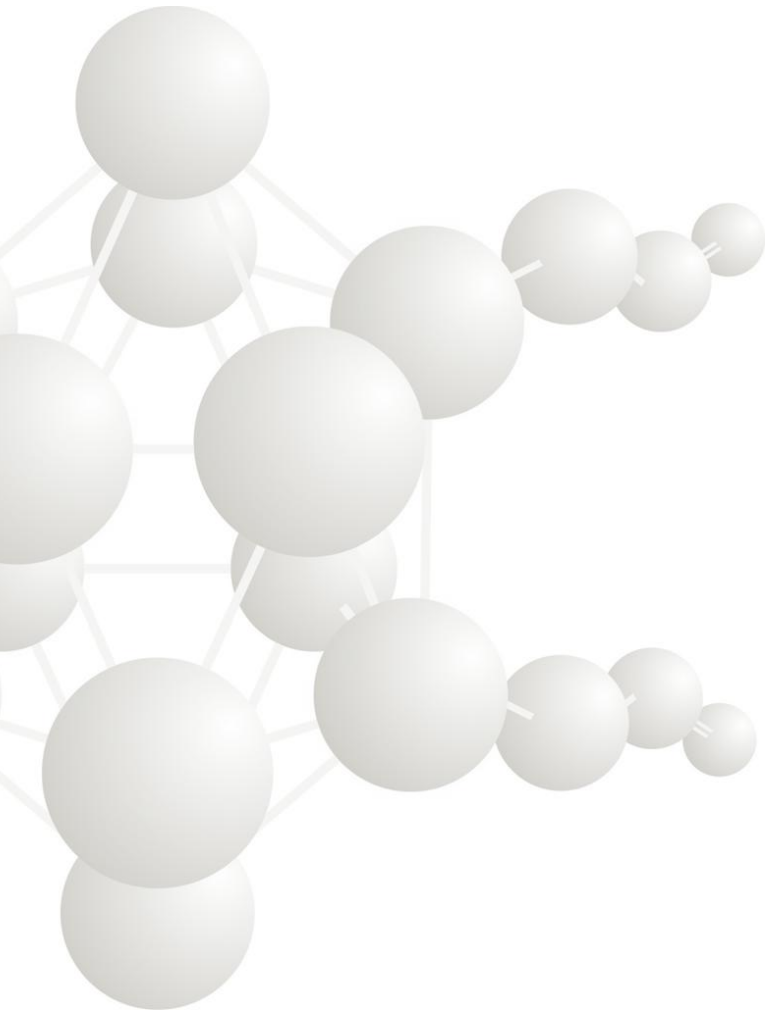

Biomaterials 32 (2011) 6389–6398

Contents lists available at ScienceDirect

Biomaterials

journal homepage: www.elsevier.com/locate/biomaterials

A highly radiopaque vertebroplasty cement using tetraiodinated o-carborane additive

Ariadna Pepiol [a,1], Francesc Teixidor [a], Ketie Saralidze [b], Cees van der Marel [c], Paul Willems [d], Laura Voss [d], Menno L.W. Knetsch [b], Clara Vinas [a,**], Leo H. Koole [b,*]

[a] Materials Science Institute of Barcelona ICMAB-CSIC, Department of Molecular and Supra-molecular Materials, Barcelona, Spain
[b] Maastricht University, Department of Biomedical Engineering/Biomaterials Science, Faculty of Health, Medicine and Life Sciences, Maastricht, The Netherlands
[c] Philips Research, Mi-Plaza Center for Materials Science, Eindhoven, The Netherlands
[d] Maastricht University Medical Center, Department of Orthopaedic Surgery, Maastricht, The Netherlands

ARTICLE INFO

Article history:
Received 1 May 2011
Accepted 18 May 2011
Available online 12 June 2011

Keywords:
Bone cement
Vertebroplasty
Radiopacity
Injectable cement

ABSTRACT

Bone cements for vertebroplasty must have a much better radiocontrast level than cements for knee or hip arthroplasty. This is generally accomplished by adding a relatively large portion of $BaSO_4$, although this affects the physical-mechanical and biological properties of the cement. This prompted us to develop an alternative radiopaque cement, on the basis of unique highly radiopaque methacrylic microspheres. These contain iodine in two modalities: (i) covalently linked to the methacrylic polymer, and (ii) as constituent of the stable tetraiodocarborane 8,9,10,12-I_4-1,2-closo-$C_2B_{10}H_8$. The total iodine content in these particles exceeded 30% by mass. These radiopaque microspheres as well as the cement made thereof were characterized extensively, e.g., by scanning electron microscopy, X-ray contrast measurements, X-ray photoelectron spectroscopy, measurements of compressive strength, infrared spectroscopy, and solid state $^{11}B\{^1H\}$ NMR spectroscopy. Furthermore, the new cement was subjected to several biocompatibility tests in vitro. The results show that the new bone cement fulfills all physico-chemical criteria for use in vertebroplasty. Further data on the cement's biocompatibility (in vitro), as well as on the handling parameters and doughviscosity, indicate that this material has a potential to become an alternative to vertebroplasty cements with a high $BaSO_4$ content. The new cement provides two significant advantages: (i) controlled viscosity in the dough phase, which facilitates precise injection during the vertebroplasty procedure; (ii) excellent structural stability, which precludes leaching of contrast post-implantation.

1. Introduction

Vertebroplasty has become a widely used technique to treat patients with one or more vertebral compression fractures [1–3]. Such fractures are usually related to osteoporosis, i.e., age-related demineralization and weakening of bone. Osteoporotic vertebral compression fractures constitute a major health care problem; it has been estimated that there are around 1.4 million new cases annually around the globe [4]. In essence, vertebroplasty comprises percutaneous injection of cement into a weakened osteoporotic vertebral element. The cement provides additional strength and stiffness after hardening in situ, causing effective pain reduction, both in the short term and in the long term.

Two recent randomized studies on the clinical outcome of vertebroplasty have caused enormous controversy [5,6]. Both studies compared vertebroplasty with sham treatment, 1 and 6 months post procedure. Patients with osteoporotic vertebral fractures up to 1 year old were included. Surprisingly, both studies indicated that vertebroplasty and sham treatment are equally effective. It was emphasized that vertebroplasty, however widespread and popular, is not an evidence-based treatment. A very recent study from 7 clinics in the Netherlands and Belgium, comprising 202 patients with persistent pain, has indicated that vertebroplasty is effective and safe [7]. The effects of the technique, in terms of immediate and long-term (>1 year) pain relief are substantially greater in comparison with conservative treatment. Furthermore, the cost of vertebroplasty appears to be acceptable [7].

Looking at vertebroplasty from the perspective of biomaterials science, it seems clear that the cements as they are currently provided by industry are, in fact, a point of weakness. It has already been suggested that new cement formulations, tailored to

* Corresponding author.
** Corresponding author.
E-mail address: l.koole@bioch.unimaas.nl (L.H. Koole).
[1] A. Pepiol is enrolled in the PhD Program of the UAB.

0142-9612/$ – see front matter © 2011 Elsevier Ltd. All rights reserved.
doi:10.1016/j.biomaterials.2011.05.056

vertebroplasty, could help to further improve clinical outcome of the procedure [8–11]. Current commercial vertebroplasty cements are –essentially- derived from the classical formulations of cements for hip and knee arthroplasty. The most important adjustment is the addition of extra BaSO4, since higher X-ray contrast is required in vertebroplasty. Accurate real-time monitoring of the flowing cement during injection is critical to detect possible cement leakage [12,13]. Displaced cement can cause severe complications. Cement in the spinal canal can cause neuropathic pain or even paralysis, cement in the azygos vein can cause pulmonary embolism [14–16]. Some of the commercial vertebroplast cements contain no less than 30% of $BaSO_4$ in the powder. Such high loadings of contrast agent have negative impacts on (i), the viscosity/injectability of the cement dough; (ii), physical properties of the cement (especially fatigue resistance), and (iii), the long-term biocompatibility; release of Ba^{2+} ions has been associated with increased activity of osteoclasts (locally) and –hence- increased bone resorption [17,18].

It has already been shown that interesting new methacrylic cements can be developed on the basis of all-polymeric formulations, in which enhanced X-ray contrast is introduced via covalently bound iodine [9,19–21]. Previously, we have used copolymers of methylmethacrylate (MMA) and 4-iodobenzoyl-oxo-ethylmethacrylate (4-IEMA, Fig. 1) for this purpose. 4-IEMA was our building block of choice, since it is a crystalline compound that can be manufactured relatively easily in a highly pure form, even on a multi-kg scale. This method has yielded more homogeneous cements, which is explained by the absence of inorganic contrast agents. Radiopaque cements containing the MMA/4-IEMA copolymer have relatively low viscosity in the dough-phase (i.e. they are easily injectable), and post-curing they have improved fatigue resistance properties and they are significantly less cytotoxic, at least in vitro.

However, MMA/4-IEMA copolymers could not provide the high level of radiopacity that is required for vertebroplasty. Here, we introduce an original new method to boost the radiopacity of the iodine-containing cement, while its attractive features are maintained. We again used the MMA/4-IEMA copolymer concept, and in addition to this, we used 8,9,10,12-I_4-1,2-*closo*-$C_2B_{10}H_8$ (Fig. 1) as a contrast additive [22]. Due to its high iodine content, its exceptional stability, its complete insolubility in aqueous media, and the fact that $I_4C_2B_{10}H_8$ can be prepared on large (kg) scale, we hypothesized that this compound would be particularly suitable to improve radiopacity of our cements. Recently, we reported the

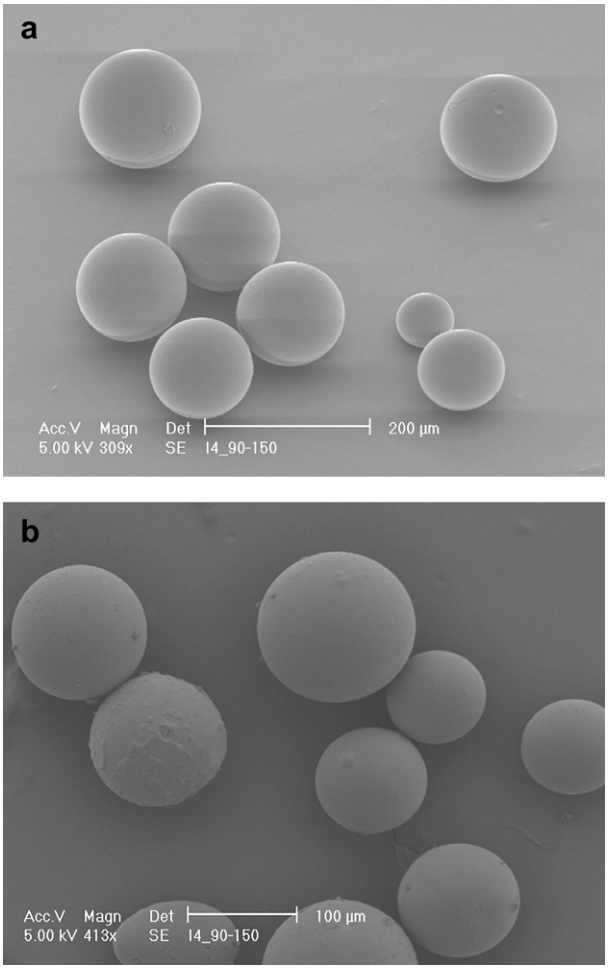

Fig. 2. Scanning electron micrographs of the radiopaque iodine-containing microspheres that were prepared and used in this work. (a) I-microspheres; (b) IC-microspheres.

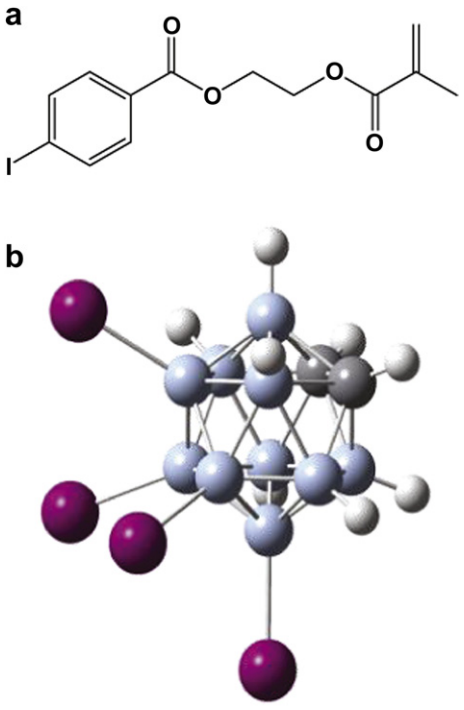

Fig. 1. (a) Structural formula of the iodine-containing methacrylic monomer (4IEMA) that was used in this work. (b) Molecular structure of 8,9,10,12-I_4-1,2-closo-$C_2B_{10}H_8$.

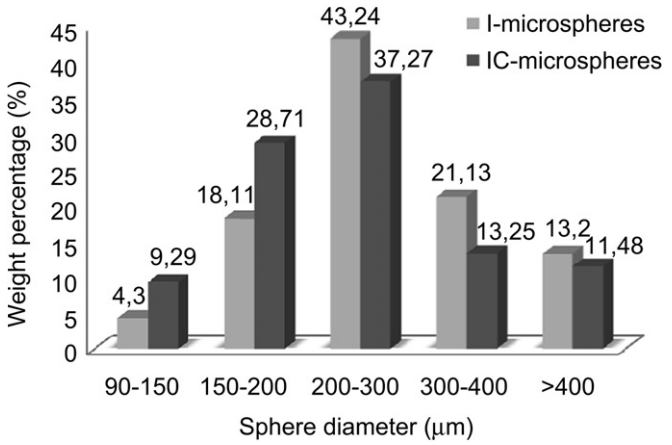

Fig. 3. Size distribution diagrams of I-microspheres and IC-microspheres (mass distribution).

Table 1
Composition of the threecementsthatwerecompared in thiswork.

Cement	Powder part					Liquid part		
	PMMA (g)	I-spheres (g)	IC-spheres (g)	$BaSO_4$ (g)	BPO (mg)	MMA (g)	DMPT (mg)	HQ[a] (ppm)
Vertaplex™	14	–	–	6	360	8.75	100	80
I-cement	5	5	–	–	150	12.00	125	–
IC-cement	5	–	5	–	150	12.00	125	–

[a] HQ = hydroquinone.

synthesis of highly iodinated orthocarborane derivatives that have iodine contents in the range 88.2–90.5% in mass [23–25]. Carboranes already find use in Boron Neutron Capture Therapy (BNCT) and in the design of new antiviral, antibacterial and antitumor drugs [26–31].

We report synthesis of new radiopaque microspheres, built from MMA, 4-IEMA, and a dimethacrylate crosslinker, with $I_4C_2B_{10}H_8$ embedded therein. The microspheres and the cement prepared thereof were studied with different techniques; all data were compared with microspheres and cement without $I_4C_2B_{10}H_8$, as well as with a commercial vertebroplasty cement that owes its radiopacity to the incorporation of $BaSO_4$.

2. Materials and methods

2.1. Materials

Chemicals were purchased from Sigma/Aldrich/Fluka (Zwijndrecht, The Netherlands), Acros Organics (Landsmeer, The Netherlands) or Jansen Chimica (Geel, Belgium). MMA was distilled at atmospheric pressure and stored at −20 °C. 4-IEMA was synthesized from 4-iodobenzoyl chloride as described previously [32]. The cluster compound 8,9,10,12-I_4-1,2-*closo*-$C_2B_{10}H_8$was synthesized according to the literature [22]. Benzoyl peroxide (BPO), Trigonox-C (t-butylperoxybenzoate), N,N-dimethyl 4-toluidine (DMPT, 99%), tetraethylene glycol dimethacrylate (TEGDMA), poly(vinyl alcohol) (PVA; MW 86000; 99–100% hydrolyzed), poly(ethylene glycol) (PEG; MW 1000) and poly(vinyl pyrrolidone) (PVP; K-23–32; MW 5800) were used as purchased. Commercial vertebroplastycment (Vertaplex™) was obtained from the company EMCM BV, Nijmegen, The Netherlands). Cell culture medium (DMEM/F12, MEM), fetal bovine serum (FBS), and antibiotics were from Invitrogen (Breda, The Netherlands). PMMA microspheres were prepared in house through a suspension polymerization reaction, as described previously [20].

2.2. Preparative procedures

The first step was to synthesize microspheres on the basis of three methacrylic monomers: MMA, 4-IEMA, and TEGDMA. Our attempts to maximize the iodine content showed that the polymerization becomes troublesome if the content of 4-IEMA in the feed exceeds 30 M %. For this reason, we prepared microspheres with the following composition: MMA : 4-IEMA : TEGDMA = 32.5 : 13.9 : 1 (molar ratios). Trigonox-C (t-butylperoxybenzoate, [33]) was used as the polymerization initiator at a concentration of 10 M %, relative to all other monomers. These microspheres and the cement derived thereof are designated as "I-microspheres", and the "I-cement", respectively. These materials served as controls throughout this study.

The second step was the preparation of microspheres with elevated iodine content, through addition of the cluster $I_4C_2B_{10}H_8$. Keeping the formulation of the methacrylic monomers unchanged, we added the $I_4C_2B_{10}H_8$ as long as solubility permitted. This led to the composition: MMA : 4-IEMA : TEGDMA : $I_4C_2B_{10}H_8$ = 32.5 : 13.9 : 1 : 0.74 (molar ratios). The same amount of Trigonox-C was used in the suspension polymerization. The resulting microspheres and the cement derived thereof are designated "IC- microspheres" and "IC-Cement", respectively. Further synthetic details are given below.

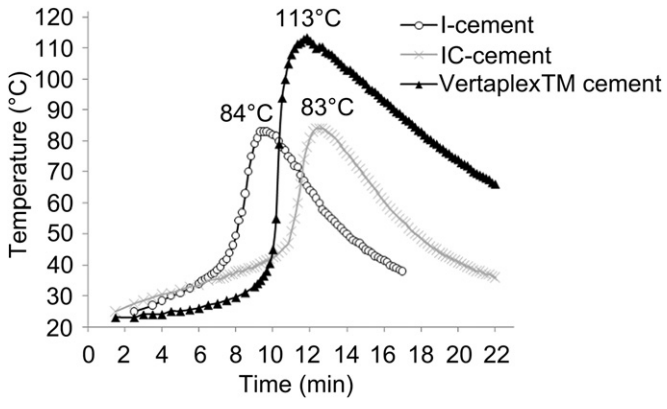

Fig. 4. Temperature-time curves measured during the preparations of I-cement, IC-cement, and Vertaplex™.

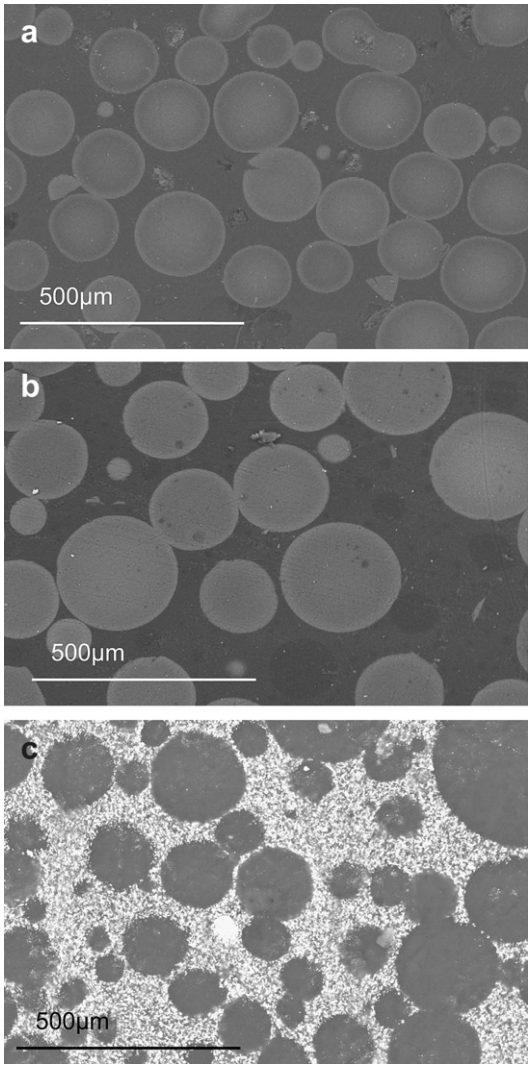

Fig. 5. Backscatter Scanning Electron Micrographs showing characteristic morphologic details of the three cements. (a) I-cement; note the reflective iodine-containing microspheres embedded in the non-reflective PMMA matrix. (b) IC-cement. Note the close resemblance between micrographs 5(a) and 5(b). The microspheres in 5(b) appear lighter, due to the combined effect of iodine that is linked to the copolymer and iodine that is part of the iodocarborane cluster compound. (c) Vertaplex™ cement. Here, the microspheres (PMMA) are surrounded by a PMMA matrix that is loaded with highly reflective white BaSO4 granules.

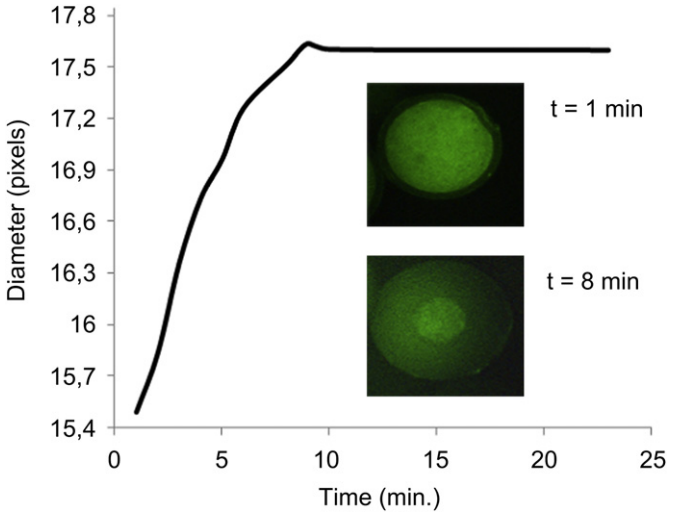

Fig. 6. Swelling of an IC-microsphere upon immersion in MMA, observed with fluorescence microscopy. Uptake of MMA leads to a volume increase of appr. 40% within 10 min. Afterward, equilibrium swelling is achieved. The 10 min time interval coincides with the time scale of cement mixing, handling and hardening. Most probably, uptake of MMA by the microspheres prior to polymerization is a critical parameter governing the hardened cement's physical–mechanical properties.

2.2.1. Preparation of I-microspheres

A solution of poly(vinyl alcohol) (3.75 g), poly(ethylene glycol) (2.50 g), and poly(vinyl pyrrolidinone) (0.375 g) in 150 mL distilled water was magnetically stirred (900 rpm) and heated to 90 °C. A mixture of MMA (3.25 g, 32.46 mmol), 4IEMA monomer (4.25 g, 11.8 mmol), Trigonox-C (1 mL, 5.35 mmol) and TEGDMA (0.33 mL, 1.08 mmol) was added dropwise. Heating and stirring were continued for 3 h. The microspheres precipitated immediately as stirring was stopped, and the supernatant was decanted carefully. The microspheres were allowed to cool to room temperature, and washed with water (6×). The microspheres were decanted, frozen (−180 °C, liquid nitrogen), and lyophilized. Yield: 6.2 g (83%). Microspheres between 200 and 300 mm were separated through sieving, and these particles were used subsequently in our cement preparations.

2.2.2. Preparation of IC-microspheres

Essentially same procedure was followed, except that a mixture of MMA (812 mg, 8.11 mmol), 4IEMA (1.06 g, 2.94 mmol), $I_4C_2B_{10}H_8$ (120 mg, 0.183 mmol), Trigonox-C (0.25 mL, 1.34 mmol) and TEGDMA (76.2 μL, 0.25 mmol) was added dropwise to 75 mL of the stirred aqueous phase. The yield of the IC microspheres was: 1.65 g (88%). IC microspheres with a diameter between 200 and 300 mm were used in the preparation of IC-cement.

2.2.3. Preparation of I-cement and IC-cement

The powder portion of each cement batch was prepared by mixing equal amounts of PMMA microspheres (vide supra) with either I-microspheres or IC-microspheres. Typically, 5.00 g of PMMA microspheres was mixed with 5.00 g of the iodine-containing microspheres. Then, we added benzoylperoxide to the combined microspheres (150 mg per 10.00 g). The liquid portion of the cement was prepared by dissolving 125 mg of DMPT in 12.00 g of MMA.

Cements were prepared in the fume hood in an open bowl, by mixing powder and liquid with a spatula. After mixing for about 3 min, a slightly viscous homogenous mixture was obtained. The material was carefully poured into vertically placed polypropylene cylinders with the dimensions: 8 mm diameter and 80 mm height, avoiding inclusion of air bubbles. The ongoing polymerization could be noted clearly; a clear rise in temperature occurred after 10–12 min. Samples were left untouched for 24 h at least.

Table 2
Apparent concentrations (atom %) measuredwith XPS at: (i) the fracturesurface of the three cement specimens (spot size 100 mm scannedacrossan area of 1200 × 500 mm), and (ii) at the surface of radiopaquemicrospheres (spot size 100 mm, non-scanning).

Atom	B1s	C1s			I3d5	I4d5	I4s	O1s
Line position (eV)	190.5	284.8	286.5	288.7	620.7	50.7	187.8	
		C–H	C–O	CO(O)				
IC-cement	0.34	41.1	16.9	13.4	0.6	0.6	0.6	26.5
I-cement	–	42.6	16.6	13.7	0.1	0.2	0.1	26.7
IC-microspheres	1.9	38.9	16.6	6.5	1.9	2.2	2.2	24.1
I-microspheres	–	37.9	16.8	6.4	0.8	1.1	0.8	30.6

2.2.4. Preparation of test specimens

The cement rods were carefully removed from the polypropylene molds using a sharp knife, and were then processed with a computer-controlled lathe-machine into two types of specimens: (i) 8.0 mm diameter/2.0 mm height discs for cell-contact experiments, and (ii) 8.0 mm diameter/8.0 mm height cylinders for several physical-mechanical characterization methods.

2.3. Methods

2.3.1. Microscopy

Morphology and size of the microspheres were characterized using scanning electron microscopy (SEM) analysis (Philips XL30, Eindhoven, The Netherlands). The microspheres were stuck on an aluminum stub with double-face adhesive carbon tape. The stubs were coated under vacuum for 2 min with a thin layer of gold and examined at an accelerating voltage of 5 kV. The morphology of the cements has been studied with a Philips XL30 equipped with a solid-state backscattered electron detector operated at an accelerating voltage of 25 kV. All cement samples were supplied with a thin carbon conductive layer. Sputter coating was performed with a 108 auto/SE sputter coater (Cressington Scientific Instruments Ltd., Watford, U.K.). Fluorescence microscopy was performed with Nikon Eclipse E800, equipped with a RS photometric cooled CCD camera.

2.3.2. Time-temperature curves during cement curing

Liquid (2.4 g) and powder (2.0 g) portions were hand-mixed with a spatula. The resulting cement dough was wrapped in aluminum foil, and a thermometer was inserted into the center of the cement mass. Temperatures were recorded every 30 s; when a rise of the temperature was noted (after appr. 8 min), temperatures were recorded every 10 s.

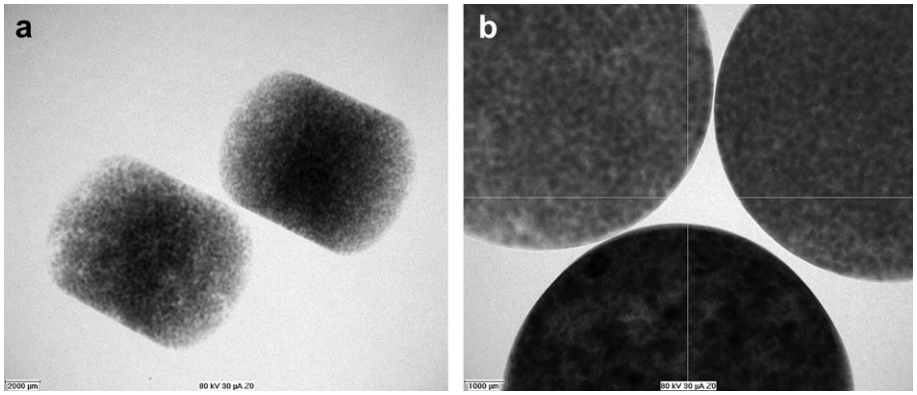

Fig. 7. X-Ray fluoroscopic images of the cylindrical specimens (height = diameter = 8 mm) of the three cements.(X-ray beam of 80 kV). (a) IC-cement (left) and I-cement (right). Note that the samples were placed under a 45° angle with respect to the X-beam. (b) IC-cement (upper right), I-cement (upper left) and Vertaplex™ (below). Now, the vertical axes of the cylinders are aligned with the X-beam. Note the improved contrast of IC-cement vs. I-cement, as well as the granular contrast of Vertaplex™.

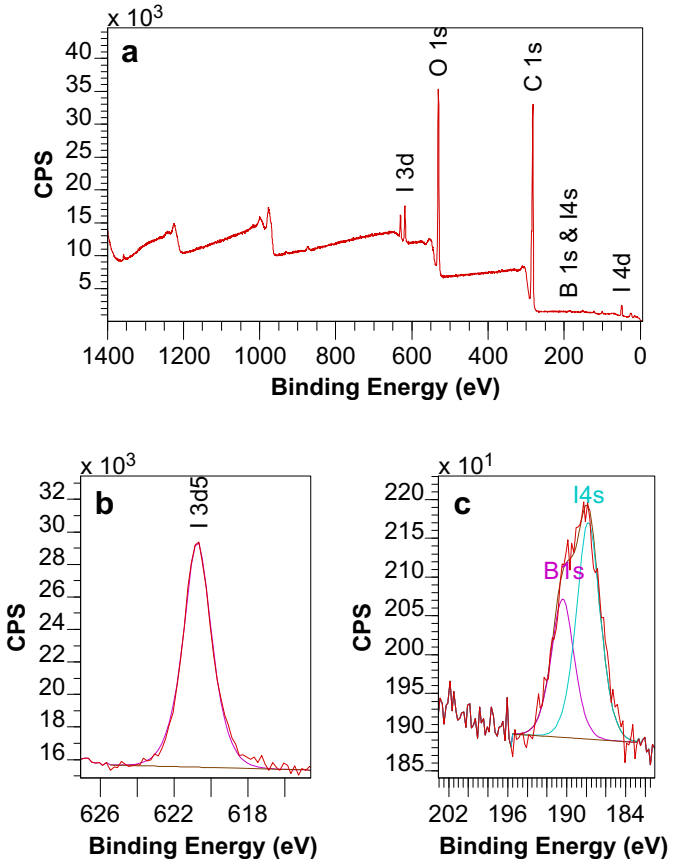

Fig. 8. XPS spectra of a fresh fractured surface of the IC-cement, measured with a measurement spot size of 1200 × 500 μm. (a) Survey spectrum. (b) Narrow-scan spectrum showing the I3d5 line at 621 eV. (c) Narrow-scan spectrum showing the overlapping B1s and I4s lines. Blue spectra were obtained after deconvolution; B1s is at 190 eV, and I4s is at 188 eV.

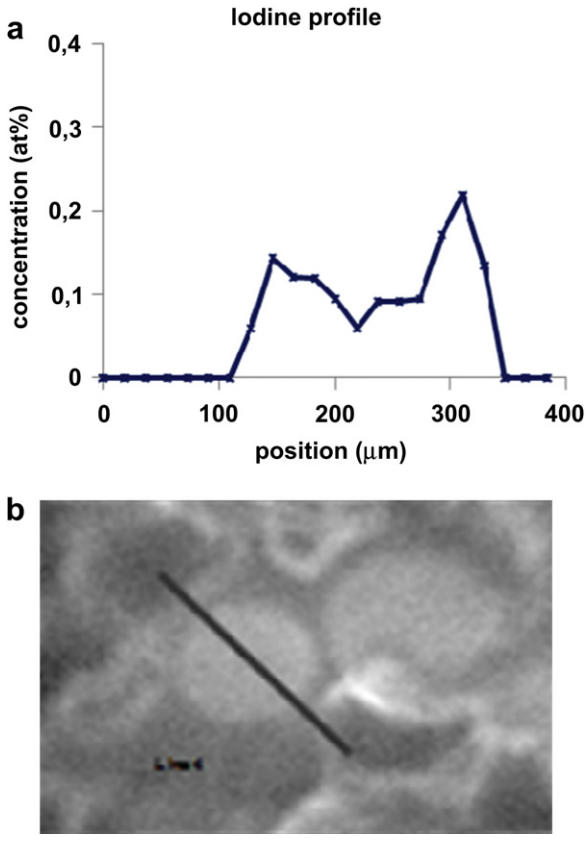

Fig. 9. Results of the XPS line-scan experiments on the fresh fractured surface of the IC-cement; the measurement spot size (focussed X-ray beam) now used was 8 × 8 μm. (a) Measured profile of the iodine at the surface concentration. The position of the spot is on the *x*-axis. (b) Secondary X-ray induced image of a part of the fresh fractured of the IC cement, also showing the trajectory of the measurement spot (diagonal black line). This was exactly across a broken iodine containing microsphere at the surface. Note that the profile in (a) corresponds with the absence of iodine between 0 and 120 μm, and beyond 300 μm; this is outside the microsphere. Between 120 and 350 μm, iodine is definitely present. The profile is M-shaped, which reveals that the $I_4C_2B_{10}H_8$ cluster is localized predominantly near the inner surface of the microsphere, rather than in the core.

2.3.3. X-Ray visibility

The three cements were studied with a high-resolution X-ray imaging system (Philips BV Pulsera; 46 kV, 1.04 mAs, autofocus). X-ray imaging during injection of the IC-cement in the human vertebra was performed with a C-arm system that is in routine clinical use.

2.3.4. Cytocompatibility

Two cell lines have been used to test the cytocompatibility of the cements, 3T3 mouse fibroblasts and Saos-2 osteoblasts. 3T3 mouse fibroblasts were routinely grown in DMEM/F12 + Glutamax medium containing 10% FBS and antibiotics (100 U/mL penicillin, 100 μg/mL streptomycin, 0.25 μg/mL amphotericin B). Saos-2 osteoblasts were grown in MEM with 10% FBS, 2 mM L-glutamine, and antibiotics (100 U/mL penicillin, 100 μg/mL streptomycin, 0.25 μg/mL amphotericin B) [34].The two cell lines were harvested using trypsin/EDTA (0.05%/0.53 mM) and grown at 37 °C/5%CO_2. To eliminate as much as possible the effect of residual MMA, the experiments were performed two months after cement preparation. Two different experiments were performed to test the cytocompatibility of the cements (i) Live/Dead assay and (ii) MTT test [35,36].

(i) Live/Dead assay (Molecular Probes, Reduced Biohazard Viability/Cytotoxicity Kit #1 (L-3224)) was used to test the surface cytotoxicity of the cements (8 mm diameter, 2 mm thickness disks). After washing each disk with at least 5 mL of FBS, 10.000 Saos-2 osteoblasts were inoculated and incubated for 42 h at 37 °C/5% CO_2. The cells on the disks were washed with PBS and then incubated with PBS containing 2 μM calcein-AM and 4 μM ethidium-homodimer-1 for 30 min at room temperature. The cells were directly observed with a fluorescence microscope. All tests were run in duplicate.

(ii) Cement extracts cytotoxicity was performed with MTT test using Minimum essential medium with Earle's salts, Glutamax-I, and 25 mM HEPES and supplemented with 10 wt.% fetal bovine serum and antibiotic/antimycotic solution (1×) as a culture medium. Small fragments (total mass of approx. 1 g) of the cured cements, exposed to ambient laboratory air for 2 months were sterilized using ultra-violet light and then put in approx. 10 mL (final concentration 0.1 g/mL) of cell culture medium at 37 °C. The medium was removed after 2 days (stored at 4 °C) and fresh medium was added. This was repeated twice. The collected media were put on 3T3 fibroblasts in a 96-wells plate (10.000 cells/well) and the cells were allowed to grow for 24 or 48 h at 37 °C/5% CO_2. MTT assay was conducted by adding methyl thiazol tetrazolium in medium (0.5 mg/mL) to the cells for 1.5 h at 37 °C. Conversion of soluble MTT into the dark blue insoluble MTT formazan is directly related to mitochondrial activity and subsequently to cell viability. The resulting blue crystals were dissolved in isopropanol and the optical absorbance at 550 nm was measured using a micro-plate reader. The cell survival in pure culture medium was set to 100% and latex extract was set as a negative control.

2.3.5. Compressive modulus

All specimens (machined cylinders with diameter = height = 8.0 mm) were first incubated in sterile PBS buffer during 4 weeks (pH 7.4, ambient temperature). Then, each specimen was compressed at ambient temperature at a true strain rate of 3×10^{-3} s^{-1}. Force and displacement were recorded continuously. Although the ASTM F451-99a standard specification for acrylic bone cements prescribes the sample height to be twice the diameter, we used samples with $h/d = 1$. This low ratio proved to be favorable to study large strain deformations since buckling of the sample is avoided. A minimum of 8 independent measurements was done for each of the three cements.

2.3.6. XPS

These experiments were carried out with a Quantera SXM™ instrument from Ulvac-PHI. The measurements were performed using monochromatic AlKα-radiation. Various spot sizes have been used. The take-off angle of the detected electrons was 45°, which corresponds to an information depth of 7 nm. By means of wide-scan measurements, all elements present at the surface have been identified. The

Table 3
Results of the measurements of the compressive modulus of the three cements.

Experiment #	Compressive modulus (MPa)		
	I-cement	IC-cement	Vertaplex
1	79.1	98.9	97.3
2	85.3	111.2	94.2
3	85.4	100.0	76.3
4	76.9	98.2	76.0
5	65.6	102.5	74.2
6	81.5	86.9	100.4
7	78.8	102.3	96.6
8	55.9	111.0	76.6
9	75.2	94.3	105.0
Average	76.0	100.6	88.5
Standard deviation	9.6	7.6	12.4

chemical state and the atomic concentrations of the elements were obtained from accurate narrow-scan measurements. Standard sensitivity factors were used to convert peak areas into atomic concentrations. Consequently, concentrations may deviate from reality in the absolute sense (generally not more than 20% relative).

2.3.7. Solid-state NMR

One-dimensional ^{1}H-NMR and ^{11}B{^{1}H}-NMR spectra of $I_4C_2B_{10}H_8$, I-microspheres, IC-microspheres, I-cement, and IC-cement were recorded at room temperature on a Bruker WB 400 MHz spectrometer at a MAS spinning rate of 12 kHz. The ^{11}B{^{1}H}-NMR spectra were run with a pulse program *hpdec.av;* frequency of observed channel (SF): 128.38 MHz; time domain size (TD): 16384; number of scans (NS): 32-2048; sweep width (SW): 4099.44 ppm; acquisition time (AQ): 0.0156 s ^{1}H-NMRspectra were run using the pulse program *zg*,; frequency of observed channel: 400.16 MHz; time domain size: 4096; number of scans: 2; sweep width: 374.84 ppm; acquisition time: 0.0137 s.

3. Results and discussion

3.1. Microsphere synthesis and cement preparation

The suspension polymerization reactions leading to either the I- or IC-microspheres proved to be sensitive to a multitude of experimental parameters, such as stirring speed, method of addition of the monomer droplets, concentration of the radical initiator, reaction temperature, scale, etc. Also, the composition of the aqueous phase (PVA, PVP, and PEG dissolved in water) was critical. After a number of trial experiments in which we optimized the experimental conditions, we succeeded in the reproducible fabrication of the desired iodine-containing spherical particles (Fig. 2) on a scale of 6–7 g per batch for the I-microspheres, and 1.5–2 g per batch for the IC-microspheres. The size distribution diagrams of a typical batch are displayed in Fig. 3; the average diameter is between 200 and 300 μm. Clearly, there is no significant difference between the sizes of the I-microspheres and IC-microspheres. Size distributions were reproducible.

Preparation of the two experimental cements (I- and IC-cement) proceeded without technical difficulties. For benchmarking, we also included a commercial vertebroplasty cement in this study; this cement (Vertaplex™ cement) was obtained from the company EMCM (Nijmegen, the Netherlands). Vertaplex™ is a methacrylic cement that contains $BaSO_4$ in its powder part, in a concentration of 35% by mass. The detailed compositions of the 3 cements used in this study are compiled in Table 1. During ourcement preparations, we transferred the dough that was obtained after approx. 3 min. of mixing, into cylindrical molds (vide supra). In one case per cement, we used the material to monitor the temperature of the curing cement as a function of time. The resulting time-temperature curves for each of the three cements are shown in Fig. 4. These data clearly reflect the well-known exothermic nature of methacrylic polymerizations. The commercial cement achieved a maximum temperature of approx. 113 °C, whereas both experimental cements did not become hotter than approx. 84 °C. The curing parameters were approximately equal for the three cements. For example, the setting times were 8.1, 11.1 and 10.3 min for I-, IC-cement and Vertaplex™, respectively.

3.2. Physical characterization of the cements

3.2.1. Scanning electron microscopy

SEM in the backscatter mode was first used to characterize the three cements. This required careful polishing of the cement specimens, followed by sputter coating with carbon. Fig. 5 shows

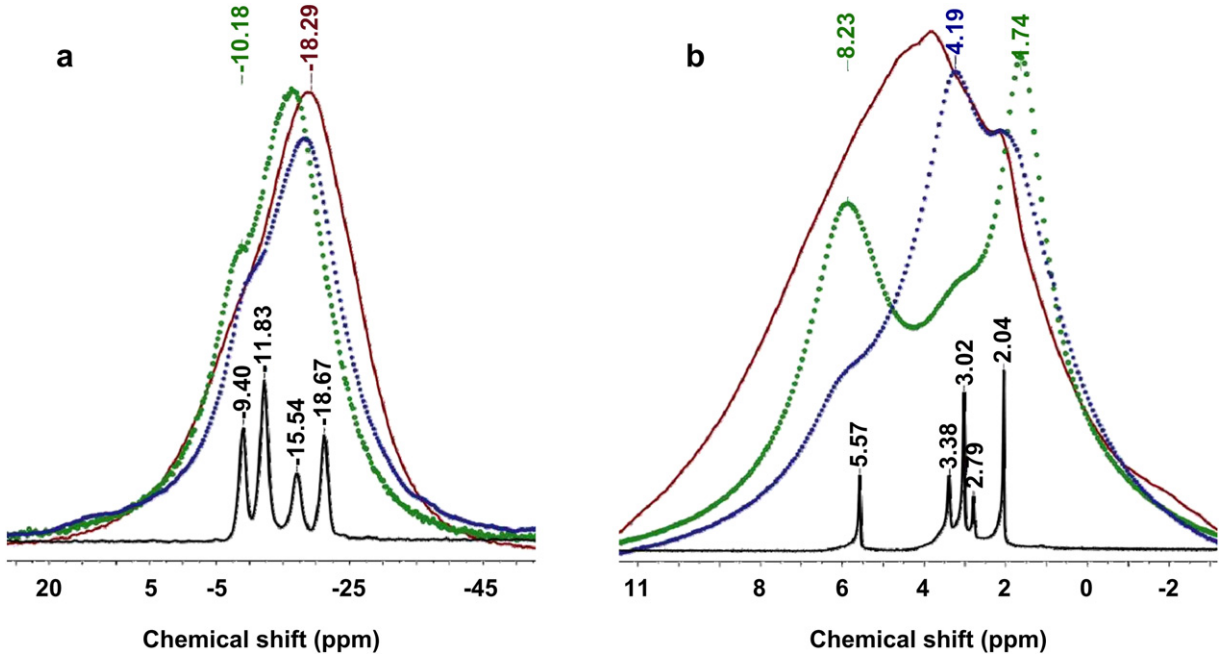

Fig. 10. (a) ^{11}B{^{1}H}-CPMAS NMR solid state spectra of $I_4C_2B_{10}H_8$ (red), IC-microspheres (green), IC-cement (blue). ^{11}B-{^{1}H} NMR spectrum of $I_4C_2B_{10}H_8$ in d6-acetone (black) shows a pattern 2 : 4 : 2 : 2 in the range - ppm. (b) ^{1}H CPMAS NMR spectra of $I_4C_2B_{10}H_8$, IC-microspheres, IC-cement, and ^{1}H NMR spectrum of $I_4C_2B_{10}H_8$in d6-acetone. (For interpretation of the references to colour in this figure legend, the reader is referred to the web version of this article.)

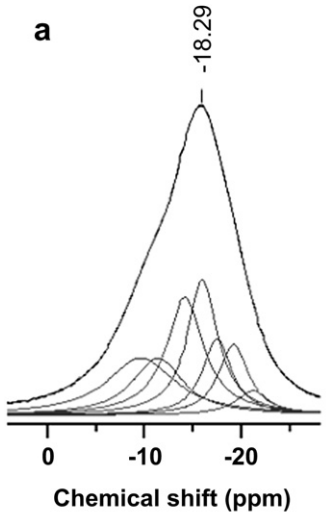

Relative Area	Chemical Shift (ppm)
4	-5.39
3	-8.93
4	-14.62
4	-18.28
2	-21.34
2	-24.73
1	-28.78

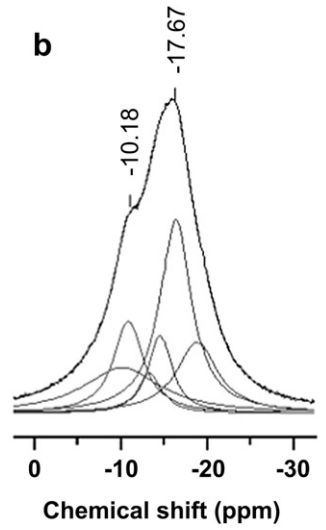

Relative Area	Chemical Shift (ppm)
4	-7.88
3	-9.17
1	-13.39
2	-15.47
7	-18.57
3	-22.82

Fig. 11. (a) Deconvolution of $I_4C_2B_{10}H_8$CPMAS spectrum $^{11}B\{^1H\}$-NMR, (b) deconvolution of IC-microspheres CPMAS spectrum $^{11}B\{^1H\}$-NMR .The tables summarize the disarticulation of the ^{11}B NMR spectra for $I_4C_2B_{10}H_8$ and IC-microspheres together with peak assignments.

a representative SEM backscatter micrograph for each of the three cements. I-cement (Fig. 5a) consists of I-microspheres embedded in a continuous matrix of PMMA. The iodine (bound to the MMA-4IEMA copolymer) in the I-microspheres explains why the particles appear lighter than the matrix. The IC-microspheres, shown analogously in Fig. 5b, are lighter than the I-microspheres, due to the combined effect of iodine bound to the MMA-4IEMA copolymer and iodine in $I_4C_2B_{10}H_8$. Note that the microspheres in Fig. 5a and b all have a corona, indicating that some swelling has occurred during the cement mixing phase, through uptake of MMA. This swelling dilutes the contrast, and this explains why the outer ring of most particles appears relatively dark. We believe that this absorption of MMA is, actually, a positive feature. Polymerization of the MMA molecules after the diffusion will lead to integration of the contrast particles in the continuous phase, and this structural merging is expected to be beneficial for the physical properties of the material. Fig. 5c shows the backscatter SEM image of Verteplex™ cement (containing $BaSO_4$). Clear discrete black circles due to (radiolucent) PMMA are seen. The continuous matrix contains granular particles of $BaSO_4$ (white), embedded in PMMA. Although no clumping of contrast particles appears in Fig. 5c, it seems clear that such a high loading of contrast particles in the continuous matrix will have a profound impact on the material as a whole. We decided to study swelling of the I- and IC-microspheres in MMA in some more detail. We immersed microspheres in a thin (approx. 1-mm) layer of MMA under continuous examination with fluorescence microscopy. Photographs were taken every min., and the images clearly verified that expansion (swelling) through MMA uptake takes place (Fig. 6). Image analysis revealed that the diameter of a typical IC-microsphere expanded by approximately 13% during 10 min immersion in MMA. Note that this corresponds with a volume expansion of 44%. Although swelling during cement hardening can occur only during the first few minutes, it seems clear that this effect is significant, and −probably- essential with regard to the physical properties of the resulting materials.

3.2.2. X-ray imaging

Fig. 7 shows high-resolution images of the three cements; the measurements were performed on cylindrical specimens with diameter = height = 8.0 mm. Note that the images of the three materials are clearly different. As expected, the contrast of materials increases in the order: I-cement < IC-cement < Vertaplex™. In the left image, the cylindrical specimens were tilted by appr. 30° with respect to the X-beam, this explains why the images appear darker in the centre than at the top or bottom parts. The right image shows X-absorption images of the three cements when the specimens are exactly parallel to the X-beam. The contrast in the I- and IC-cement is distributed more evenly throughout the volume, in comparison with Vertaplex™. On the latter cement, clumps of contrast could be clearly discerned.

3.2.3. X-ray photoelectron spectroscopy

These experiments were also based on the cylindrical specimens with diameter = 8.0 mm; height = 8.0 mm. First, we treated the specimens with a saw in a radial plane close to the specimen's centre. After removing approximately 60%, sawing was stopped. Then, the sample was carefully broken, and the fracture surfaces were used for XPS. This method ensures that data reflect the chemical composition of the genuine materials, free of any contaminants. The XPS spectra confirmed the chemical composition of the I-cement and the IC-cement (Table 2). A clear boron peak appeared in the spectrum of the IC-cement (190.5 eV, Fig. 8), even though boron is known to be relatively insensitive in XPS. We also subjected the IC-microspheres as well as pure $I_4C_2B_{10}H_8$ (a powder) to XPS, finding that the boron peak appears in exactly the same position in all three cases. The same holds true for the iodine peaks: both in the IC-microspheres, at fracture surfaces of the IC-cement, and in pure $I_4C_2B_{10}H_8$ we found the same peak positions. This strongly indicates that the tetraiodocarborane molecules in the IC-cement have remained fully intact during the two subsequent free-radical polymerizations that occurred around them (firstly during IC-microsphere synthesis, and secondly during bone cement hardening). Interestingly, further XPS experiments could prove that the tetraiodocarborane molecules are spread throughout the volume of the microspheres, but not in a homogeneous manner. This was demonstrated by measuring a series of high-resolution XPS spectra (using a measurement spot of 20 mm) by moving the measurement spot stepwise along a straight line across a fractured IC-microsphere at the cement's fracture surface. It was found that the element iodine (chemically bound in $I_4C_2B_{10}H_8$) has a clear tendency to accumulate near the inner walls of the microspheres (Fig. 9).

3.2.4. Compressive modulus

We again used the cylindrical specimens with diameter = height = 8.0 mm in these experiments. Specimens were weighed prior to the experiments, and discarded if the mass was low (due to enclosed air bubbles). Using 9 specimens per material, we obtained

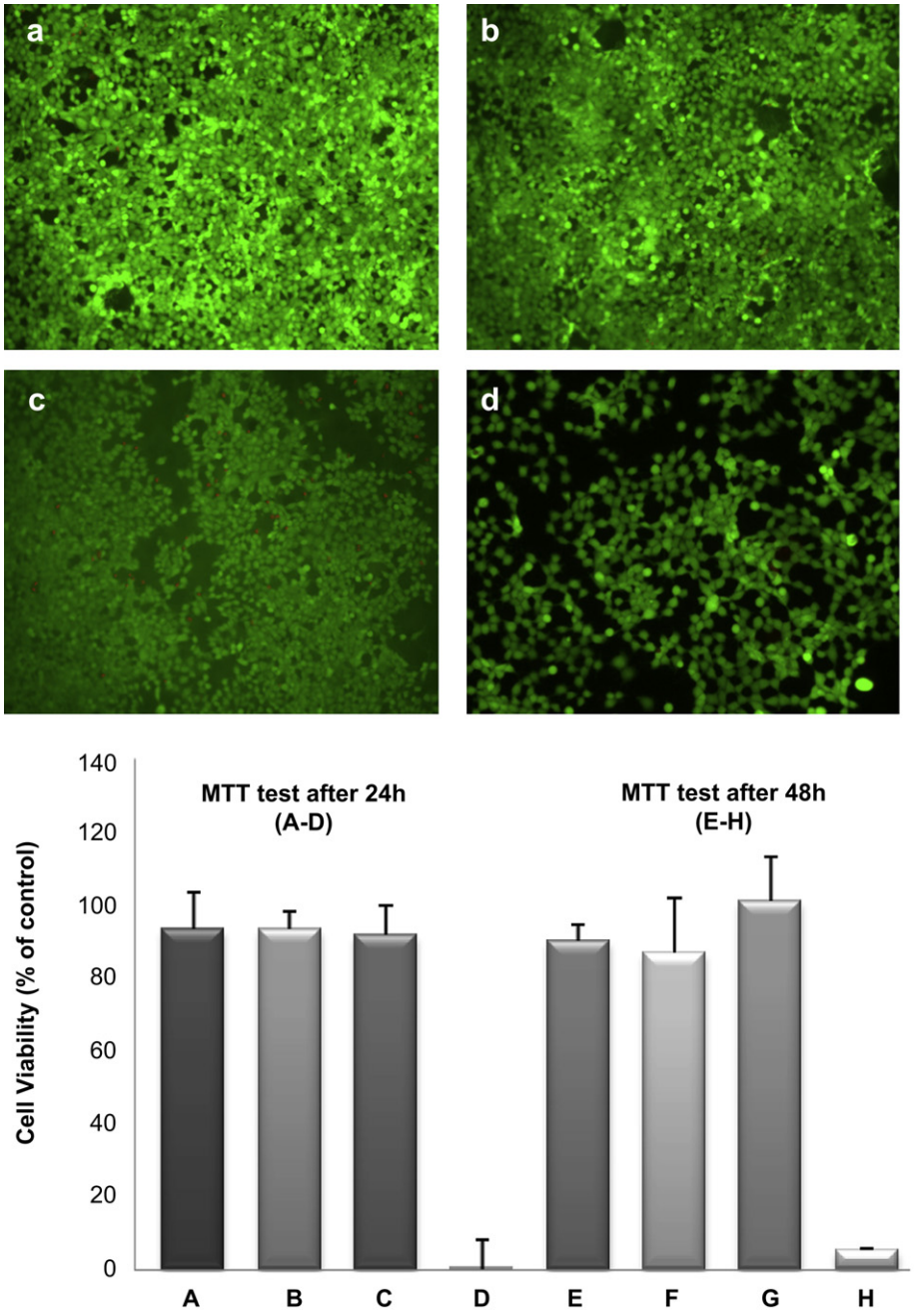

Fig. 12. Live/Dead assayfluorescentmicrographs of (a) I-cement, (b) IC-cement, (c) Vertaplex™ cementand on (d) the glass control material, and graphical representation of cell viability after 24 h, where (a) corresponds to I-cement, (b) to IC-cement, (c) to Vertaplex™ cement, and (d) Latex, negative control; and after 48 h, where (e) corresponds to I-cement, (f) to IC-cement, (g) to Vertaplex™ cement, and (h) Latex, negative control. All cement extracts do not show significant toxicity (student t test $p < 0.05$).

the compressive moduli as compiled in Table 3. Note that the specimens were first equilibrated in aqueous medium (PBS) during 4 weeks prior to these experiments. This was done to mimic the *in vivo* situation as closely as possible. It is known that acrylic bone cements absorb some water (despite their hydrophobic nature), and it is also known that absorbed water molecules act as a plasticizer. Hence, pre-incubation of the cement samples led to a more fair resemblance of the *in vivo* situation, as compared to the use of dry specimens. The I-cement has the lowest compressive modulus (76.0 ± 9.6 MPa), compared with the other cements (100.6 ± 7.6 MPa for the IC-cement, and 88.5 ± 12.4 MPa for Vertaplex™). Note that all these differences are statistically significant. Furthermore, it must be noted that the moduli for the IC-cement and for Vertaplex™ correspond very well with literature data on bone cements for hip and knee arthroplasty, for which compressive moduli between 80 and 110 MPa have been reported [37]. The relative softness of I-cement probably disqualifies this material for use as a vertebroplasty cement.

3.2.5. Solid state NMR spectroscopy

^{11}B-NMR spectroscopy has proven to be a powerful tool for the study of boron-containing compounds in solution [38]. Nevertheless, in the solid state this technique has been applied to borosilicate glasses, boron halides, and organoboron compounds, but there are very few examples for boron hydride clusters in the literature [39]. Magic-angle-spinning solid state NMR spectroscopy with a focus on boron and hydrogen was used to characterize the IC-microspheres and IC-cement. The $^{11}B\{^1H\}$-CPMAS NMR spectra of $I_4C_2B_{10}H_8$, IC-microspheres and IC-cement are shown in Fig. 10a.

The $^{11}B\{^1H\}$-CPMAS NMR spectra of IC-microspheres and IC-cement show very broad resonances typical of amorphous compounds. However, the ^{11}B resonances appear in the same chemical shift region (+10/−40 ppm) as the starting $I_4C_2B_{10}H_8$, which demonstrates its presence in IC-microspheres and IC-cement.

The ^1H CPMAS NMR spectra of the IC-microspheres (green) contains signals of all the chemical groups incorporated inside polymer (Fig. 10b), such as phenyl units from 4IEMA (8 ppm), methylene (4 ppm) and methyl groups (2 ppm). For comparison, we have also given the ^1H CPMAS NMR spectrum of the pure carborane to show where the proton bonded to the $C_{cluster}$ appears (5.57 ppm). This signal it is not detectable in our ^1H solid state NMR spectra due to the small amount of $I_4C_2B_{10}H_8$ included in our materials.

In order to understand the $^{11}B\{^1H\}$-CPMAS NMR spectra and assign the peaks corresponding to the $I_4C_2B_{10}H_8$ cluster we used computer deconvolution. The boron signal of $I_4C_2B_{10}H_8$ solid state NMR spectra is made up by seven peaks with a total relative area of 20 boron atoms (Fig. 11a), showing the two clusters per unit cell, as is previously reported in its crystal structure [22]. Analyzing the deconvolution of the $^{11}B\{^1H\}$-CPMAS NMR spectrum in the IC-microspheres (Fig. 11b) we can confirm the same solid structure of the $I_4C_2B_{10}H_8$ inside the polymer, since the same number of boron atoms (same symmetry, in fact) is obtained.

3.2.6. Interaction with cells in vitro

Fig. 12 shows fluorescence photo-micrographs as taken at the end of the LIVE-DEAD assay (48 h). Note that (i), osteoblasts cells (Saos-2) were used I these tests, and (ii), all specimens were thoroughly washed prior to the analysis, to ensure that potential toxic effects relate to the material, not to toxic leachables. The I- and IC-cements, as well as Vertaplex™ showed the presence of predominantly alive cells (green); almost no red spots (indicating.cell necrosis) could be found. The results of the MTT assay are also shown in Fig. 12. None of the three cements showed toxic effects in the aqueous extracts; survival of the cells was >90% during the first 24 h, and between 85 and 90% during the next 24 h.

4. Conclusion

The alternative radiopaque cement that is described in this work contains methacrylic radiopaque microspheres that contain iodine in two modalities: iodine is linked covalently to the methacrylic polymer, or iodine belongs to the stable iodocarborane cluster $I_4C_2B_{10}H_8$. The cluster compound is spread over the entire volume of these microspheres, but in such a manner that the periphery of each microsphere is richer in the cluster compound than the core. The structure is stabilized through H-bonding between the cluster and C═O groups of the embedding poly(methacrylate) crosslinked polymer network. Compared to existing vertebroplasty cements, the new cement is less viscous in its dough phase (i.e. several minutes after mixing of the powder and liquid portions). This facilitates fast and accurate injection of the material through the relatively thin vertebroplasty needle. It is anticipated that this will improve the clinical outcome of vertebroplasty procedures. Furthermore, the cement featured excellent cell-compatibility *in vitro,* as well as sufficient radiopacity in a realistic experimental set-up. Further work to examine the potential utility of the new cement is currently ongoing in our laboratories and clinic.

Acknowledgment

This work has been supported by Generalitat de Catalunya (2009/SGR/00279) and Ministerio de Ciencia e Innovación (CTQ2010-16237). A. Pepiol thanks to the Consejo Superior de Investigaciones Científicas for the JAE and JAE estancias breves grants.

References

[1] Patel N. Percutaneous vertebroplasty: role in treatment of vertebral compression fractures. Phys Med Rehabil Clin N Am 2010;21:869–76.
[2] Hurley MC, Kaakaji R, Dabus G, Shaibani A, Walker MT, Fessler RG, et al. Percutaneous vertebroplasty. Neurosurg Clin N Am 2009;20:341–59.
[3] Eckel TS, Olan W. Vertebroplasty and vertebral augmentation techniques. Tech Vasc Interv Radiol 2009;12:44–50.
[4] Johnell O, Kanis JA. An estimate of the worldwide prevalence and disability associated with osteoporotic fractures. Osteoporos Int 2006;17:1726–33.
[5] Kallmes DF, Comstock BA, Heagerty PJ, Turner JA, Wilson DJ, Diamond TH, et al. A randomized trial of vertebroplasty for osteoporotic spinal fractures. N Engl J Med 2009;361:569–79.
[6] Buchbinder R, Osborne RH, Ebeling PR, Wark DJ, Mitchel P, Graves S, et al. A randomized trial of vertebroplasty for painful osteoporotic vertebral fractures. N Engl J Med 2009;361:557–68.
[7] Klazen CA, Lohle PN, de Vries J, Jansen FH, Tielbeek AV, Blonk MC, et al. Vertebroplasty versus conservative treatment in acute osteoporotic vertebral compression fractures (Vertos II): an open-label randomised trial. Lancet 2010;376:1085–92.
[8] Lewis G, Towler MR, Boyd D, German MJ, Wren AW, Clarkin OM, et al. Evaluation of two novel aluminum-free, zinc-based glass polyalkenoate cements as alternatives to PMMA bone cement for use in vertebroplasty and balloon kyphoplasty. J Mater Sci Mater Med; 2010:59–66.
[9] Lewis G, Koole LH, van Hooy-Corstjens CS. Influence of powder-to-liquid monomer ratio on properties of an injectable iodine-containing acrylic bone cement for vertebroplasty and balloon kyphoplasty. J Biomed Mater Res B Appl Biomater 2009;91:537–44.
[10] Lewis G. Injectable bone cements for use in vertebroplasty and kyphoplasty: state-of-the-art review. J Biomed Mater Res B Appl Biomater 2006;76(2):456–68.
[11] Carrodeguas RG, Lasa BV, Del Barrio JS. Injectable acrylic bone cements for vertebroplasty with improved properties. J Biomed Mater Res B Appl Biomater 2004;68:94–104.
[12] Pizzoli AL, Brivio LR, Caudana R, Vittorini E. Percutaneous CT-guided vertebroplasty in the management of osteoporotic fractures and dorsolumbar metastases. Orthop Clin North Am 2009;40:449–58.
[13] Lee IJ, Choi AL, Yie MY, Yoon JY, Jeon EY, Koh SH, et al. CT evaluation of local leakage of bone cement after percutaneous kyphoplasty and vertebroplasty. Acta Radiol 2010;51:649–54.
[14] Krueger A, Bliemel C, Zettl R, Ruchholtz S. Management of pulmonary cement embolism after percutaneous vertebroplasty and kyphoplasty: a systematic review of the literature. Eur Spine J 2009;18:1257–65.
[15] Jensen ME, Evans AJ, Mathis JM, Kallmes DF, Cloft HJ, Dion JE. Percutaneous polymethyl methacrylate vertebroplasty in the treatment of osteoporotic vertebral body compression fractures: technical aspects. AJNR Am J Neuroradiol 1997;18:1897–904.
[16] Venmans A, Klazen CA, Lohle PN, van Rooij WJ, Verhaar HJ, de Vries J, et al. Percutaneousvertebroplasty and pulmonary cement embolism: results from VERTOS II. AJNR Am J Neuroradiol 2010;31:1451–3.
[17] Wang JS, Diaz J, Sabokbar A, Athanasou N, Kjellson F, Tanner KE, et al. In vitro and *in vivo* biological responses to a novel radiopacifying agent for bone cement. J R Soc Interface 2005;2:71–8.
[18] Sabokbar A, Fujikawa Y, Murray DW, Athanasou N. Radiopaque agents in bone cement increase bone resorption. J Bone Jt Surg Br 1997;79:129–34.
[19] Artola A, Gurruchaga M, Vázquez B, San Román J, Goñi I. Elimination of barium sulphate from acrylic bone cements. Use of two iodine-containing monomers. Biomaterials 2003;24:4071–80.
[20] Boelen EJ, Lewis G, Xu J, Slots T, Koole LH, van Hooy-Corstjens CS. Evaluation of a highly-radiopaque iodine-containing acrylic bone cement for use in augmentation of vertebral compression fractures. J Biomed Mater Res A 2008 Jul;86(1):76–88.
[21] Zaharia C, Zecheru T, Moreau MF, Pascaretti-Grizon F, Mabilleau G, Marculescu B, et al. Chemical structure of methylmethacrylate-2-[2',3',5'-triiodobenzoyl]oxoethyl methacrylate copolymer, radio-opacity, in vitro and *in vivo* biocompatibility. Acta Biomater 2008;4:1762–9.
[22] Vaca A, Teixidor F, Kivekäs R, Sillanpää R, Viñas C. A solvent-free regioselective iodination route of ortho-carboranes. Dalton Trans 2006;41:4884–5.
[23] Srivastava RR, Hamlin DK, Wilbur DS. Synthesis of highlyiodinatedicosahedral mono- anddicarboncarboranes. J Org Chem 1996;61:9041–4.
[24] Barberà G, Vaca A, Teixidor F, Sillanpää R, Kivekäs R, Vinas C. Designed synthesis of new orthocarborane derivatives: from mono- to polysubstituted frameworks. Inorg Chem 2008;47:7309–16.
[25] Teixidor F, Barberà G, Viñas C, Sillanpää R, Kivekäs R. Synthesis of boron-iodinated *o*-carborane derivatives. Water stability of the periodinatedmonoproticsalt. Inorg Chem 2006;45:3496–8.
[26] Barth RF, Coderre JA, Vicente MGH, Blue ET. Boron neutron capturetherapy:current status andfutureprospects. Clin Cancer Res 2005;11:3987–4002.
[27] Valliant JF, Guenther KJ, King AS, Morel P, Schaffer P, Sogbein OO, et al. The medicinalchemistry of carboranes. CoordChemRev 2002;232:173–230.

[28] Endo Y, Iijima T, Yamakoshi Y, Yamaguchi M, Fukasawa H, Shudo KJ. Potent estrogenicagonistsbearingdicarba-closo-dodecaborane as a hydrophobic-pharmacophore. J Med Chem 1999;42:1501–4.
[29] Ohta K, Iijima T, Takahashi H, Hashimoto Y, Endo Y. Novelretinoid X receptor (RXR) antagonist having a dicarba-closo-dodecaborane as a hydrophobicmoiety. Bioorg Med Chem Lett 2004;14:5913–8.
[30] Armstrong AF, Valliant JF. The bioinorganic and medicinal chemistry of carboranes: from new drug discovery to molecular imaging and therapy. Dalton Trans 2007;38:4240–51.
[31] Fujii S, Hashimoto Y, Suzuki T, Ohtac S, Endo Y. A new class of androgen receptor antagonists bearing carborane in place of a steroidal skeleton. Bioorg Med Chem Lett 2005;15:227–30.
[32] Aldenhoff YB, Kruft MA, Pijpers AP, van der Veen FH, Bulstra SK, Koole LH. Stability of radiopaque iodine-containing biomaterials. Biomaterials 2002;23:881–6.
[33] http://home.megapass.co.kr/~dooleekc/tech/cure/TrigonoxC.pdf.
[34] Fassina L, Visai L, Asti L, Benazzo F, Speziale P, Tanzi, et al. Calcified matrix production by SAOS-2 cells inside a polyurethane porous scaffold, using a perfusion bioreactor. Tissue Eng 2005;11:685–700.
[35] Poole CA, Brookes NH, Gilbert RT, Beaumont BW, Crowther A, Scott L, et al. Detection of viable and non-viable cells in connective tissue explants using the fixable fluoroprobes 5-chloromethylfluorescein diacetate and ethidium homodimer-1. Connect Tissue Res 1996;33:233–41.
[36] Stoddart MJ, Furlong PI, Simpson A, Richards RG. A comparison of non-reactive methods for assessing viability in ex vivo cultured cancellous bone: technical note. Eur Cell Mater 2006;12:16–25.
[37] "Bone Cements", Berlin Heidelberg New York. Springer Verlag; 2000. p. 142–144.
[38] Hermanek S. Boron-11 NMR spectra of boranes, main-group heteroboranes, and substituted derivatives. Factors influencingchemicalshifts of skeletalatoms. Chem Rev 1992;92:325–62.
[39] Tiritiris I, Schleid T, Muller K. Solid-state NMR studies on ionic Closo-dodecaborates. Appl Magn Reson 2007;32:459–81.

DOI: 10.1002/anie.201105668

Conducting Materials

Stepwise Sequential Redox Potential Modulation Possible on a Single Platform**

*Ariadna Pepiol, Francesc Teixidor, Reijo Sillanpää, Marius Lupu, and Clara Viñas**

In memory of Heribert Barrera i Costa

Electron transfer is fundamental to many processes of life, including oxygen binding, photosynthesis, and respiration.[1] All organisms obtain energy by transferring electrons from an electron donor to an electron acceptor.[2] For example, the electron-transport chain in photosynthesis is remarkable.[3] In this work we show the first case of an artificial energetically favorable (downhill) sequence having well-defined, characterized, and structurally similar individual electron donors and acceptors made from a common frame. This example was made possible by using a metallacarborane cluster. There has been interest in producing systems with similar characteristics in highly predominant electroactive frameworks such as ferrocene (Fc), C_{60}, or perylene diimide.[4] The results have been, however, very limited.[5]

In the early 1970s, it was realized that the geometry of boron clusters is related to the number of electron pairs available for bonding.[6] The electronic and structural relationship between boron clusters having a common number of atoms in the cluster is shown in Scheme 1 for the case in which there are 11 vertices. These relationships suggest that the reversible transition from one cluster to its neighbor in Scheme 1 could be done through a redox process. This scenario, however, is seldom the case as there are frequently chemical reactions coupled to the redox process to make them irreversible.

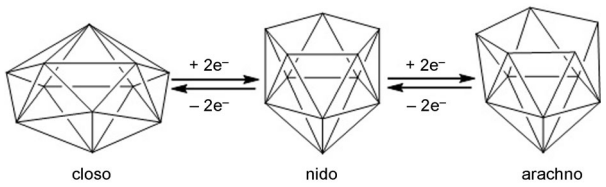

Scheme 1. Electronic and structural relationship for borane clusters having 11 vertices.

Ferrocene, C_{60}, and perylene diimide are the most predominant electroactive frameworks. C_{60} can be structurally compared with 1,2-, 1,7-, or 1,12-$C_2B_{10}H_{12}$ *closo*-carboranes because all are neutral icosahedral molecules. However, C_{60} requires much less energy to incorporate $2e^-$ than the carboranes, that is, −0.98 V for C_{60}^- and −1.37 V for C_{60}^{2-} (Fc^+/Fc)[7] versus −2.5 V (SCE)[8] (corresponding to −2.91 V (Fc^+/Fc)). Also, there is no appreciable change in the C_{60} structure after the incorporation of $4e^-$,[7] whereas the carboranes alter their shape dramatically.[6] The low reduction potential of C_{60} has made it very attractive as an electron acceptor in devices,[9] whereas carboranes have not found a parallel application. In contrast, C_{60} appeared as an excellent platform to generate a large sequential set of electron acceptors; this proposal, however, seems to be hardly attainable.[10] Therefore carboranes could not compete with C_{60} as electron acceptors. However, the B–X bond (X = halogen) in boron clusters is much more stable to reduction than the C–X bond in sp^2 carbon atoms and this could be used as an advantage for the redox tuning of boron clusters.[11]

If carboranes are geometrically analogous to C_{60}, metallacarboranes such as $[3,3'\text{-Co}(1,2\text{-}C_2B_9H_{11})_2]^-$, $[\mathbf{1}]^-$, are analogous to Fc. Therefore, to bypass the inevitable relationship between the structure and the number of electron pairs in boron clusters, and to benefit from the strength of the B–X bond, we focused our attention on the less severe electron regulated metallacarboranes, and in particular on $[\mathbf{1}]^-$.[12] Compound $[\mathbf{1}]^-$ shows three quasireversible waves in cyclic voltammetry at +1.18, −1.80, and −2.75 V (Fc^+/Fc) assigned to Co^{IV}/Co^{III}, Co^{III}/Co^{II}, and Co^{II}/Co^{I}, respectively.[13] The cathodic peaks indicate that high energy is required to introduce one and two electrons into the system, but this energy could be lowered given that B–X bonds can be produced and that their presence in the cluster could really make the cathodic peaks more positive. This assumption was supported by the $E_{1/2}(Co^{III}/Co^{II})$ values of $[\mathbf{1}]^-$ in acetonitrile: −1.80 V for $[\mathbf{1}]^-$, and −1.48 V (Fc^+/Fc) for $[3,3'\text{-Co}(8\text{-Cl-}1,2\text{-}C_2B_9H_{10})_2]^-$. These two anions can be made with good purity and their $E_{1/2}(Co^{III}/Co^{II})$ values calculated.[13] The large number of boron atoms in the cluster offer the possibility of multiple B–X substitutions that could gradually and systematically decrease the $E_{1/2}(Co^{III}/Co^{II})$ value. However, no other chlorinated derivative of $[\mathbf{1}]^-$ is available in the pure form. The commonly described $[\text{Co}(8,9,10\text{-}Cl_3\text{-}1,2\text{-}C_2B_9H_8)_2]^-$, ($Cl_6$-$[\mathbf{1}]^-$) is indeed a mixture of penta-, hexa-, and heptachlorinated $[\mathbf{1}]^-$ derivatives.[14] No higher chlorinated derivatives of

[*] A. Pepiol, Prof. F. Teixidor, M. Lupu, Prof. C. Viñas
Institut de Ciència de Materials de Barcelona (ICMAB-CSIC)
Campus UAB, 08193 Bellaterra (Spain)
E-mail: clara@icmab.es
Prof. R. Sillanpää
Department of Chemistry, University of Jyväskylä
40014 Jyväskylä (Finland)

[**] This work was supported by the Generalitat de Catalunya (2009/SGR/00279) and the Ministerio de Ciencia e Innovación (CTQ2010-16237). A. Pepiol thanks the CSIC for a JAE grant and M. Lupu thanks the MICINN for a FPU grant. A. Pepiol and M. Lupu are enrolled in the UAB PhD program. We thank Mireia Ruis and Elena Marchante for performing the electrochemical tests.

Supporting information for this article is available on the WWW under http://dx.doi.org/10.1002/anie.201105668.

$[\mathbf{1}]^-$ had been described until recently when the whole series from mono to dodecachlorinated $[\mathbf{1}]^-$ derivatives was reported.[14]

Each new dehydrochlorination step of $[\mathbf{1}]^-$ brought about a decrease of the $E_{1/2}(Co^{III}/Co^{II})$ value near 0.1 V. Thus for ten Cl substitutions, $[Co(C_2B_9H_6Cl_5)_2]^-$ (Cl_{10}-$[\mathbf{1}]^-$), an $E_{1/2}(Co^{III}/Co^{II})$ near −0.8 V (Fc^+/Fc) was expected, and this was confirmed by experiment.[14] The described $E_{1/2}$ tunability makes $[\mathbf{1}]^-$ a unique platform for achieving the targeted $E_{1/2}$ values. This valuable finding, however, faces a problem: it is impossible to get pure samples of each independent chlorinated species in practical quantities. Each sample was made of four to five components.[14] This problem precluded their use in devices, and also generated some controversy as the $E_{1/2}(Co^{III}/Co^{II})$ values of the different compounds could not be measured independently. To progress on the stepwise redox potential diminution we moved to the iodinated species of $[\mathbf{1}]^-$. The synthesis of $[3,3'\text{-}Co(8\text{-}I\text{-}1,2\text{-}C_2B_9H_{10})(1',2'\text{-}C_2B_9H_{11})]^-$ (I-$[\mathbf{1}]^-$),[15] $[3,3'\text{-}Co(8\text{-}I\text{-}C_2B_9H_{10})_2]^-$ (I_2-$[\mathbf{1}]^-$),[16] and $[3,3'\text{-}Co(8,9,10\text{-}I_3\text{-}1,2\text{-}C_2B_9H_8)_2]^-$ (I_6-$[\mathbf{1}]^-$)[13c] in pure form and in practical quantities had been described. Also their $E_{1/2}(Co^{III}/Co^{II})$ values had been measured,[13,15,17] but no relationship between them had been highlighted. To prove the $E_{1/2}(Co^{III}/Co^{II})$ dependence upon the number of iodine substituents in the platform, $[3,3'\text{-}Co(9,10\text{-}I_2\text{-}1,2\text{-}C_2B_9H_9)_2]^-$ (I_4-$[\mathbf{1}]^-$) and $[3,3'\text{-}Co(8,9,10,12\text{-}I_4\text{-}1,2\text{-}C_2B_9H_7)_2]^-$ (I_8-$[\mathbf{1}]^-$) needed to be prepared. Considering the stepwise lowering of the $E_{1/2}(Co^{III}/Co^{II})$ value with added chlorine substituents on $[\mathbf{1}]^-$, and the $E_{1/2}(Co^{III}/Co^{II})$ values for I-$[\mathbf{1}]^-$, I_2-$[\mathbf{1}]^-$, and I_6-$[\mathbf{1}]^-$, it was expected that with I_8-$[\mathbf{1}]^-$ it would be possible to reach $E_{1/2}(Co^{III}/Co^{II})$ values in the −0.6 to −0.8 V (Fc^+/Fc) range. Indeed this was the case. The synthesis of I_8-$[\mathbf{1}]^-$ was possible by using the steps and reaction conditions indicated in Scheme 2.

I_8-$[\mathbf{1}]^-$ is the highest iodinated derivative of $[\mathbf{1}]^-$ reported so far and can be made in useful quantities as the NMe_4^+ salt for its possible applications. Its ^{11}B and ^1H NMR spectroscopy, MALDI-TOF and EA data (see the Supporting Information) confirmed its structure, along with the structure from the X-ray analysis that is presented in Figure 1.[18]

The X-ray crystal structure of the intermediate $[HNMe_3][1,5,6,10\text{-}I_4\text{-}7,8\text{-}C_2B_9H_8]$ shown in Figure 2,[18] was also solved. In a similar way the missing $[NMe_4][4,5\text{-}I_2\text{-}7,8\text{-}C_2B_9H_{10}]$ and $[NMe_4][3,3'\text{-}Co(9,10\text{-}I_2\text{-}1,2\text{-}C_2B_9H_9)_2]$ have also been synthesized. See reaction conditions and steps needed in Scheme 3 (R = H). The $E_{1/2}(Co^{III}/Co^{II})$ values for $[\mathbf{1}]^-$,I-$[\mathbf{1}]^-$, I_2-$[\mathbf{1}]^-$, I_4-$[\mathbf{1}]^-$, I_6-$[\mathbf{1}]^-$, and I_8-$[\mathbf{1}]^-$ were experimentally determined by

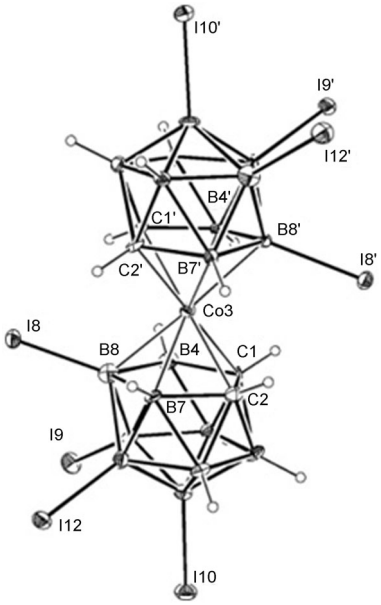

Figure 1. Ortep plot of $[3,3'\text{-}Co(8,9,10,12\text{-}I_4\text{-}1,2\text{-}C_2B_9H_7)_2]^-$ anion (I_8-$[\mathbf{1}]^-$). Thermal ellipsoids are shown at 30% probability. Selected bond lengths [Å] and angles [°]: C1–C2 1.64(2), C1′–C2′ 1.68(2), Co–C from 2.00(1) to 2.05(1), Co–B from 2.09(1) to 2.17(1), I–B from 2.15(2) to 2.23(2), C1-Co3-C2′ 179.0(5), C1′-Co3-C2 179.5(5) C1-Co3-C1′ 132.1(4) and C2–Co3–C2′ 131.4(5).

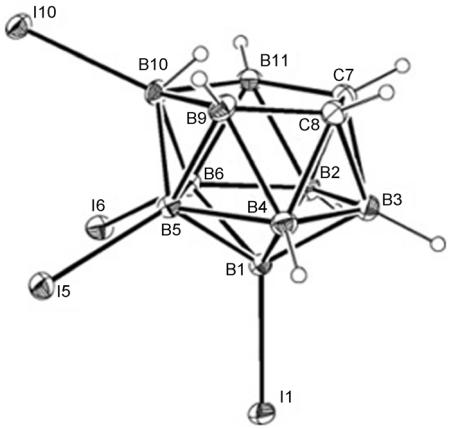

Figure 2. Ortep plot of $[1,5,6,10\text{-}I_4\text{-}7,8\text{-}nido\text{-}C_2B_9H_8]^-$ anion. Thermal ellipsoids are shown at 30% probability. Selected bond lengths [Å] and angles [°]: C7-C8 1.533(9), I–B from 2.183(6) to 2.197(6), C7-C8-B9 113.3(5), C8–C7 B11-114.8(5) and B9-B10-B11 102.1(5).

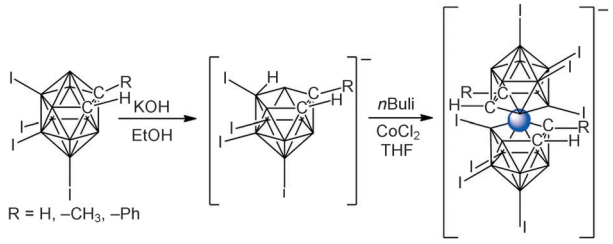

Scheme 2. Synthesis of I_8-$[\mathbf{1}]^-$ and its $C_{clusters}$ derivatives (R = H, Me, Ph). THF = tetrahydrofuran.

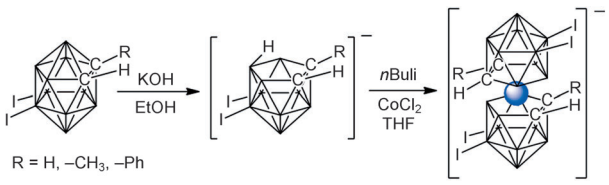

Scheme 3. Synthesis of I_4-$[\mathbf{1}]^-$ and its $C_{clusters}$ derivatives (R = H, Me, Ph).

cyclic voltammetry and their values versus Fc^+/Fc are tabulated in Table 1.

A plot of the $E_{1/2}(Co^{III}/Co^{II})$ values against the number of iodine substituents on the platform is given in the Supporting Information. Each new iodine averages a shift of +0.133 V, thus the not yet produced $[Co(C_2B_9H_6I_5)_2]^-$ would have an $E_{1/2}(Co^{III}/Co^{II})$ value near −0.48 V (Fc^+/Fc). Therefore just by the addition of ten iodine substituents on boron in $[\mathbf{1}]^-$ the $E_{1/2}(Co^{III}/Co^{II})$ value drops from −1.80 V to −0.48 V (Fc^+/Fc).

Table 1: $E_{1/2}$ data for I_n-$[\mathbf{1}]^-$ (n = 0, 1, 2, 4, 6, 8) and $C_{clusters}$ derivatives.[a]

Compound	$E_{1/2}$ vs. Fc^+/Fc [V]	Compound	$E_{1/2}$ vs. Fc^+/Fc [V]
$[\mathbf{1}]^-$	−1.80	Me_2I_4-$[\mathbf{1}]^-$	−1.00
I-$[\mathbf{1}]^-$	−1.50	I_6-$[\mathbf{1}]^-$	−0.82
I_2-$[\mathbf{1}]^-$	−1.32	I_8-$[\mathbf{1}]^-$	−0.68
I_4-$[\mathbf{1}]^-$	−1.15	Ph_2I_8-$[\mathbf{1}]^-$	−0.61
Ph_2I_4-$[\mathbf{1}]^-$	−1.03	Me_2I_8-$[\mathbf{1}]^-$	−0.54

[a] Cyclic voltammogram responses were recorded at the glassy carbon electrode in MeCN $5x10^{-3}$ I_n-$[\mathbf{1}]^-$ using $[NBu_4][PF_6]$ (0.1 M) as the supporting electrolyte. The electrochemical cell contained $Ag/AgCl/KCl_{sat}$ as the reference electrode and a platinum wire as the auxiliary electrode. All experiments were performed at room temperature. The potential values have been referenced to the Fc^+/Fc couple [$E_{1/2}(Fc^+/Fc)$ = 0.64 V versus a standard hydrogen electrode (SHE)].

This is an unprecedented finding that allows the tuning of the redox potential of a platform with a minor change in its shape and dimensions so as to adjust its $E_{1/2}$ value to a specific purpose. To compare the $E_{1/2}(Co^{III}/Co^{II})$ value after substitution on C or on B anions $[3,3'\text{-}Co(1\text{-}Ph\text{-}9,10\text{-}I_2\text{-}1,2\text{-}C_2B_9H_8)_2]^-$ (Ph_2I_4-$[\mathbf{1}]^-$), $[3,3'\text{-}Co(1\text{-}Me\text{-}9,10\text{-}I_2\text{-}1,2\text{-}C_2B_9H_8)_2]^-$ (Me_2I_4-$[\mathbf{1}]^-$), $[3,3'\text{-}Co(1\text{-}Ph\text{-}8,9,10,12\text{-}I_4\text{-}1,2\text{-}C_2B_9H_6)_2]^-$ (Ph_2I_8-$[\mathbf{1}]^-$), and $[3,3'\text{-}Co(1\text{-}Me\text{-}8,9,10,12\text{-}I_4\text{-}1,2\text{-}C_2B_9H_6)_2]^-$ (Me_2I_8-$[\mathbf{1}]^-$) were synthesized using similar strategies as those used for I_4-$[\mathbf{1}]^-$ and I_8-$[\mathbf{1}]^-$. Their $E_{1/2}(Co^{III}/Co^{II})$ values are tabulated in Table 1. The first noticeable point is that the $C_{cluster}$ substitution produces an anodic shift as it does on B, but it is smaller; second, the effect of Me, near 0.07, is larger than the effect of Ph, in the range from +0.04 to +0.06.

Once it had been demonstrated that $[\mathbf{1}]^-$ allows a stepwise tunable redox potential system, it was our goal to observe if the latter tunable property transcended into a different observable one.

We chose the growth of polypyrrole (PPy) to explore this possibility. The motivation of this study was the potential use of conducting polymers for practical applications in active areas of research in fields as varied as rechargeable batteries, electrochromic displays, information memory, antistatic materials, anticorrosives, electrocatalysis, sensors, electromechanical devices, infrared polarizers, radars, and biomedical applications, among others.[19]

Besides, it was already known that $[\mathbf{1}]^-$ facilitated the electrochemical growth of PPy from pyrrole, thus producing an extraordinary overoxidation resistance to the material.[20] The electrochemical synthetic procedure we have used for PPy doped with the iodinated derivatives of $[\mathbf{1}]^-$ consists of applying a linear potential ramp versus time to a solution of pyrrole and the doping anion, up to a certain oxidizing voltage.[21] The current is measured between the working electrode and the reference electrode. Once the oxidizing potential target is reached, the polarity of the working electrode is reversed to a specified reducing voltage. This cycle is applied repeatedly and in each cycle a higher intensity is observed, thus indicating the growth of the material.

The synthetic procedure is similar to that of the cyclic voltammetry electrochemical method of a reversible system, and in favorable cases produces an oxidation peak that has a similar shape to the reduction peak. As can be seen in Figure 3 for PPy/$[I_n\text{-}\mathbf{1}]^-$, both the forward and reverse scans produce current peaks. The separation between the anodic and cathodic peaks is, however, much larger than the equivalent separation in an electrochemical reversible system.

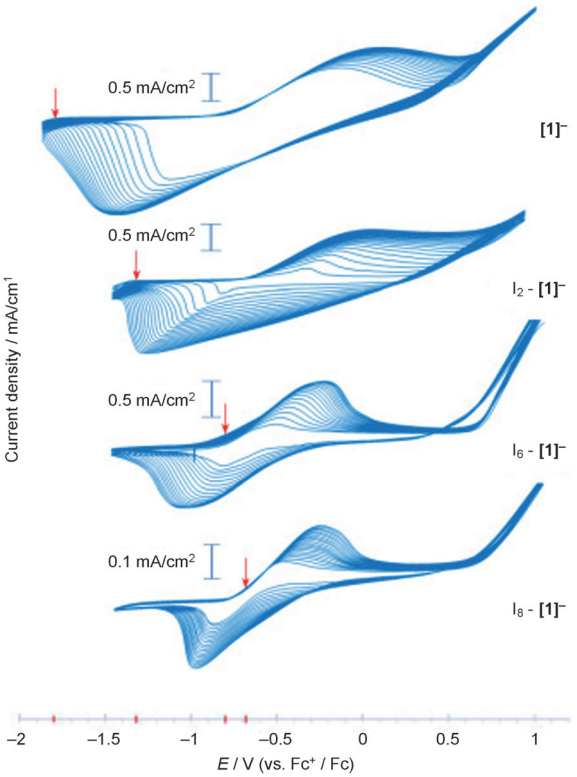

Figure 3. Growth curves of PPy doped with I_n-$[\mathbf{1}]^-$ (n = 0, 2, 6, 8). The red arrows correspond to the $E_{1/2}$ value for I_n-$[\mathbf{1}]^-$.

One could argue that the obvious difference between the PPy/$[I_n\text{-}\mathbf{1}]^-$ growth traces is due to the different shape of the anions. This difference should not be the case as it has been demonstrated that the geometry and apparent size of the boron clusters with different numbers of like substituents is strongly influenced by the type of boron cluster framework. This influence is observed in the ease of the formation of solid solutions by different types of boron clusters. For instance, a mixture of 9-X-12-Y-3,4,5,6,7,8,10,11-Me_8-1,2-$C_2B_{10}H_2$, in which (X,Y) are (I,Cl), (I,H), (H,H), and (H,Cl) combines into a single crystal to produce an average formula of 9-$I_{0.707}H_{0.293}$-12-$Cl_{0.566}H_{0.434}$-3,4,5,6,7,8,-10,11-Me_8-1,2-$C_2B_{10}H_2$.[21] Other examples are found in $[PdBr_{1.133}Cl_{0.867}$-

$(1,2\text{-}(PPh_2)_2\text{-}1,2\text{-}C_2B_{10}H_{10})]\cdot CH_2Cl_2$ and $[PdBrCl_{0.541}Me_{0.459}\text{-}(1,2\text{-}(PPh_2)_2\text{-}1,2\text{-}C_2B_{10}H_{10})]\cdot CH_2Cl_2$, which were made from $[PdBr_2(1,2\text{-}(PPh_2)_2\text{-}1,2\text{-}C_2B_{10}H_{10})]$, $[PdCl_2(1,2\text{-}(PPh_2)_2\text{-}1,2\text{-}C_2B_{10}H_{10})]$, $[PdBrCl(1,2\text{-}(PPh_2)_2\text{-}1,2\text{-}C_2B_{10}H_{10})]$, and $[PdBrMe(1,2\text{-}(PPh_2)_2\text{-}1,2\text{-}C_2B_{10}H_{10})]$ mixtures.[22]

Therefore, it shall be assumed that any differences in the growth of PPy doped with derivatives of the platform $[3,3'\text{-}Co(1,2\text{-}C_2B_9H_{11})_2]^-$ will depend little on the number of iodine substituents and largely on their $E_{1/2}$ redox potential. Figure 3 shows the growth of four PPy/I_n-[**1**]$^-$ conducting organic polymers with $n=0$, 2, 6, and 8 and with the $E_{1/2}$ value for I_n-[**1**]$^-$ $=-1.80$ ($n=0$), $-1{,}32$ ($n=2$), -0.82 ($n=6$), and -0.68 ($n=8$) V (Fc^+/Fc). The $E_{1/2}$ potentials for I_n-[**1**]$^-$ are more negative than the cathodic peak for PPy/[**1**]$^-$ and PPy/I_2-[**1**]$^-$, and in between the cathodic and anodic peaks for PPy/I_6-[**1**]$^-$ and PPy/I_8-[**1**]$^-$. The red arrows in Figure 3 indicate $E_{1/2}$ value for the doping of I_n-[**1**]$^-$.

The traces for the couple PPy/[**1**]$^-$ and PPy/I_2-[**1**]$^-$, on one side and the couple PPy/I_6-[**1**]$^-$, and PPy/I_8-[**1**]$^-$, on the other are very different. Notably, PPy/I_6-[**1**]$^-$ and PPy/I_8-[**1**]$^-$ display: 1) a much smaller separation between the anodic and cathodic peaks, 2) more slender peaks, and 3) have a well-defined plateau between the anodic peak and the slope starting between 0.65 and 1 V. All these differences are related to how close the $E_{1/2}$ value for I_n-[**1**]$^-$ is to the gravity center between the anodic and cathodic peaks, $(E_a-E_c)/2$. Remarkably, the gravity center for the anodic and cathodic peaks is $-0.63(2)$ V (Fc^+/Fc) for all four PPy/I_n-[**1**]$^-$ materials ($n=0$, 2, 6, 8). As seen in Figure 3 the effect of the electroactive anion, all other conditions being equal, on the growth of the PPy/I_n-[**1**]$^-$ material is clear.

What are the implications of a predictable and accessible $E_{1/2}$ tunable platform? Our opinion is that the possibilities are numerous, mainly in nanoscience and molecular materials. They offer a unique opportunity to combine different, but highly compatible materials with different electron-transfer characteristics. At this moment we are studying the generation of electron-transfer-cascade materials made of thin layers, each with distinct electron-transfer characteristics. The [**1**]$^-$ platform, as a result of its high stability, availability, possibility for functionalization, and tunable electroactivity, offers a wide range of possibilities that are not encountered for other popular electroactive platforms.

Received: August 10, 2011
Published online: ■■ ■■, ■■■■

Keywords: cluster compounds · conducting materials · electron transport · iodine · redox chemistry

[1] R. E. Blankenship in *Molecular Mechanisms of Photosynthesis*, Blackwell Science, Oxford, **2002**, chap. 6–7.
[2] R. Cotterill, *Biophysics: An Introduction*, Wiley, Chichester, **2003**, chap. 9.
[3] a) A. Amunts, O. Drory, N. Nelson, *Nature* **2007**, *447*, 58–63; b) M. R. Wasielewski, *J. Org. Chem.* **2006**, *71*, 5051–5066; c) R. Lomoth, A. Magnuson, M. Sjödin, P. Huang, S. Styring, L. Hamarström, *Photosynth. Res.* **2006**, *87*, 25–40; d) J. H. Alstrum-Acevedo, M. K. Brennaman, T. J. Meyer, *Inorg. Chem.* **2005**, *44*, 6802–6827.
[4] a) Y. Araki, R. Chitta, A. S. D. Sandanayaka, K. Langewalter, S. Gadde, M. E. Zandler, O. Ito, F. D'Souza, *J. Phys. Chem. C* **2008**, *112*, 2222–2229; b) M. Morisue, D. Kalita, N. Haruta, Y. Kobuke, *Chem. Commun.* **2007**, 2348–2350; c) A. Sautter, B. K. Kaletaş, D. G. Schmid, R. Dobrawa, M. Zimine, G. Jung, I. H. M. van Stokkum, L. De Cola, R. M. Williams, F. Würthner, *J. Am. Chem. Soc.* **2005**, *127*, 6719–6729; d) T. Konishi, A. Ikeda, S. Shinkai, *Tetrahedron* **2005**, *61*, 4881–4899.
[5] a) A. Laiho, R. H. A. Ras, S. Valkama, J. Ruokolainen, R. Österbacka, O. Ikkala, *Macromolecules* **2006**, *39*, 7648–7653; b) Z. R. Hong, Z. H. Huang, X. T. Zeng, *Chem. Phys. Lett.* **2006**, *425*, 62–65; c) V. Shrotriya, J. Ouyang, R. J. Tseng, G. Li, Y. Yang, *Chem. Phys. Lett.* **2005**, *411*, 138–143; d) R. H. Xie, G. W. Bryant, G. Sun, T. Kar, Z. Chen, V. H. Smith, Jr., Y. Araki, N. Tagmatarchis, H. Shinohara, O. Ito, *Phys. Rev. B* **2004**, *69*, 201403.
[6] a) R. E. Williams, *Inorg. Chem.* **1971**, *10*, 210–214; b) K. Wade, *J. Chem. Soc. D* **1971**, 792–793; c) D. M. P. Mingos, *Nature Phys. Sci.* **1972**, *236*, 99–102; d) R. W. Rudolph, W. R. Pretzer, *Inorg. Chem.* **1972**, *11*, 1974–1978.
[7] L. Echegoyen, L. E. Echegoyen, *Acc. Chem. Res.* **1998**, *31*, 593–601.
[8] J. H. Morris, H. J. Gysling, D. Reed, *Chem. Rev.* **1985**, *85*, 51–76.
[9] a) T. C. Clarke, J. R. Durrant, *Chem. Rev.* **2010**, *110*, 6736–6767; b) S. Günes, H. Neugebauer, N. S. Saricifti, *Chem. Rev.* **2007**, *107*, 1324–1338; c) J. L. Segura, N. Martin, D. M. Guldi, *Chem. Soc. Rev.* **2005**, *34*, 31–47; d) J. Roncali, *Chem. Soc. Rev.* **2005**, *34*, 483–495; e) L. Sánchez, M. Sierra, N. Martín, A. J. Myles, T. J. Dale, J. Rebek, Jr., W. Seitz, D. M. Guldi, *Angew. Chem.* **2006**, *118*, 4753–4757; *Angew. Chem. Int. Ed.* **2006**, *45*, 4637–4641.
[10] a) M. Zheng, F. F. Li, Z. J. Shi, X. Gao, K. M. Kadish, *J. Org. Chem.* **2007**, *72*, 2538–2542; b) M. Carano, M. Marcaccio, F. Paolucci, P. Birkett, *Photochem. Photobiol. Sci.* **2006**, *5*, 1132–1136; c) F. Zhou, G. J. Van Berkel, B. T. Donovan, *J. Am. Chem. Soc.* **1994**, *116*, 5485–5486; d) A. A. Popov, I. E. Kareev, N. B. Shustova, E. B. Stukalin, S. F. Lebedkin, K. Seppelt, S. H. Strauss, O. V. Boltalina, L. Dunsch, *J. Am. Chem. Soc.* **2007**, *129*, 11551–11568.
[11] U. Páramo-Garcío, M. Ávila-Rodríguez, M. G. García-Jiménez, S. Gutiérrez-Granados, J. G. Ibáñez-Cornejo, *Electroanalysis* **2006**, *18*, 904–910.
[12] a) I. B. Sivaev, V. I. Bregadze, *Collect. Czech. Chem. Commun.* **1999**, *64*, 783–805; b) D. A. Rudakov, V. L. Shirokii, V. A. Knizhnikov, A. V. Bazhanov, E. I. Vecher, N. A. Maier, V. I. Potkin, A. N. Ryabtsev, P. V. Petrovskii, I. B. Sivaev, V. I. Bregadze, I. L. Eremenko, *Russ. Chem. Bull. Int. Ed.* **2004**, *53*, 2554–2557.
[13] a) L. Matel, R. Cech, F. Macasek, S. Hermanek, J. Plesek, *Radiochem. Radioanal. Lett.* **1978**, *35*, 241–246; b) L. Mátel, F. Macášek, P. Rajec, S. Heřmánek, J. Plešek, *Polyhedron* **1982**, *1*, 511–519; c) M. D. Mortimer, C. B. Knobler, M. F. Hawthorne, *Inorg. Chem.* **1996**, *35*, 5750–5751.
[14] P. Gonzalez-Cardoso, A. I. Stoica, P. Farràs, A. Pepiol, C. Viñas, F. Teixidor, *Chem. Eur. J.* **2010**, *16*, 6660–6665.
[15] I. Rojo, F. Teixidor, C. Viñas, R. Kivekäs, R. Sillanpää, *Chem. Eur. J.* **2003**, *9*, 4311–4323.
[16] I. Rojo, F. Teixidor, C. Viñas, R. Kivekäs, R. Sillanpää, *Organometallics* **2003**, *22*, 4642–4646.
[17] M. Corsini, F. Fabrizi de Biani, P. Zanello, *Coord. Chem. Rev.* **2006**, *250*, 1351–1372.
[18] See the Supporting Information for details for the X-ray structure analyses. CCDC 837895 ($[HNMe_3][1,5,6,10\text{-}I_4\text{-}7,8\text{-}C_2B_9H_8]$) and 837896 ($[NMe_4][3,3'\text{-}Co(8,9,10,12\text{-}I_4\text{-}1,2\text{-}C_2B_9H_7)_2]$) contain the supplementary crystallographic data for this paper. These data can be obtained free of charge from The

Cambridge Crystallographic Data Centre via www.ccdc.cam.ac.uk/data_request/cif.

[19] a) D. D. Ateh, H. A. Navsaria, P. Vadgama, *J. R. Soc. Interface* **2006**, *3*, 741 – 752; b) S. F. Michael, B. A. Deore in *Self-Doped Conducting Polymers* (Eds.: Wiley-*Blackwell)*, Blackwell Science, Oxford, **2007**, p. 338.

[20] a) C. Masalles, J. Llop, C. Viñas, F. Teixidor, *Adv. Mater.* **2002**, *14*, 826 – 829; b) C. Masalles, S. Borrós, C. Viñas, F. Teixidor, *Adv. Mater.* **2002**, *14*, 449 – 452.

[21] F. Teixidor, G. Barberà, A. Vaca, R. Kivekäs, R. Sillanpää, J. Oliva, C. Viñas, *J. Am. Chem. Soc.* **2005**, *127*, 10158 – 10159.

[22] S. Paavola, F. Teixidor, C. Viñas, R. Kivekäs, *J. Organomet. Chem.* **2002**, *657*, 187 – 193.

Communications

Conducting Materials

A. Pepiol, F. Teixidor, R. Sillanpää, M. Lupu, C. Viñas* ——— ■■■■–■■■■

Stepwise Sequential Redox Potential Modulation Possible on a Single Platform

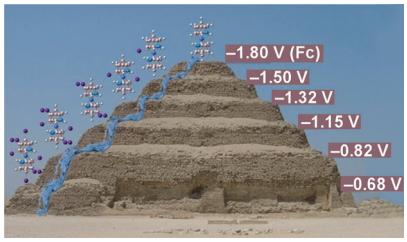

Step by step: The cluster [3,3′-Co(1,2-$C_2B_9H_{11})_2]^-$ is an excellent platform for making a stepwise tunable redox potential system by dehydroiodination. With the addition of up to eight iodine substituents (purple; see picture), there is a fall in the $E_{1/2}(Co^{III}/Co^{II})$ value from −1.80 V to −0.68 V (vs. Fc^+/Fc; Fc = ferrocene). A practical application of this tunability has been observed in the growth of polypyrrole.

SUPPORTING INFORMATION

Stepwise Sequential Redox Potential Modulation is Possible in a Single Platform

*Ariadna Pepiol, Francesc Teixidor, Reijo Sillanpää, Marius Lupu and Clara Viñas**

A. Pepiol, M. Lupu, Prof. F. Teixidor, Prof. C. Viñas; Institut de Ciència de Materials de Barcelona (ICMAB-CSIC); Campus UAB, 08193 Bellaterra (Spain); Fax: (+34)935805729; E-mail: clara@icmab.es.

Prof. R. Sillanpää; Department of Chemistry, University of Jyväskylä, FIN-40014, Finland

Experimental Section

Materials and instrumentation: All metallacarborane anions prepared are air and moisture stable. All manipulations were carried out under inert atmosphere. 1,2-dimethoxyethane (DME) and THF were distilled from sodium benzophenone prior to use. Reagents were obtained commercially and used as purchased. 1,2-*closo*-$C_2B_{10}H_{12}$, 1-Me-1,2-*closo*-$C_2B_{10}H_{12}$, 1-Ph-1,2-*closo*-$C_2B_{10}H_{12}$ were obtained from Katchem. [3,3'-Co(8-I-1,2-$C_2B_9H_{10}$)(1',2'-$C_2B_9H_{11}$)]$^-$, (I-[**1**]$^-$); [1] [3,3'-Co(8-I-$C_2B_9H_{10}$)$_2$]$^-$, (I$_2$-[1]$^-$);[2] 3,3'-Co(8,9,10-I_3-1,2-$C_2B_9H_8$)$_2$]$^-$, (I_6-[1]$^-$)[3] were synthesised as reported at the literature.

Elemental analyses were performed in our laboratory using a Carlo Erba EA1108 micro analyzer. IR spectra (ν, cm^{-1}; KBr pellets) were obtained on a Shimadzu FTIR-8300 spectrophotometer. The ^{1}H- and ^{1}H{^{11}B}-NMR (300.13 MHz), ^{13}C{^{1}H}-NMR (75.47 MHz) and ^{11}B- and ^{11}B{^{1}H}-NMR (96.29 MHz) spectra were recorded on a Bruker ARX 300 instrument equipped with the appropriate decoupling accessories. All NMR spectra were performed in deuterated solvents at 22ºC. The ^{11}B- and ^{11}B{^{1}H}-NMR

shifts were referenced to external $BF_3 \cdot OEt_2$, while the ^1H, $^1H\{^{11}B\}$, and $^{13}C\{^1H\}$-NMR shifts were referenced to $SiMe_4$. Chemical shifts are reported in units of parts per million downfield from reference, and all coupling constants in Hz. The mass spectra were recorded in the negative ion mode using a Bruker Biflex MALDI-TOF-MS [N_2 laser; λ_{exc} 337 nm (0.5 ns pulses); voltage ion source 20.00 kV (Uis1) and 17.50 kV (Uis2)].

For voltammetric determinations, an electrochemical system, VoltaLab (Universal Electrochemical Laboratory System) interfaced with a PGZ100 potentiostat (Radiometer Analytical) and controlled by the VoltaMaster 4 software, was used. The electrochemical cell contained glassy carbon electrode as working electrode, a reference $Ag/AgCl/KCl_{sat}$ electrode and platinum wire as auxiliary electrode. The solutions were deaerated with analytical grade nitrogen at the start of each experiment to prevent oxygen interference. All experiments were performed at room temperature. All the potential values were referred to the Fc^+/Fc couple [$E_{1/2}$ (Fc^+/Fc) = 0.64 V *vs*. Standard Hydrogen Electrode (SHE)].

Synthesis of [$HNMe_3$][5,6-I_2-7,8-*nido*-$C_2B_9H_{10}$]. To a solution of KOH (177 mg, 3.15mmol) in degassed EtOH (4 mL) was added 9,12-I_2-1,2-*closo*-$C_2B_{10}H_{10}$ (250 mg, 0.63 mmol). The solution was refluxed for 5 h. After cooling to room temperature, the solvent was removed under reduced pressure and the solid residue was dissolved in 10 mL of water. The solution was neutralized with 1M HCl. Afterwards, an aqueous solution of [$HNMe_3$]Cl was added dropwise until no more precipitate was formed. The white solid was filtered and rinsed with water obtaining [$HNMe_3$][5,6-I_2-7,8-*nido*-$C_2B_9H_{10}$]. Yield: 230 mg (82%). Elemental analysis for $C_5B_9H_{20}I_2N$: calc: C 13.47, H 4.99, N 3.14; found C 13.13, H 4.51, N 2.97; IR (KBr): ν= 3024 (s; $\nu_s(C_c\text{-}H)$, 2970 (s; $\nu_s(C_{alkyl}\text{-}H)$, 2723 (vs; ν_s(N-H)), 2538 (s; ν_s(B-H)), 1465 cm^{-1} (s; $\nu_s(N\text{-}CH_3)$); ^1H NMR (300 MHz, [D_6]acetone, 25º, TMS): δ= 3.50-1.00 (s, 7H, B-*H*), 3.08 (s, 9H, $NH(CH_3)_3$), 2.32 (s, 1H, N-*H*), 2.08 (s, 2H, $C_{cluster}$-*H*), -2.00--2.20 ppm (s, 1H, B-H_{bridge}); $^1H\{^{11}B\}$ NMR (300 MHz, [D_6]acetone, 25º, TMS): δ= 3.08 (s, 9H, $NH(CH_3)_3$), 2.38 (br s, 3H, B-*H*), 2.32 (s, 1H, N-*H*), 2.08 (br s, 2H, $C_{cluster}$-*H*), 1.86 (s, 3H, B-*H*), 1.76 (s, 1H, B-*H*), 1.14 (s, 1H, B-*H*), 1.08 (d, $^1J(H_{bridge},H)$= 9.5 Hz, 1H, B-*H*), -2.15 ppm (d, $^1J(H_{bridge},H)$= 9.6 Hz, 1H, B-H_{bridge}); $^{13}C\{^1H\}$ NMR (75 MHz, [D_6]acetone, 25º, TMS): δ= 44.66 ppm (s, $HN(CH_3)_3$); ^{11}B RMN (96 MHz, [D_6]acetone, 25º, BF_3OEt_2): δ= -9.3 (d, ^1J(B,H)=

142 Hz, 2B, B(9,11)), -16.9 (d, ^1J(B,H)= 164 Hz, 1B, B(3), -21.1 (d, ^1J(B,H)=152 Hz, 2B, B(2,4)), -24.0 (br s, 2B, B(5,6)), -27.7 (d, ^1J(B,H)=137 Hz, 1B, B(10), -33.5 ppm (d, ^1J(B,H)= 147 Hz, 1B, B(1)); MALDI-TOF MS: *m/z* (%): 386.4 (70) $[M-1]^-$, 126.9 (100) $[I^-]$.

Synthesis of [$HNMe_3$][1,5,6,10-I_4-7,8-$C_2B_9H_8$]. To a solution of KOH (120 mg, 2.14 mmol) in degassed EtOH (4 mL) was added 8,9,10,12-I_4-1,2-$C_2B_{10}H_8$ (300 mg, 0.463 mmol). The solution was refluxed for 5 h. After cooling to room temperature, the solvent was removed under reduced pressure and the solid residue was dissolved in 10 mL of water. The solution was neutralized with 1 M HCl. Afterwards, an aqueous solution of [$HNMe_3$]Cl was added dropwise until no more precipitate was formed. The white solid was filtered and rinsed with water obtaining [$HNMe_3$][1,5,6,10-I_4-7,8-$C_2B_9H_8$]. Yield: 258 mg (80%). Elemental analysis for $C_5B_9H_{18}I_4N$: calc: C 8.61, H 2.60, N 2.01; found C 8.94, H 2.55, N 2.07; IR (KBr): ν= 3121 (s; ν_s(N-H)), 2567 cm^{-1} (s; ν_s(B-H)). ^{1}H NMR (300 MHz, [D_6]acetone, 25º, TMS): δ= 3.5–1.5 (br s, 5H, B*H*), 3.15 (s, 9H, C*H*$_3$NH), 2.50 (br s, 2H, $C_{cluster}$*H*), 0.4--0.6 ppm (br s, 1H, BH_{bridge}); ^{1}H{^{11}B} NMR (300 MHz, [D_6]acetone, 25º, TMS): δ= 3.15 (s, 9H, C*H*$_3$NH), 2.83 (br s, 3H, B*H*), 2.50 (br s, 2H, $C_{cluster}$*H*), 2.18 (s, 2H, B*H*), -0.09 ppm (br s, 1H, BH_{bridge}); ^{13}C{^{1}H} NMR (75 MHz, [D_6]acetone, 25º, TMS): δ= 54.1 ppm (s, *C*H$_3$NH); ^{11}B NMR (96 MHz, [D_6]acetone, 25º, BF_3OEt_2): δ= -7.0 (d, 2B, ^1J(B,H)= 148 Hz, B(9,11)*H*), -14.5 (d, 1B, ^1J(B,H)= 174 Hz, B(3)*H*), -16.4 (m, 4B, B(5,6)*I* + B(2,4)*H*), -33.9 ppm (s, 2B, B(1,10)*I*); MALDI-TOF MS: *m/z* (%): 636.9 (100) $[M]^-$, 126.9 (81) $[I^-]$.

Synthesis of [NMe_4][3,3'-Co-(9,12-I_2-1,2-*closo*-$C_2B_9H_9)_2$], I_4-[**1**]$^-$**.** To a stirring solution of [$HNMe_3$][5,6-I_2-7,8-$C_2B_9H_{10}$] (220 mg, 0.5 mmol) in THF (5mL) cooled to 0 ºC in an ice-water bath was added, drop wise, a solution of butyllithium in hexanes (0.63mL, 1.6M, 1.01mmol). The suspension was stirred for 1 hour at 0ºC at room temperature. Volatiles were removed under reduced pressure. The resulting solution was then transferred via a syringe onto solid $CoCl_2$ anhydrous (196mg, 1.5mmol), following which the reaction was heated to reflux for 15 minutes. After stirring for 1 hour, the solvent was removed under reduced pressure. Then, 10mL of diethyl ether and 10mL of water were added to the residue. The mixture was thoroughly shaken, and the two layers separated. The organic layer was separated from the mixture, and the aqueous layer was extracted with diethyl ether (3 x 10mL). The combined organic phase was dried over

$MgSO_4$, filtered and the solvent removed under reduced pressure. Afterwards, an aqueous solution of $[NMe_4]Cl$ was added drop wise until no more precipitate was formed. The orange solid was filtered and rinsed with water obtaining $[NMe_4][3,3'\text{-}Co\text{-}(9,12\text{-}I_2\text{-}1,2\text{-}\textit{closo}\text{-}C_2B_9H_9)_2]$. Yield: 160 mg (76%). Elemental analysis for $C_8B_{18}H_{30}CoI_4N$: calc: C 10.72, H 3.23, N 1.58; found C 10.65, H 3.23, N 1.55; IR (KBr): ν= 3020 (s; $\nu_s(C_{cluster}\text{-}H)$), 2950, 2921 (s; $\nu_s(C_{alkyl}\text{-}H)$, 2578 (vs; ν_s(B-H)), 1479 ($\nu_s(N\text{-}CH_3)$), 945 cm^{-1} (s; $\nu_{as}(CH_3)$). ^{1}H NMR (300 MHz, [D_6]acetone, 25º, TMS): δ= 4.44 (br s, 4H, $C_{cluster}H$), 4.0–1.5 (br s, 5H, B-*H*), 3.45 ppm (s, 12H, $N(CH_3)_4$); $^1H\{^{11}B\}$ NMR (300 MHz, [D_6]acetone, 25º, TMS): δ= 4.44 (br s, 4H, $C_{cluster}H$), 4.20 (br s, 2H, B-*H*), 3.63 (br s, 4H, B-*H*), 3.45 (s, 12H, $N(CH_3)_4$)), 3.36 (br s, 8H, B-*H*), 1.63 ppm (br s, 2H, B-*H*); $^{13}C\{^1H\}$ NMR (75 MHz, [D_6]acetone, 25º, TMS): δ= 68.35 ($C_{cluster}$), 55.29 ppm ($N(CH_3)_4$); ^{11}B NMR (96 MHz, [D_6]acetone, 25º, BF_3OEt_2): δ= 6.9 (d, ^1J(B,H)= 161 Hz, 2B, B(8,8'), 4.6 (d, ^1J(B,H)= 146 Hz, 2B, B(10,10'), -5.6 (d, 4B, ^1J(B,H)= 155 Hz, B(4,4',7,7'), -15.5 (d, 4B, ^1J(B,H)= 149 Hz, B(5,5',11,11')), -15.3 (br s, 4B, B(9,9',12,12')), -22.3 ppm (d, ^1J(B,H)= 167 Hz, 2B, B(6,6')); MALDI-TOF MS: *m/z* (%): 828.6 (100) $[M\text{-}1]^-$.

Synthesis of $[NMe_4][3,3'\text{-}Co\text{-}(8,9,10,12\text{-}I_4\text{-}1,2\text{-}\textit{closo}\text{-}C_2B_9H_7)_2]$. To a stirring solution of $[HN(CH_3)_3]$ [1,5,6,10-I_4-7,8-$C_2B_9H_8$] (125mg, 0.18mmol) in THF (5mL) cooled to 0 ºC in an ice-water bath was added, dropwise, a solution of butyllithium in hexanes (0.24mL, 1.6M, 0.38mmol). The suspension was stirred for 1 hour at 0ºC at room temperature. Volatiles were removed under reduced pressure. The resulting solution was then transferred via a syringe onto solid $CoCl_2$ anhydrous (73.5 mg, 0.56mmol), following which the reaction was heated to reflux for 15 minutes. After stirring for 1 hour, the solvent was removed under reduced pressure. Then, 10mL of diethyl ether and 10mL of water were added to the residue. The mixture was thoroughly shaken, and the two layers separated. The organic layer was separated from the mixture, and the aqueous layer was extracted with diethyl ether (3 x 10mL). The combined organic phase was dried over $MgSO_4$, filtered and the solvent removed under reduced pressure. Afterwards, an aqueous solution of $[NMe_4]Cl$ was added dropwise until no more precipitate was formed. The orange solid was filtered and rinsed with water obtaining $[NMe_4][3,3'\text{-}Co\text{-}(8,9,10,12\text{-}I_4\text{-}1,2\text{-}\textit{closo}\text{-}C_2B_9H_7)_2]$. Yield: 155 mg (73%). Elemental analysis for $C_5B_9H_{18}I_4N$: calc: C 8.61, H 2.60, N 2.01; found C 8.94, H 2.55, N 2.07; IR (KBr): ν= 3022 (s; $\nu_s(C_{cluster}\text{-}H)$), 2956, 2921 (s; $\nu_s(C_{alkyl}\text{-}H)$, 2621, 2584 (s; ν_s(B-H)),

1477 cm^{-1} (s; ν_s(N-C)); ^{1}H NMR (300 MHz, [D_6]acetone, 25º, TMS): δ= 5.12 (br s, 4H, $C_{cluster}H$), 3.5–1.5 (br s, 5H, B-*H*), 3.43 ppm (s, 12H, N(CH_3)$_4$)); ^{1}H{^{11}B} NMR (300 MHz, [D_6]acetone, 25º, TMS): δ=5.12 (br s, 4H, $C_{cluster}H$), 3.62 (br s, 4H, B-*H*), 3.43 (s, 12H, N(CH_3)$_4$), 2.75 (br s, 4H, B-*H*), 2.65 ppm (br s, 2H, B-*H*); ^{13}C{^{1}H} NMR (75 MHz, [D_6]acetone, 25º, TMS): δ= 60.78 ($C_{cluster}$), 55.32 ppm (N(CH_3)$_4$); ^{11}B NMR (96 MHz, [D_6]acetone, 25º, BF_3OEt_2): δ= -3.0 (d, ^1J(B,H)=170 Hz, 4B, B(4,4',7,7'), -5.1 (s, 2B, B(8,8')), -8.0 (s, 2B, B(10,10'), -10.9 (s, 4B, B(9,9',12,12')), -14.4 (d, ^1J(B,H)=157 Hz, 4B, B(5,5',11,11')), -21.6 ppm (d, ^1J(B,H)= 174 Hz, 2B, B(6,6')); MALDI-TOF MS: *m/z* (%): 1331.2 (100) $[M-1]^-$.

X-ray structure analysis

X-ray crystal structure analyses were performed by using an Enraf Nonius CCD area detector diffractometer with MoK$_\alpha$ radiation (λ = 0.71073 Å) equipped with an Oxford Cryostream low-temperature unit. The data sets were corrected for abortion using SADABS program [4] .The structures were solved with the program SIR97[5]; full-least-squares refinements on F^2 were performed with SHELXL97 [6] using anisotropic displacement parameters for most of the non-H atoms: two B atoms in [NMe_4][3,3'-Co-(8,9,10,12-I_4-1,2-*closo*-$C_2B_9H_7$)$_2$] were refinened isotropically. The hydrogen atoms were treated as riding atoms using the SHELX97 default parameters or their positional parameters were refined isotropically according to the riding model. All calculations and graphics were done at WinGX [7] platform.

[$HNMe_3$][1,5,6,10-I_4-7,8-$C_2B_9H_8$]: $C_5H_{18}B_9I_4N$, M_r = 697.09, crystal dimensions 0.20 x 0.18 x 0.16 mm^3, monoclinic, space group $P2_1/c$ (No.14), a = 8.1945(3), b = 14.7772(8), 16.3516(6) Å; α = 90, β =102.154(6), γ = 90 °, V = 1935.66(15) $Å^3$, Z = 4, T = 173(2), ρ_{calcd} = 2.392 g cm^{-3}, μ =6.42 mm^{-1}, 10297 reflections collected, 4218 unique reflections (R_{int} = 0.0336), 199 parameters, R1 = 0.0369 (I >2σ(I)); wR2 = 0.0748 (all data).

[NMe_4][3,3'-Co-(8,9,10,12-I_4-1,2-*closo*-$C_2B_9H_7$)$_2$]: $C_8H_{26}B_9CoI_8N$, M_r = 1405.01, crystal dimensions 0.12 x 0.10 x 0.08 mm^3, monoclinic, space group $P2_12_12_1$ (No.2), a = 9.5648(4), b = 14.0855(6), 26.9740(12) Å; α = β = γ = 90 °, V = 3634.1(3) $Å^3$, Z = 4, T = 173(2), ρ_{calcd} = 2.568 g cm^{-3}, μ = 7.275 mm^{-1}, 21164 reflections collected, 5943 unique reflections (R_{int} = 0.0501), 324 parameters, R1 = 0.0434 (I >2σ(I)); wR2 = 0.0729 (all data).

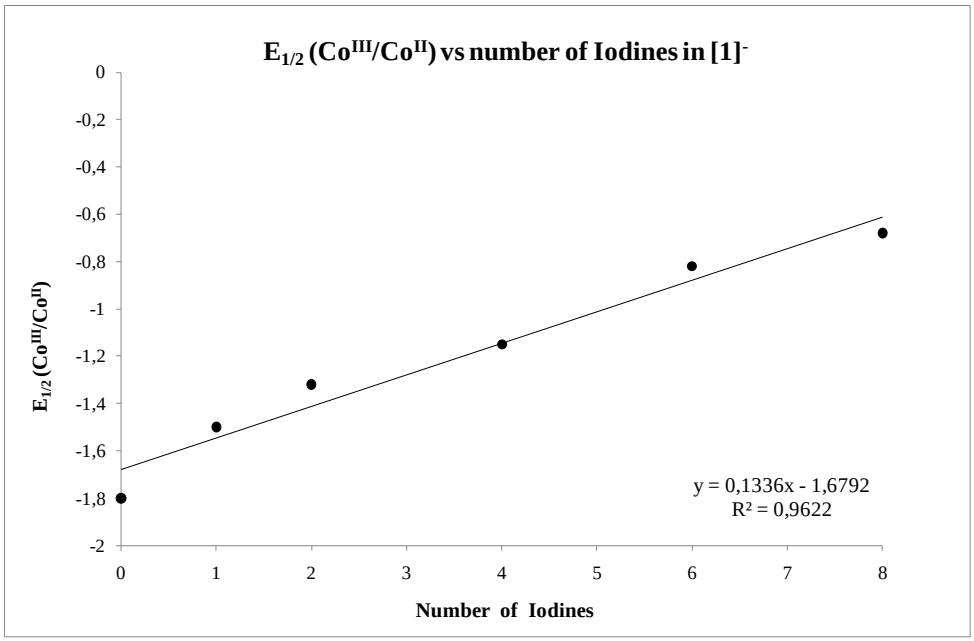

Figure S1. $E_{1/2}(Co^{III}/Co^{II})$ values with regard to the number of iodine substituents on the $[3,3'\text{-}Co(1,2\text{-}C_2B_9H_{11})_2]^-$ platform.

[1] I. Rojo, F. Teixidor, C. Viñas, R. Kivekäs, R. Sillanpää, *Chem.-Eur. J.*, **2003**, 9, 4311.

[2] I. Rojo, F. Teixidor, R. Kivekäs, R. Sillanpää, C. Vinas, *Organometallics*, **2003**, 22, 4642.

[3] M.D. Mortimer, C.B. Knobler, M.F. Hawthorne, *Inorg. Chem.* **1996**, *35*, 5750.

[4] G. M. Sheldrick *SADABS*, University of Göttingen, Germany, **2008**.

[5] A. Altomare, M. C. Burla, M. Camalli, G. L. Cascarano, C. Giacovazzo, A. Guagliardi, A.G. G. Moliterni, G. Polidori, R. Spagna, SIR 97: A new tool for crystal structure determination and refinement. *J. Appl. Cryst.* **1999**, *32*, 115-119.

[6] G. M. Sheldrick *Acta Crystallogr. , Sect. A: Found. Crystallogr.* **2008**, *A64*, 112-122.

[7] L. J. Farrugia, WinGX suite for small-molecule single-crystal crystallography. *J. Appl.Cryst*. **1999**, *32*, 837-838.

5.- ANNEX I

(Articles publicats anteriors a la

Comissió de Doctorat del setembre de 2011)

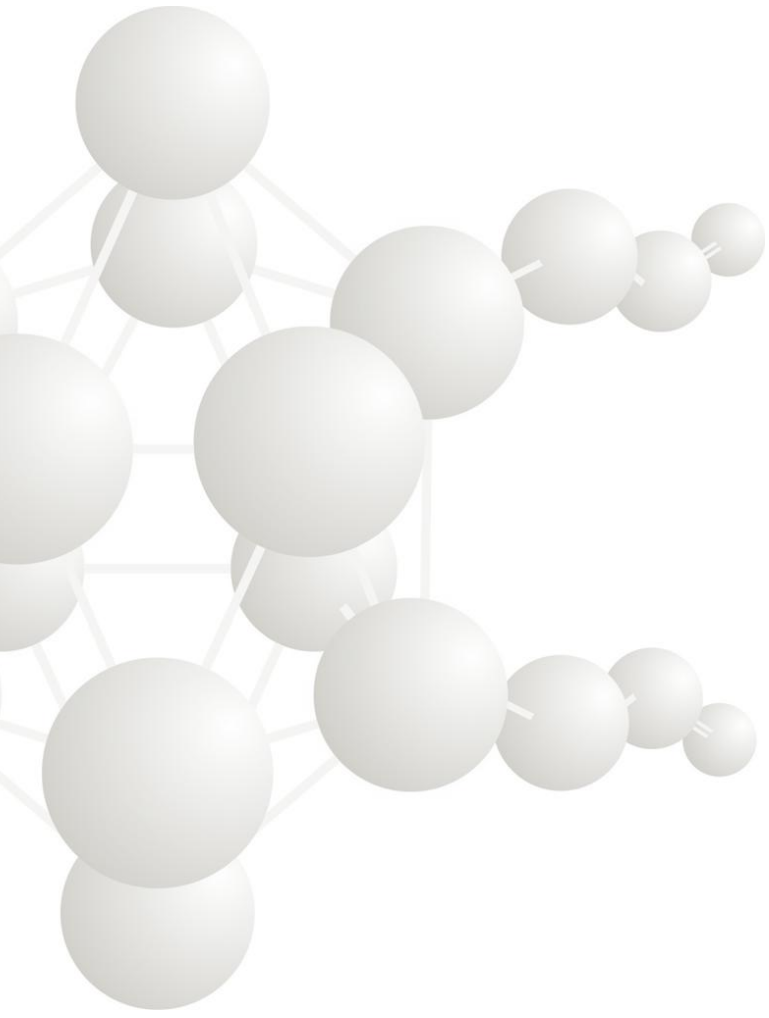

ORGANOMETALLICS
Article

Organometallics **2009,** *28,* 6031–6035 6031
DOI: 10.1021/om900443v

Investigations on the Reactivity of Li/Cl Phosphinidenoid Tungsten Complexes toward Various Iodine Compounds

Rainer Streubel,*,† Aysel Özbolat-Schön,† Maren Bode,† Jörg Daniels,† Gregor Schnakenburg,† Francesc Teixidor,‡ Clara Viñas,*,‡ Albert Vaca,‡ Ariadna Pepiol,‡ and Pau Farràs‡

†*Institut für Anorganische Chemie, Rheinische Friedrich-Wilhelms-Universität Bonn, Gerhard-Domagk-Strasse 1, 53121 Bonn, Germany, and* ‡*Institut de Ciència de Materials de Barcelona (CSIC), Campus de la UAB, E-08193 Bellaterra, Spain*

Received May 26, 2009

Reactivity studies of Li/Cl phosphinidenoid $W(CO)_5$ complexes **2a**,**b** toward various iodine compounds are reported. Transiently generated complexes **2a**,**b** yielded no selective reactions with 3-, 9-, and 9,12-diiodo *o*-carbaboranes **3a**−**c**, whereas clean transfer-iodination reaction occurred with *C*-iodo-substituted *o*-carbaboranes **3d**,**e**, thus giving chloro(iodo)phosphane complex **6a** in the case of **2a**. Complex **2a** was also reacted with iodo(phenyl)acetylene to yield complexes **6a**, **8**, and **9** in competing reactions. An independent pathway to chloro(iodo)phosphane complexes **6a**,**b** was reaction of complexes **2a**,**b** with elemental iodine at low temperature. All compounds were unambiguously characterized by elemental analysis, multinuclear NMR, IR, MS studies, and, in the case of **6a** and **9**, single-crystal X-ray diffraction.

Introduction

Carbenoids **I**[1] and silylenoids **II**[2] are versatile reactive intermediates in organic synthesis (Scheme 1). In contrast, phosphinidenoids **III** are still unknown, although some authors speculated[3] about their existence.

Recently, we reported the first examples of Li/X phosphinidenoid $W(CO)_5$ complexes (**IV**; X = F,[4] Cl[5]), stable in THF solution (X = F) up to 10 °C but unstable in the case of X = Cl above −40 °C, which decomposed upon warming to give mono- and dinuclear diphosphene complexes.[4,5] Reaction of the complex $[W(CO)_5(Li/ClPCH(SiMe_3)_2)]$ with methyl iodide yielded the corresponding *P*-Me-substituted phosphane complex and thus provided evidence for a nucleophilic, phosphanide complex-like reactivity. In addition, reactions of the same Li/Cl phosphinidenoid complex with π-systems such as dimethyl cyanamide, phenylacetylene, or benzaldehyde led to three-membered heterocycle complexes, which demonstrated a phosphinidene complex-like behavior. More recently, we obtained the first strong NMR spectroscopic evidence for complexes $[W(CO)_5(Li/FPCH(SiMe_3)_2)]$ and $[W(CO)_5(Li/ClPC_5Me_5)]$, although the bonding of lithium remained unclear. The latter complex also decomposed above −40 °C, giving a P,C-cage complex (cf. Scheme 2) comprising formally two phosphinidene complex units and revealing that one C_5Me_5 (= Cp*) ring was involved.[6] Here, results on new nucleophilic as well as iodination and exchange reactions of Li/Cl phosphinidenoid complexes are reported.

Scheme 1. Carbenoids, Silylenoids, Phosphinidenoids, and Complexes Thereof[a]

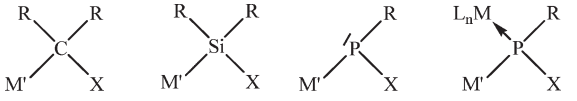

I **II** **III** **IV**

[a] R = ubiquitous organic substitutents; M′ = main group element metal; X = halogen; ML_n = transition metal complex.

Results and Discussion

In order to start examining the scope of nucleophilic reactions while focusing on iodine derivatives, we decided to start first on multifunctional iodocarbaboranes. These present C_c−H, B−H, B−I, and C−I functional groups and a

*Corresponding authors. (R.S.) E-mail: r.streubel@uni-bonn.de. Fax: (49)228-739616. Tel: (49)228-735345. (C.V.) E-mail: clara@icmab.es. Fax: (34) 935805729. Tel: (34) 935801853.

(1) (a) Köbrich, G. *Angew. Chem.* **1967**, *79*, 15; Angew. Chem., Int. Ed. 1967, 6, 41. (b) Kirmse, W. *Angew. Chem.* **1965**, *77*, 1; Angew. Chem., Int. Ed. 1965, 4, 1. (c) Boche, G.; Lohrenz, J. W. *Chem. Rev.* **2001**, *101*, 697.

(2) (a) Tamao, K.; Kawashi, A. *Angew. Chem.* **1995**, *107*, 886; Angew. Chem., Int. Ed. 1995, 34, 818. (b) Tamao, K.; Kawashi, A.; Asahara, M.; Toshimitsu, A. *Pure Appl. Chem.* **1999**, *71*, 393. (c) Lee, M. E.; Cho, H. M.; Lim, Y. M.; Choi, J. K.; Park, C. H.; Jeong, S. E.; Lee, U. *Chem.—Eur. J.* **2004**, *10*, 377. (d) Antolini, F.; Gehrhus, B.; Hitchcock, P. B.; Lappert, M. F. *J. Chem. Soc., Chem. Commun.* **2005**, 5112. (e) Flock, M.; Marschner, C. *Chem.—Eur. J.* **2005**, *11*, 4635. (f) Weidenbruch, M. *Angew. Chem.* **2006**, *118*, 4347; Angew. Chem., Int. Ed. 2006, 45, 4241. (g) Molev, G.; Bravo-Zhivotovskii, D.; Karni, M.; Tumanski, B.; Botoshansky, M.; Apeloig, Y. *J. Am. Chem. Soc.* **2006**, *128*, 2784.

(3) For speculations on ClMg/Cl phosphinidenoids, see: Yoshifuji, M. *J. Chem. Soc., Dalton Trans.* **1998**, 3343.

(4) Özbolat, A.; von Frantzius, G.; Marinas Pérez, J.; Nieger, M.; Streubel, R. *Angew. Chem.*, **2007**, *119*, 9488; *Angew. Chem., Int. Ed.* **2007**, *46*, 9327.

(5) Özbolat, A.; von Frantzius, G.; Hoffbauer, W.; Streubel, R. *J. Chem. Soc., Dalton Trans.* **2008**, 2674.

(6) Bode, M.; Daniels, J.; Streubel, R. *Organometallics* **2009**, *28*, 4636.

Published on Web 09/23/2009

Scheme 2. Generation and Reaction of Li/Cl Phosphinidenoid Complexes 2a,b in the Presence of *B*-Iodo-Substituted *o*-Carbaborane 3b (shown as example)

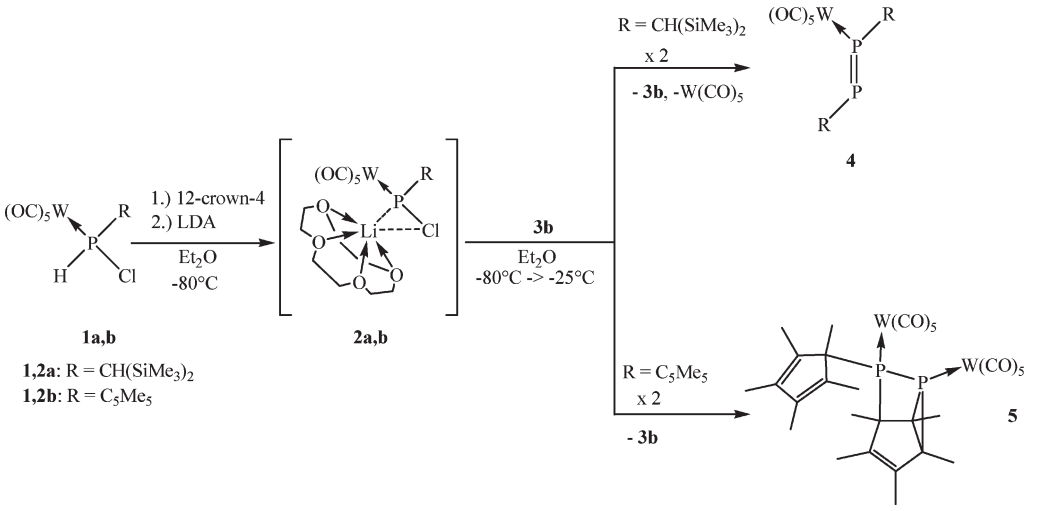

modulated reactivity depending on the occupied site in the cluster;[7] C_c corresponds to the cluster's carbon atoms. Another strong motivation was to get access to *B*-phosphanyl functional *o*-carbaboranes (hitherto unknown) by reacting phosphinidenoid complexes with various carbaborane species (Figure 1). With this aim in mind we generated Li/Cl phosphinidenoid complexes **2a**,**b** as previously described from complexes **1a**[8] and **1b**[9] in the presence of 3-iodo-, 9-iodo-, and 9,12-diiodo *o*-carbaboranes **3a**−**c**[7,10−12] (Scheme 2).

Unfortunately, ^{31}P and ^{11}B NMR studies of the reactions did not provide spectroscopic evidence of products possessing a B−P bond. Instead exclusively formation of **4**[5] and **5**[6] was observed. Nevertheless, in one of the reactions of complex **2a** with 9,12-diiodo *o*-carbaborane **3c** new products were observed by ^{31}P NMR spectroscopy that displayed resonances at 190.9 (^1J(W,P) = 268.3 Hz) and 170.6 (^1J(W,P) = 260.7 Hz, ^2J(P,H) = 15.3 Hz), which perhaps point to *o*-carbaboranyl-substituted chloro-(organo)-phosphane complexes, but due to rapid decomposition further investigations were prevented. Thus, after having observed the lack of reactivity of complexes **2a**,**b** toward B−I bonds, we addressed the question whether *C*-iodo *o*-carbaboranes might be better substrates for substitution reactions. To learn more about this possibility, 1-iodo-2-methyl- and 1-iodo-2-phenyl-substituted carbaboranes **3d**,**e** were synthesized on purpose by reaction of 1-methyl and 1-phenyl carbaborane, **7a**,**b**, respectively, with butyllithium and iodine at 0 °C. Li/Cl phosphinidenoid complexes **2a**,**b** were generated and reacted with 1-iodo-2-methyl- or 1-iodo-2-phenyl-substituted carbaboranes **3d**,**e**. Instead of a nucleophilic iodine substitution, we obtained an unprecedented intermolecular iodine-transfer reaction, thus resulting in the formation of *P*-iodo-substituted chlorophosphane complexes **6a**,**b** together with deiodinated carboranes **7a**,**b** (Scheme 3) as the major products. During these studies it did not became apparent if *C*-Li-carbaborane derivatives were transiently formed that eventually yielded **7a**,**b** (Scheme 3). The ^{31}P NMR spectra of complexes **6a**,**b** displayed data (**6a**: δ = 78.2, ^1J(W,P) = 311.5 Hz; **6b**: δ = 98.6, ^1J(W,P) = 309.0 Hz) with downfield-shifted resonances and increased tungsten−phosphorus coupling constant magnitudes, which both reflect the formal exchange of hydrogen by iodine in **1a**,**b**.

One straightforward way to deal with the relative acidity of the C_c−H bonds in carboranes is to consider that the C_c−H bond is the result of the overlap of an sp orbital on C with the hydrogen s orbital, and a similar picture can be drawn for the C−H bond in acetylene, and thus for the C−I bond in iodoacetylene derivatives. To check the consistency of the model, *in situ* generated iodo(phenyl)acetylene was mixed with the Li/Cl phosphinidenoid complex **2a** (instead of the carbaborane **3d**). Again, complex **6a** was formed but not as the major product, thus partly fulfilling our expectations. If the ratio of complex **2a** to iodo phenylacetylene was 1:1.6, a mixture of complexes **6a**, **8**, and **9** (ratio 6:1:11.7) was obtained (Scheme 4); if the ratio of the starting materials was 1:1, we obtained a different product ratio of 6:1:2. Formation of **6a** may be interpreted as substitution of Li^+ by I^+, partly meeting our expectations and thus backing the beforehand made assumption on the *C*-iodo carbaborane acting as a clean source of iodonium. In contrast, the formation of **8** and **9** is not understood.

Comparing the reactions of the alkyne or the carbaboranes with **2a**, the formation of **9** is of particular interest, as it clearly evidences the disparity in behavior of "1-R-1,2-$C_2B_{10}H_{10}R$" and "R-C≡C$^-$" units. The idea that complex **6a** was formed via some kind of iodine-atom transfer reaction (from **3c**,**d**) prompted us to investigate the reaction of *in situ* generated **2a**,**b** with elemental iodine at low temperature. Under these conditions complexes **6a**,**b** and lithium iodide were selectively formed; noteworthy is that oxidation of the Li/Cl phosphinidenoid complexes was not observed.

All final products were obtained in pure form by low-temperature column chromatography and were unambiguously

(7) Barberà, G.; Vaca, A.; Teixidor, F.; Sillanpää, R.; Kivekäs, R.; Viñas, C. *Inorg. Chem.* **2008**, *47*, 7308.
(8) **1a**: Streubel, R.; Priemer, S.; Ruthe, F.; Jones, P. G. *Eur. J. Inorg. Chem.* **2000**, 1253.
(9) **1b**: Streubel, R.; Rohde, U.; Jeske, J.; Ruthe, F.; Jones, P. G. *Eur. J. Inorg. Chem.* **1998**, *2005*, 7308.
(10) Li, J.; Logan, C. F.; Jones, M. *Inorg. Chem.* **1991**, *30*, 4866.
(11) (a) Zakharkin, L. I.; Kalinin, V. N. *Izv. Akad. Nauk SSSR, Ser. Khim.* **1966**, *3*, 590. (b) Zakharkin, L. I.; Ol'Shevskaya, V. A.; Poroshin, T. Y.; Balgurova, E. V. *Zh. Obshch. Khim.* **1987**, *57*, 2012. (c) Andrews, J. S.; Zayas, J.; Jones, M.Jr. *Inorg. Chem.* **1985**, *24*, 3715.
(12) (a) Li, J.; Logan, C. F.; Jones, M.Jr. *Inorg. Chem.* **1991**, *30*, 4866. (b) Batsanov, A. S.; Fox, M. A.; Howard, J. A. K.; Hughes, A. K.; Johnson, A. L.; Martindale, S. J. *Acta. Crystallogr. C* **2003**, *59*, O74.

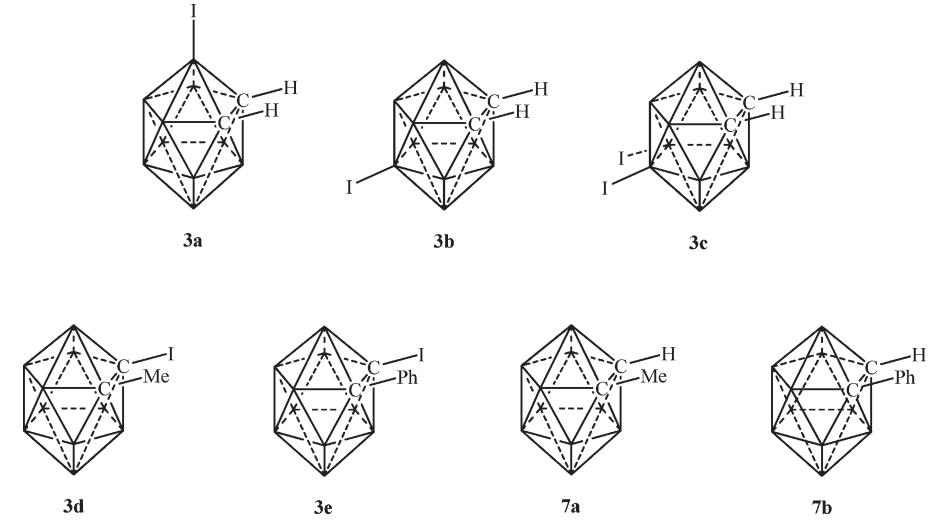

Figure 1. Carbaborane derivatives.

Scheme 3. Reaction of Li/Cl Phosphinidenoid Complexes 2a,b with *C*-Iodo-Substituted *o*-Carboranes 3d,e

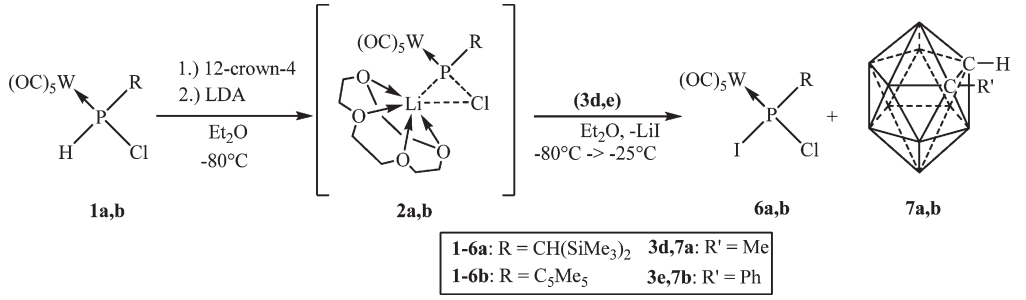

Scheme 4. Reaction of Li/Cl Phosphinidenoid Complex 2a with Iodo(phenyl)acetylene

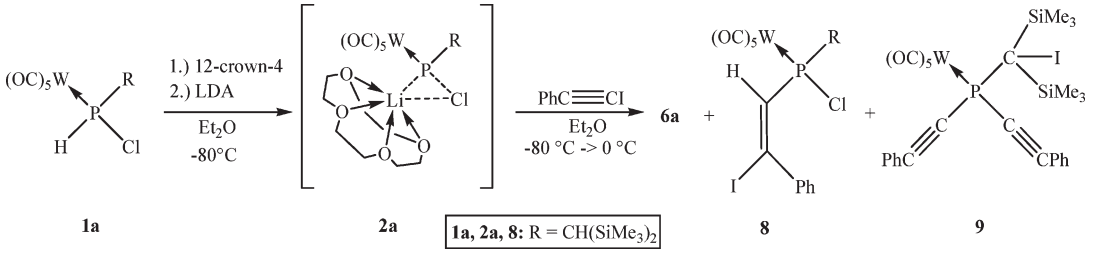

characterized by elemental analysis, NMR and IR spectroscopy, mass spectrometry, and single-crystal X-ray diffraction studies in the cases of complexes **6a** and **9** (Figures 1 and 2).[13]

Structure Discussion

The unambiguously confirmed molecular structures of **6a** and **9** are displayed in Figures 2 and 3.[13] Complex **6a** shows a typical tetrahedral environment at the phosphorus center with a small C1−P−I (95.78(6)°) and a large W−P−C1 angle (120.05(16)°). In complex **6a** P−W, P−C1, and P−Cl bond lengths are slightly elongated compared to the corresponding dichlorophosphane tungsten complex reported before (P−W 2.4589(7), P−C 1.804(3), P−Cl 2.0598(9) Å), which probably is due to the larger iodine atom.[14]

A comparison of selected distances in complex **9** with corresponding bonds of $[Cr(CO)_5P(C{\equiv}CPh)_3]$[15] (C≡C 1.176, P−C 174.8 and 175.3 Å) revealed more elongated C≡C and P−C bonds in the case of **9** (C8−C9 1.202(4), C16−C17 1.205(4), P−C8 1.762(3), and P−C16 1.762(3) Å). The P−C≡C bond angles of **9** are 167.5(3)° and 167.0(3)° and, thus, slightly bent toward the $W(CO)_5$ group.

Conclusions

The reactivity of the transient Li/Cl phosphinidenoid complexes **2a**,**b** toward various iodine-containing compounds was examined in a series of experiments. With B−I containing *o*-carbaboranes **3a**−**c** no selective reactions were obtained with complexes **2a**,**b**, whereas with 1-iodo *o*-carbaboranes **3d**,**e** reacted with **2a**,**b** to yield the I/Cl mixed-substituted organophosphane complexes **6a**,**b** via iodine-transfer

(13) The constitution of **8** was confirmed by X-ray structure analysis, too, but because of disorder of phenyl carbon atoms the data will not be discussed further.

(14) Khan, A. A.; Wismach, C.; Jones, P. G.; Streubel, R. *Dalton Trans.* **2003**, 2483.

(15) Kunishima, M.; Nakata, D.; Tanaka, S.; Hioki, K.; Tani, S. *Tetrahedron* **2000**, *56*, 9927.

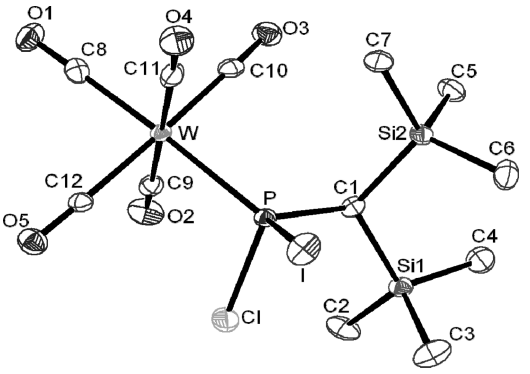

Figure 2. Structure of complex **6a** (50% probability level; hydrogen atoms are omitted for clarity). Selected bond lengths [Å] and angles [deg]: W−P 2.4742(12), P−C1 1.819(5), P−Cl 2.0988(17), P−I 2.4489(12), W−P−C1 120.05(16), Cl−P−I 95.78(6), C1−P−I 105.21(16), C1−P−Cl 106.89(17), W−P−C1 107.64(6).

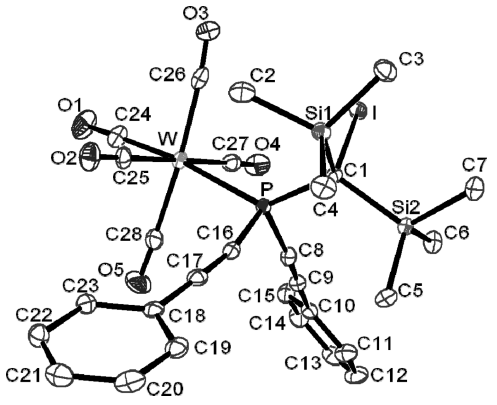

Figure 3. Structure of complex **9** (50% probability level; hydrogen atoms are omitted for clarity). Selected bond lengths [Å] and angles [deg]: W−P 2.5426(8), P−C1 1.859(3), P−C16 1.762(3), C16−C17 1.205(4), C17−C18 1.436(4), P−C8 1.762(3), C8−C9 1.202(4), C9−C10 1.440(4), I−C1 2.191(3); W−P−C1 130.35(10), C16−P−C8 102.12(14), C17−C16−P 178.5(3), C9−C8−P 167.0(3), P−C1−I 103.66, P−C1−Si1 112.43(15), P−C1−Si2 115.63(15).

reaction. Complexes **6a**,**b** could also be obtained with elemental iodine. Further studies using complex **2a** as a good case in point and iodo(phenyl)acetylene showed the formation of a mixture of complexes **6a**, **8**, and **9**, thus revealing multiple reaction pathways in this particular case; current studies are devoted to elucidate this problem. In total, these first results reveal that these novel reactive intermediates have a rich and surprisingly new chemistry.

Experimental Section

All operations were performed in an atmosphere of purified and dried argon. Solvents were distilled from sodium. NMR data were recorded on a Bruker Avance 300 spectrometer at 25 °C (if not mentioned otherwise) using C_6D_6 (**6a**,**b**) or $CDCl_3$ (**8**, **9**) as solvent and internal standard; shifts are given relative to tetramethylsilane (^{1}H, 300.1 MHz; ^{13}C, 75.5 MHz), external BF_3←OEt_2 (^{11}B and ^{11}B{^{1}H} 96.29 MHz), and 85% H_3PO_4 (^{31}P:, 121.5 MHz) in ppm. Mass spectra were recorded on a Kratos MS 50 spectrometer (EI, 70 eV); only m/z values are given. Elemental analyses were performed using an Elementa (Vario EL) analytical gas chromatograph. Infrared spectra were collected on a FT-IR Nicolet 380. Melting points were obtained on a Büchi 535 capillary apparatus. For compounds **3d**,**e**, elemental analyses were performed using a Carlo Erba EA1108 microanalyser, and IR spectra were recorded from KBr pellets on a Shimadzu FTIR-8300 spectrophotometer. X-ray crystallographic analysis of **6a** and **9**: Data were collected on a Nonius KappaCCD diffractometer at 100 K using Mo Kα radiation (λ = 0.71073 Å). The structures were refined by full-matrix least-squares on F^2 (SHELXL-97[16]). All non-hydrogens were refined anisotropically. The hydrogen atoms were included in calculated positions using a riding model.

Synthesis of 1-Me,2-I-1,2-*closo*-$C_2B_{10}H_{10}$ (3d). To a stirring solution of 1-Me,1,2-*closo*-$C_2B_{10}H_{11}$ (500 mg, 3.16 mmol) in diethyl ether (20 mL) cooled to 0 °C in an ice−water bath was added, dropwise, a solution of *n*-butyllithium in hexane (2 mL, 1.6 M, 3.32 mmol) under nitrogen atmosphere. The suspension was stirred at room temperature for 0.5 h, then cooled again to 0 °C, at which point I_2 (842.0 mg, 3.32 mmol) was added in a single portion. The resulting solution was stirred at 0 °C for 30 min and at room temperature for a further 30 min, then extracted with 5% aqueous $Na_2S_2O_3$ (20 mL) and washed with water (2 × 5 mL). The organic phase was dried over $MgSO_4$, filtered, and evaporated *in vacuo* to give a pale yellow solid. The crude product was purified by silica gel flash chromatography at −10 °C under argon atmosphere, using diethyl ether as the eluting solvent to yield 1-Me,2-I-1,2-*closo*-$C_2B_{10}H_{10}$ (691 mg, 77%).

3d: ^{1}H NMR (CD_3COCD_3) [ppm] δ 2.25 (3 H, s); ^{1}H{^{11}B} NMR (CD_3COCD_3) [ppm] δ 2.83 (s, 3H), 2.66 (s, 3H), 2.31 (s, 2H), 2.25 (s, 3H), 2.13 (s, 2H), 1.91 (s, 1H); ^{13}C{^{1}H} NMR (CD_3COCD_3) [ppm] δ 75.68 (s), 27.81 (s), 16.93 (s); ^{11}B NMR (CD_3COCD_3) [ppm] δ −3.3 (d, ^1J(B,H) = 75 Hz, 2B), −5.4 (d, ^1J(B,H) = 90 Hz, 1B), −6.4 (d, ^1J(B,H) = 90 Hz, 2B), −6.9 (d, ^1J(B,H) = 87 Hz, 2B), −8.7 (d, ^1J(B,H) = 83 Hz, 2B), −9.5 (d, ^1J(B,H) = 80 Hz, 2B); FTIR (KBr) ν (cm^{-1}) 2937 (s, C_{alkyl}−H), 2590 (s, B−H). Anal. Calcd for $C_3B_{10}H_{13}I$: C 12.62, H 4.61. Found: C 13.04, H 4.74.

Synthesis of 1-Ph,2-I-1,2-*closo*-$C_2B_{10}H_{10}$ (3e). The synthetic procedure was the same as for **3d** using 1-Ph,1,2-*closo*-$C_2B_{10}H_{11}$ (250 mg, 1.14 mmol) in diethyl ether (25 mL) and a solution of *n*-butyllithium in hexane (0.75 mL, 1.6 M, 1.2 mmol) and I_2 (303.0 mg, 1.2 mmol). The workup was followed to obtain 1-Ph,2-I-1,2-*closo*-$C_2B_{10}H_{10}$ (278 mg, 71%).

3e: ^{1}H NMR (CD_3COCD_3) [ppm] δ 7.77 (d, ^3J(H,H) = 3 Hz, 2H), 7.55 (m, 3H); ^{1}H{^{11}B} NMR (CD_3COCD_3) [ppm] δ 7.77 (d, ^3J(H,H) = 3 Hz, 2H), 7.55 (m, 3H), 3.23 (br s, 2H), 2.88 (br s, 3H), 2.44 (br s, 2H), 2.26 (br s, 3H), 2.15 (br s, 1H); ^{13}C{^{1}H} NMR (CD_3COCD_3) [ppm] δ 132.87 (s), 131.34 (s), 128.98 (s), 84.67 (s), 20.89 (s); ^{11}B NMR (CD_3COCD_3) [ppm] δ −2.9 (d, ^1J(B,H) = 72 Hz, 2B), −6.9 (d, ^1J(B,H) = 81 Hz, 2B), −8.8 (m, ^1J(B,H) = 76 Hz, 6B); FTIR (KBr) ν (cm^{-1}) 3064, 2962 (w, C_{aryl}−H), 2632, 2599, 2574, 2572 (s, B−H), 1494 (s, C_{aryl}−C_{aryl}).

Reaction of Complexes 2a,b with 3d,e. To a solution of 0.11 mmol of lithium diisopropylamide (LDA, freshly prepared from 0.07 mL (0.11 mmol) of *n*-butyllithium and 16 μL (0.11 mmol) of diisopropylamine) in 0.5 mL of diethyl ether cooled to −80 °C was slowly added a solution of 55.1 mg (0.1 mmol) of **1a** (or 53.0 mg (0.1 mmol) of **1b**) and 17 μL (0.11 mmol) of 12-crown-4 in 0.5 mL of diethyl ether. Then a solution of 0.2 mmol of **3d** (57 mg) or **3e** (69 mg) in 0.5 mL of XXXX was added, and the reaction mixture was stirred for 2.5 h while gently warming to 0 °C. The solvent was removed under vacuum, and the residue was dissolved in C_6D_6 and analyzed by multinuclear NMR spectroscopy.

Synthesis of Complex 6a. To a solution of 0.44 mmol of lithium diisopropylamide (LDA, freshly prepared from

(16) Hengefeld, A.; Kopf, J.; Rehder, D. *Organometallics* **1983**, *2*, 114.
(17) Sheldrick, G. M. *SHELXL-97*; Universität Göttingen, 1997.

0.28 mL (0.44 mmol) of *n*-butyllithium and 0.06 mL (0.44 mmol) of diisopropylamine) in 10 mL of diethyl ether cooled to −80 °C was slowly addded a solution of 221 mg (0.4 mmol) of **1a** and 65 μL (0.4 mmol) of 12-crown-4 in 5 mL of diethyl ether. Then a solution of 112 mg (0.44 mmol) of iodine in 5 mL of diethyl ether was dropped into the phosphinidenoid complex solution, and the reaction mixture was stirred for 3.5 h while gently warming to +10 °C. The solvent was removed under vacuum. The product was extracted five times with 3 mL of *n*-pentane. After evaporation, the yellow solid was dissolved with 2 mL of *n*-pentane and cooled to −80 °C. The precipitated crystals were separated from the solution by a syringe. The residue was dried under vacuum.

6a: yellow solid; yield 195 mg (0.29 mmol, 72%); mp 64−69 °C (dec); NMR spectroscopy (C_6D_6, 30 °C): ^{1}H NMR [ppm] δ 0.21 (s, 9H, $SiMe_3$), 0.27 (d, ^4J(P,H) = 0.57 Hz, 9H, $SiMe_3$), 2.55 (d, ^2J(P,H) = 5.19 Hz, 1H, PCH); ^{13}C{^{1}H} NMR [ppm] δ 0.0 (d, ^3J(P,C) = 4.5 Hz, $SiMe_3$), 1.0 (d, ^3J(P,C) = 3.2 Hz, $SiMe_3$) 39.5 (d, ^1J(P,C) = 31.7 Hz, PC), 195.8 (d_{Sat}, ^1J(W,C) = 128.0 Hz, ^2J(P,C) = 7.1 Hz, *cis*-CO), 196.8 (d_{Sat}, ^2J(P,C) = 44.3 Hz, *trans*-CO); ^{31}P{^{1}H} NMR [ppm] δ 78.2 (s_{Sat}, ^1J(W,P) = 311.5 Hz); MS *m*/*z* (%) 675.9 (4) [(M)$^+$]; FTIR (KBr) ν(CO) $\tilde{\nu}$ = 1951 (s), 1997 (m), 2079 (m) [cm^{-1}]. Anal. Calcd: C 21.30, H 2.83. Found: C 21.50, H 3.04. X-ray crystallographic analysis: Suitable pale yellow single crystals were obtained from concentrated *n*-pentane solutions. $C_{12}H_{19}ClIO_5PSi_2W$; crystal size 0.54 × 0.16 × 0.10 mm^3, monoclinic, *P*21/*n*, *a* = 14.7403(4) Å, *b* = 9.6381(2) Å, *c* = 15.3230(3) Å, α = 90°, β = 101.3970(10)°, γ = 90°, *V* = 2133.99(8) Å^3, *Z* = 4, $2\theta_{max}$ = 55°, collected (independent) reflections = 20 403 (4838), R_{int} = 0.0856, μ = 7.188 mm^1, 218 refined parameters, R_1 (for $I > 2\sigma(I)$) = 0.0394, wR_{21} (for all data) = 0.1042, max./min. residual electron density = 1.749/−4.643 e Å^3.

Synthesis of Complex 6b. To a solution of 0.5 mmol of lithium diisopropylamide (LDA, freshly prepared from 0.32 mL (0.5 mmol) of *n*-butyllithium and 0.07 mL (0.5 mmol) of diisopropylamine) in 5 mL of diethyl ether cooled to −80 °C was slowly added a solution of 221 mg (0.42 mmol) of **1b** and 68 μL (0.42 mmol) of 12-crown-4 in 5 mL of diethyl ether. Then a solution of 107 mg (0.42 mmol) of iodine in 1 mL of diethyl ether was dropped into the phosphinidenoid complex solution, and the reaction mixture was stirred for 3.5 h while gently warming to 0 °C. The liquid was filtered from the solid and dried under vacuum. The raw product was purified further by column chromatography (Al_2O_3, −20 °C) using *n*-pentane.

6b: orange solid; yield 161 mg (0.25 mmol, 59%); mp 104 °C (dec); NMR spectroscopy (C_6D_6, 30 °C): ^{1}H NMR [ppm] δ 1.37 (d, *J*(P,H) = 16.4 Hz, 3H, Cp*(C1)-CH_3), 1.56 (ddq, *J*(P,H) = 7.4 Hz, *J*(H,H) = 3.2 Hz, *J*(H,H) = 1.1 Hz, 6H, Cp*-CH_3), 1.75 (br s, 3H, Cp*-CH_3), 1.79 (br s, 3H, Cp*-CH_3); ^{13}C{^{1}H} NMR [ppm] δ 10.4 (d, *J*(P,C) = 2.6 Hz, Cp*-CH_3) 10.5 (d, *J*(P,C) = 2.6 Hz, Cp*-CH_3) 11.8 (d, *J*(P,C) = 0.6 Hz, Cp*-CH_3) 12.1 (s, Cp*-CH_3) 16.5 (d, ^2J(P,C) = 6.8 Hz, Cp*(C1)-CH_3) 65.5 (d, ^1J(P,C) = 19.4 Hz, Cp*(C1)), 133.5 (d, *J*(P,C) = 3.2 Hz, Cp*), 133.6 (d, *J*(P,C) = 1.3 Hz, Cp*), 145.0 (d, *J*(P,C) = 10.0 Hz, Cp*), 145.1 (d, *J*(P,C) = 9.7 Hz, Cp*), 195.6 (d_{Sat}, ^2J(P,C) = 7.1 Hz, *cis*-CO), 196.7 (d_{Sat}, ^2J(P,C) = 44.9 Hz, *trans*-CO); ^{31}P{^{1}H} NMR δ 98.6 (s_{Sat}, ^1J(W,P) = 309.0 Hz); MS *m*/*z* (%) 652 (1) [(M)$^+$]; FTIR (KBr; ν(CO)) $\tilde{\nu}$ = 1939 (s), 1995 (m), 2078 (m) [cm^{-1}]. Anal. Calcd: C 27.61, H 2.32. Found: C 28.26, H 2.50.

Synthesis of Complexes 8 and 9. To a solution of 1.1 mmol of lithium diisopropylamide (LDA, freshly prepared from 0.69 mL (1.0 mmol) of *n*-butyllithium and 0.14 mL (1.0 mmol) of diisopropylamine) in 10 mL of diethyl ether cooled to −90 °C was slowly added a solution of 550 mg (1 mmol) of **1a** and 180 μL (1.1 mmol) of 12-crown-4 in 10 mL of diethyl ether. After 5 min an *in situ* prepared solution of iodo phenylacetylene was added. The reaction mixture was stirred for 2 h while slowly warming to 0 °C. Then the solvents were evaporated, and the residue was suspended with 10 mL of diethyl ether. The products were adsorbed on Al_2O_3 purified by column chromatography (Al_2O_3, −20 °C) using (1) petroleum ether and (2) a mixture of petroleum ether and diethyl ether (19:1 and 18:2). The second fraction contained **8**, which after removal of the solvents was obtained as a pale yellow solid and was subsequently washed with 2 mL of *n*-pentane. **9** was obtained from the third and fourth fraction as a sunflower yellow powder, which was subsequently washed three times with 2 mL of *n*-pentane to yield the pure product as a pale yellow powder.

8: pale yellow solid; yield 74 mg (0.095 mmol, 10%); mp 132−135 °C (dec); ^{1}H NMR [ppm] δ 0.30 (s, 18H, $(SiMe_3)_2$), 1.69 (d, 1H, ^2J(P,H) = 4.96 Hz, PC*H*), 7.40 (d, 1H, ^2J(P,H) = 16.8 Hz, PC*H*), 7.45 (m, 2H, Ph), 7.28 (m, 3H, Ph); ^{13}C{^{1}H} NMR [ppm] δ 1.6 (d, ^1J(P,C) = 4.1 Hz, $SiMe_3$), 2.2 (d, ^1J(P,C) = 2.7 Hz, $SiMe_3$), 33.1 (d, ^{1}(P,C) = 9.1 Hz, P-*C*H), 112.6 (d, ^3J(P,C) = 3.3 Hz, i-Ph), 127.6 (s, o-Ph), 127.7 (s, m-Ph), 128.8 (s, p-Ph), 139.8 (d, ^2J(P,C) = 4.4 Hz, PCH*C*IPh), 140.7 (d, ^1J(P,C) = 11.0 Hz, P*C*HCIPh), 195.7 (d, ^1J(W,C) = 127.6 Hz, ^2J(P,C) = 7.1 Hz, *cis*-CO), 197.8 (d, ^2J(P,C) = 33.0 Hz, *trans*-CO) ppm; ^{31}P{^{1}H} NMR [ppm] δ 89.7 (d_{Sat}, ^1J(W,P) = 283.6 Hz); MS *m*/*z* (%) 777.9 (1) [(M)$^+$]; FTIR (KBr) ν(CO) $\tilde{\nu}$ = 2074 (m), 1984 (m), 1923 (s); ν(C=C): 1598 (w), 1967 (w), 1581 (w) [cm^{-1}]. Anal. Calcd C 30.85, H 3.24. Found: C 30.53, H 3.32.

9: pale yellow solid; yield 159 mg (0.19 mmol, 19%); mp 116−120 °C (dec); ^{1}H NMR [ppm]: δ 0.5 (s, 18H, $(SiMe_3)_2$), 7.4 (m, 10H, CCPh 2×); ^{13}C{^{1}H} NMR [ppm] δ 3.5 (s, $(SiMe_3)_2$), 85.5 (d, ^1J(P,C) = 73.9 Hz, P-*C*C-Ph), 109.1 (d, ^2J(P,C) = 13.7 Hz, P-C*C*-Ph), 120.7 (s, ipso-Ph−C), 128.3 (s, ortho-Ph-CH), 129.9 (s, para-Ph-CH), 131.7 (s, meta-Ph-CH), 198.0 (d, ^2J(P,C) = 6.6 Hz, *cis*-CO), 200.1 (d, ^2J(P,C) = 28.6 Hz, *trans*-CO); ^{31}P{^{1}H} NMR [ppm] δ 19.2 (d_{Sat}, ^1J(W,P) = 265.8 Hz); MS *m*/*z* (%): 715.1 (0.5) [(M)$^+$ − I]; FTIR (KBr) ν(CO) $\tilde{\nu}$ = 2070 (m), 1981 (m), 1924 (s); ν(C≡C) 2163 (m) [cm^{-1}]. Anal. Calcd: C 39.92, H 3.35. Found: C 39.77, H 3.42.

X-ray Crystallographic Analysis. Suitable pale yellow single crystals were obtained from concentrated diethyl ether solutions. $C_{28}H_{28}IO_5PSi_2W$; crystal size 0.44 × 0.40 × 0.39 mm^3, monoclinic, *P*21/*n*, *a* = 12.4156(3) Å, *b* = 14.4943(5) Å, *c* = 17.6597(5) Å, α = 90°, β = 91.404(2)°, γ = 90°, *V* = 3177.00(16) Å^3, *Z* = 4, $2\theta_{max}$ = 55°, collected (independent) reflections = 31 420 (7154), R_{int} = 0.0535, μ = 4.767 mm^1, 349 refined parameters, R_1 (for $I > 2\sigma(I)$) = 0.0263, wR_{21} (for all data) = 0.0685, max./min. residual electron density = 1.726/−1.684 e Å^3.

Acknowledgment. Financial support by the DFG (STR 411/26-1), the COST action cm0802, the DAAD PPP Program "Acciones Integradas", and Ministerio de Ciencia e Innovación (HA-2005-0141) is gratefully acknowledged.

Supporting Information Available: CIF files giving X-ray crystallographic data for **6a** and **9**. This material is available free of charge via the Internet at http://pubs.acs.org. Crystallographic data of **6a** and **9** have also been deposited at the Cambridge Crystallographic Data Centre under the numbers CCDC-729255 (**6a**) and CCDC-729255 (**9**). These data can be obtained free of charge from the Cambridge Crystallographic Data Centre via www.ccdc.cam.ac.uk/data _request/cif.

CHEMISTRY
A EUROPEAN JOURNAL

DOI: 10.1002/chem.200902558

Additive Tuning of Redox Potential in Metallacarboranes by Sequential Halogen Substitution

Patricia González-Cardoso,[a] Anca-Iulia Stoica,[a, b] Pau Farràs,[a] Ariadna Pepiol,[a] Clara Viñas,[a] and Francesc Teixidor*[a]

Abstract: The first artificially made set of electron acceptors is presented that are derived from a unique platform Cs[3,3′-Co($C_2B_9H_{11}$)$_2$], for which the redox potential of each differs from its predecessor by a fixed amount. The sequence of electron acceptors is made by substituting one, two, or more hydrogen atoms by chlorine atoms, yielding Cs[3,3′-Co($C_2B_9H_{11-y}Cl_y$)($C_2B_9H_{11-z}Cl_z$)]. The higher the number of chlorine substituents, the more prone the platform is to be reduced. The effect is completely additive, so if a single substitution implies a reduction of 0.1 V of the redox potential of the parent complex, then ten substitutions imply a reduction of 1 V.

Keywords: chlorination · electron transport · metallacarboranes · redox chemistry · voltammetry

Introduction

Electron transfer (ET) is fundamental in many processes of life, including oxygen binding, photosynthesis and respiration.[1] All organisms obtain energy by transferring electrons from an electron donor to an electron acceptor.[2] Besides, ET attracts considerable attention because of the possible application in energy storage and photovoltaic energy conversion.[3–6]

Maximum efficiency in photosynthesis is obtained when electrons pass from one carrier molecule to another in a downhill direction. Nature has found its way to succeed in this task, but this appears hard with man-made molecules, as incompatibility among the different donors and acceptors may easily occur.[7] By using a unitary platform, this problem could be largely eliminated facilitating ET. However, tuning of a redox potential in an additive and stepwise fashion by fixed increments on a single platform has never been achieved. Typical electrochemical platforms, such as ferrocene, C_{60}, or perylene diimide, have never been proven capable to produce such stepwise tuning. These first-choice platforms have available sites to produce successive substitutions to get a redox potential modulation, but the resulting $E_{1/2}$ is not additive.[8–18]

In this work, we describe the largest set of molecules based on a unique frame that show a stepwise and additive tuning of the redox potential. This platform is [3,3′-Co($C_2B_9H_{11}$)$_2$]$^-$ (**1**$^-$) and it has many sites for substitution; in addition, the B–Cl bonds are very strong, stronger than the C–Cl sites. This may have been the reason for such uniqueness.

Boron clusters approximate to deltahedra or to deltahedra with one or more vertices missing. In the early 1970s, it was realised that the geometry of boron clusters is related to the number of electron pairs available for bonding; therefore, redox processes should be able to produce structural change.[19–22]

Although C_{60} and 1,2-, 1,7- and 1,12-$C_2B_{10}H_{12}$ *closo*-carboranes, see Figure 1, are all neutral molecules characterised by a closed-cage structure, the first requires much less energy to incorporate $2e^-$ than the carboranes, −0.87 versus −2.50 V, respectively, being both values referred to saturated calomel electrode (−1.03 and −2.66 V, respectively, referred to the Fc^+/Fc couple; onwards, all the potential values in this paper will be referred to this couple).[23,24] The low-lying LUMO in C_{60} and the structural rearrangement required upon ET for the carboranes account for this large voltage difference. The low reduction potential of C_{60} has made it very valuable as an electron acceptor in devices,[14–18]

[a] P. González-Cardoso, Dr. A.-I. Stoica, Dr. P. Farràs, A. Pepiol, Prof. Dr. C. Viñas, Prof. Dr. F. Teixidor
Institut de Ciència de Materials de Barcelona (CSIC)
Campus de la U.A.B., 08193 Bellaterra (Spain)
Fax: (+34) 935805729
E-mail: teixidor@icmab.es

[b] Dr. A.-I. Stoica
On leave from the Department of Analytical Chemistry
University of Bucharest (Romania)

Supporting information for this article is available on the WWW under http://dx.doi.org/10.1002/chem.200902558.

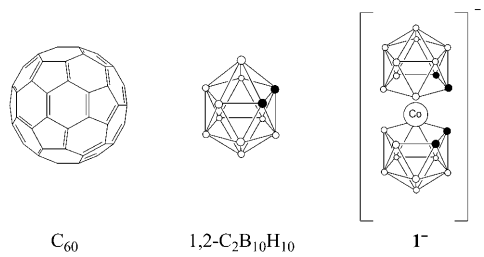

Figure 1. Schematic representation of C_{60}, 1,2-$C_2B_{10}H_{10}$ and Cs[3,3′-Co-(1,2-$C_2B_9H_{11}$)$_2$] (Cs[**1**])molecules.

and could have been an excellent platform to generate a large sequential set of electron acceptors. However, up to now, this has not been achieved,[25–27] and does not seem to be possible.

According to their reduction potentials, carboranes could not compete with C_{60} as electron acceptors; however, the B–X bond (X = halogen) in boron clusters is much more stable to reduction than the C–X bond in sp^2 carbon atoms and this could make it valuable for the sought redox tuning.[28]

As borane clusters are not suited to be redox modulated due to the structural changes caused by addition or removal of electrons, we considered a system that keeps the properties of boron clusters, but avoids rearrangement. Thus, attention was set on the less severe electron-counting rules demand of metallacarboranes, and in particular to the known Co^{III} species Cs[3,3′-Co($C_2B_9H_{11}$)$_2$], Cs[**1**].[29,30] In this work, we show how the stepwise chlorination of **1**$^-$ parallels an easier electron reduction in all three redox couples existing in Cs[**1**]. Besides, the ease of electron reduction is additive by a fixed amount upon each new chlorination step.

Results and Discussion

Experimental studies: [3,3′-Co($C_2B_9H_{11}$)$_2$]$^-$ shows three quasi-reversible waves in cyclic voltammetry at +1.47, −1.51 and −2.46 V versus Fc+/Fc assigned to Co^{IV}/Co^{III}, Co^{III}/Co^{II} and Co^{II}/Co^{I}, respectively.[29,31] The negative $E_{1/2}$ peaks indicate that introducing one and two electrons into the Co^{III} system is energy intensive. It is known that the redox potential of the dichlorinated anion [NMe_4][3,3′-Co($C_2B_9H_{10}Cl$)$_2$] is −1.19 V for the couple Co^{III}/Co^{II},[32] about 0.3 V more positive than for **1**$^-$. This corresponds to 0.3 V for two steps of chlorination, and we wanted to learn if it was possible that with a higher number of chlorination steps whether the ease of reduction would increase accordingly. To prove the potential tuning of Cs[**1**], it was necessary to have a wide set of consecutive halogenated derivatives. The only reported synthesis of chlorinated derivatives of Cs[**1**] was based on the reaction of Cl_2 with Cs[**1**]; this reaction produced mixtures of complexes with several Cl atoms ranging from 2 to 6.[33] On the other hand, pure [$HNMe_3$][3,3′-Co($C_2B_9H_{10}Cl$)$_2$] has been reported to be synthesised by reaction of *N*-chlorosuccinimide with Cs[**1**] in THF.[34] To easily correlate the number of Cl substituents on platform **1**$^-$ and the additive potential shift described in this work, we have named the halogenated species Cs[3,3′-Co($C_2B_9H_{11-y}Cl_y$)($C_2B_9H_{11-z}Cl_z$)] as Cs[Cl$_x$-**1**], with x being the total number of chlorine atoms exchanged for hydrogen atoms in Cs[**1**].

As previously said, only [$HNMe_3$][Cl$_2$-**1**] and Cs[Cl$_6$-**1**] were known before this work, the latter being indeed a mixture of species from Cs[Cl$_2$-**1**] to Cs[Cl$_6$-**1**].[33] This had prevented an accurate calculation of $E_{1/2}$ for Cs[Cl$_6$-**1**] as the cyclic voltammetry (CV) wave was very complex (see Figure 2 a). Even so, the CV wave corresponding to the Cs

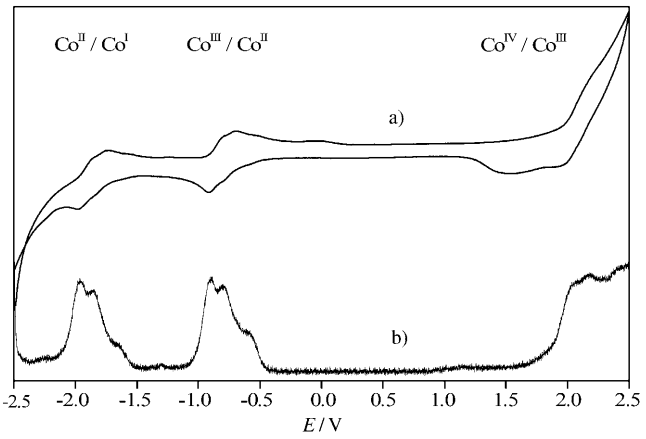

Figure 2. a) Cyclic voltammogram and b) square wave voltammogram responses recorded at a glassy carbon electrode in MeCN of 5×10^{-3} M Cs-[Cl$_x$-**1**] (x = 2–6) with [NBu_4][PF_6] (0.1 M) as the supporting electrolyte. The electrochemical cell contained Ag/AgCl/KCl$_{sat}$ as the reference electrode and a platinum wire as the auxiliary electrode. The potential values have been referred to Fc^+/Fc. Scan rate: a) 0.2 V s^{-1}, b) 0.025 V s^{-1}.

[Cl$_2$-**1**] to Cs[Cl$_6$-**1**] mixture was shifted to more positive $E_{1/2}$ values than for Cs[Cl$_2$-**1**] and, furthermore, the CV wave corresponding to Cs[Cl$_2$-**1**] was shifted to more positive values than that for Cs[**1**]. These facts motivated us to find a more efficient chlorination method that eventually would lead to more chlorine-enriched mixtures.

The objective was to see if the CV wave really moved towards more anodic voltages with an increase in the degree of chlorination of Cs[**1**]. After several unsuccessful trials, we discovered a useful method to increase the chlorination degree of Cs[**1**] by reacting *N*-chlorosuccinimide with Cs[**1**] in the oven at 200(±6)°C in a vacuum sealed tube. By varying the ratio of reagents, a set of series of Cs[Cl$_x$-**1**] ($x > 2$) was obtained, each series consisting of a limited number of x values in an approximately Gaussian distribution (see Supporting Information). The Gaussian curve shifted to more enriched chlorinated derivatives of Cs[**1**] by increasing the NCS/Cs[**1**] ratio. The CV of the synthesised mixtures proved our hypothesis that the higher the degree of chlorination, the more positive the redox potential became. To unambiguously validate the former experiments, it was necessary to

find a reliable analytical tool that provided a measure of the components of each mixture. The molecular composition was obtained by MALDI-TOF-MS analysis by comparing the areas under each peak envelope (see Table S1 in Supporting Information). This was possible because the Cs[Cl_x-**1**] mixtures are made of chemically and structurally very similar compounds, so their MALDI-TOF-MS represent the chemical composition of the studied samples extremely well. Each peak in each mixture had the appropriate isotopic composition and was separated from its neighbour either 35 or 36 mass units. The most chlorine-enriched derivative produced was the Cs[Cl_9-**1**] salt.

Electrochemistry of chlorinated mixtures: The CV of each of these mixtures is very similar to the wave shown in Figure 2a, but all of them were consistently shifted to anodic potentials as the average x value in the Cs[Cl_x-**1**] mixture was increased. Therefore, our hypothesis was qualitatively proven by the CV of the different mixtures, but we had not yet proven the additivity by a fixed amount upon each new chlorination step on the platform Cs[**1**]. To reach this point, we needed a set of adequate mixtures and an electrochemical method capable of providing $E_{1/2}$ values for each individual species. Thus, we prepared samples A–F (see Table 1) to study their redox potentials. The square wave voltammetry (SWV) was the technique that provided more fine structure

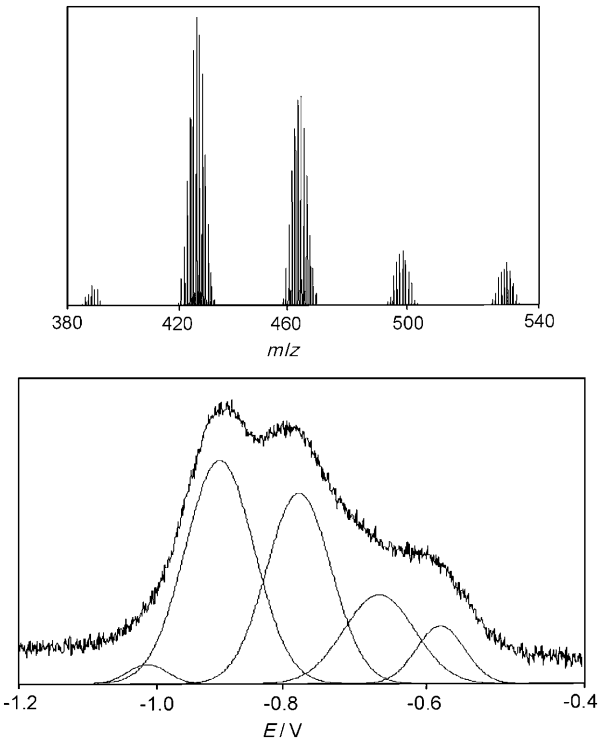

Figure 3. MALDI-TOF mass spectrum of Cs[Cl_x-**1**] with $x=2$–6 (top) and deconvolution into Gaussians of its Co^{III}/Co^{II} SWV (bottom) from sample B.

Table 1. Percentage composition of the mixtures of Cs[Cl_x-**1**] used for the calculation of the $E_{1/2}$ values displayed in Figure 4. The composition of each sample has been determined by the analysis of the corresponding MALDI-TOF mass spectrum.

	[Cl_2-**1**]$^-$	[Cl_3-**1**]$^-$	[Cl_4-**1**]$^-$	[Cl_5-**1**]$^-$	[Cl_6-**1**]$^-$	[Cl_7-**1**]$^-$	[Cl_8-**1**]$^-$	[Cl_9-**1**]$^-$
A	20.4	62.8	16.8	–	–	–	–	–
B	2.7	49.1	34.1	8.2	5.9	–	–	–
C	–	–	5.2	14.2	16.4	31.1	30.7	2.3
D	–	–	–	–	22.6	42.9	32.4	2.1
E	29.9	25.1	13.7	3.2	11.4	12.9	3.7	–
F	18.4	11.1	15.4	4.7	21.2	23.5	5.8	–

in the electrochemical wave to warrant individual $E_{1/2}$ calculations. In Figure 2b, the SWV for Cs[Cl_x-**1**] ($x=2$–6) is indicated. When the chemical composition, drawn from MALDI-TOF MS, and deconvolution into Gaussian curves of the corresponding SWV were combined, a set of self-consistent $E_{1/2}$ values for each x value could be obtained for the Co^{III}/Co^{II} redox process, as outlined in Figure 3. The MALDI-TOF MS and SWV data are periodic, the first with regard to mass, and the second with regard to potential. Importantly, both also present the same intensity pattern, a property that is related to the quantity of different components in the mixture.

The MALDI-TOF MS in Figure 3 (top) corresponds to sample B, made up of Cs[Cl_2-**1**], Cs[Cl_3-**1**], Cs[Cl_4-**1**], Cs[Cl_5-**1**] and Cs[Cl_6-**1**]; each peak shows the proper isotopic distribution centred at 391.51, 426.53, 461.53, 495.51 and 530.50, respectively. The difference in m/z between these peaks is constant and due to the addition of an extra chlorine atom and the loss of hydrogen; that is, the chlorination step. The SWV plot in Figure 3 deconvolutes into five Gaussian curves that correspond to the number of chlorinated species in the mixture. The intensities of each Gaussian parallel the intensity of each peak in the MALDI-TOF MS and they are separated from its neighbours by a fixed potential, as also happens in the MALDI-TOF MS in which the peaks are separated a fixed m/z. In consequence, the change in mass and potential proceeds in a parallel fashion and one can conclude that the periodic anodic shift in the SWV is also due to the influence of one extra chloride on Cs[Cl_{x-1}-**1**]. The periodicity in the $E_{1/2}$ values shown in Figure 3 (bottom) proves the chlorination mass and potential additivity described above for the first six members of the series. Similar studies have been conducted with directly out of the oven mixtures with higher chlorination patterns or with purposely prepared mixtures after combining different synthetic procedures. The results are displayed in Table 2, together with the whole sequence of $E_{1/2}$ potentials. For each x value, $E_{1/2}$ has been calculated as many times as Cs[Cl_x-**1**] has been found in the different synthetic mixtures; the dispersion of $E_{1/2}(x)$ is very low, proving that the values are self-consistent (see Figure 4). The $E_{1/2}$ values for the higher Cs[Cl_x-**1**] members of the series are not given, only

Table 2. Calculated energy values of the HOMO and LUMO of Cs[Cl_x-**1**] compared with the $E_{1/2}$ value for their corresponding Co^{III}/Co^{II} process (versus Fc^+/Fc).

	$E_{1/2}$ [V]	$-E_{HOMO}$ [eV]	$-E_{LUMO}$ [eV]	CTC
Cs[**1**]	−1.51	3.963	−0.546	−3.48
Cs[Cl_1-**1**]	–	4.060	−0.379	−3.25
Cs[Cl_2-**1**]	−1.21	4.163	−0.153	−3.10
Cs[Cl_3-**1**]	−1.09	4.261	0.019	−2.94
Cs[Cl_4-**1**]	−0.98	4.409	0.195	−2.79
Cs[Cl_5-**1**]	−0.88	4.492	0.344	−2.65
Cs[Cl_6-**1**]	−0.77	4.609	0.496	−2.51
Cs[Cl_7-**1**]	−0.67	4.698	0.596	−2.37
Cs[Cl_8-**1**]	−0.56	4.784	0.698	−2.24
Cs[Cl_9-**1**]	−0.52	4.838	0.819	−2.13
Cs[Cl_{10}-**1**]	–	4.984	0.925	−2.01
Cs[Cl_{11}-**1**]	–	5.017	1.026	−1.90
Cs[Cl_{12}-**1**]	–	5.149	1.130	−1.78

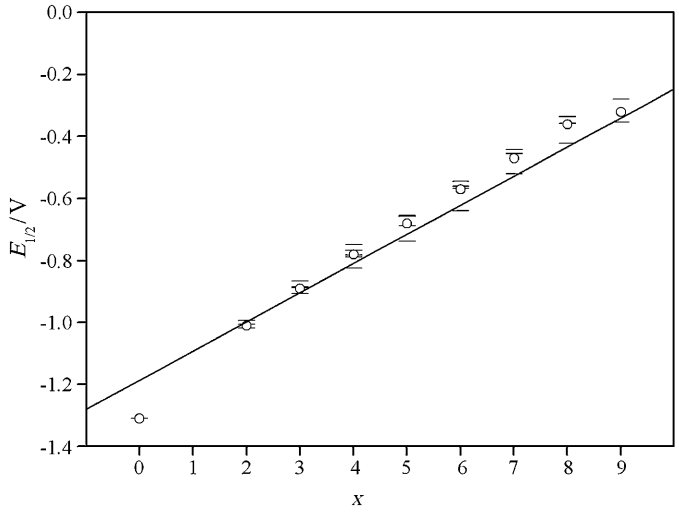

Figure 4. $E_{1/2}$ of all the Cs[Cl_x-**1**] calculated from the deconvolution into Gaussians of the SW voltammograms of the mixtures which contain them. The horizontal lines (——) represent the individual $E_{1/2}$ values whereas the empty circles (○) represent the average $E_{1/2}$ versus Fc^+/Fc for each number of chlorine atoms.

traces of such species were found in all the mixtures prepared, preventing an accurate measure of $E_{1/2}$.

Examining the $E_{1/2}$ values, one can see that each Cl addition results in an increase of 0.12 V. Thus, the addition of eight chloride ions would imply an increase of 0.96 V. For Cs[Cl_8-**1**], an estimated $E_{1/2}$ value near $-0.55\,V = -1.51 + 0.96\,V$ would be expected, and the real value is found at −0.56 V. The additivity is satisfied very reasonably and also applies to the Co^{II}/Co^{I} couple and most probably to the Co^{IV}/Co^{III} couple. Some values are slightly out of the rule, for example, the $E_{1/2}$ value for Cs[Cl_9-**1**], but this may be due to the always low yield of this particular anion in any sample produced, more than to a failure of the additivity. In Figure 2b, the SWV for the Co^{III}/Co^{II} and Co^{II}/Co^{I} look very similar. This has allowed us to double check the goodness of fit of the Gaussian deconvolution. Less data has been obtained for the Co^{IV}/Co^{III} couple due to the overall anodic shift upon higher chlorination that has taken the $E_{1/2}$ value for this couple to the anodic edge of the solvent.

Preliminary results show that the $E_{1/2}$ additivity modulation also occurs with Br and I derivatives of Cs.[1] For the same number of halogen substituents, the anodic shift follows the next order: $E_{1/2}(Cl) < E_{1/2}(Br) < E_{1/2}(I)$. Each redox potential is shifted near 0.10 V for Co^{III}/Co^{II} and 0.07 V for Co^{II}/Co^{I} when moving from Cl to Br and 0.10 V for both redox processes when moving from Br to I.

DFT calculations: To find a theoretical basis on the redox tunability of Cs[Cl_x-**1**] species, the $E_{1/2}$ values for the redox couple Co^{III}/Co^{II} have been correlated with their HOMO and LUMO energies. Table 2 displays the HOMO and the LUMO energies along with the $E_{1/2}$ for the couple Co^{III}/Co^{II}. The cluster total charge (CTC) is also shown.[35] CTC is a useful property to interpret the behaviour of boron clusters, since it computes all charges on the cluster atoms, not only these in the periphery. In this case, CTC has been computed with the natural population analysis (NPA) method.[36]

There is a good parallel between the plots of $E_{1/2}$ and $-E_{LUMO}$, as well as between $E_{1/2}$ and $-E_{HOMO}$. Although the $E_{1/2}$ correlation with both E_{LUMO} and E_{HOMO} may seem contradictory, it is not if the first relates to the reduction of Co^{III} to Co^{II} and the second relates to the oxidation of Co^{III} to Co^{IV}. The easiest Cs[Cl_x-**1**] compound to be oxidised is that with $x = 0$, which is the one with the more positive HOMO energy, in agreement with the Koopman's theorem. Conversely, the easiest Cs[Cl_x-**1**] to be reduced is that with $x = 12$, as it has the more stable LUMO. There is also noticeable correlation between $E_{1/2}$ and the CTC: the species with a more negative CTC charge are more difficult to reduce; see, for example, Cs[**1**], which has the highest negative CTC. In contrast, the compounds that are reduced most easily are those with the more positive CTC charge.

Conclusion

These redox values are very comparable to the first two reduction waves of C_{60} at −0.64 V for $[C_{60}]^{0/-I}$ and −1.03 V for $[C_{60}]^{-I/-II}$ versus Fc^+/Fc, which is remarkable considering that C_{60} is a neutral molecule, whereas $[3,3'\text{-}Co(C_2B_9H_{11})_2]^-$ is an anionic species. These results show that, with a higher degree of chlorination, it should be possible to attain even positive values of $E_{1/2}$. We are currently developing a new method of synthesis that should allow us to synthesise specific species up to the Cs[Cl_{12}-**1**].

Experimental Section

Materials and instrumentation: All metallacarborane anions prepared were air and moisture stable. *N*-Chlorosuccinimide (NCS) was purchased from Aldrich and used as received. Cs[$3,3'\text{-}Co(C_2B_9H_{11})_2$] was supplied by Katchem. The mass spectra were recorded in the negative ion mode

by using Bruker Biflex MALDI-TOF MS [N_2 laser; λ_{exc} 337 nm (0.5 ns pulses); voltage ion source 20.00 kV]. For voltammetric determinations, an electrochemical system, VoltaLab (Universal Electrochemical Laboratory System) interfaced with a PGZ100 potentiostat (Radiometer Analytical) and controlled by the VoltaMaster 4 software was used. The electrochemical cell contained a glassy carbon electrode as working electrode, a reference $Ag/AgCl/KCl_{sat}$ electrode and platinum wire as auxiliary electrode. The solutions were deaerated with analytical grade nitrogen at the start of each experiment to prevent oxygen interference. All experiments were performed at room temperature. All the potential values were referred to the Fc^+/Fc couple [$E_{1/2}$ (Fc^+/Fc) = 0.20 V versus $Ag/AgCl/KCl_{sat}$].

General synthetic procedure for the preparation of chlorinated derivatives of [3,3′-Co(1,2-$C_2B_9H_{11}$)$_2$]$^-$: Cs[**1**] (≈0.1 mmol), and the corresponding molar quantity of N-chlorosuccinimide (NCS), for the main target anion expected in the resulting mixture, were crushed together in a glove box until a homogeneous powder was obtained. As an example, if [Cl_6-**1**]$^-$ was the desired dominant anion in the mixture, a 1:6 ratio of Cs[**1**] and NCS was to be mixed. A thick-walled Pyrex tube (20 cm long, 5 mm id and 8 mm od) was charged with the powder. The lower part of the tube was then cooled with liquid N_2, evacuated and sealed under vacuum with an energetic flame. Afterwards, the tube was placed inside a protective iron cylinder and put inside a preheated tubular furnace. The temperature of the furnace was maintained for 2 h at 194 ± 6 °C. The protective cylinder containing the tube was then carefully removed and the whole cooled down to room temperature. The tube was then opened and THF was added in order to perform the characterisation by negative MALDI-TOF MS and get the CV and SWV for the mixture of anions.

Computational methods: Calculations were performed with the Gaussian 03 suite of programs.[37] Geometries of [3,3′-Co(1,2-$C_2B_9H_{11}$)$_2$]$^-$ and its chlorinated derivatives were fully optimised and HOMO–LUMO energies and NPA (natural population analysis) charges calculated at the B3LYP/3–21G* and B3LYP/6–31+G(d,p) level of theory, respectively.[36] All stationary points were found to be true minima (number of imaginary frequencies, N_{imag} = 0).

Acknowledgements

This work was supported by MEC (MAT2006-05339, SAB2006-0127) and Generalitat de Catalunya (2005/SGR/00709). P.G.-C., P.F. and A.P. thank CSIC for a pre-doctoral grant. We are also thankful to CESCA for providing the computational resources.

[1] R. E. Blankenship in *Molecular Mechanisms of Photosynthesis*, Blackwell Science, Oxford, **2002**, Chapter 6; R. E. Blankenship in *Molecular Mechanisms of Photosynthesis*, Blackwell Science, Oxford, **2002**, Chapter 7.
[2] R. Cotterill in *Biophysics: An Introduction*, Wiley-VCH, Weinheim, **2003**, Chapter 9.
[3] R. Eisenberg, H. B. Gray, *Inorg. Chem.* **2008**, *47*, 1697.
[4] C. Herrero, B. Lassalle-Kaiser, W. Leibl, A. W. Rutherford, A. Aukauloo, *Coord. Chem. Rev.* **2008**, *252*, 456.
[5] K. Sanderson, *Nature* **2008**, *452*, 400.
[6] X. Sala, I. Romero, M. Rodríguez, L. Escriche, A. Llobet, *Angew. Chem.* **2009**, *121*, 2882; *Angew. Chem. Int. Ed.* **2009**, *48*, 2842.
[7] R. Liegghio, P. G. Potvin, A. B. P. Lever, *Inorg. Chem.* **2001**, *40*, 5485.
[8] Y. Araki, R. Chitta, A. S. D. Sandanayaka, K. Langewalter, S. Gadde, M. E. Zandler, O. Ito, F. D'Souza, *J. Phys. Chem. C* **2008**, *112*, 2222.
[9] M. Morisue, D. Kalita, N. Haruta, Y. Kobuke, *Chem. Commun.* **2007**, 2348.
[10] A. Sautter, B. K. Kaletaş, D. G. Schmid, R. Dobrawa, M. Zimine, G. Jung, I. H. M. Van Stokkum, L. De Cola, R. M. Williams, F. Würthner, *J. Am. Chem. Soc.* **2005**, *127*, 6719.
[11] T. Konishi, A. Ikeda, S. Shinkai, *Tetrahedron* **2005**, *61*, 4881.
[12] N. Martín, L. Sanchez, B. Illescas, I. Perez, *Chem. Rev.* **1998**, *98*, 2527.
[13] J. L. Segura, N. Martin, D. M. Guldi, *Chem. Soc. Rev.* **2005**, *34*, 31.
[14] A. Laiho, R. H. A. Ras, S. Valkama, J. Ruokolainen, R. Osterbacka, O. Ikkala, *Macromolecules* **2006**, *39*, 7648.
[15] Z. R. Hong, Z. H. Huang, X. T. Zeng, *Chem. Phys. Lett.* **2006**, *425*, 62.
[16] V. Shrotriya, J. Ouyang, R. J. Tseng, G. Li, Y. Yang, *Chem. Phys. Lett.* **2005**, *411*, 138.
[17] R. H. Xie, G. W. Bryant, G. Y. Sun, T. Kar, Z. F. Chem, V. H. Smith, Y. Araki, N. Tagmatarchis, H. Shinohara, O. Ito, *Phys. Rev. B* **2004**, *69*, 201403.
[18] A. A. Popov, I. E. Kareev, N. B. Shustova, E. B Stukalin, S. F. Lebedkin, K. Seppelt, S. H. Strauss, O. V. Boltalina, L. Dunsch, *J. Am. Chem. Soc.* **2007**, *129*, 11551.
[19] R. E. Williams, *Inorg. Chem.* **1971**, *10*, 210.
[20] K. Wade, *Chem. Commun.* **1971**, 792.
[21] D. M. P. Mingos, *Nature Phys. Sci.* **1972**, *236*, 99.
[22] E. D. Jemmis, M. M. Balakrishnarajan, P. D. Pancharatna, *Chem. Rev.* **2002**, *102*, 93.
[23] L. Echegoyen, L. E. Echegoyen, *Acc. Chem. Res.* **1998**, *31*, 593. According to this reference, the measured potential ($E_{1/2}$) for $C_{60}^{0/-1}$ was −0.98 V versus Fc^+/Fc. For comparison purposes, we have converted it to SCE by adding 0.5 V.
[24] J. H. Morris, H. J. Gysling, D. Reed, *Chem. Rev.* **1985**, *85*, 51.
[25] M. Zheng, F. F. Li, Z. J. Shi, X. Gao, K. M. Kadish, *J. Org. Chem.* **2007**, *72*, 2538.
[26] M. Carano, M. Marcaccio, F. Paolucci, P. Birkett, *Photochem. Photobiol. Sci.* **2006**, *5*, 1132.
[27] F. Zhou, G. J. Van Berkel, B. T. Donovan, *J. Am. Chem. Soc.* **1994**, *116*, 5485.
[28] U. Páramo-Garcío, M. Ávila-Rodríguez, M. G. García-Jiménez, S. Gutiérrez-Granados, J. G. Ibáñez-Cornejo, *Electroanalysis* **2006**, *18*, 904.
[29] M. F. Hawthorne, D. C. Young, T. D. Andrews, D. V. Howe, R. L. Pilling, A. D. Pitts, M. Reintjes, L. F. Warren, Jr., P. A. Wegner, *J. Am. Chem. Soc.* **1968**, *90*, 879.
[30] I. B. Sivaev, V. I. Bregadze, *Collect. Czech. Chem. Commun.* **1999**, *64*, 783.
[31] M. Corsini, F. Fabrizi de Biani, P. Zanello, *Coord. Chem. Rev.* **2006**, *250*, 1351.
[32] D. A. Rudakov, V. L. Shirokii, V. A. Knizhnikov, A. V. Bazhanov, E. I. Vecher, N. A. Maier, V. I. Potkin, A. N. Ryabtsev, P. V. Petrovskii, I. B. Sivaev, V. I. Bregadze, I. L. Eremenko, *Russ. Chem. Bull.* **2004**, *53*, 2554.
[33] L. Mátel, F. Macasek, P. Rajec, *Polyhedron* **1982**, *1*, 511.
[34] P. K. Hurlburt, R. L. Miller, K. D. Abney, T. M. Foreman, R. J. Butcher, S. A. Kinkead, *Inorg. Chem.* **1995**, *34*, 5215.
[35] a) F. Teixidor, G. Barberà, A. Vaca, R. Kivekäs, R. Sillanpää, J. Oliva, C. Viñas, *J. Am. Chem. Soc.* **2005**, *127*, 10158; b) A. V. Puga, F. Teixidor, R. Sillanpää, R. Kivekäs, M. Arca, G. Barberà, C. Viñas, *Chem. Eur. J.* **2009**, *15*, 9755.
[36] a) A. D. Becke, *J. Chem. Phys.* **1993**, *98*, 5648; b) A. E. Reed, L. A. Curtiss, F. Weinhold, *Chem. Rev.* **1988**, *88*, 899; c) P. C. Hariharan, J. A. Pople, *Theor. Chim. Acta* **1973**, *28*, 213.
[37] Gaussian 03, Revision C.02, M. J. Frisch, G. W. Trucks, H. B. Schlegel, G. E. Scuseria, M. A. Robb, J. R. Cheeseman, J. A. Montgomery, Jr., T. Vreven, K. N. Kudin, J. C. Burant, J. M. Millam, S. S. Iyengar, J. Tomasi, V. Barone, B. Mennucci, M. Cossi, G. Scalmani, N. Rega, G. A. Petersson, H. Nakatsuji, M. Hada, M. Ehara, K. Toyota, R. Fukuda, J. Hasegawa, M. Ishida, T. Nakajima, Y. Honda, O. Kitao, H. Nakai, M. Klene, X. Li, J. E. Knox, H. P. Hratchian, J. B. Cross, V. Bakken, C. Adamo, J. Jaramillo, R. Gomperts, R. E. Stratmann, O. Yazyev, A. J. Austin, R. Cammi, C. Pomelli, J. W. Ochterski, P. Y. Ayala, K. Morokuma, G. A. Voth, P. Salvador, J. J. Dannenberg, V. G. Zakrzewski, S. Dapprich, A. D. Daniels, M. C. Strain, O. Farkas, D. K. Malick, A. D. Rabuck, K. Raghavachari, J. B. Foresman, J. V. Ortiz, Q. Cui, A. G. Baboul, S. Clifford, J. Cio-

slowski, B. B. Stefanov, G. Liu, A. Liashenko, P. Piskorz, I. Komaromi, R. L. Martin, D. J. Fox, T. Keith, M. A. Al-Laham, C. Y. Peng, A. Nanayakkara, M. Challacombe, P. M. W. Gill, B. Johnson, W. Chen, M. W. Wong, C. Gonzalez, J. A. Pople, Gaussian, Inc., Wallingford CT, **2004**.

Received: September 16, 2009
Revised: January 5, 2010
Published online: April 21, 2010

CHEMISTRY
A EUROPEAN JOURNAL

Supporting Information

Additive Tuning of Redox Potential in Metallacarboranes by Sequential Halogen Substitution

Patricia González-Cardoso,[a] Anca-Iulia Stoica,[a, b] Pau Farràs,[a] Ariadna Pepiol,[a] Clara Viñas,[a] and Francesc Teixidor*[a]

chem_200902558_sm_miscellaneous_information.pdf

Experimental Section

$Cs[3,3'\text{-}Co(1,2\text{-}C_2B_9H_{11})_2]$, Cs[**1**], near 0.1 mmol, and the corresponding molar quantity of N-chlorosuccinimide, NCS, for the main target anion in the expected resulting mixture, were crushed together in a glove box until a homogeneous powder was obtained. As an example, if $[Cl_6\text{-}\mathbf{1}]^-$ was aimed as one of the dominant anions in the mixture, a 1:6 ratio of $Cs[3,3'\text{-}Co(1,2\text{-}C_2B_9H_{11})_2]$ and NCS would be mixed. A thick-walled Pyrex tube (20 cm long, 5 mm id and 8 mm od) was charged with the powder. The lower part of the tube was then cooled with liquid N_2, evacuated and sealed under vacuum with an energetic flame. Afterwards, the tube was placed inside a protective iron cylinder and put inside a preheated tubular furnace. The temperature of the furnace was maintained for 2 hours at 194±6ºC. The protective cylinder containing the tube was then carefully removed and the whole cooled down to room temperature. The tube was then opened and THF was added in order to perform the characterization by negative MALDI-TOF-MS and get the CV and SWV for the mixture of anions.

Table S1. Experimental results for the mixture [3,3'-Co(1,2-$C_2B_9H_{11})_2$]$^-$ and NCS from reagent ratios 1:1 to 1:20. Experiments are done at 194±6ºC for 2 h. In the column headed by **y**, the species observed by MALDI-TOF-MS are indicated in bold numbers, indicative of the number of inserted chlorine atoms. In parenthesis is indicated the molar fraction of the different chlorinated species.

Reagent ratio	**y**
1:1	**0** (0.24), **1** (0.46), **2** (0.31)
1:2	**0** (0.05), **1** (0.15), **2** (0.52), **3** (0.19), **4** (0.09)
1:3	**2** (0.25), **3** (0.35), **4** (0.26), **5** (0.11)
1:4	**2** (0.09), **3** (0.14), **4** (0.25), **5** (0.35), **6** (0.18)
1:5	**4** (0.11), **5** (0.34), **6** (0.46), **7** (0.09)
1:6	**5** (0.25), **6** (0.54), **7** (0.22)
1:7	**5** (0.09), **6** (0.35), **7** (0.39), **8** (0.12)
1:8	**6** (0.21), **7** (0.46), **8** (0.31)
1:9	**7** (0.32), **8** (0.51), **9** (0.17)
1:10	**7** (0.10), **8** (0.54), **9** (0.33)
1:11	**7** (0.19), **8** (0.50), **9** (0.28)
1:12	**7** (0.04), **8** (0.42), **9** (0.40), **10** (0.14)
1:13	**7** (0.09), **8** (0.44), **9** (0.38), **10** (0.09)
1:14	**7** (0.06), **8** (0.45), **9** (0.39), **10** (0.10)
1:15	**7** (0.04), **8** (0.44), **9** (0.39), **10** (0.11)
1:16	**8** (0.32), **9** (0.45), **10** (0.21)
1:17	**8** (0.33), **9** (0.46), **10** (0.21)
1:18	**8** (0.36), **9** (0.46), **10** (0.18)
1:19	**8** (0.16), **9** (0.45), **10** (0.31), **11** (0.08)
1:20	**8** (0.19), **9** (0.47), **10** (0.29), **11** (0.05)

6.- ANNEX II

(Manuscrits pendents de publicació posteriors a la Comissió de Doctorat del setembre de 2011)

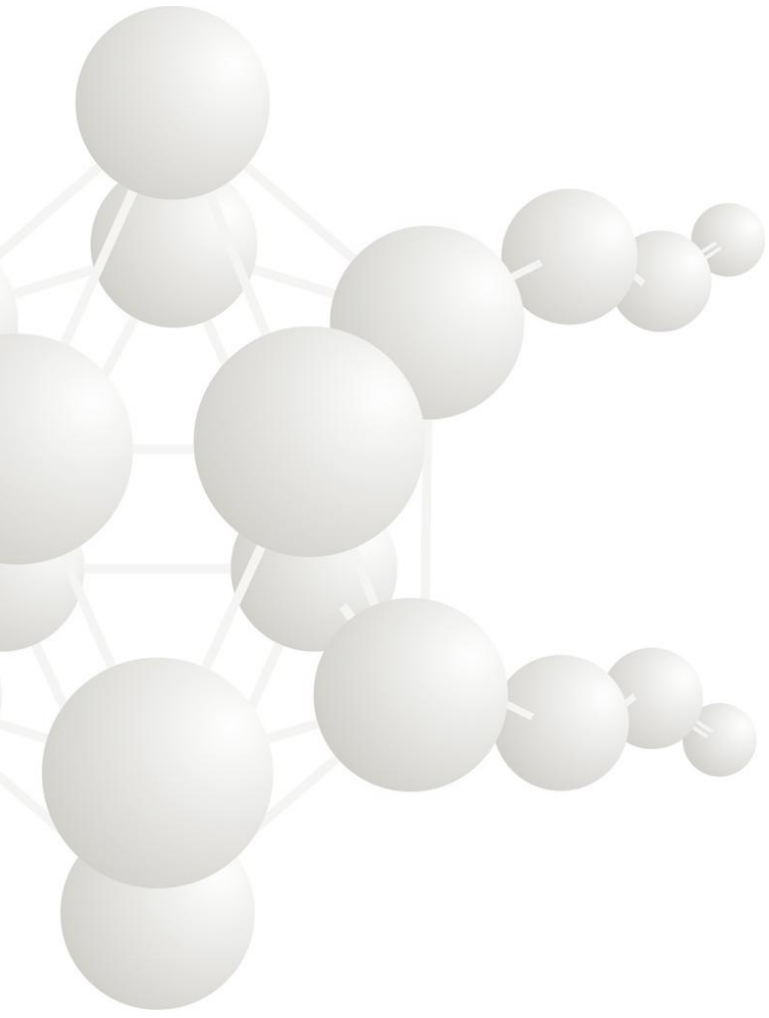

Designed Synthesis of New Poly-iodinated *Nido* and Cobaltabisdicarbollide Frameworks

Ariadna Pepiol[a], Marius Lupu[a], Francesc Teixidor[a], Reijo Sillanpää[b], Clara Viñas[a*]

[a] *Institut de Ciencia de Materials de Barcelona (CSIC) Campus UAB, 08193 Bellaterra, Spain. e-Mail clara@icmab.es*

[b] *Department of Chemistry, University of Jyväskylä, 40351 Jyväkylä, Finland*

Highly iodinated molecules have been of interest in materials science and medical applications[1] including the potential use of iodinated *ortho*-carboranes as next-generation radiopaque contrast agents for X-ray diagnostic imaging.[2] These compounds have a much greater proportion of iodine in the structures compared to the iodinated organic compounds currently used in X-ray contrast agents. Clean and effective syntheses are still the critical issue for the consideration of highly iodinated *ortho*-carboranes as realistic candidates for X-ray contrast agents.[3] However, the recent development of a fast and solvent free synthetic procedure has allowed the preparation of 1-R-9,12-I_2-1,2-*closo*-$C_2B_{10}H_{10}$ and 1-R-8,9,10,12-I_4-1,2-*closo*-$C_2B_{10}H_8$ (R = H, Me, Ph) derivatives by direct reaction of *o*-carboranes (1,2-*closo*-$C_2B_{10}H_{12}$, 1-Me-1,2-*closo*-$C_2B_{10}H_{11}$, 1-Ph-1,2-*closo*-$C_2B_{10}H_{11}$) and iodine in sealed tubes.[4] Additionally, the procedure does not require any further solvent-based workup and an excess the of iodine is recovered and re-utilized. For the C-substituted counterparts slightly shorter reaction times for the same degree of iodination compared to the parent *o*-carborane were needed. This result is consistent with both theoretical[5] and experimental data[6] reported by Lipscomb and co-workers, which showed that the electron-donating effect of methyl groups bonded to the $C_{cluster}$ atoms causes a uniform increase in electron density on the B atoms while having little or no effect on the sequence of substitution.

Since the best method to obtain halocarboranes is by electrophilic halogenation with iodine or bromine of the boron atom vertices, the most common halogenated *nido* carboranes are those substituted at the 9 and 11 positions, the sites of highest electron density as a result of their position in the open pentagonal face of the nido cluster.[7] Consequently, producing iodo and bromo derivatives substituted in other positions of the *nido* cluster is relatively difficult, due to the insusceptibility of these sites to electrophilic attack. As far as we are aware, bromination of a *nido* carborane is only known at the 9 and 11 positions. For iodocarboranes the *nido* anion enantiomers 5-I-nido-7,8-dicarbaundecaborate and 6-I-nido-7,8-dicarbaundecaborate have been additionally been obtained, through the deboronation of 9-I-*o*-carborane with KOH[8] or tetrabutylammonium fluoride hydrate, TBAFH.[9]

In spite of the fact that halogenated *nido* carboranes have potential relevance to important topics such as radioiodine carry and as boron neutron capture therapy (BNCT) reagents;[10] relatively few iodinated and brominated *nido* carboranes are known.

The synthetic strategy leading to selective *B*-iodinated cobaltabisdicarbollide [3,3'-Co(1,2-

$C_2B_9H_{11})_2]^-$ derivatives. As far as we are aware, regioselective substitutions have not been possible, and specific derivatives could only be obtained after careful separations of complex mixtures. Here, we first describe the deboronation with EtOK in EtOH of a series of *closo* iodinated derivatives of o-carborane which leads us to achieve highly regioselective *B*-iodinated *nido* counterparts. Upon controlled deboronation, new iodinated derivatives of cobaltabisdicarbollide [3,3'-Co-(1-R-9,12-I_2-1,2-*closo*-$C_2B_9H_8)_2]^-$ and [3,3'-Co-(1-R-8,9,10,12-I_4-1,2-*closo*-$C_2B_9H_6)_2]^-$ (R= H, Me, Ph) through the complexation reaction with cobalt (II) of the appropriate *nido* compounds [7-R-5,6-I_2-1,2-*nido*-$C_2B_9H_9]^-$ and [7-Ph-8,9,10,12-I_4-1,2-*nido*-$C_2B_9H_7]^-$ have been synthesized.

In this work we show a first case of an artificial large downhill sequence with well defined and characterized, and structurally very similar, individual electron donors and acceptors made from a common frame. This has been possible by using a metallacarborane cluster. There has been interest in producing systems with similar characteristics in highly prevailing electroactive frameworks such as ferrocene, C_{60}, or perylene diimide.[11] The results have been, however, very limited.[12] Metallacarboranes are part of the boron clusters family of compounds with the particularity that have a metal in its framework. Boron clusters have a molecular structure that approximates to deltahedra or to deltahedra with one or more vertices missing.

The low reduction potential of C_{60} has made it very attractive as an electron acceptor in devices,[13] whereas carboranes have not found a parallel application. On the other hand, C_{60} appeared as an excellent platform to generate a large sequential set of electron acceptors; this, however, seems to be hardly attainable.[14] Therefore, from the reduction potentials point of view, carboranes could not compete with C_{60} as electron acceptors, however the B-X bond, (X= halogen), in boron clusters is much more stable to reduction than the C-X bond in sp^2 carbon atoms and this could be taken in advantage for the boron clusters to be redox tuned.[15]

The *closo* halogenated compounds 1-R-9,12-I_2-1,2-*closo*-$C_2B_{10}H_9$ and 1-R-8,9,10,12-I_4-1,2-*closo*-$C_2B_{10}H_7$ (R= H, Me, Ph) have been synthesized as previously reported[16] and used as starting materials for partial degradation to respective *nido* clusters and subsequent complexation with Co(II) to the metallacarboranes formation.

The deboronation of these compounds with KOH-EtOH under reflux conditions for 3 h and following precipitation with $[HNMe_3]Cl$ lead to the formation of $[HN(CH_3)_3]$[7-R-5,6-I_2-7,8-*nido*-$C_2B_9H_9$] and $[HN(CH_3)_3]$[7-R-1,5,6,10-I_4-7,8-*nido*-$C_2B_9H_8$] in good to high yield (Scheme 1). Compounds **1, 4** and **7** were synthesized as previously reported. [17]

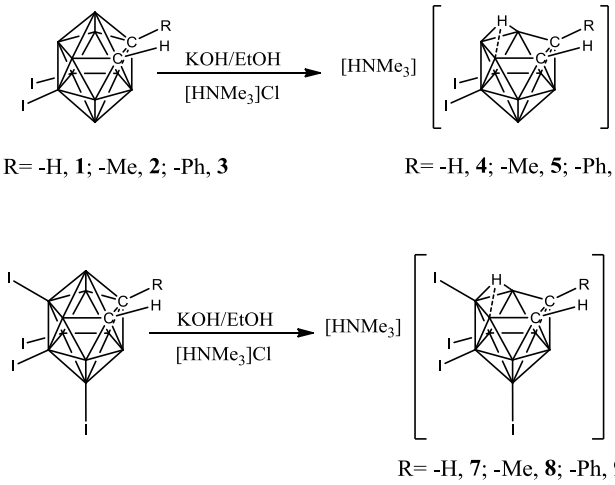

Scheme 1. Partial degradation process of iodinated *closo* carboranes 1-R-9,12-I_2-1,2-*closo*-$C_2B_{10}H_{10}$ and 1-R-8,9,10,12-I_4-1,2-*closo*-$C_2B_{10}H_8$ (R = H, Me, Ph).

Complexation reaction of each *nido* compound was performed by extracting the bridging proton with *t*BuOK or *n*-butillitium. The addition of one more equivalent of *n*-butillitium permits the trimethylamonium acidic proton extraction and consequent trimethylamine elimination in vacuum.

After the addition of $CoCl_2$ the reaction was refluxed for 15 minutes and precipitated with $[N(Me)_4]Cl$ to obtain $[N(Me)_4][3,3'\text{-Co-}(1\text{-R-}9,12\text{-}I_2\text{-}1,2\text{-}closo\text{-}C_2B_9H_9)_2]$ and $[N(Me)_4][3,3'\text{-Co-}(1\text{-R-}8,9,10,12\text{-}I_4\text{-}1,2\text{-}closo\text{-}C_2B_9H_7)_2]$ (R= H, Me, Ph) in good to high yield (Scheme 2).

Compounds [**10]** and [**13]** were synthesized as reported in the literature. [17]

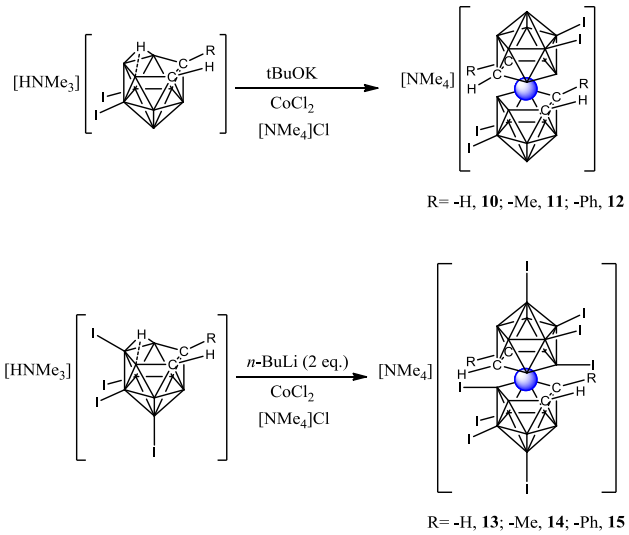

Scheme 2. Complexation reaction of *nido* clusters to metallacarboranes of Co(III) to obtain $[N(Me)_4][3,3'\text{-Co-}(1\text{-R-}9,12\text{-}I_2\text{-}1,2\text{-}closo\text{-}C_2B_9H_9)_2]$ and $[N(Me)_4][3,3'\text{-Co-}(1\text{-R-}8,9,10,12\text{-}I_4\text{-}1,2\text{-}closo\text{-}C_2B_9H_7)_2]$ (R= H, Me, Ph).

All the synthesized compounds have been fully characterized using ^1H-, ^{11}B-, ^{13}C-NMR and MALDI-TOF spectroscopy, and in the case of 1-Me-9,12-I_2-1,2-*closo*-$C_2B_{10}H_9$ and $[HNMe_3][7\text{-Ph-}1,5,6,10\text{-}I_4\text{-}7,8\text{-}nido\text{-}C_2B_9H_7]$ using X-ray diffraction.

An example of MALDI-TOF spectrum is displayed in Figure 1, showing a peak with isotopic distribution at m/z = 1332.4 corresponding to $[I_8C_4B_{18}H_{14}Co]^-$, whereas the peak at m/z = 1458.3 corresponds to $[I_8C_4B_{18}H_{14}Co + I]^-$.

Crystals suitable for X-ray diffraction of 1-Me-9,12-I_2-1,2-*closo*-$C_2B_{10}H_9$ [**2**] (Figure 2) and of the trimethylammonium salt of the protonated monoanion, $[NHMe_3][7\text{-Ph-}1,5,6,10\text{-}I_4\text{-}7,8\text{-}nido\text{-}C_2B_9H_7]$ [**9**] were grown from a chloroform solution (Figure 3).

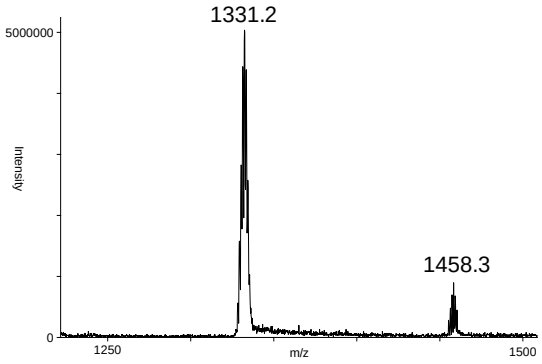

Figure 1. MALDI-TOF spectrum of $[3,3'\text{-Co-}(8,9,10,12\text{-}I_4\text{-}1,2\text{-}closo\text{-}C_2B_9H_7)_2]^-$

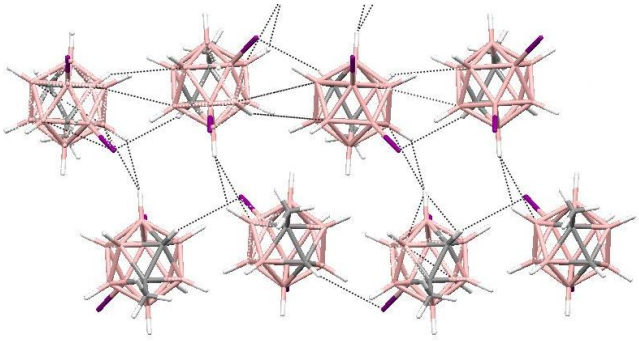

Figure 2. Crystal packing of [**2**] showing the periodical C_c-H···I-B interactions. White = H, pink = B, grey = C). Contacts shorter than the sum of Van der Waals radii (-0.2Å) are plotted as dashed dark lines.

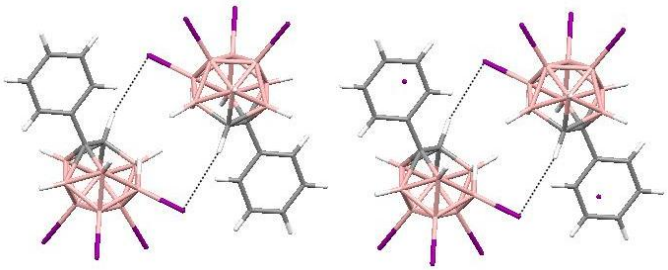

Figure 3. Crystal packing of [**9**] showing the periodical C_c-H···I-B interactions. White = H, pink = B, grey = C). Contacts shorter than the sum of Van der Waals radii (-0.2Å) are plotted as dashed dark lines.

Influence of B-I vertexes on the bridging proton of *nido* species: The bridging proton in [7,8-nido-$C_2B_9H_{12}]^-$ derivatives is relatively acidic and can be removed by the addition of a strong base. Comparing

the chemical shift (δ) of this bridging proton in unhalogenated [7,8-nido-$C_2B_9H_{12}$]$^-$ with di- and tetra-iodinated *nido* compounds, we observe that the presence of halogen groups on boron vertexes shift δ to lower fields[18] (Table 1). The presence of an iodine substituent on the open face boron vertex of *nido* compounds produces even a larger effect on the bridging proton chemical shift to lower fields compared to the di-iodinated counterparts. In addition, methyl or phenyl groups in *C*-monosubstituted *B*-iodinated *nido* carboranes produce an electron donating effect towards the cluster shifting the bridging proton signal to lower fields in comparison to *C*-unsubstituted carboranes.

Compounds	Chemical shift of bridge BHB protons (ppm)
[7,8-nido-$C_2B_9H_{12}$]$^-$	-2.90
[5,6-I_2-7,8-*nido*-$C_2B_9H_{10}$]$^-$	-2.15
[7-Me-5,6-I_2-7,8-*nido*-$C_2B_9H_9$]$^-$	-1.89
[7-Ph-5,6-I_2-7,8-*nido*-$C_2B_9H_9$]$^-$	-1.58
[1,5,6,10-I_4-7,8-*nido*-$C_2B_9H_8$]$^-$	-0.09
[7-Me1,5,6,10-I_4-7,8-*nido*-$C_2B_9H_7$]$^-$	+0.19
[7-Ph-1,5,6,10-I_4-7,8-*nido*-$C_2B_9H_7$]$^-$	+0.40

Table 1. Chemical shift of bridge BHB protons in *nido*-carboranes.

Although it is possible to calculate *nido*-carborane *p*K_a values from DFT methods,[12] can be found little experimental data in the literature. The reported *pka* value for this bridging proton in [7,8-nido-$C_2B_9H_{12}$]$^-$ is 14.25 (in water),[19] and considering the variation on δ of BHB protons on iodinated *nido* compounds we decided to study the protonation process of dicarbollide anions: [7-R-5,6-I_2-7,8-*nido*-$C_2B_9H_8$]$^{2-}$ and [7-R-1,5,6,10-I_4-7,8-*nido*-$C_2B_9H_6$]$^{2-}$ in order to determinate the acidity of the bridging proton and, consequently, the influence of iodine groups attached to boron vertexes.

A straightforward way was recording ^{11}B NMR spectra of its potassium salt in aqueous solution, as a function of *p*H. Significant shifts were observed from acidic to basic solutions. Figure 4 shows a comparison of spectra recorded from *p*H = 0 to *p*H= 8 of the dianion [1,5,6,10-I_4-7,8-*nido*-$C_2B_9H_7$]$^{2-}$ (left) and at *p*H = 3 to *p*H= 11 of the [7-Me-1,5,6,10-I_4-7,8-*nido*-$C_2B_9H_6$]$^{2-}$ (right). Spectra recorded at basic solution are identical to that of compound [$HNMe_3$][**7**] and [$HNMe_3$][**8**] indicating that the monoanions are present. The basic forms show a quite different pattern.

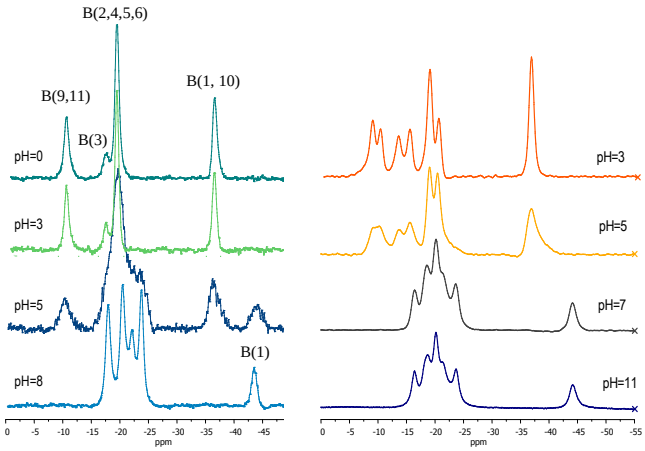

Figure 4. ^{11}B{^{1}H} NMR spectra of the acid/base pair [1,5,6,10-I_4-7,8-*nido*-$C_2B_9H_8$]$^-$/[1,5,6,10-I_4-7,8-*nido*-$C_2B_9H_7$]$^{2-}$ (left) and [7-Me-1,5,6,10-I_4-7,8-*nido*-$C_2B_9H_7$]$^-$/[7-Me-1,5,6,10-I_4-7,8-*nido*-$C_2B_9H_6$]$^{2-}$ in water. The highest field peaks in the spectra at *p*H = 3 (*ca.* -33.9 and -35.2 ppm) are assigned to the overlapped signals of B(1) and B(10). At *p*H = 8 or *p*H = 11 the peaks of B(1) are shifted to higher field (*ca.* -8 and -9.1 ppm, respectively) whereas that of B(10) are shifted to low field (*ca.* +12.0 and +15.2 ppm, respectively).

Upon deprotonation, the resonance due to B(10) are shifted to low field, whereas that of B(1) are clearly shifted upfield, in the same way as for the cases of [7,8-*nido*-$C_2B_9H_{11}$]$^{2-}$,[20] [7,8-μ-SCH_2CH_2S-7,8-*nido*-$C_2B_9H_9$]$^{2-}$ [21] and [1,2,3,4,5,6,9,10,11-I_9-7,8-*nido*-$C_2B_9H_2$]$^{2-}$.[22] A more accurate value could be determined by reacting the dianion with different acids in aqueous solution. The strongest acid which is unable to protonate [1,5,6,10-I_4-7,8-*nido*-$C_2B_9H_7$]$^{2-}$ is [NH_3OH]$^+$. In addition, acetic acid readily protonates it. Thus, *p*K_a of the bridging proton of [**7**]$^-$ must lie near 5.5, which means that iodine substitution on *nido*-carboranes enhances their acidity. Nevertheless, for the

case of $[5,6\text{-}I_2\text{-}7,8\text{-}nido\text{-}C_2B_9H_9]^{2-}$ the addition of distillated water was enough to introduce the bridging proton into the open face.

Influence of B-I vertexes on the $^{11}B\{^1H\}$-NMR spectrum: In Figure 5 can be noticed that the presence of iodine atoms attached to boron vertexes cause the ^{11}B resonance to appear at higher field in comparison to non halogenated counterparts.

Since the same effect is observed for iodinated-*nido* clusters, either for iodinated-cobaltabisdicarbollide complexes, only the iodine atom effect on boron chemical shift for *nido* compounds will be largely discussed.

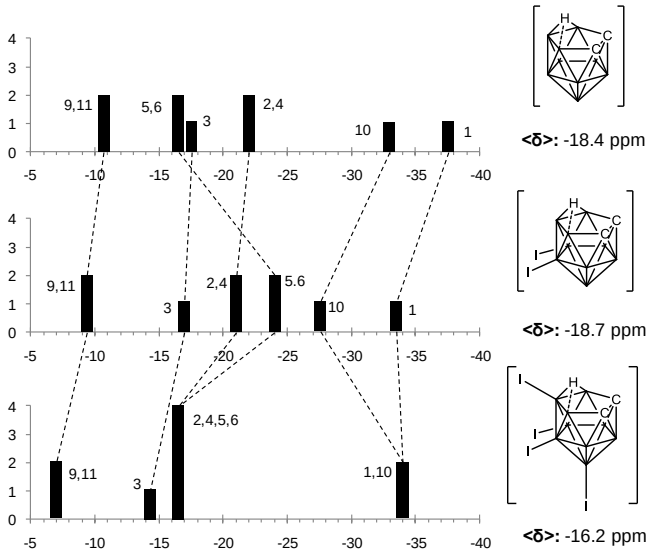

Figure 5. Diagram $^{11}B\{^1H\}$-NMR spectra with the peak assignments for the compounds: $[HN(CH_3)_3][7,8\text{-nido-}C_2B_9H_{12}]$, $[HN(CH_3)_3][5,6\text{-}I_2\text{-}7,8\text{-}nido\text{-}C_2B_9H_{10}]$ [**4**] and $[HN(CH_3)_3][1,5,6,10\text{-}I_4\text{-}7,8\text{-}nido\text{-}C_2B_9H_8]$ [**7**].

The $^{11}B\{^1H\}$-NMR spectra of $[HN(CH_3)_3][7,8\text{-nido-}C_2B_9H_{12}]$, $[HN(CH_3)_3][5,6\text{-}I_2\text{-}7,8\text{-}nido\text{-}C_2B_9H_{10}]$ [**4**], and $[HN(CH_3)_3][1,5,6,10\text{-}I_4\text{-}7,8\text{-}nido\text{-}C_2B_9H_8]$ [**7**], are in the range -7 to -38 ppm**,** characteristic of *o*-carborane *nido* species. [23] The $[HNMe_3][5,6\text{-}I_2\text{-}7,8\text{-}nido\text{-}C_2B_9H_{10}]$ spectrum displays a 2:1:2:2:1:1 pattern (low to high field), same as uniodinated *nido* cluster. Instead, for the case of $[HNMe_3][1,5,6,10\text{-}I_4\text{-}7,8\text{-}nido\text{-}C_2B_9H_8]$, the pattern is 2:1:4:2 (low to high field). For the case of $[HNMe_3][5,6\text{-}I_2\text{-}7,8\text{-}nido\text{-}C_2B_9H_{10}]$ ($\delta_{B(5,6)}$ = -24.0 ppm), the presence of iodine on B(5,6) causes the resonance to appear at clear higher field in comparison to unsubstituted $[HNMe_3][7,8\text{-nido-}C_2B_9H_{12}]$ ($\delta_{B(5,6)}$ = -16.6 ppm).

In a different way, for $[HNMe_3][1,5,6,10\text{-}I_4\text{-}7,8\text{-}nido\text{-}C_2B_9H_8]$ the presence of the iodine atoms have no significant effect on the chemical shift of B(5,6), either on B(10,1), in comparison to unsubstituted *nido* cluster. The only considerable variation observed on $^{11}B\{^1H\}$-NMR spectrum of $[HNMe_3]$[**7**], is the spectrum pattern, due to the simultaneous peak position of B(1,10) at δ = -33.9 ppm, and B(2,4,5,6) at δ = -16.4 ppm.

Influence of B-I vertexes on the redox potential $E_{1/2}(Co^{III}/Co^{II})$: The $E_{1/2}(Co^{III}/Co^{II})$ for $[3,3'\text{-Co}(1,2\text{-}C_2B_9H_{11})_2]^-$, [**10**]$^-$, [**11**]$^-$, [**12**]$^-$, [**13**]$^-$, [**14**]$^-$ and [**15**]$^-$ were experimentally determined by cyclic voltammetry and their values with regard to Fc^+/Fc are tabulated in Table 2.

Compound	$E_{1/2}$ *vs* Fc^+/Fc
$[3,3'\text{-Co}(8\text{-I-}1,2\text{-}C_2B_9H_{10})_2]^-$	-1.80
$[3,3'\text{-Co}(8\text{-I-}1,2\text{-}C_2B_9H_{10})(1,2\text{-}C_2B_9H_{11})]^-$	-1.50
$[3,3'\text{-Co}(8\text{-I-}1,2\text{-}C_2B_9H_{10})_2]^-$	-1.32
$[3,3'\text{-Co}(9,12\text{-}I_2\text{-}1,2\text{-}C_2B_9H_9)_2]^-$	-1.15
$[3,3'\text{-Co}(1\text{-Ph-}9,12\text{-}I_2\text{-}1,2\text{-}C_2B_9H_8)_2]^-$	-1.03
$[3,3'\text{-Co}(1\text{-Me-}9,12\text{-}I_2\text{-}1,2\text{-}C_2B_9H_8)_2]^-$	-1.00
$[3,3'\text{-Co}(8,9,12\text{-}I_3\text{-}1,2\text{-}C_2B_9H_8)_2]^-$	-0.82
$[3,3'\text{-Co}(8,9,10,12\text{-}I_4\text{-}1,2\text{-}C_2B_9H_7)_2]^-$	-0.68
$[3,3'\text{-Co}(1\text{-Ph-}8,9,10,12\text{-}I_4\text{-}1,2\text{-}C_2B_9H_6)_2]^-$	-0.61
$[3,3'\text{-Co}(1\text{-Me-}8,9,10,12\text{-}I_4\text{-}1,2\text{-}C_2B_9H_6)_2]^-$	-0.54

Table 2. $E_{1/2}$ data for $[3,3'\text{-Co}(I_n\text{-}1,2\text{-}C_2B_9H_{11\text{-}n})_2]^-$ (n=0,1,2,3,4) and C_c derivatives.

A representation of the $E_{1/2}(Co^{III}/Co^{II})$ values with regard to the number of iodine substituents on the platform are given in Figure 6, which indicates that each new iodine averages a shift of +0.133V, therefore

the up to now not yet produced $[Co(C_2B_9H_6I_5)_2]^-$ expectedly would have a $E_{1/2}(Co^{III}/Co^{II})$ near -0.48V (*vs* Fc^+/Fc).

Therefore just by the addition of 10 iodine substituents on boron in $[3,3'\text{-}Co(1,2\text{-}C_2B_9H_{11})_2]^-$ the $E_{1/2}(Co^{III}/Co^{II})$ drops from -1.80 V to -0.48V (*vs* Fc^+/Fc). This is an unprecedented finding that allows tuning the redox potential of a platform with a minor change in its shape and dimensions so to adjust its $E_{1/2}$ to a specific purpose.

To compare the effect on $E_{1/2}(Co^{III}/Co^{II})$ of the substitution on C instead on B in the platform, anions $[3,3'\text{-}Co(1\text{-}Ph\text{-}9,10\text{-}I_2\text{-}1,2\text{-}C_2B_9H_8)_2]^-$ [**12**], $[3,3'\text{-}Co(1\text{-}Me\text{-}9,12\text{-}I_2\text{-}1,2\text{-}C_2B_9H_8)_2]^-$ [**11**], $[3,3'\text{-}Co(1\text{-}Ph\text{-}8,9,10,12\text{-}I_4\text{-}1,2\text{-}C_2B_9H_6)_2]^-$ [**15**] and $[3,3'\text{-}Co(1\text{-}Me\text{-}8,9,10,12\text{-}I_4\text{-}1,2\text{-}C_2B_9H_6)_2]^-$ [**14**] were synthesized. The corresponding $E_{1/2}(Co^{III}/Co^{II})$ values are tabulated in Table 2. First noticeable point is that the effect of the $C_{cluster}$ substitution is an anodic shift as upon substitution on B, but it is smaller; second, the effect of –Me, near 0.07, is larger than the effect of –Ph, in the range +0.04 to +0.06.

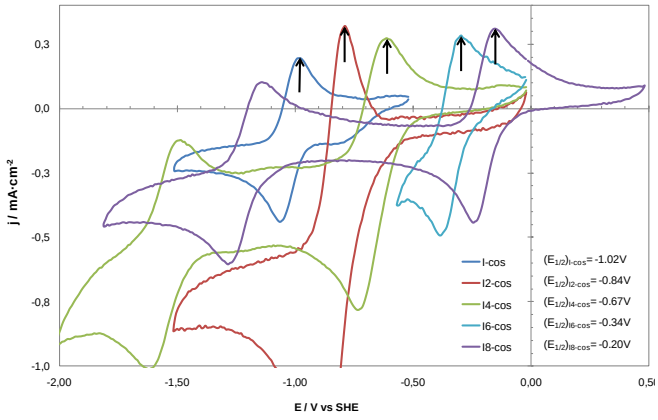

Figure 6. Cyclic voltammetries of $[3,3'\text{-}Co(I_n\text{-}1,2\text{-}C_2B_9H_{11\text{-}n})_2]^-$ (n=0,1,2,3,4) and C_c derivatives.

Experimental Section

Materials and instrumentation: All metallacarborane anions prepared are air and moisture stable. All manipulations were carried out under inert atmosphere. 1,2-dimethoxyethane (DME) and THF were distilled from sodium benzophenone prior to use. Reagents were obtained commercially and used as purchased. 1,2-*closo*-$C_2B_{10}H_{12}$, 1-Me-1,2-*closo*-$C_2B_{10}H_{12}$, 1-Ph-1,2-*closo*-$C_2B_{10}H_{12}$ were obtained from Katchem. $[5,6\text{-}I_2\text{-}7,8\text{-}nido\text{-}C_2B_9H_{10}]^-$,[17] $[1,5,6,10\text{-}I_4\text{-}7,8\text{-}nido\text{-}C_2B_9H_8]^-$,[17] $[3,3'\text{-}Co\text{-}(9,12\text{-}I_2\text{-}1,2\text{-}closo\text{-}C_2B_9H_9)_2]^-$,[17] $[3,3'\text{-}Co\text{-}(8,9,10,12\text{-}I_4\text{-}1,2\text{-}closo\text{-}C_2B_9H_7)_2]^-$,[17] $[3,3'\text{-}Co(8\text{-}I\text{-}1,2\text{-}C_2B_9H_{10})(1',2'\text{-}C_2B_9H_{11})]^-$,[24] $[3,3'\text{-}Co(8\text{-}I\text{-}C_2B_9H_{10})_2]^-$,[25] $3,3'\text{-}Co(8,9,10\text{-}I_3\text{-}1,2\text{-}C_2B_9H_8)_2]^-$,[26] were synthesised as reported at the literature.

Elemental analyses were performed using a Carlo Erba EA1108 micro analyzer. IR spectra (ν, cm^{-1}; KBr pellets) were obtained on a Shimadzu FTIR-8300 spectrophotometer. The ^1H- and $^1H\{^{11}B\}$-NMR (300.13 MHz), $^{13}C\{^1H\}$-NMR (75.47 MHz) and ^{11}B- and $^{11}B\{^1H\}$-NMR (96.29 MHz) spectra were recorded on a Bruker ARX 300 instrument equipped with the appropriate decoupling accessories. All NMR spectra were performed in deuterated acetone at 22ºC. The ^{11}B- and $^{11}B\{^1H\}$-NMR shifts were referenced to external $BF_3{\cdot}OEt_2$, while the ^1H, $^1H\{^{11}B\}$, and $^{13}C\{^1H\}$-NMR shifts were referenced to $SiMe_4$. Chemical shifts are reported in units of parts per million downfield from reference, and all coupling constants in Hz. The mass spectra were recorded in the negative ion mode using a Bruker Biflex MALDI-TOF-MS [N_2 laser; λ_{exc} 337 nm (0.5 ns pulses); voltage ion source 20.00 kV (Uis1) and 17.50 kV (Uis2)].

For voltammetric determinations, an electrochemical system, VoltaLab (Universal Electrochemical Laboratory System) interfaced with a PGZ100 potentiostat (Radiometer Analytical) and controlled by the VoltaMaster 4 software, was used. The electrochemical cell contained glassy carbon electrode as working electrode, a reference $Ag/AgCl/KCl_{sat}$ electrode and platinum wire as auxiliary electrode. The solutions were deaerated with analytical grade nitrogen at the start of each experiment to prevent oxygen interference. All experiments were performed at room temperature. All the potential values were referred to the Fc^+/Fc couple [$E_{1/2}$ (Fc^+/Fc) = 0.64 V *vs*. Standard Hydrogen Electrode (SHE)].

Synthesis of 1-Me-9,12-I_2-1,2-$C_2B_{10}H_9$ [2]: *Method A*. A thick-walled Pyrex tube charged with 1-Me-1,2-*closo*-$C_2B_{10}H_{11}$ (250 mg, 1.57 mmol) and iodine (4002 mg, 15.79 mmol) was put under vacuum, cooled down with liquid nitrogen and sealed. The tube was then placed in a furnace and the temperature was raised to 170°C during 30 minutes, maintained for 3.5 hours and allowed to drop slowly to room temperature. Then, diethyl ether enough to dissolve the product and a 10% aqueous solution of sodium metabisulphite were added to the residue. The mixture was hardly shaken and the two layers were separated. The organic layer was washed in this

way several times, until the complete quenching of the excess iodine. The organic phase was then dried over $MgSO_4$, filtered and the solvent removed under reduced pressure, to give *1-CH_3-9,12-I_2-1,2-closo-$C_2B_{10}H_9$* as a yellowish solid. (470 mg, 73 %).

Method B. A thick-walled Pyrex tube charged with 1-Me-1,2-*closo*-$C_2B_{10}H_{11}$ (250 mg, 1.57 mmol) and iodine (4002 mg, 15.79 mmol) was put under vacuum, cooled down with liquid nitrogen and sealed. The tube was then placed in a furnace and the temperature was raised to 170°C during 30 minutes, maintained for 3.5 hours and allowed to drop slowly to room temperature. Excess iodine was effectively separated by sublimation from the reaction mixture at 50 °C under reduced pressure to give *1-Me-9,12-I_2-1,2-closo-$C_2B_{10}H_9$* as a yellowish solid. (485 mg, 75 %). IR (KBr): ν= 3041 (C_c-H), 2936, 2863 (C_{alkyl}-H), 2621, 2575 (B-H). ^{1}H ($CDCl_3$): δ= 4.01 (br s, 1H, C_c-H), 3.75–1.75 (B-*H*), 1.98 (s, 3H, CH_3). ^{1}H{^{11}B} (CD_3COCD_3): δ= 4.01 (br s, 1H, C_c-H), 2.85 (br s, 2H, B-*H*), 2.78 (br s, 4H, B-*H*), 2.49 (br s, 2H, B-*H*), 1.98 (s, 3H, CH_3). ^{13}C{^{1}H} ($CDCl_3$): δ= 68.11 (s, C_c-CH_3), 59.17 (s, C_c-H), 25.49 (s, CH_3). ^{11}B ($CDCl_3$): δ= -10.5 (d, ^1J(B,H)= 156, 2B), -14.8 (d, ^1J(B,H)= 177, 2B), -15.9 (d, ^1J(B,H)=173, 2B), -16.7 (d, ^1J(B,H)=184, 2B), -18.4 (br s, 1B), -21.7 (br s, 1B). MALDI-TOF MS: *m/z*= 408.69 (23%) [M], 525.09 [M + I -B] (100%), 536.25 [M + I] (75%).

Synthesis of 1-Ph-9,12-I_2-1,2-*closo*-$C_2B_{10}H_9$ [**3**]: A thick-walled Pyrex tube charged with 1-Ph-1,2-*closo*-$C_2B_{10}H_{11}$ (250 mg, 1.12 mmol) and iodine (4002 mg, 11.29 mmol) was put under vacuum, cooled down with liquid nitrogen and sealed. The tube was then placed in a furnace and the temperature was raised to 170°C during 30 minutes, maintained for 3.5 hours and allowed to drop slowly to room temperature. Then, diethyl ether enough to dissolve the product and a 10% aqueous solution of sodium metabisulphite were added to the residue. The mixture was hardly shaken and the two layers were separated. The organic layer was washed in this way several times, until the complete quenching of the excess iodine. The organic phase was then dried over $MgSO_4$, filtered and the solvent removed under reduced pressure, to give *1-Ph-9,12-I_2-1,2-closo-$C_2B_{10}H_9$* as a brownish oil. (470 mg, 79 %). IR (KBr): ν= 3042 (aromatic CH), 2923 (C_c-H), 2610 (B-H). ^{1}H ($CDCl_3$): δ= 7.47 (d, 3H, ^3J(H,H)= 6, C_{aryl}-H), 7.39 (dd, 2H, ^3J(H,H)= 6, C_{aryl}-H), 4.38 (br s, 1H, C_c-H), 3.75–1.75 (B-*H*). ^{1}H{^{11}B} (CD_3COCD_3): δ= 7.47 (d, 3H, ^3J(H,H)= 6, C_{aryl}-H), 7.39 (dd, 2H, ^3J(H,H)= 6, C_{aryl}-H), 4.38 (br s, 1H, C_c-H), 4.38 (br s, 1H, C_c-H), 3.09 (br s, 2H, B-*H*), 3.00 (br s, 2H, B-*H*), 2.86 (br s, 2H, B-*H*), 2.76 (br s, 2H, B-*H*). ^{13}C{^{1}H} ($CDCl_3$): δ= 131.81, 131.00, 130.79, 130.05, 129.30, 127.52 (C_6H_5), 57.91 (C_c-H). ^{11}B ($CDCl_3$): δ= -5.8 (d, ^1J(B,H)= 160, 2B), -10.4, -11.4, -12.1 (6B), -14.0 (br s, 1B), -15.1 (br s, 1B).

Synthesis of [$HNMe_3$][7-CH_3-5,6-I_2-7,8-*nido*-$C_2B_9H_9$] [**5**]: To a solution of KOH (102 mg, 1.829 mmol) in degassed EtOH (5 ml) 1-Me-9,12-I_2-1,2-*closo*-$C_2B_{10}H_9$ (150 mg, 0.365 mmol) was added. The solution was refluxed for 2 h. After cooling down to room temperature, the solvent was removed under reduced pressure and the solid residue was dissolved in 10 ml of water. The solution was neutralized with HCl 0.25 M. Afterwards, aqueous solution of [$HNMe_3$]Cl was added dropwise until no more precipitate was formed. The white solid was filtered and rinsed with water to give *[$HNMe_3$][7-CH_3-5,6-I_2-7,8-nido-$C_2B_9H_9$]* (151 mg, 87%). IR (KBr): ν= 3026 (N-H), 2957 (C_c-H), 2925 (C_{alkyl}-H), 1480 (N-C), 2541 (B-H). ^{1}H (CD_3COCD_3): δ= 3.47 (s, 12H, $N(CH_3)_4$), 1.30 (s, 3H, CH_3). ^{1}H{^{11}B} (CD_3COCD_3): δ= 3.47 (s, 12H, $N(CH_3)_4$), 2.40-1.05 (s, B-H), 1.30 (s, 3H, CH_3), -1.89 (s, 1H, H_{bridge}). ^{13}C{^{1}H} ($CDCl_3$): δ= 55.38 ($N(CH_3)_4$), 23.91 (CH_3). ^{11}B ($CDCl_3$): δ= -7.6 (d, ^1J(B,H)= 144, 1B), -8.8 (d, ^1J(B,H)= 140, 1B), -12.2 (d, ^1J(B,H)=164, 1B), -16.4 (d, ^1J(B,H)=171, 1B), -20.2 (d, ^1J(B,H)=156, 1B), -23.4 (br s, 1B), -24.2 (br s, 1B), -27.3 (d d, ^1J(B,H)=138, ^1J(H,H)=34, 1B), -31.8 (d, ^1J(B,H)=150, 1B). MALDI-TOF MS: *m/z*= 398.60 [M, 100%].

Synthesis of [$HNMe_3$][7-Ph-5,6-I_2-*nido*-7,8-$C_2B_9H_9$] [**6**]: The same procedure as for the obtaining of compound [**5**] was followed. The used reactants quantities were: KOH (0.5 g, 1.06 mmol), EtOH (15 ml), 1-Ph-9,12-I_2-1,2-*closo*-$C_2B_{10}H_7$ (500 mg, 1.06 mmol). The final white solid product, *[$HNMe_3$][7-Ph-5,6-I_2-7,8-nido-$C_2B_9H_9$]* was obtained with a yield of 73% *(*395 mg). IR (KBr): ν= 3077 (N-H), 3026 (C_c-H), 2543 (B-H) 1479 (N-C). ^{1}H (CD_3COCD_3): δ= 7.22-7.07 (m, 5H,C_6H_5), δ= 3.46 (s, 12H, $N(CH_3)_4$). ^{1}H{^{11}B} (CD_3COCD_3): δ= 7.22-7.07 (m, 5H,C_6H_5), δ= 3.46 (s, 12H, $N(CH_3)_4$), 2.81-1.24 (s, B-H), -1.58 (s, 1H, H_{bridge}). ^{13}C{^{1}H} ($CDCl_3$): δ= 55.35 ($N(CH_3)_4$), 127.56, 126.65, 125.22 (C_6H_5). ^{11}B ($CDCl_3$): δ= -6.4 (d, ^1J(B,H)= 153, 1B), -8.1 (d, ^1J(B,H)= 151, 1B), -12.3 (d, ^1J(B,H)= 162, 1B), -17.7 (d, ^1J(B,H)= 162, 1B), -20.4 (d, ^1J(B,H)= 152, 1B), -22.5 (br s, 1B), -23.8 (br s, 1B), -26.4 (d d, ^1J(B,H)= 150), -30.9 (d, ^1J(B,H)= 147, 1B). MALDI-TOF MS: *m/z*= 462.81 [M, 100%].

Synthesis of [$HN(CH_3)_3$][7-Me-1,5,6,10-I_4-7,8-*nido*-$C_2B_9H_7$] [**8**]: The same procedure as for the obtaining of compound [**5**] was followed. The used reactants quantities were: KOH (0.63 g, 1.13 mmol), EtOH (5 ml), 1-Me-8,9,10,12-I_4-1,2-*closo*-$C_2B_{10}H_7$ (150 mg, 0.226 mmol). The final white solid product, *[$HNMe_3$][7-Me-1,5,6,10-I_4-7,8-nido-$C_2B_9H_7$]*, was obtained with a yield of 63% *(*100 mg, 0.14mmol). IR (KBr): ν = 3115 (s, ν(N-H)), 2923 (w, ν($C_{cluster}$-H st.)), 2865 (w, ν(C_{alkyl}-H st.)), 2555 (s, ν(B-H st.)), 1462 (w, ν(N-C)). ^{1}H-NMR (CD_3COCD_3) δ = 8.51, (t, ^{1}J(N,H) = 111, 1H,

$NH(CH_3)_3$), 3.2 (d, $^3J(H,H)$ = 3, 9H, $NH(CH_3)_3$), 2.37 (s, 3H, CH_3 $_{cluster}$). $^1H\{^{11}B\}$-NMR (CD_3COCD_3) δ = 8.51, (t, $^1J(N,H)$ = 111, 1H, $NH(CH_3)_3$), 3.2 (d, $^3J(H,H)$ = 3, 9H, $NH(CH_3)_3$), 2.60 (m, 4H, B-H), 2.37 (s, 3H, CH_3 $_{cluster}$), 2.19 (s, 1H, B-H), 0.19 (s, 1H, H_{bridge}). $^{13}C\{^1H\}$ (CD_3COCD_3): δ=45.5 (s, $HN(CH_3)_3$), 23.5 (CH_3). ^{11}B-NMR (CD_3COCD_3) δ = -7.50 (d, ^1J (B,H) = 144, 1B), -8.73 (d, ^1J (B,H) = 131, 1B), -12.18 (d, ^1J (B,H) = 195, 1B), -14.21 (d, ^1J (B,H) = 160, 1B), -17.97 (s, 2B, B-I), -17.97 (d, ^1J (B,H) = 93, 1B), -35.23 (s, 2B, B-I). MALDI-TOF-MS: m/ z (%) = 524.98 (M-I, 24%), 651.40 (M, 100%).

Synthesis of $[HN(CH_3)_3][7\text{-Ph-}1,5,6,10\text{-}I_4\text{-}7,8\text{-}nido\text{-}C_2B_9H_7]$ [**9**]: The same procedure as for the obtaining of compound [**8**] was followed. The used reactants quantities were: KOH (0.77 g, 1.38 mmol), EtOH (5 ml), 1-Ph-8,9,10,12-I_4-1,2-*closo*-$C_2B_{10}H_7$ (200 mg, 0.27 mmol). The final white solid product, *$[HNMe_3][7\text{-Ph-}1,5,6,10\text{-}I_4\text{-}7,8\text{-nido-}C_2B_9H_7]$*, was obtained with a yield of 73% *(*156 mg, 0.20 mmol). IR (KBr): ν = 3111 (s, ν(N-H)), 2548 (s, ν(B-H st.)), 1463 (w, ν(N-C)). ^{1}H-NMR (CD_3COCD_3) δ = 8.71 (s, $^1J(N,H)$ = 102, 1H, $NH(CH_3)_3$), 7.23-7.17 (m, 5H, C_6H_5), 3.19 (d, $^3J(H,H)$ = 6, 9H, $NH(CH_3)_3$). $^1H\text{-}\{^{11}B\}$-NMR (CD_3COCD_3) δ = 8.71 (s, $^1J(N,H)$ = 102, 1H, $NH(CH_3)_3$), 7.23-7.17 (m, 5H, C_6H_5), 3.19 (d, $^3J(H,H)$ = 6, 9H, $NH(CH_3)_3$), 2.93-1.2 (m, 5H, B-H), 0.4 (s, 1H, H_{bridge}). $^{13}C\{^1H\}$ (CD_3COCD_3): δ= 141.7 (C_{ipso} of C_6H_5), 128.0, 126.6, 126.1 (C_6H_5), 45.5 (s, $HN(CH_3)_3$). ^{11}B-NMR (CD_3COCD_3) δ = -6.5 (d, ^1J (B,H) = 147, 1B), -8.0 (d, ^1J (B,H) = 148, 1B), -12.4 (s, 1B, B-I), -15.5 (d, ^1J (B,H) = 135, 1B), -17.2 (m, 1B, B-I), -18.2 (m, 2B, B-H), -34.5 (s, 2B, B-I, B(1,10)).

MALDI-TOF-MS: m/ z (%) = 587 (M-I, 55%), 713 (M, 100%).

Synthesis of $[N(CH_3)_4][3,3'\text{-Co-}(1\text{-Me-}9,12\text{-}I_2\text{-}1,2\text{-}closo\text{-}C_2B_9H_8)_2]$ [**11**]: To a stirring solution of *$[HNMe_3][7\text{-Me-}5,6\text{-}I_2\text{-}7,8\text{-nido-}C_2B_9H_9]$* (120 mg, 0.25 mmol) in THF (10 ml) cooled to 0 ºC in an ice-water bath was added, dropwise, a solution of K*t*BuO in THF (1.3ml, 1M, 1.26mmol). In parallel a $CoCl_2$ (165mg, 01.26mmol) solution in THF (5ml) was prepared. The solution was then transferred via a syringe over the initial reaction mixture, previously cooled to 0 ºC. The resulted mixture was heated to reflux for 6 hours. The solvent was then removed under reduced pressure. 10ml of diethyl ether and 10ml of HCl (37%, 1M) aqueous solution were then added to the residue. The mixture was hardly shaken and the two layers separated. The organic layer was separated from the mixture and the aqueous layer was extracted with diethyl ether (3 x 10ml). The combined organic phase was dried over $MgSO_4$, filtered and the solvent removed under reduce pressure. Afterwards, an aqueous solution of $[NMe_4]Cl$ was added dropwise until no more precipitate was formed. The orange solid was filtered and rinsed with water to give *$[NMe_4][3,3'\text{-Co-}(1\text{-}CH_3\text{-}9,12\text{-}I_2\text{-}1,2\text{-closo-}C_2B_9H_8)_2]$* (165 mg, 70%). IR (KBr): ν=3020 (C_c-H), 2922, 2853 (C_{alkyl}-H), 2577 (B-H), 1479 (N-CH_3). $^1H(CD_3COCD_3)$: δ= 3.45 ($N(CH_3)_4$), 2.42 (s, 3H, $C_{cluster}$-CH_3), 2.29 (s, 3H, $C_{cluster}$-CH_3)). $^1H\{^{11}B\}$ NMR (CD_3COCD_3): 3.76-1.71 (m, B-*H*), 3.48 (s, 12H, $N(CH_3)_4$), 2.42 (s, 3H, $C_{cluster}$-CH_3), 2.29 (s, 3H, $C_{cluster}$-CH_3)) $^{13}C\{^1H\}$ NMR (CD_3COCD_3): δ=65.47 ($C_{cluster}$-CH_3), 55.52 ($N(CH_3)_4$), 54.13 ($C_{cluster}$-H), 22.45 (CH_3). ^{11}B NMR (CD_3COCD_3): δ=8.9, 5.0, -2.7, -4.2 (m, B-H), -8.8, -12.9, -14.9 (m, B-I). MALDI-TOF MS: *m/z*=1117.6 [M+2I, 47%], 990.1 [M+I, 100%], 862.6 [M, 88%].

Synthesis of $[N(CH_3)_4][3,3'\text{-Co-}(1\text{-Ph-}9,12\text{-}I_2\text{-}1,2\text{-}closo\text{-}C_2B_9H_8)_2]$ [**12**]: The same procedure as for the obtaining of compound [**11**] was followed. The used reactants quantities were: *$[HN(CH_3)_3][7\text{-Ph-}5,6\text{-}I_2\text{-}7,8\text{-nido-}C_2B_9H_9]$* (200 mg, 0.39 mmol), THF (10 ml), solution of K*t*BuO in THF (1.95 ml, 0.195 mmol), $CoCl_2$ (254 mg, 1.95 mmol), 5ml of THF, 10ml of HCl (37%, 0.25M) aqueous solution. The final orange solid compound, *$[N(CH_3)_4][3,3'\text{-Co-}(1\text{-}C_6H_5\text{-}9,12\text{-}I_2\text{-}1,2\text{-closo-}C_2B_9H_8)_2]$* was obtained with a yield of 71% (295 mg). IR (KBr): ν=3027 (C_c-H), 2951, 2923, 2854 (C_{alkyl}-H), 2558 (B-H), 1479 (**N-C**H_3). $^1H(CD_3COCD_3)$: δ=7.66-7.14 (m, 10H, C_6H_5), 4.63 (s, 2H, $C_{cluster}$-H), 3.47 ($N(CH_3)_4$). $^1H\{^{11}B\}$ (CD_3COCD_3): δ=7.66-7.14 (m, 10H, C_6H_5), 4.80-1.53 (m, B-H), 4.63 (s, 2H, $C_{cluster}$-H), 3.47 ($N(CH_3)_4$). $^{13}C\{^1H\}(CD_3COCD_3)$: δ=141.45, 140.70 ($C_{ipso}$ of C_6H_5), 129.15, 128.45, 127.97, 127.29, 125.59, 122.88 (C_6H_5), 71.29 ($C_{cluster}$-C_6H_5), 55.46 ($N(CH_3)_4$), 53.94, 50.59 ($C_{cluster}$-H). ^{11}B NMR (CD_3COCD_3): δ=9.4, 5.6, -3.7, -9.4 (m, B-H), -14.6 (s, B-I). MALDI-TOF MS: *m/z*=1115.8 [M+I, 17%]. 988.2 [M, 100%], 860.8 [M-I, 17%].

Synthesis of $[N(CH_3)_4][3,3'\text{-Co-}(1\text{-Me-}8,9,10,12\text{-}I_4\text{-}1,2\text{-}closo\text{-}C_2B_9H_6)_2]$ [**14**]: The same procedure as for the obtaining of compound [**11**] was followed. The used reactants quantities were: *$[HNMe_3][7\text{-Me-}1,5,6,10\text{-}I_4\text{-}7,8\text{-nido-}C_2B_9H_7]$* (60 mg, 0.08 mmol), THF (5 ml), solution of butyllithium in hexane (0.105ml, 1.6M, 0.168mmol), $CoCl_2$ (32.8g, 0.253mmol), 10ml of diethyl ether, 10ml of HCl (37%, 0.25M) aqueous solution. The final orange solid compound, *$[NMe_4][3,3'\text{-Co(1-Me-}8,9,10,12\text{-}I_4\text{-}1,2\text{-closo-}C_2B_9H_6)_2]$*, was obtained with a yield of 65% *(64 mg, 0.04 mmol)*. IR (KBr): ν = 3022 (w, ν($C_{cluster}$-H)), 2952, 2924, 2853 (s, ν($C_{cluster}$-CH_3), ($N(CH_3)_4$)), 2590 (s, ν(B-H)). ^{1}H-NMR (CD_3COCD_3) δ = 5.18 (s, 2H, $C_{cluster}$-H), 3.45 (s, 12H, $N(CH_3)_4$), 2.55 (s, 3H, $C_{cluster}$-CH_3). $^1H\text{-}\{^{11}B\}$-NMR (CD_3COCD_3) δ = 5.18 (s, 2H, $C_{cluster}$-H), 4.25 (s, B-H), 3.45 (s, 12H, $N(CH_3)_4$), 2,93 (s, B-H), 2.84 (s, 3H, $C_{cluster}$-CH_3), 2.55 (s, 3H, $C_{cluster}$-CH_3). $^{13}C\{^1H\}$ NMR (CD_3COCD_3): δ = 69.77 ($C_{cluster}$-CH_3), 60.66 ($C_{cluster}$-H), 55.36 ($N(CH_3)_4$), 22.42 (CH_3). ^{11}B-

NMR (CD_3COCD_3) δ = -0.5, -1.3, -3.2, -4.9 (m, B-H), -7.4, -9.4 (m, 4B, B-I), -11.7, -13.2 (m, B-H). MALDI-TOF-MS: m/ z (%) = 1363 (M, 27%), 1237 (M-I, 10%), 837 (M-4I, 100%).

Synthesis of [NMe_4][3,3'-Co-(1-Ph-8,9,10,12-I_4-1,2-*closo*-$C_2B_9H_6)_2$] [**15**]: The same procedure as for the obtaining of compound [**11**] was followed. The used reactants quantities were: *[$HNMe_3$][7-Ph-1,5,6,10-I_4-7,8-nido-$C_2B_9H_7$]* (100 mg, 0.12 mmol), THF (5 ml), solution of butyllithium in hexane (0.16ml, 1.6M, 0.258mmol), $CoCl_2$ (50.2g, 0.387mmol), 10ml of diethyl ether, 10ml of HCl (37%, 0.25M) aqueous solution. The final orange solid compound, *[NMe_4][3,3'-Co(1-Ph-8,9,10,12-I_4-1,2-closo-$C_2B_9H_6)_2$]*, was obtained with a yield of 69% *(42 mg, 0.02 mmol)*. IR (KBr): ν = 3030 (w, ν($C_{cluster}$-H)), 2952, 2923, 2853 (s, ν($N(CH_3)_4$), 2606 (s, ν(B-H). ^{1}H-NMR (CD_3COCD_3) δ = 7.26-6.98 (m, 10H, C_6H_5), 5.71 (s, 2H, $C_{cluster}$-H), 3.45 (s, 12H, $N(CH_3)_4$). $^1H\{^{11}B\}$-NMR (CD_3COCD_3) δ = 7.26-6.98 (m, 10H, C_6H_5), 5.71 (s, 2H, $C_{cluster}$-H), 4.50 (s, B-H), 2.63 (s, B-H), 2.41 (s, B-H), 3.45 (s, 12H, $N(CH_3)_4$). $^{13}C\{^1H\}$ NMR (CD_3COCD_3): δ = 137.40 (C_{ipso} of C_6H_5), 129.93, 128.73, 128.12, 127.03, 126.63 (C_6H_5) 64.01 ($C_{cluster}$-H), 55.29 ($N(CH_3)_4$). ^{11}B-NMR (CD_3COCD_3) δ = -1.89, -6.70, -11.30, -14.02 (m, 18B, B-H + B-I). MALDI-TOF-MS: m/ z (%) = 1486 (M, 17%), 1359 (M-I, 33%), 1232 (M-2I, 20%), 1104 (M-3I, 12%), 978 (M-4I, 16%), 840 (M-5I, 32%), 713 (M-6I, 100%).

X-ray structure analysis

X-ray crystal structure analyses were performed by using an Enraf Nonius CCD area detector diffractometer with MoK_α radiation (λ = 0.71073 Å) equipped with an Oxford Cryostream low-temperature unit. The data sets were corrected for abortion using SADABS program.[27] The structures were solved with the program SIR97;[28] full-least-squares refinements on F^2 were performed with SHELXL97[29] using anisotropic displacement parameters for most of the non-H atoms: two B atoms in [NMe_4][3,3'-Co-(8,9,10,12-I_4-1,2-*closo*-$C_2B_9H_7)_2$] were refinened isotropically. The hydrogen atoms were treated as riding atoms using the SHELX97 default parameters or their positional parameters were refined isotropically according to the riding model. All calculations and graphics were done at WinGX[30] platform.

1-Me-9,12-I_2-1,2-*closo*-$C_2B_{10}H_9$ [2]: $C_3H_{12}B_{10}I_2$, M_r = 410.05, monoclinic, space group $P2_1/n$, a = 8.9345(3), b = 12.7332(3), c = 11.4559 (3) Å; α = 90, β =97.6710(10), γ = 90 °, V = 1291.61 Å^3, Z = 2, T = 173(2).

[$NHMe_3$][7-Ph-1,5,6,10-I_4-7,8-*nido*-$C_2B_9H_7$] [**9**]: $C_9H_{22}B_9CoI_4N$, M_r = 749.19, monoclinic, space group $P2_1/c$, a = 13.5502(2), b = 12.3860(2), c = 14.9886(2) Å; α = 90, β = 113.7250(10), γ = 90 °, V = 2302.98 Å^3, Z = 2, T = 173(2).

Notes and references

[1] P. J. Ell and S. Gambhir, in *Nuclear Medicine in Clinical Diagnosis and Treatment*, 3rd edn, Churchill Livingstone, Oxford, UK, **2004**.

[2] S.-B. Yu and A. D. Watson, *Chem. Rev.* **1999**, *99*, 2353.

[3] (*a*) R. R. Srivastava, D. K. Hamlin and D. S. Wilbur, *J. Org. Chem.* **1996**, *61*, 9041; (*b*) *PCT Int. Appl.*, WO9526353, **1995**; *Eur. Pat. Appl.*, EP0700918, **1996**.

[4] Vaca, A.; Teixidor, F.; Kivekäs, R.; Sillanpää, R.; Viñas, C. Dalton Trans. 2006, 4884.

[5] (a) Newton, M. D.; Boer, F. P.; Lipscomb, W. N. *J. Am. Chem. Soc.* **1966**, *88*, 2353. (b) Boer, F. P.; Potenza, J. A.; Lipscomb, W. N. *Inorg. Chem.* **1966**, *5*, 1301.

[6] Potenza, J. A.; Lipscomb, W. N. *Inorg. Chem.* **1966**, *5*, 1483.

[7] F.P. Olsen, M.F. Hawthorne, *Inorg. Chem*. **1965**, 4, 1839.

[8] G. K. Semin, L. I. Zakharkin, S. I. Kuznetsov, G. G. Zhigareva, E. V. Bryukhova, *Russ. J. Gen. Chem.* **1998**, 68, 919.

[9] E. C. Santos, A. B. Pinkerton, S. A. Kinkead, P. K. Hurlburt, S. A. Jasper, C. W. Sellers, J. C. Huffman, L. J. Todd, *Polyhedron* **2000**, *19*, 1777.

[10] E. A. Mizusawa, M. R. Thompson, M. F. Hawthorne, *Inorg. Chem*. **1985**, *24*, 1911.

[11] a) Y. Araki, R. Chitta, A. S. D. Sandanayaka, K. Langewalter, S. Gadde, M. E. Zandler, O. Ito, F. D'Souza, *J. Phys. Chem. C*. **2008**, *112*, 2222-2229; b) Morisue, D. Kalita, N. Haruta, Y. Kobuke, *Chem. Commun*. **2007**, 2348-2350; c) A. Sautter, B. K. Kaletaş, D. G. Schmid, R. Dobrawa, M. Zimine, G. Jung, I. H. M. Van Stokkum, L. De Cola, R. M. Williams, F. Würthner, *J. Am. Chem. Soc*. **2005**, *127*, 6719-6729; d) T. Konishi, A. Ikeda, S. Shinkai, *Tetrahedron* **2005**, *61*, 4881-1899.

[12] a) A. Laiho, R. H. A. Ras, S. Valkama, J. Ruokolainen, R. Österbacka, O. Ikkala, *Macromolecules* **2006**, *39*, 7648-7653; b) 8. Z. R. Hong, Z. H. Huang, X. T. Zeng, *Chem. Phys. Lett.* **2006**, *425*, 62-65; c) V. Shrotriya, J. Ouyang, R. J. Tseng, G. Li, Y. Yang, *Chem. Phys. Lett.* **2005**, *411*, 138-143; d) R. H. Xie, G. W. Bryant, G. Sun, T. Kar, Z. Chen, V. H. Smith, Jr., Y. Araki, N. Tagmatarchis, H. Shinohara, O. Ito, *Phys. Rev. B: Condens. Matter. Mater. Phys.* **2004**, *69*, 201403 (4 pages).

[13] (a) T. C. Clarke, J. R. Durrant, *Chem. Reviews* **2010**, *110*, 6736-6767. (b) S. Günes, H. Neugebauer, N. S. Saricifti, *Chem. Reviews* **2007**, *107*, 1324-1338. (c) J. L. Segura, N. Martin, D. M. Guldi, *Chem. Soc. Reviews* **2005**, *34*, 31-47. (d) J. Roncali, *Chem. Soc. Reviews* **2005**, *34*, 483-495. (e) *L. Sánchez, M. Sierra, N. Martín*, A. J. Myles, T. J. Dale, J. Rebek Jr., W. Seitz, D. M. Guldi, *Angew. Chem. Int. Ed*. **2006**, *45*, 4637-4641.

[14] a) M. Zheng, F. F. Li, Z. J. Shi, X. Gao, K. M. Kadish, *J. Org. Chem.* **2007**, *72*, 2538-2542; b) M. Carano, M. Marcaccio, F. Paolucci, P. Birkett, *Photochem. Photobiol. Sci.* **2006**, *5*, 1132-1136; c) F. Zhou, G. J. Van Berkel, B. T. Donovan, *J. Am. Chem. Soc.* **1994**, *116*, 5485-5486. d) A. A. Popov, I. E. Kareev, N. B. Shustova, E. B Stukalin, S. F. Lebedkin, K. Seppelt, S. H. Strauss, O. V. Boltalina, L. Dunsch, *J. Am. Chem. Soc.* **2007,** *129*, 11551-11568.

[15] U. Páramo-Garcío, M. Ávila-Rodríguez, M. G. García-Jiménez, S. Gutiérrez-Granados, J. G. Ibáñez-Cornejo, *Electroanalysis* **2006**, *18*, 904-910.

[16] A. Vaca, F. Teixidor, R. Kivekäs, R. Sillanpää, C. Viñas, Dalton Trans., **2006**; 4884.

[17] A. Pepiol, F. Teixidor, R. Sillanpää, M. Lupu, C. Viñas, Angwandte Chemie International Edition, 2011, accepted.

[18] G. Barberà C. Viñas, F. Teixidor, A. J. Welch, G. M. Rosair, *J. Organomet. Chem*., **2001**; *40*, 6555-6562.

[19] G. G. Hlatky, D. J. Crowther, *Inorg. Synth*., **1998**; *32*, 229.

[20] M. A. Fox, A. K. Hughes, A. L. Johnson, M. A. J. Paterson, *J. Chem. Soc., Dalton Trans.*, **2002**, 2009.

[21] G. Barberà, C. Viñas, F. Teixidor, G. M. Rosair, A. J. Welch, *J. Organomet. Chem.* **2002**, *663*, 221.

[22] F. Teixidor, G. Barberà, R. Kivekäs, R. Sillanpää, C. Viñas, *Dalton Trans*. **2007**, 1668-1670.

[23] J. Buchanan, E. M. Hamilton, D. Reed, A. J. Welch, *J. Chem. Soc., Dalton Trans*. **1990**, 677.

[24] I. Rojo, F. Teixidor, C. Viñas, R. Kivekäs, R. Sillanpää, *Chem.-Eur. J.*, **2003**, *9*, 4311.

[25] I. Rojo, F. Teixidor, R. Kivekäs, R. Sillanpää, C. Vinas, *Organometallics*, **2003**, *22*, 4642.

[26] M.D. Mortimer, C.B. Knobler, M.F. Hawthorne, *Inorg. Chem.* **1996**, *35*, 5750.

[27] G. M. Sheldrick *SADABS*, University of Göttingen, Germany, **2008**.

[28] A. Altomare, M. C. Burla, M. Camalli, G. L. Cascarano, C. Giacovazzo, A. Guagliardi, A.G. G. Moliterni, G. Polidori, R. Spagna, SIR 97: A new tool for crystal structure determination and refinement. *J. Appl. Cryst.* **1999**, *32*, 115-119.

[29] G. M. Sheldrick *Acta Crystallogr. , Sect. A: Found. Crystallogr*. **2008**, *A64*, 112-122.

[30] L. J. Farrugia, WinGX suite for small-molecule single-crystal crystallography. *J. Appl.Cryst*. **1999**, *32*, 837-838.

Building Highly Dense Multibranched *o*-Carborane Derivatives by means of Kumada Cross Coupling Reaction

Ariadna Pepiol[a], Francesc Teixidor[a], Reijo Sillanpää[b], Clara Viñas[a*]

[a] *Institut de Ciencia de Materials de Barcelona (CSIC) Campus UAB, 08193 Bellaterra, Spain. e-Mail clara@icmab.es*

[b] *Department of Chemistry, University of Jyväskylä, 40351 Jyväkylä, Finland*

Abstract

o-Carborane derivatives with precisely defined patterns of substitution have been prepared from 9,12-I_2-1,2-*closo*-$C_2B_{10}H_{10}$ and 8,9,10,12-I_4-1,2-*closo*-$C_2B_{10}H_8$ by replacing the iodine atoms, bonded to adjacent boron vertices in the cluster, with allyl, phenyl and phenylethynyl groups through a Kumada cross coupling reaction. Moreover, the $C_{cluster}$–H vertices on the rigid *o*-carborane head are available as further linking points for organic moieties, hydrogen bond acceptors, transition metals, nanoparticles or surfaces. The generation of diverse macromolecules and supramolecular assemblies constitutes a main focus for our current research and related advances will be reported in the near future.

Introduction

Carborane clusters are molecules of great interest as building blocks in macromolecular and supramolecular chemistry. Moreover, despite showing remarkable chemical inertness, they can be functionalized by different straightforward reactions. Thus, a number of dendrimers,[1] macrocycles,[2] self-assembled monolayers[3] and supramolecular assemblies,[4, 5] with special mention for host-guests adducts[6] incorporating *ortho*-carboranes have been prepared and structurally characterized.

A useful and general method for the functionalization of *o*-carboranes through their boron atoms is electrophilic iodination followed by Kumada cross-coupling reaction that allows the introduction of organic moieties. This has led to mono- and disubstituted compounds, starting from 9-I-1,2- *closo*-$C_2B_{10}H_{11}$, 9,12-I_2-1,2-*closo*-$C_2B_{10}H_{10}$, 3-I-1,2-*closo*-$C_2B_{10}H_{11}$ or 3,6-I_2-1,2-*closo*-$C_2B_{10}H_{10}$,[7] but, as we are aware, never to a higher degree of substitution. Recently, we reported the regioselective synthesis of 9,12-I_2-1,2-*closo*-$C_2B_{10}H_{10}$ [**1**] and 8,9,10,12-I_4-1,2-*closo*-$C_2B_{10}H_8$ [**2**],[8] where the B–I vertices reside at the compacted adjacent positions antipodal to the two carbon atoms. By substitution of iodine with the appropriate organic groups, the *o*-carborane cluster can be envisaged as a robust dendritic core for multiple and diverse types of ramifications. Two or four arms may be densely appended to the cluster through four boron vertices located at a compact area of the cluster, whilst the two C–H vertices occupying the two positions furthest away from them remain ready for further functionalization or complexation. These prospects prompted us to study the reactivity of [**1**] and [**2**] in order to performe polyfunctionalized synthons.

Here, we report the synthesis of such structures, which may offer a unique platform for the construction

of large molecules with full control over the position of the substituents.

In the present study, both boron di- and tetraiodinated *o*-carborane have been chosen as the platform to prepare multiple regioselective derivatives with different patterns of substitution (Figure 1). It was our main target to elucidate if the highly crowded iodine atoms in a compact region of the boron cluster could be replaced. To achieve so, the cross-coupling reaction on *B*-iodinated *o*-carboranes with Grignard reagents in the presence of Pd(II) and Cu(I) catalysts was studied.

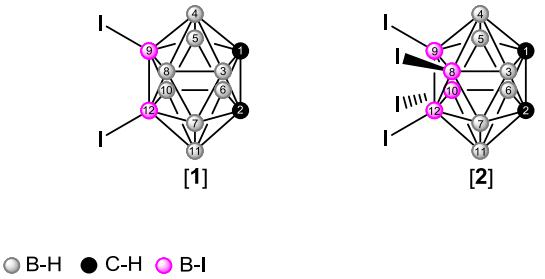

Figure 1. Vertex numbering in di- and tetra-iodinated o-carborane derivatives [**1**] and [**2**].

Results and Discussion

In order to obtain the desired products, three types of Grignard reagents were used, allylmagnesium, phenylethynylmagnesium and phenylmagnesium chlorides. The first produce a more relaxed space and, in addition it could provide ‘‘free’’ ends for further reactions whereas, the second and the third, were chosen to produce a highly congested region in *o*-carborane derivatives.

The same synthetic procedure was performed in all cases, first the corresponding organomagnesium chloride and the catalyst *cis*-$[PdCl_2(PPh_3)_2]$ were added to a solution of the *B*-iodinated derivative in anhydrous THF and the mixture was left under reflux overnight. The corresponding crude products were purified through a bed of silica, modulating the eluent polarity (Table 1).

The reaction of [**1**] with allylmagnesium chloride proceeded completely after several hours to give 9,12-$(CH_2CHCH_2)_2$-1,2-*closo*-$C_2B_{10}H_{10}$ [**3**] as a colourless oil in high yield (see Scheme 1, (i)), and 8,9,10,12-$(CH_2CHCH_2)_4$-1,2-*closo*-$C_2B_{10}H_8$ [**4**] (see Scheme 2, (i)) was synthesized according to the literature.[9]

Grignard Reagent	Reagent	Catalyst (% molar)	Purification eluent (volume)	Product	Yield (%)
CH_2=$CHCH_2MgCl$	[**1**]	4	Hexane/$CHCl_3$ (1:1)	[**3**]	92
	[**2**]	4	Hexane/$CHCl_3$ (5:1)	[**4**]	92
	[**8**]	4	Hexane/$CHCl_3$ (3:1)	[**9**]	75
PhC≡CMgCl	[**1**]	8	$CHCl_3$	[**5**]	70
	[**2**]	8	$CHCl_3$	[**6**]	65
PhMgCl	[**1**]	4	$CHCl_3$	[**7**]	72
	[**2**]	4	$CHCl_3$	[**8**]	81

Table 1. Experimental details for Palladium-catalyzed Kumada cross coupling reactions.

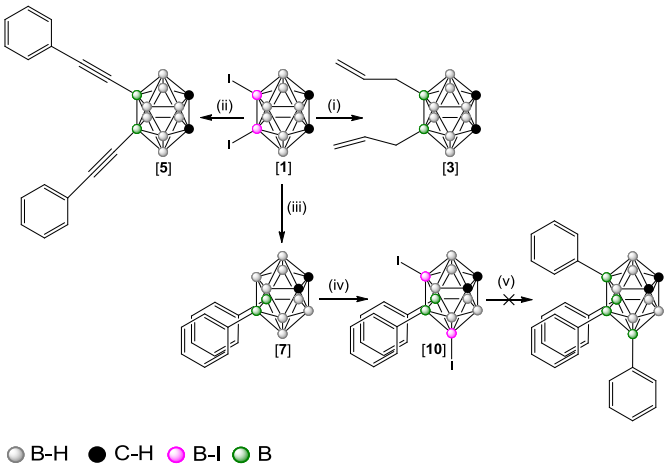

Scheme 1. Kumada cross coupling reactions on [**1**] using *cis*-$[Pd(PPh_3)_2Cl_2]$ and CuI as a catalysts, in THF refluxing overnight. (i) CH_2=$CHCH_2MgCl$, (ii) PhC≡CMgCl, (iii) PhMgCl, (iv) solvent free electrophilic iodination with I_2 (10 eq.) at 210ºC during 4h and (v) PhMgCl.

The allylation of both *o*-carborane clusters in [**3**] and [**4**] was confirmed by multinuclear NMR and FT-IR spectroscopic techniques, mass spectrometry and elemental analysis.

Crystals suitable for X-ray diffraction of compound [**4**] were obtained from the reaction mixture. The crystal structure proved the identity of [**4**] as 8,9,10,12-$(CH_2CHCH_2)_4$-1,2-*closo*-$C_2B_{10}H_8$ (Figure 2). The crystal lattice packing is directed by intermolecular interactions between the C_c-H vertexes and the terminal olefinic branches, which drives to infinite layers perpendicular to the crystallographic *bc* plane.

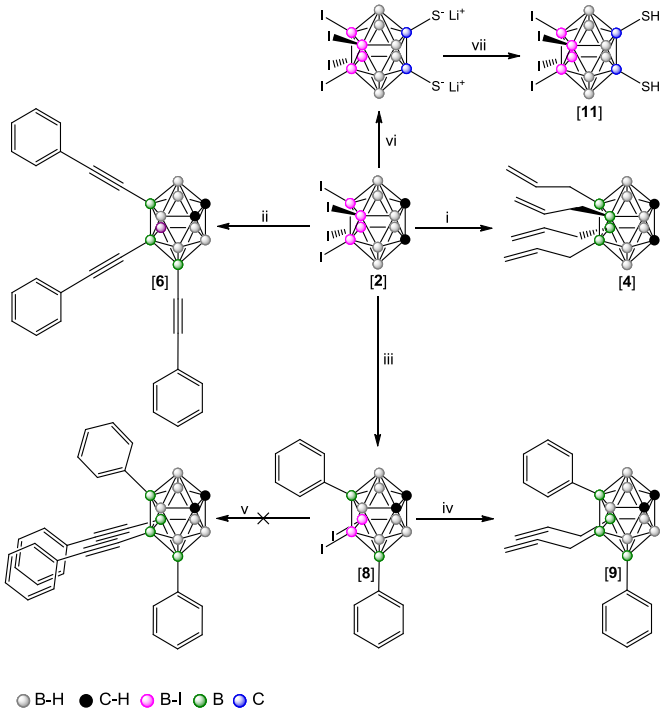

Scheme 2. Kumada cross coupling reactions on [**2**] using *cis*-$[Pd(PPh_3)_2Cl_2]$ and CuI as a catalysts, in THF refluxing overnight. (i) CH_2=$CHCH_2MgCl$, (ii) PhC≡CMgCl, (iii) PhMgCl, (iv) CH_2=$CHCH_2MgCl$ and (v) PhC≡CMgCl. *C*-dithiolation reaction of [**2**] with 2 equivalents of n-butillitium and ¼ S_8 to generate the C-dithiolate salt of [**2**] (vi) and acidification with diluted HCl to obtain tetraiodinated *C*-dithiol *o*-carborane [**11**], (vii).

While the cross coupling reaction of [**1**] with phenylethynylmagnesium chloride proceeded completely to give 9,12-$(PhC{\equiv}C)_2$-1,2-*closo*-$C_2B_{10}H_{10}$ [**5**] in good to high yield (Scheme 1, (ii)), the same coupling with [**2**] lead to the exchange of three of the four iodine atoms to give 8,9,10,12-$(PhC{\equiv}C)_3$I-1,2-*closo*-$C_2B_{10}H_8$ [**6**] (Scheme 2, (ii)). The identity of both products was confirmed by mult inuclear NMR and FT-IR spectroscopic techniques, mass spectrometry and elemental analysis. Although, the exact position of the iodine atom in the cluster remains unclear, taking into account esteric impediments in the compact region of B(9) and B(12) vertexes, one can consider the unsubstituted iodine to remain in one of these two positions.

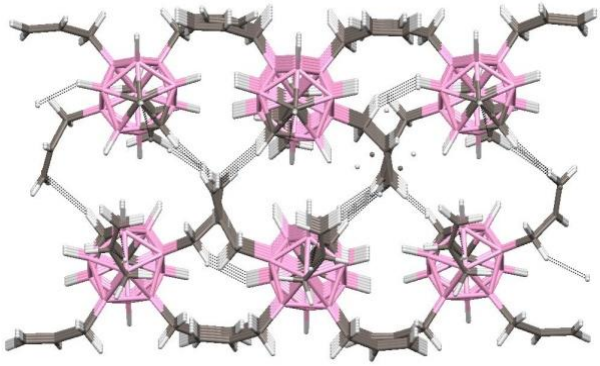

Figure 2. Crystal packing of [**4**] showing the periodical $C_{cluster}$-H/olefinic group interactions, view down crystallographic *a* axis. White = H, pink = B, grey = C). Contacts shorter than the sum of Van der Waals radii are plotted as dashed dark lines.

Crystals suitable for X-ray diffraction of compound [**5**] were grown in chloroform. Resolution of the crystal structure proved that the obtained compound was 9,12-$(PhC{\equiv}C)_2$-1,2-*closo*-$C_2B_{10}H_{10}$ [**5**]. An interesting packing driven by strong $C_{cluster}$–H/π interactions, established between $C_{cluster}$-H vertices and the centers of benzene ring planes, is observed in the crystal lattice (Figure 3). Directed by such interactions, the molecules of [**5**] pack into infinite layers perpendicular to the crystallographic *ab* plane. Thus, the crystal structure of [**5**] clearly reflects the ability of $C_{cluster}$–H vertices in *o*-carboranes to participate in non conventional hydrogen bonds with aromatic π systems. As previously reported, these interactions may serve as useful vectors in crystal engineering and supramolecular recognition. [5], [10]

In contrast, and as previously reported at the literature,[9] when [**2**] reacted with phenylmagnesium chloride, two iodine atoms were readily exchanged, but

the coupling of a third phenyl ring into the cage was extremely slow, as observed by ^{11}B NMR monitoring. The resulting diiodo-diphenyl-mixed substituted *o*-carborane was isolated and characterized by different spectroscopy techniques. The resolution of the crystal structure proved that the obtained compound was 8,10-Ph_2-9,12-I_2-1,2-*closo*-$C_2B_{10}H_8$ [**8**].

Steric hindrance could be the reason for the substitution restriction to B(8,10), since these B–I vertices are the furthest removed from each other in 2, whereas the iodine atoms at B(9,12) lie at crowded positions. The system also offers the possibility for uneven substitution, e.g., 8,10-aryl-9,12-I_2-1,2-*closo*-$C_2B_{10}H_8$ in which the two iodine atoms are ready for substitution with less crowded substituents.

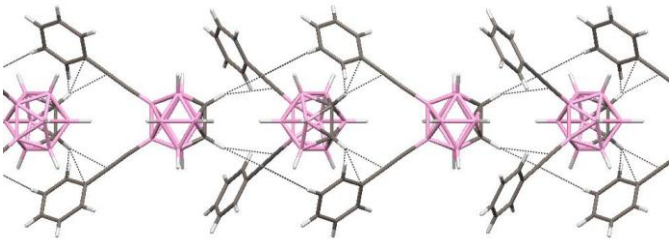

Figure 3. Crystal packing of [**5**] showing the periodical $C_{cluster}$-H/π interactions. White = H, pink = B, grey = C). Contacts shorter than the sum of Van der Waals radii are plotted as dashed dark lines.

In addition, [**8**] was also used as starting material for the cross coupling reaction with phenylethynylmagnesium chloride, but the coupling was unsuccessful since any iodine was exchanged (Scheme 2, (v)). Instead, when using a less crowded organomagnesium chloride, such as CH_2=$CHCH_2MgCl$, the coupling reaction with [**8**] lead to the formation of 8,10-Ph_2-9,12-$(CH_2CHCH_2)_2$-1,2-*closo*-$C_2B_{10}H_8$ [**9**] in good to high yields (Scheme 2, (iv)). The diallyl-diphenyl-mixed substituted *ortho*-carborane was isolated and characterised. Crystals suitable for X-ray diffraction were grown from a chloroform solution. Resolution of the crystal structure proved that the obtained compound was 8,10-Ph_2-9,12-$(CH_2CHCH_2)_2$-1,2-*closo*-$C_2B_{10}H_8$ [**9**] (Figure 4). The $C_{cluster}$–H vertices on the rigid *o*-carborane head are available as further linking points for organic moieties, hydrogen bond acceptors, transition metals, nanoparticles or surfaces. The generation of diverse macromolecules and supramolecular assemblies constitutes a main focus for our current research and related advances will be reported in the near future.

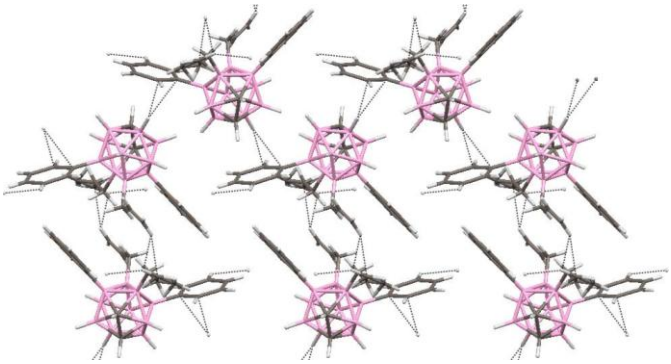

Figure 4. Crystal packing of [**9**] showing the periodical $C_{cluster}$-H/π interactions. White = H, pink = B, grey = C). Contacts shorter than the sum of Van der Waals radii are plotted as dashed dark lines.

Since the four-fold phenylation of the *o*-carborane was proved to be unsuccessful when reacting [**2**] with phenylmagnesium chloride, we design a new synthetic strategy in order to get the 8,9,10,12-Ph_4-1,2-*closo*-$C_2B_{10}H_8$. First, we perform the cross coupling reaction of [**1**] with phenylmagnesium chloride to obtain 9,12-Ph_2-1,2-*closo*-$C_2B_{10}H_{10}$ [**7**] as previously reported at the literature.[7c] Then we induce an electrophilic iodination over the unsubstituted boron vertexes B(8) and B(10) by a solvent free reaction with I_2 in a sealed tub at 210ºC during 4h, to finally obtain [**10**] in good yield (see Scheme 1, (iv)).

The different allocation of the four substituents in [**10**] may decrease the esteric effect of the two bulky phenyl groups since they are displayed in neighboring vertexes B(9,12), and the two remaining iodine atoms

are placed one far from the other, so the substitution for phenyl groups is, in principle, esterically viable. Unfortunately, the cross coupling reaction of [**10**] with PhMgCl did not lead to the expected four-fold phenylation of the *o*-carborane.

Figure 5 shows a comparison of ^{11}B NMR diagram spectra for unsubstituted *o*-carborane and two synthesized geometrical isomers [**8**] and [**10**]. While the presence of phenyl groups on B(9,12) in [**10**] and on B(8,10) on [**8**] causes the boron resonance to appear at clear lower field in comparison to unsubstituted *o*-carborane cluster (*ca.* +8 and +9 ppm, respectively), the iodine substituents on B(8,10) on [**10**] and on B(9,12) on [**8**] shift the NMR boron peak to higher field (*ca.* -11 and -8 ppm, respectively).

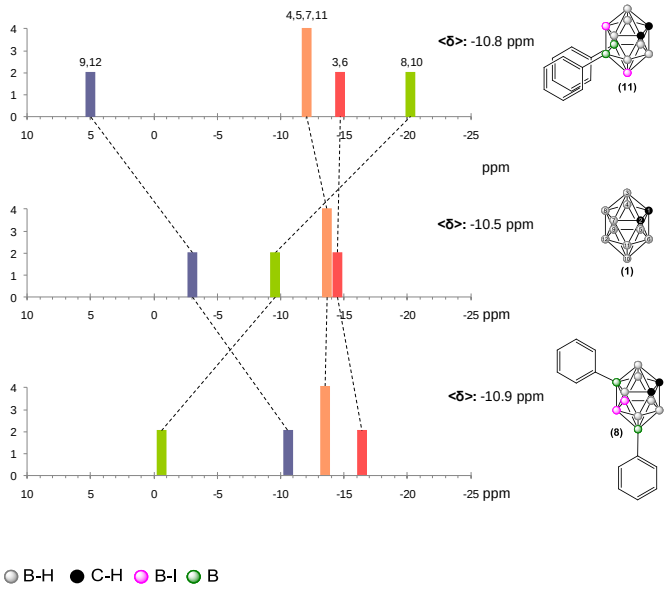

Figure 5. Diagram ^{11}B{^{1}H}-NMR spectra with the peak assignments for the *o*-carborane and the geometric isomers 8,10-I_2-9,12-Ph_2-1,2-*closo*-$C_2B_{10}H_8$ [**10**] and 8,10-Ph_2-9,12-I_2-1,2-*closo*-$C_2B_{10}H_8$ [**8**].

The di-*C*-thiolate salt of [**2**] was obtained according to an adaptation of a previously reported methodology[11] using *n*-butillitium and S_8 (see Scheme 2, (vi)). It is known that iodine substitution on the cluster boron atoms makes electron density decrease on the carbon atoms, making hydrogen atoms more acidicSo, sulfur atoms in the dithiolate salt of [**2**] are expected to be less basic, but their coordination ability is not completely lost, they can still bind to metals.

It should be noticed that the relative acidity of the C–H vertices in these clusters is useful in supramolecular chemistry, due to the possibility to participate in weak H-bonding.[5] In addition, a range of organic moieties, heteroatoms and metal centres can be bonded to the carbon atoms in straightforward pathways, *i. e.* deprotonation followed by treatment with the proper electrophile. It is our purpose to study the *C*-thiolate formation on these systems, as good coordination abilities are known for them, both to metal centres and nanoparticles.

Nevertheless, during the isolation of the corresponding dithiol by acidification of the dithiolate with diluted HCl to give 1,2-$(SH)_2$-8,9,10,12-I_4-1,2-*closo*-$C_2B_{10}H_6$ [**11**], a certain tendency to oxidation was observed, possibly due to the above mentioned decrease in the electron density of the sulfur atoms (see Scheme 2, (vii)). The oxidation reaction was forced by the use of iodine under basic conditions, giving the corresponding dimer where the carborane units are linked through disulfide bridges. [12]

Conclusion

The synthetic importance of *B*-iodo-*o*-carboranes relies on the possibility of exchanging iodine with organic moieties using the Kumada cross-coupling reaction, opening new possibilities of constructing macromolecules. These boron substituted *o*-carborane derivatives can in turn serve as synthons for many applications.

Experimental Section

Materials and instrumentation: All *o*-carboranes prepared are air and moisture stable. All manipulations were carried out under inert atmosphere. THF were distilled from sodium benzophenone prior to use. Reagents were obtained commercially and used as purchased.

1,2-*closo*-$C_2B_{10}H_{12}$ was obtained from Katchem. 9,12-I_2-1,2-*closo*-$C_2B_{10}H_{10}$ [**1**], [8] 8,9,10,12-I_4-1,2-*closo*-$C_2B_{10}H_8$ [**2**], [8] 8,9,10,12-$(CH_2CHCH_2)_4$-1,2-*closo*-$C_2B_{10}H_8$ [**4**] [9] and 8,10-Ph_2-9,12-I_2-1,2-*closo*-$C_2B_{10}H_8$ [**8**] [9] were synthesised as reported at the literature.

Elemental analyses were performed using a Carlo Erba EA1108 micro analyzer. IR spectra (ν, cm^{-1}; KBr pellets) were obtained on a Shimadzu FTIR-8300 spectrophotometer. The ^1H- and $^1H\{^{11}B\}$-NMR (300.13 MHz), $^{13}C\{^1H\}$-NMR (75.47 MHz) and ^{11}B- and $^{11}B\{^1H\}$-NMR (96.29 MHz) spectra were recorded on a Bruker ARX 300 instrument equipped with the appropriate decoupling accessories. All NMR spectra were performed in deuterated acetone at 22ºC. The ^{11}B- and $^{11}B\{^1H\}$-NMR shifts were referenced to external $BF_3{\cdot}OEt_2$, while the ^1H, $^1H\{^{11}B\}$, and $^{13}C\{^1H\}$-NMR shifts were referenced to $SiMe_4$. Chemical shifts are reported in units of parts per million downfield from reference, and all coupling constants in Hz. The mass spectra were recorded in the negative ion mode using a Bruker Biflex MALDI-TOF-MS [N_2 laser; λ_{exc} 337 nm (0.5 ns pulses); voltage ion source 20.00 kV (Uis1) and 17.50 kV (Uis2)], and using a FIA-ES/MS (Shimadzu AD VP/ API 150) instrument for neutral species.

Synthesis of 9,12-$(CH_2=CHCH_2)_2$-1,2-*closo*-$C_2B_{10}H_{10}$ [**3**]: To a stirring solution of 9,12-I_2-1,2-*closo*-$C_2B_{10}H_{10}$ (0.50 g, 1.26 mmol) in THF (10 mL) cooled to 0 ºC in an ice-water bath was added dropwise to a solution of allylmagnesium chloride in THF (2.6 mL, 2M, 5.2 mmol). After stirring at room temperature for 30 minutes, *cis*-$[PdCl_2(PPh_3)_2]$ (35.0 mg, 4% equiv.) and CuI (9.6 mg, 4% equiv.) were added in a single portion, following the reaction was heated to reflux overnight. The solvent was removed and 20 mL of diethyl ether were added to the residue. The excess of Grignard reagent was destroyed by slow addition of dilute HCl. The organic layer was separated from the mixture, and the aqueous layer was extracted with diethyl ether (3 x 10 mL). The combined organic phase was dried over $MgSO_4$, filtered and the solvent removed under reduced pressure. The crude product was dissolved in hexane/chloroform mixture (1:1 by volume, *ca*. 5 mL) and passed through a bed of silica. The solvent was removed *in vacuo* to give 9,12-$(CH_2=CHCH_2)_2$-1,2-*closo*-$C_2B_{10}H_{10}$ as a yellowish oil. Yield: 260 mg (92 %). Elemental Analysis for $C_{14}B_{10}H_{28}$: calc: C 42.50, H 8.80; found: C 42.56, H 8.27. IR (KBr): ν [cm^{-1}] =3072 (vs, $\nu_s(C_{cluster}$-H i $=CH_2)$), 2995, 2962, 2900, 2885 (vs, ν_s(=CH and $CH_2)$), 2594 (vs, ν_s(B-H)), 1633 (vs, ν_s(C=C)), 1089, 1022 (s, $\nu_{as}(=CH_2)$). ^1H NMR: δ [ppm] =5.77 (m, 2H, CH_2=C*H*-CH_2), 4.84-4.76 (m, 4H, C*H*$_2$=CH-CH_2), 3.42 (s, 2H, $C_{cluster}$-*H*), 3.10–1.00 (m, 8H, B-$H_{terminal}$), 1.64 (s, 4H, CH_2=CH-C*H*$_2$). $^1H\{^{11}B\}$ NMR: δ [ppm]=5.77 (m, 2H, CH_2=C*H*-CH_2), 4.84-4.76 (m, 4H, C*H*$_2$=CH-CH_2), 3.42 (s, 2H, $C_{cluster}$-*H*), 2.23 (s, 2H, B(3,6)-$H_{terminal}$), 2.10 (s, 2H, B(8,10)-$H_{terminal}$), 2.05 (s, 4H, B(4,5,7,11)-$H_{terminal}$), 1.64 (d, ^3J(H,H)=7.9 Hz, 4H, CH_2=CH-C*H*$_2$). $^{13}C\{^1H\}$ NMR: δ [ppm]=140.2 (s, CH_2=*C*H-CH_2), 111.8 (s, *C*H_2=CH-CH_2), 48.3 (s, $C_{cluster}$), 22.6 (m, CH_2=CH-*C*H_2). ^{11}B NMR: δ [ppm]=7.5 (s, 2B, B(9,12)), -8.6 (d, ^1J(B,H)=145 Hz, 2B, B(8,10)), -14.3 (d, ^1J(B,H)=164 Hz, 4B, B(4,5,7,11)), -16.3 (d, ^1J(B,H)=195 Hz, 2B, B(3,6)). MALDI-TOF MS: *m/z* (%)=224.4 (100) $[M-1]^-$.

Synthesis of 9,12-$(Ph\text{-}C{\equiv}C)_2$-1,2-*closo*-$C_2B_{10}H_{10}$ [**5**]**:** To a stirring solution of 9,12-I_2-1,2-*closo*-$C_2B_{10}H_{10}$ (295 mg, 0.8 mmol) in dry THF (5 mL) cooled to 0 ºC in an ice-water bath was added dropwise a solution of phenylethynylmagnesium bromide solution in THF (3 mL, 1M, 3 mmol). After stirring at room temperature for 30 minutes, *cis*-$[PdCl_2(PPh_3)_2]$ (42.0 mg, 8% equiv.) and CuI (11.4 mg, 8% equiv.) were added in a single portion, following the reaction was heated to reflux overnight. The solvent was removed and 20 mL of diethyl ether were added to the residue. The excess of Grignard reagent was destroyed by slow addition of dilute HCl. The organic layer was separated from the mixture, and the aqueous layer was extracted with diethyl ether (3 x 10 mL). The combined organic phase was dried over $MgSO_4$, filtered and the solvent removed under reduced pressure. The crude product was dissolved in chloroform (5 mL) and passed through a bed of silica. The solvent was removed *in vacuo* to give 9,12-$(Ph\text{-}C{\equiv}C)_2$-1,2-*closo*-$C_2B_{10}H_{10}$ as a brown oil. Yield: 180 mg (70 %). Elemental Analysis for $C_{18}B_{10}H_{20}$: calc: C 62.79, H 5.81; found: C 62.70, H 5.93. IR (KBr): ν [cm^{-1}] =3211 (m, $\nu_s(C_{phenyl}$-H)), 3065 (vs, $\nu_s(C_{cluster}$-H)), 2607 (vs, ν_s(B-H)), 2189 (s, ν_s(C≡C)), 1597, 1489 (vs, $\nu_s(C\text{-}C_{phenyl})$).$^1H$ NMR: δ [ppm]=7.44 (s, 2H, $H_{phenyl\text{-}para}$), 7.27 (s, 8H, $H_{phenyl\text{-}ortho}$, $H_{phenyl\text{-}meta}$), 3.43 (s, 2H, $C_{cluster}$-*H*), 2.50–1.50 (m, 8H, B-$H_{terminal}$). $^1H\{^{11}B\}$ NMR: δ [ppm]=7.44 (s, 2H, $H_{phenyl\text{-}para}$), 7.27 (s, 8H, $H_{phenyl\text{-}ortho}$, $H_{phenyl\text{-}meta}$), 3.43 (s, 2H, $C_{cluster}$-*H*), 2.58 (s, 2H, B(8,10)-$H_{terminal}$), 2.34 (s, 4H, B(4,5,7,11)-$H_{terminal}$), 2.29 (s, 2H, B(3,6)-$H_{terminal}$). $^{13}C\{^1H\}$ NMR: δ [ppm]=131.9 (s, $C_{phenyl\text{-}para}$), 128.0 (s, $C_{phenyl\text{-}ortho}$, $C_{phenyl\text{-}meta}$), 124.1 (s, $C_{phenyl\text{-}ipso}$), 48.3 (s, $C_{cluster}$). ^{11}B NMR: δ [ppm]=-0.7 (s, 2B, B(9,12)), -6.9 (d, ^1J(B,H)=125 Hz, 2B, B(8,10)), -13.5 (m, 4B, B(4,5,7,11)), -15.7 (m, 2B, B(3,6)). ESI MS: *m/z* (%)=344.3 (100) $[M-1]^-$.

Synthesis of 8,9,10,12-{$(Ph\text{-}C{\equiv}C)_3$I}-1,2-*closo*-$C_2B_{10}H_8$ [**6**]: To a stirring solution of 8,9,10,12-I_4-1,2-*closo*-$C_2B_{10}H_8$ (300 mg, 0.46 mmol) in dry THF (5 mL) cooled to 0 ºC in an ice-water bath was added dropwise a solution of phenylethynylmagnesium bromide solution in THF (5.6 mL, 1M, 5.6 mmol). After stirring at room temperature for 30 minutes, *cis*-$[PdCl_2(PPh_3)_2]$ (25.0 mg, 8% equiv.) and CuI (7.0 mg, 8% equiv.) were added in a single portion,

following which the reaction was heated to reflux overnight. The solvent was removed and 20 mL of diethyl ether were added to the residue. The excess of Grignard reagent was destroyed by slow addition of dilute HCl. The organic layer was separated from the mixture, and the aqueous layer was extracted with diethyl ether (3 x 10 mL). The combined organic phase was dried over $MgSO_4$, filtered and the solvent removed under reduced pressure. The crude product was dissolved in chloroform (5 mL) and passed through a bed of silica. The solvent was removed *in vacuo* to give 8,9,10,12-{(Ph-C≡C)$_3$I}-1,2-*closo*-$C_2B_{10}H_8$ as brown oil. Yield: 155 mg (60 %). Elemental Analysis for $C_{26}B_{10}H_{23}I$: calc: C 54.73, H 4.03; found: C 55.82, H 4.24. IR (KBr): ν [cm^{-1}] =3211 (m, ν_s($C_{aromatic}$-H)), 3059 (vs, ν_s($C_{cluster}$-H)), 2617 (s, ν_s(B-H)), 2195 (vs, ν_s(C≡C)), 1597, 1490 (vs, ν_s(C-C_{ring})).^{1}H NMR: δ [ppm]=7.41 (s, 15 H, H_{pheny}), 5.04 (s, 1H, $C_{cluster}$-*H*), 4.77 (s, 1H, $C_{cluster}$-*H*), 2.50–1.50 (m, 6H, B-$H_{terminal}$). ^{1}H{^{11}B} NMR: δ [ppm]=7.41 (s, 2H, H_{pheny}), 5.04 (s, 1H, $C_{cluster}$-*H*), 4.77 (s, 1H, $C_{cluster}$-*H*), 2.63 (s, 6H, B-$H_{terminal}$). ^{13}C{^{1}H} NMR: δ [ppm]=132.1 (s, $C_{phenyl\text{-}para}$), 128.2 (s, $C_{phenyl\text{-}ortho}$, $C_{phenyl\text{-}meta}$), 124.0 (s, $C_{phenyl\text{-}ipso}$), 46.4, 45.5 (s, $C_{cluster}$). ^{11}B NMR: δ [ppm]=0.0 (s, 2B, B(8,10)), -11.8, -6.9 (s, 2B, B(9,12)), -13.4 (d, ^{1}J(B,H)=126 Hz, 4B, B(4,5,7,11)), -16.9 (m, ^{1}J(B,H)=107 Hz 2B, B(3,6)). ESI MS: *m*/*z* (%)=570 (100) [M-1]$^-$.

Synthesis of 8,10-Ph_2-9,12-$(CH_2$=$CHCH_2)_2$-1,2-*closo*-$C_2B_{10}H_8$ [9]: To a stirring solution of 8,10-Ph-9,12-I_2-1,2-*closo*-$C_2B_{10}H_8$ (120 mg, 0.27 mmol) in THF (5 mL) cooled to 0 ºC in an ice-water bath was added, dropwise, a solution of allylmagnesium chloride in THF (0.55 mL, 2 M, 1.1 mmol). After stirring at room temperature for 30 minutes, *cis*- [$PdCl_2(PPh_3)_2$] (7.7 mg, 4% equiv.) and CuI (2.1 mg, 4% equiv.) were added in a single portion, following which the reaction was heated to reflux overnight. The solvent was removed and 5 mL of diethyl ether were added to the residue. The excess of Grignard reagent was destroyed by slow addition of dilute HCl. The organic layer was separated from the mixture, and the aqueous layer was extracted with diethyl ether (3 x 5 mL). The combined organic phase was dried over $MgSO_4$, filtered and the solvent removed under reduced pressure. The crude product was purified by flash silica gel chromatography, using hexane/chloroform (3:1 by volume) mixture as eluent, to give 8,10-Ph-9,12-$(CH_2$=$CHCH_2)_2$-1,2-*closo*-$C_2B_{10}H_8$. Yield: 130 mg (75%). Elemental Analysis for $C_{20}B_{10}H_{28}$: calc: C 63.82, H 7.45; found: C 63.97, H 7.39. IR (KBr): ν [cm^{-1}] =3200 (m, ν_s(C_{phenyl}-H)), 3065 (vs, ν_s($C_{cluster}$-H and =CH_2)), 2995, 2962, 2900, 2885 (vs, ν_s(=CH and CH_2)), 2607 (vs, ν_s(B-H)), 1633 (vs, ν_s(C=C)), 1597, 1489 (vs, ν_s(C-C_{phenyl})), 1089, 1022 (s, ν_{as}(=CH_2)). ^{1}H NMR: δ [ppm]=7.70 (m, 4H, H_{phenyl}), 7.36 (m, 6H, H_{phenyl}), 5.93 (m, 2H, CH_2=C*H*-CH_2), 4.87-4.82 (m, 4H, CH_2=CH-CH_2), 3.62 (s, 2H, $C_{cluster}$-*H*), 3.10–1.00 (m, 6H, B-$H_{terminal}$), 1.33 (s, 4H, CH_2=CH-CH_2).^{1}H{^{11}B} NMR: δ [ppm]=7.70 (m, 4H, H_{phenyl}), 7.36 (m, 6H, H_{phenyl}), 5.93 (m, 2H, CH_2=C*H*-CH_2), 4.87-4.82 (m, 4H, CH_2=CH-CH_2), 3.62 (s, 2H, $C_{cluster}$-*H*), 2.41 (br s, 4H, B(4,5,7,11)*H*), 2.32 (br s, 2H, B(3,6)*H*), 1.33 (d, ^{3}*J*(B,H)=9.0 Hz, 4H, CH_2=CH-CH_2).^{13}C{^{1}H} NMR: δ [ppm] =139.4 (s, CH_2=*C*H-CH_2), 134.3, 127.3 (C_{phenyl}), 112.4 (s, *C*H_2=CH-CH_2), 49.3 (s, $C_{cluster}$), 21.4 (br m, CH_2=CH-*C*H_2). ^{11}B NMR: δ [ppm] =7.3 (s, 2B, B(9,12)), 2.2 (s, 2B, B(8,10)-*Ph*), -14.9 (d, ^{1}*J*(B,H)=161 Hz, 4B, B(4,5,7,11)), -17.0 (d, ^{1}*J*(B,H)=167 Hz, 2B, B(3,6)). ESI MS: *m*/*z* (%)= 399.4 (100) [M+23]$^+$.

Synthesis of 9,12-Ph_2-8,10-I_2-1,2-*closo*-$C_2B_{10}H_8$ [10]: A thick-walled Pyrex tube charged with 9,12-Ph-1,2-*closo*-$C_2B_{10}H_{10}$ (50 mg, 0.2 mmol) and iodine (432 mg, 1.7 mmol) was put under vacuum, cooled down with liquid nitrogen and sealed. The tube was then placed in a furnace and the temperature gradually raised to 210ºC during 20 minutes, maintained for 5h and allowed to drop slowly to room temperature. The excess of iodine was effectively separated by sublimation from the reaction mixture a 50ºC under reduced pressure. The resulting solid was purified by thin layer chromatography (TLC), using chloroform as the eluting solvent, to give 9,12-Ph-8,10-I_2-1,2-*closo*-$C_2B_{10}H_8$. Yield: 45 mg (49%). IR (KBr): ν [cm^{-1}] = 3045 (s, $C_{cluster}$-H st.), 2972, 2924, 2858 (vs, ν_s(CH_2)), 2609 (s, B-H st.), 1430 (vs, ν_s(C-C_{phenyl})). ^{1}H NMR: δ [ppm] =7.52 (d, ^{1}J(H,H)=9 Hz, 4H, $H_{phenyl\text{-}meta}$), 7.24 (m, 6H, $H_{phenyl\text{-}ortho,para}$), 5.06 (br s, 2H, $C_{cluster}$*H*), 4.0–1.6 (br m, 6H, B*H*). ^{1}H{^{11}B} NMR: δ [ppm]=7.52 (d, ^{1}J(H,H)=9 Hz, 4H, $H_{phenyl\text{-}meta}$), 7.24 (m, 6H, $H_{phenyl\text{-}ortho,para}$), 5.06 (br s, 2H, $C_{cluster}$*H*), 3.36 (br s, 4H, B(4,5,7,11)*H*), 2.88 (br s, 2H, B(3,6)*H*).^{13}C{^{1}H} NMR: δ [ppm] =134.3, 127.9, 126.8 (C_{phenyl}), 52.7 ($C_{cluster}$). ^{11}B NMR: δ [ppm] =5.01 (s, 2B, B(9,12)-*Ph*), -12.1 (d, ^{1}*J*(B,H)=164 Hz, 4B, B(4,5,7,11)), -14.8 (d, ^{1}*J*(B,H)=186 Hz, 2B, B(3,6)). -20.1 (s, 2B, B(8,10)-*I*). ESI MS: *m*/*z* (%)= 537 (100) [M-B-H]$^-$, 547 (20) [M-H]$^-$, 663 (75) [M-B+I]$^-$.

Synthesis of 1,2-$(SH)_2$-8,9,10,12-I_4-1,2-*closo*-$C_2B_{10}H_6$ [11]: To a stirring solution of 8,9,10,12-I_4-1,2-*closo*-$C_2B_{10}H_8$ (200 mg, 0.31 mmol) in THF (5 mL) cooled to 0 ºC in an ice-water bath was added, dropwise, a solution of butyllithium in hexanes (0.41 mL, 1.6 M, 0.65 mmol). The suspension of the 1,2-dilithio derivative was stirred at room temperature for 0.5 h, then cooled again to 0 ºC, where S_8 (21.6 mg, 0.084 mmol) was slowly added. The resulting solution of the thus formed 1,2-dithiolate salt was stirred at room temperature for 0.5 h. Volatiles were removed under reduced pressure, and 5 mL of diethyl ether were added. A solution of HCl (2 mL, 0.5 M, 1 mmol) was slowly added stirring. The mixture was thoroughly

shaken, and the two layers separated. The aqueous layer was extracted with diethyl ether (3 x 5 mL). The combined organic phase was dried over $MgSO_4$, filtered and evaporated *in vacuo* to yield 1,2-$(SH)_2$-8,9,10,12-I_4-1,2-*closo*-$C_2B_{10}H_8$ (191 mg, 87%). IR (KBr), ν [cm^{-1}] = 2623 (s, S-H st.), 2513 (s, B-H st.). ^1H NMR: δ [ppm]= 5.93 (2 H, br s, SH), 4.6 – 2.2 (6 H, br m, BH). $^1H\{^{11}B\}$ NMR: δ [ppm]= 5.93 (2 H, br s, SH), 3.45 (4 H, br s, B(4,5,7,11)H), 3.12 (2 H, br s, B(3,6)H). $^{13}C\{^1H\}$ NMR: δ [ppm]= 58.1 (s, $C_{cluster}$). ^{11}B NMR: δ [ppm]= -4.2, broad shoulder at -5.3 (6 B, br m, B(3,4,5,6,7,11)), -7.5 (2 B, s), -17.4 (2 B, s). ESI MS: *m*/*z* = 710.6 ($M - H^+$, 100%).

X-ray structure analysis

X-ray crystal structure analyses were performed by using an Enraf Nonius CCD area detector diffractometer with MoK_α radiation (λ = 0.71073 Å) equipped with an Oxford Cryostream low-temperature unit. The data sets were corrected for abortion using SADABS program [21] .The structures were solved with the program SIR97[22]; full-least-squares refinements on F^2 were performed with SHELXL97[23] using anisotropic displacement parameters for most of the non-H atoms. The hydrogen atoms were treated as riding atoms using the SHELX97 default parameters or their positional parameters were refined isotropically according to the riding model. All calculations and graphics were done at WinGX [24] platform.

Notes and references

[1] a) R. Núñez, A. Gonzalez-Campo, C. Viñas, F. Teixidor, R. Sillanpää, R. Kivekäs, *Organometallics*, **2005**, *24*, 6351; b) R. Núñez, A. González, C. Viñas, F. Teixidor, R. Sillanpää, R. Kivekäs, *Org. Lett.*, **2005**, *7*, 231; c) D. Armspach, M. Cattalini, E. C. Constable, C. E. Housecroft, D. Phillips, *Chem. Commun.*, **1996**, 1823; d) M. C. Parrott, E. B. Marchington, J. F. Valliant, A. Adronov, *J. Am. Chem. Soc.*, **2005**, *127*, 12081.

[2] a) I. T. Chizhevsky, S. E. Johnson, C. B. Knobler, F. A. Gomez, M. F. Hawthorne, *J. Am. Chem. Soc.*, **1993**, *115*, 6981; b) M. A. Fox, J. A. K. Howard, J. A. H. MacBride, A. Mackinnon, K. Wade, *J. Organomet. Chem.*, **2003**, *680*, 155; c) M. J. Bayer, A. Herzog, M. Diaz, G. A. Harakas, H. Lee, C. B. Knobler, M. F. Hawthorne, *Chem. Eur. J.*, **2003**, *9*, 2732; d) C. Viñas, M. R. Cirera, F. Teixidor, R. Kivekäs, R. Sillanpää, J. Llibre, *J. Organomet. Chem.*, **1998**, *568*, 149; e) W. Jiang, I. T. Chizhevsky, M. D. Mortimer, W. L. Chen, C. B. Knobler, S. E. Johnson, F. A. Gomez, M. F. Hawthorne, *Inorg. Chem.*, **1996**, *35*, 5417; f) F. Teixidor, J. Casabó, C. Viñas, E. Sánchez, L. Escriche, R Kivekäs, *Inorg. Chem.*, **1991**, *30*, 3053; g) F. Teixidor, C. Viñas, J. Rius, C. Miravitlles, J. Casabó, *Inorg. Chem.*, **1990**, *29*, 149.

[3] a) T. Baše, Z. Bastl, Z. Plzák, T. Grygar, J. Plešek, M. J. Carr, V. Malina, J. Šubrt, J. Boháček, E. Večerníková, O. Kříž, *Langmuir*, **2005**, *21*, 7776; b) G. B. Khomutov, E. S. Soldatov, S. P. Gubin, S. A. Yakovenko, A. S. Trifonov, A. Y. Obydenov, V. V. Khanin, *Thin Solid Films*, **1998**, *329*, 550.

[4] a) R. N. Grimes, *Angew. Chem.-Int. Edit. Engl.*, **1993**, *32*, 1289; P. C. Andrews, C. L. Raston, *J. Organomet.Chem.* **2000**, *600*, 174; b) R. J. Hardie, P. D. Godfrey, C. L. Raston, *Chem.-Eur. J.*, **1999**, *5*, 1828; c) M. J. Hardie, C. L. Raston, *Chem. Commun.*, **1999**, 1153; d) R. J. Blanch, M. Williams, G. D. Fallon, M. G. Gardiner, R. Kaddour, C. L. Raston, *Angew. Chem.-Int. Edit. Engl.*, **1997**, *36*, 504.

[5] a) M. A. Fox, A. K. Hughes, *Coord. Chem. Rev.*, **2004**, *248*, 457; b) P. C. Andrews, M. J. Hardie, C. L. Raston, *Coord. Chem. Rev.*, **1999**, *189*, 169; c) G. Barberà, C. Viñas, F. Teixidor, G. M. Rosair, A. J. Welch, *J. Chem. Soc., Dalton Trans.*, **2002**, 3647.

[6] a) T. J. Wedge, M. F. Hawthorne, *Coord. Chem. Rev.*, **2003**, *240*, 111; b) M. F. Hawthorne, Z. P. Zheng, *Acc. Chem. Res.*, **1997**, *30*, 267.

[7] a) L. I. Zakharkin, A. I. Kovredov, V. A. Olshevskaya and Z. S. Shaugumbekova, *J. Organomet. Chem.*, **1982**, 226, 217; b) J. Li, C. F. Logan and M. Jones, *Inorg. Chem.*, **1991,** 30, 4866; c) Z. P. Zheng, W. Jiang, A. A. Zinn, C. B. Knobler and M. F. Hawthorne, *Inorg. Chem.*, **1995**, 34, 2095; d) G. Barberà , A. Vaca, F. Teixidor, R. Sillanpää , R. Kivekäs and C. Viñas, *Inorg. Chem.*, **2008**, 47, 7309 and references therein.

[8] A. Vaca, F. Teixidor, R. Kivekäs, R. Sillanpää and C. Viñas, *Dalton Trans*., **2006**, 4884.

[9] A. Vaca, F. Teixidor, R. Sillanpää , R. Kivekäs, C. Viñas, *Chem. Commun.*, **2011**, 47, 2252–2254.

[10] A. V. Puga, F. Teixidor, R. Sillanpaää, R. Kivekäs, M. Arca, G. Barberà and C. Viñas, *Chem.–Eur. J.* **2009**, *15*, 9764.

[11] F. Teixidor, G. Barberà, C. Viñas, R. Sillanpää, R. Kivekäs, *Inorg. Chem.*, **2006**, *45*, 3496.

[12] F. Teixidor, R. W. Rudolph, *J. Organomet. Chem.*, **1983**, *241*, 301.

[13] G. M. Sheldrick *SADABS*, University of Göttingen, Germany, **2008**.

[14] A. Altomare, M. C. Burla, M. Camalli, G. L. Cascarano, C. Giacovazzo, A. Guagliardi, A.G. G. Moliterni, G. Polidori, R. Spagna, SIR 97: A new tool for crystal structure determination and refinement. *J. Appl. Cryst.* **1999**, *32*, 115-119.

[15] G. M. Sheldrick *Acta Crystallogr. , Sect. A: Found. Crystallogr.* **2008**, *A64*, 112-122.

[16] L. J. Farrugia, WinGX suite for small-molecule single-crystal crystallography. *J. Appl.Cryst.* **1999**, *32*, 837-838.

[17] G. M. Sheldrick *SADABS*, University of Göttingen, Germany, **2008**.

[18] A. Altomare, M. C. Burla, M. Camalli, G. L. Cascarano, C. Giacovazzo, A. Guagliardi, A.G. G. Moliterni, G. Polidori, R.

Spagna, SIR 97: A new tool for crystal structure determination and refinement. *J. Appl. Cryst.* **1999**, *32*, 115-119.

[19] G. M. Sheldrick *Acta Crystallogr., Sect. A: Found. Crystallogr*. **2008**, *A64*, 112-122.

[20] L. J. Farrugia, WinGX suite for small-molecule single-crystal crystallography. *J. Appl.Cryst*. **1999**, *32*, 837-838.

[21] G. M. Sheldrick *SADABS*, University of Göttingen, Germany, **2008**.

[22] A. Altomare, M. C. Burla, M. Camalli, G. L. Cascarano, C. Giacovazzo, A. Guagliardi, A.G. G. Moliterni, G. Polidori, R. Spagna, SIR 97: A new tool for crystal structure determination and refinement. *J. Appl. Cryst.* **1999**, *32*, 115-119.

[23] G. M. Sheldrick *Acta Crystallogr. , Sect. A: Found. Crystallogr*. **2008**, *A64*, 112-122.

[24] L. J. Farrugia, WinGX suite for small-molecule single-crystal crystallography. *J. Appl.Cryst*. **1999**, *32*, 837-838.

Supporting Information

Table S1. ^{11}B- NMR chemical shifts (in ppm) for several 9,12-R_2-1,2-*closo*-$C_2B_{10}H_{10}$ and 8,9,10,12-R_4-1,2-*closo*-$C_2B_{10}H_8$ derivatives related to the parent *o*-carborane. Spectra were run in acetone-d_6 solutions.

Compound	Substituent	B(3,6)	B(4,5,7,11)	B(8,10)	B(9,12)	<δ>
1,2-*closo*-$C_2B_{10}H_{12}$	H	-14.3	-13.6	-9.6	-3.1	-10.8
[**1**]	9,12-I_2	-14.2	-12.8	-6.3	-14.9	-12.2
[**2**]	8,9,10,12-I_4	-13.2	-9.5	-16.3	-7.1	-11.1
[**3**]	9,12-$(CH_2{=}CHCH_2)_2$	-16.3	-14.3	-8.6	7.5	-9.2
[**4**]	8,9,10,12-$(CH_2{=}CHCH_2)_4$	-17.8	-13.7	1.9	7.8	-7.1
[**5**]	9,12-$(PhC{\equiv}C)_2$	-15.7	-13.5	-6.9	-0.7	-10.1
[**6**]	8,9,10,12-$(PhC{\equiv}C)_3I$	-16.9	-13.4	0.0	-6.9, -11.8	-10.6
[**7**]	9,12-Ph_2	-15.2	-13.0	-8.8	8.3	-8.3
[**8**]	8,10-I_2-9,12-Ph_2	-14.8	-12.1	-20.1	5.0	-10.8
[**9**]	8,10-Ph_2-9,12-$(CH_2{=}CHCH_2)_2$	-17.0	-14.9	2.2	7.3	-10.6
[**10**]	8,10-Ph_2-9,12-I_2	-16.3	-13.4	-0.6	-10.6	-10.9
[**11**]	1,2-$(SH)_2$-8,9,10,12-I_4	-8.2	-4.0, -5.7	-16.2, -17.2	-7.1	-8.5

Table S2. ^{1}H-, ^{13}C{^{1}H}- NMR and in acetone-d_6 (ppm) and stretching frequencies in (cm^{-1}) for several 9,12-R_2-1,2-*closo*-$C_2B_{10}H_{10}$ and 8,9,10,12-R_4-1,2-*closo*-$C_2B_{10}H_8$ derivatives related to the parent *o*-carborane. *Spectra run in $CDCl_3$ solutions.

		δ (^{1}H) ppm	**δ (^{13}C{^{1}H})**	**υ (cm^{-1})**	
Compost	**Substituents**	$C_{clúster}$-*H*	*C*$_{clúster}$-H	υ (C_c-*H*)	υ (B-H)
1,2-*closo*-$C_2B_{10}H_{12}$	H	3.65	56.1	3070	2576
[**1**]	9,12-I_2	5.15	54.5	3060, 3037	2645, 2611
[**2**]	8,9,10,12-I_4	5.57	56.2	3024	2623
[**3**]	9,12-$(CH_2{=}CHCH_2)_2$	3.42*	48.3*	3072	2594
[**4**]	8,9,10,12-$(CH_2{=}CHCH_2)_4$	3.37*	46.5*	3072	2617, 2596
[**5**]	9,12-$(PhC{\equiv}C)_2$	3.43	48.3	3065	2607
[6]	8,9,10,12-$(PhC{\equiv}C)_3I$	5.04, 4.77	46.4, 45.5	3059	2617
[7]	9,12-Ph_2	4.67	51.5	3069	2610
[8]	8,10-I_2-9,12-Ph_2	5.38	56.3	3046	2609
[9]	8,10-Ph_2-9,12-$(CH_2{=}CHCH_2)_2$	3.62	49.3	3065	2607
[10]	8,10-Ph_2-9,12-I_2	5.06	52.7	3047	2600
[**11**]	1,2-$(SH)_2$-8,9,10,12-I_4	-	57.1	-	2513

Table S3. Crystallographic Data and Structural Refinement Details for Compounds ,9,10,12-$(CH_2CHCH_2)_4$-1,2-*closo*-$C_2B_{10}H_8$ [**4**], 9,12-$(PhC{\equiv}C)_2$-1,2-*closo*-$C_2B_{10}H_{10}$ [**5**] and 8,10-Ph_2-9,12-$(CH_2CHCH_2)_2$-1,2-*closo*-$C_2B_{10}H_8$ [**9**].

Compound	**[4]**	**[5]**	**[9]**
empirical formula	$C_{14}H_{28}B_{10}$	$C_{18}B_{10}H_{20}$	$C_{20}B_{10}H_{28}$
formula weight	304.48	344.46	376.54
space group	P 2_1/c	P n m a	C 2/c
a (Å)	9.3307(3)	28.315(8)	18.046(4)
b (Å)	13.4930(4)	21.003(6)	11.550(2)
c (Å)	30.6348(10)	8.077(2)	24.941(5)
β (deg)	90.729	90	106.334(3)
V (Å^3)	3856.58	4803.39	4988.67
Z	8	4	8
T (ºC)	21	21	21
R-Factor (%)	10.64	7.78	9.31

Synthesis “on Demand” of Unimolecular Nanoparticles as a Versatile Dendritic Precursors

Ariadna Pepiol[a], Francesc Teixidor[a], Reijo Sillanpää[b], Clara Viñas[a*]

[a] *Institut de Ciencia de Materials de Barcelona (CSIC) Campus UAB, 08193 Bellaterra, Spain. e-Mail clara@icmab.es*
[b] *Department of Chemistry, University of Jyväskylä, 40351 Jyväkylä, Finland*

Abstract

Precisely defined patterns of substitution on terminal olefinic groups have been performed either with Heck cross coupling reactions and hydroxylations. This leads to new versatile dendritic precursors with terminal hydroxyl groups in which higher generations could be attained from it. Polyanionic species have been obtained in high yield by a new route in the ring-opening reaction of cyclic oxonium [3,3′-Co(8-$C_4H_8O_2$-1,2-$C_2B_9H_{10}$)(1′,2′-C_2B_9-H_{11})] by using hydroxyl terminal groups as nucleophiles. These new polyanionic compounds that contain multiple metallacarborane clusters at their periphery may prove useful as new classes of boron neutron capture therapy compounds with enhanced water solubility and as a core to make a new class of dendrimers.

Introduction

Carboranes are molecules with unique structural features due to their rigid geometry and rich derivative chemistry, which make them of great interest as building blocks for macromolecular or supramolecular entities.[1] Of particular interest is the generation of dendrimers of high boron content, given their potential use in boron neutron capture therapy (BNCT).[2] This has been usually achieved by bonding boron cluster units to the periphery of dendritic compounds or precursors.[3] In addition, globular dendrimers with twelve identical branches appending from a central icosahedral closo-borane cluster (closomers) have been produced. [4] Nevertheless, much less attention has been paid to carboranes as cores or focal points for dendrimer growth, despite their possibilities for multiple and versatile functionalization.

Derivatization reactions on the o-carborane cluster (1,2-*closo*-$C_2B_{10}H_{12}$) can be executed on either carbon or boron vertices. [6] In most of the occasions these transformations are carried out through the carbon atoms, whereas the chemistry of boron-substituted o-carboranes is relatively underdeveloped.

In this regard, we have recently reported the synthesis of dendrons where o-carborane cluster carbon atoms are located at the focal points. [5] Subsequently, we became interested in exploring similar molecular construction from the boron vertices of the cluster.

B–H vertices in o-carboranes exhibit electrophilic substitution chemistry in many ways reminiscent of arenes.[7] Furthermore, boron vertices react at different rates depending on their position in the cluster, [8] which may enable an accurate control of the degree and regioselectivity of substitution, while maintaining the integrity of the underlying geometry.

A useful and general method for the

functionalization of *o*-carboranes through their boron atoms is electrophilic iodination followed by Kumada cross-coupling reaction that allows the introduction of organic moieties. This has led to di- and tetrasubstituted compounds, starting from 9,12-I_2-1,2-*closo*-$C_2B_{10}H_{10}$, 8,9,10,12-I_4-1,2-*closo*-$C_2B_{10}H_8$,[9] where the B–I vertices reside at the compacted adjacent positions antipodal to the two carbon atoms. By substitution of iodine with the appropriate organic groups, the *o*-carborane cluster can be envisaged as a robust dendritic core for multiple and diverse types of ramifications.

Kumada cross coupling reaction with allylmagnesium chloride lead to the formation of 9,12-$(CH_2CHCH_2)_2$1,2-*closo*-$C_2B_{10}H_{10}$ [**1**][10] and 8,9,10,12-$(CH_2CHCH_2)_4$-1,2-*closo*-$C_2B_{10}H_8$ [**2**],[10] as illustrated in Scheme 1.

In this work we perform further reactions on the terminal olefinic groups with two different synthetic pathways, a Heck cross coupling reactions with organic moieties and a transformation of the double bonds to hydroxyl groups. Afterwards, in order to set up new versatile dendritic precursors we perform several functionalization reactions of the terminal hydroxyl groups to attain higher generations from it.

Results and Discussion

Heck cross coupling reaction on terminal olefinic groups. Heck reaction, which was discovered by Mizokori in 1971[11] and later improved by Heck in 1972,[12] allows the formation of new C-C bonds by cross-coupling of aryl halides with alkenes, due to the action of catalytic palladium. Over the years, this reaction has been developed and optimized to make possible the coupling of olefins with less reactive halides such as bromides,[13] chlorides[14] or even with vinyl halides. [15] Generally Heck reactions enable a highly regioselective and stereospecific introduction of aryl groups into double bonds. However, many factors can influence on the development of the catalytic cycle giving rise to the possible formation of undesired byproducts, factors such as the temperature, the palladium complex, the aryl halide, the base involved in the regeneration process of palladium active species, among others.

In the present study, phenyl groups has been successfully coupled to both branches of [**1**] through a Heck cross-coupling reaction with phenyl iodide as a coupling agent and 2,6-lutidine as a base, thus obtaining 9,12-$(PhCH_2CHCH_2)_2$1,2-*closo*-$C_2B_{10}H_{10}$ [**3**] in acceptable yield, 65%, as shown in Scheme 2.

In contrast, only two of the four branches of 8,9,10,12-$(CH_2CHCH_2)_4$-1,2-*closo*-$C_2B_{10}H_8$ [**2**] have been coupled to phenyl groups to achieve 8,9,10,12-$(PhCH_2CHCH_2)_2(CH_2CHCH_2)_2$-1,2-*closo*-$C_2B_{10}H_8$ [**4**] in 54% yield.

Synthesized compounds [**3**] and [**4**] have been fully characterized by multinuclear NMR and FT-IR spectroscopic techniques, mass spectrometry and elemental analysis. However, the position of the two unsubstituted branches in the cluster remains unclear, but taking into account the esteric impediments in the compact region of B(9) and B(12) vertexes, one can consider the terminal olefinic branches remain in these two positions.

MALDI-TOF spectra are displayed in Figure 1, showing a peak with isotopic distribution at m/z 376.84 corresponding to $[C_{20}H_{30}B_{10}+H]^+$ of [**3**], on the left, and m/z 457.20 corresponding to $[C_{26}H_{38}B_{10}+H]^+$ of [**4**], on the right.

Hydroboration/oxidation reaction on terminal olefinic groups. The terminal olefinic groups in [**1**] and [**2**] are free to perform further reactions on them, enabling the *ortho*-carborane cluster to become the core for the design of a new type of dendrimers, having a

rigid head and four branches appending from it.

As a first approach to the development of these molecules a hydroboration/oxidation reaction has been carried out to transform the terminal double bonds to hydroxyl groups. BH3·THF was used as the hydroborating agent. Subsequent oxidation was performed by treatment with H_2O_2 in a basic aqueous solution.

After work up, crystalline white solids were obtained. The spectroscopic characterization revealed that the reaction had proceeded through specific anti-Markovnikov additions, yielding pure 9,12-($HOCH_2CH_2CH_2$)$_2$-1,2-*closo*-$C_2B_{10}H_{10}$ [**5**] and 8,9,10,12-($HOCH_2CH_2CH_2$)$_4$-1,2-*closo*-$C_2B_{10}H_8$ [**6**], [10] i.e. with all hydroxyl groups at terminal positions (see Scheme 3).

No hindered hydroboranes were thus needed for the control of the regioselectivity. This anticipates a versatile chemistry for dendritic growth, given the availability of the four terminal hydroxyl groups for further elongation of the chains. Moreover, the $C_{cluster}$–H vertices on the rigid head remain ready for derivatization or supramolecular assembly. The *o*-carborane cluster then provides a unique platform for the construction of highly dense multibranched molecules with a wide range of possibilities for derivatization. Derivatives of *o*-carborane with precise patterns of substitution can be prepared by judicious choice of the synthetic procedure. We have coupled four hydroxyl terminated arms onto a specific, compact area of the cluster occupied by two and four adjacent boron vertices, ultimately leading to a structure which might serve as a versatile dendritic precursor.

Exchanging terminal hydroxyl unites for better leaving groups: chlorination, bromination and tosylation. The generation of diverse macromolecules and supramolecular assemblies constitutes a main focus for our current research. To achieve this proposal, the insertion of new functional better leaving groups into terminal positions of the cluster branches was required, in order to make the dendron nucleolus grow in a divergent way and to construct dendrimer structures. Substitution of the terminal hydroxyl unites in [**5**] and [**6**] for chloride, bromide or tosyl groups enable the dendrimer growth by subsequent coupling reaction with nucleophilic agents.

Chlorination in [**5**] and [**6**] has been achieved by adding $SOCl_2$ and a non nucleophilic base in a catalytic proportion, such as NBu_4Cl, leading to the formation of 9,12-($ClCH_2CH_2CH_2$)$_2$-1,2-*closo*-$C_2B_{10}H_{10}$ [**7**] and 8,9,10,12-($ClCH_2CH_2CH_2$)$_4$-1,2-*closo*-$C_2B_{10}H_8$ [**8**] in good to high yield, over 90% in both cases (see Scheme 4 and 5, (i)). Crystals suitable for X-ray diffraction of compound [**8**] were grown in hexane. Resolution of the crystal structure showed two clusters for unite cell and proved that the four-fold chlorination was achieved.

The crystal packing is driven by intermolecular interactions between the hydrogen of the carbon clusters and chlorine atoms. In the structure of [**8**] the intermolecular C_c-H···Cl-C hydrogen bonds link molecules together into chains perpendicular to the crystallographic *ab* plane.

In the other hand, Apple reaction[16] has been carried out in order to exchange terminal hydroxyl groups in [**5**] and [**6**] by bromide atoms, using PPh_3 and CBr_4 to achieve 9,12-($BrCH_2CH_2CH_2$)$_2$-1,2-*closo*-$C_2B_{10}H_{10}$ [**9**] and 8,9,10,12-($BrCH_2CH_2CH_2$)$_4$-1,2-*closo*-$C_2B_{10}H_8$ [**10**] (Scheme 4 and 5, (ii)). Only for the compound [**6**] a four-fold tosylation has been performed with tosil chloride, NEt_3 as a base and NMe_3Cl as a catalyst base, [17] obtaining 8,9,10,12-($TsOCH_2CH_2CH_2$)$_4$-1,2-*closo*-$C_2B_{10}H_8$ [**11**] in good yield (Scheme 5, (iii)).

In Figure 3, $^{13}C\{^1H\}$-NMR spectra of [**6**], [**8**], [**10**] and [**11**] are displayed. Halogenated terminal methylene groups (chlorinated or brominated) are shifted to higher

field (*ca*. -17.2 and -27.7 ppm, respectively) in comparison to hydroxylated methylene in [**6**] which appears at +64.5 ppm. In contrast, tosylated methylene unites are shifted to lower field (*ca*. +8.2 ppm) in comparison to [**6**].

Oxidation reaction on terminal hydroxyl groups. Jones reagent, [18] which consists of a chromium oxide (VI) and dilute sulphuric acid in acetone solution, has been used to oxidize hydroxyl groups of [**6**] into carboxylic acid units to obtain 8,9,10,12-$(HOCOCH_2CH_2)_4$-1,2-*closo*-$C_2B_{10}H_8$ [**12**] (Scheme 5, (iv)). Again, this molecule allows the dendritic growth over the four branches regioselectively extended on furthest boron vertexes from carbon cluster. Besides, two carbon vertexes remain intact and available to be functionalized either to anchor them on surfaces or to establish supramolecular interactions through hydrogen bonds.

Steglich esterification reaction. Derivatization reaction of terminal hydroxyl unites by Steglich esterification[19] process with benzoic acid has been successfully accomplished. Instead of carrying out a traditional pyridine-based esterification reaction, which can cause partial degradation on *closo* clusters, Steglich kind was choosen. N,N-dimethylaminopyridine (DMAP) was used as a catalyst base and N,N'-dicyclohexylcarbodiimide (DCC) as a coupling reagent. No partial degradation was detected when Steglich esterification was performed on [**5**] and [**6**]. The only by-product derived from the reaction was diciclohexilurea, which being insoluble in CH_2Cl_2 solvent, was removed by filtration. This procedure leads to the formation of 9,12-$(PhCOOCH_2CH_2CH_2)_2$-1,2-*closo*-$C_2B_{10}H_{10}$ [**13**] (Scheme 4, (iii)) and 8,9,10,12-$(PhCOOCH_2CH_2CH_2)_4$-1,2-*closo*-$C_2B_{10}H_8$ [**14**] (Scheme 5, (v)) in yields slightly higher than 60% in both cases.

Nucleophilic oxonium ring-opening reaction on [3,3′-Co(8-$C_4H_8O_2$-1,2-$C_2B_9H_{10}$)(1′,2′-$C_2B_9H_{11}$)].

Since the discovery of nucleophilic oxonium ring-opening (ORO) reactions in the carborane and metallacarborane series by Plešek et al.,[20] it has elapsed more than 30 years. These reactions represent an important feature of substitution boron chemistry and many examples can be found in the literature.[21-27] Moreover, a recent exhaustive review by Semioshkin et al. [28] has been published on this field. In this paper, we would like to extend this viable structural feature by our results on the isolation of di- and tetranions of structures combining both the [3,3′-Co(8-$C_4H_8O_2$-1,2-$C_2B_9H_{10}$)(1′,2′-C_2B_9-H_{11})] and *o*-carborane derivatives structural motifs. We are interested in exploring the possibility of using both known and new types of nucleophiles to get high-boron-content compounds. In order to enchance the nucleophilic character of the terminal hydroxyl groups of [**5**] and [**6**] we used *n*-BuLi to deprotonate the nucleophile. The addition of the base was done dropwise at low temperatures, and it was left stirring for 1 h. Afterwards, the reaction was cooled down again to 0 °C, followed by the addition of [3,3′-Co(8-$C_4H_8O_2$-1,2-$C_2B_9H_{10}$)(1′,2′-C_2B_9-H_{11})]. After stirring at room temperature for 30 minutes, compounds $[N(CH_3)_4]_2$[9,12-(3,3'-Co-{8-($C_4H_8O_2$-1,2-$C_2B_9H_{10}$-1',2'-$C_2B_9H_{11}$}-$O(CH_2)_3)_2$-1,2-$C_2B_{10}H_{10}$] [**15**] and $[N(CH_3)_4]_4$[8,9,10,12-(3,3'-Co-{8-($C_4H_8O_2$-1,2-$C_2B_9H_{10}$-1',2'-$C_2B_9H_{11}$}-$O(CH_2)_3)_4$-1,2-$C_2B_{10}H_8$] [**16**] were isolated by a cationic metathesis to tetramethylammonium salts, getting in all cases orange solids as the final product.

It is evident that the formation of these anions is a consequence of the attack of the nucleophilic hydroxylate anions [9,12-$(OCH_2CH_2CH_2)_2$-1,2-*closo*-$C_2B_{10}H_{10}]^{2-}$ and [8,9,10,12-$(OCH_2CH_2CH_2)_4$-1,2-*closo*-$C_2B_{10}H_8]^{4-}$ at one of the dioxane carbon atoms adjacent to the oxonium O atom in structure [3,3′-Co(8-$C_4H_8O_2$-

1,2-$C_2B_9H_{10}$)(1′,2′-C_2B_9-H_{11})], followed by the ring opening under the formation of carborane-substituted 1,4-dioxahexane chain (see Scheme 6).

The nature of these two anions have been corroborated by elemental analysis, matrix-assisted laser desorption/ionization-time of flight mass spectrometry (MALDI-TOF-MS), IR and ^{1}H, ^{1}H{^{11}B}, ^{13}C{^{1}H}, ^{11}B, and ^{11}B{^{1}H} NMR spectroscopies.

Figure 4 shows MALDI-TOF-MS spectra of compound [**15**] in which the molecular ion peak of [9,12-(3,3'-Co-{8-($C_4H_8O_2$-1,2-$C_2B_9H_{10}$-1',2'$C_2B_9H_{11}$}-O$(CH_2)_3)_2$-1,2-$C_2B_{10}H_{10}$]$^{2-}$ is observed at m/z 540.5. It should be noticed the separation between isotopic peaks distribution is of m/z 0.5 unites corresponding to the dianion fragment.

Figure 5 shows the MALDI-TOF-MS spectra of compound [**16**] in which the molecular ion peak of [8,9,10,12-(3,3'-Co-{8-($C_4H_8O_2$-1,2-$C_2B_9H_{10}$-1',2'-$C_2B_9H_{11}$}-O$(CH_2)_3)_4$-1,2-$C_2B_{10}H_8$]$^{4-}$ is observed at m/z 504.6. It should be noticed that the separation between isotopic peaks distribution is of m/z 0.25 unites corresponding to the tetranion fragment.

The ^{11}B NMR spectrum of the cobaltabisdicarbollide part of compound [**15**] bears distinct similarities to that of the dioxanate [3,3′-Co(8-$C_4H_8O_2$-1,2-$C_2B_9H_{10}$)(1′,2′-C_2B_9-H_{11})], consisting of a downfield B(8) singlet (approximate area 2) and ten doublets of approximate areas 2:2:4:4:2:8:4:4:2:2, some of which being coincidentally overlapped. This section of the spectrum, however, coincides with that of the carboranyl substituent (with 10 boron atoms), the shape of which is dictated by the symmetry of the corresponding disubstituted carborane cage.

The ^{11}B NMR spectrum of the cobaltabisdicarbollide part of compound [**16**] also shows a downfield B(8) singlet (approximate area 4) and ten doublets of approximate areas 4:4:8:8:4:16:8:8:4:4, some of which being coincidentally overlapped with the 10 boron atoms of the carboranyl substituent.

The most diagnostic feature of the ^{1}H NMR spectra of [**15**] and [**16**] is the presence of cage $C_{cluster}$–H signals of integral intensity 8 and 16 (respectively) along with one carborane $C_{cluster}$–H resonance of relative area 2 for the carborane cluster. BOCH_2 and CH_2OCH_2 units of the interconnecting 1,4-dioxahexane chain usually occur within the range of 3.7-1.9 ppm, in contrast, *B*-CH_2 in carborane cluster appears at higher field, between 0.5-0.7 ppm.

It should be concluded that nucleophilic oxonium ring-opening reactions lead to di- and tetra-anionic compounds that contain both metallabisdicarbaborane and carborane structural motifs in one molecule. Moreover, these borane-cage subunits can be easily modified via attaching variable substituents onto cage carbon and boron vertices, which makes these compounds structurally flexible potential candidates for BNCT[29] of cancer and HIV-PR inhibition. One of the most important reasons for the growing interest in the use of metallacarboranes in biological systems is the suspected high lipophilicity of metallacarborane derivatives, which is a bottleneck for their application in human body. Consequently, these compounds were primarily designed to help to elucidate the effect of steric and hydrophobic interactions on the efficiency of the HIV-PR inhibition in the region of enzyme flaps and the effect of overall charge on the mechanism of the inhibition as well.

Conclusion

The *o*-carborane cluster provides a unique platform for the construction of highly dense multibranched molecules with a wide range of possibilities for derivatization. Derivatives of *o*-carborane with precise patterns of substitution can be prepared by judicious

choice of the synthetic procedure. We have coupled hydroxyl terminated arms onto a specific, compact area of the cluster occupied by adjacent boron vertices, ultimately leading to a di- and quadruped-shaped structure which might serve as a versatile dendritic precursor.

Furthermore, compounds [**15**] and [**16**] can be used as cores to make a new class of dendrimers that contain multiple carborane or metallacarborane clusters at their periphery. Further work to synthesize potential new classes of BNCT compounds is now underway.

Experimental Section

Materials and instrumentation: All *o*-carboranes prepared are air and moisture stable. All manipulations were carried out under inert atmosphere. THF and DMF were distilled from sodium benzophenone prior to use. Reagents were obtained commercially and used as purchased. 1,2-*closo*-$C_2B_{10}H_{12}$ was obtained from Katchem. 9,12-I_2-1,2-*closo*-$C_2B_{10}H_{10}$[9], 9,12-$(CH_2CHCH_2)_2$-1,2-*closo*-$C_2B_{10}H_{10}$ [**1**],[10] 8,9,10,12-I_4-1,2-*closo*-$C_2B_{10}H_8$,[9] 8,9,10,12-$(CH_2CHCH_2)_4$-1,2-*closo*-$C_2B_{10}H_8$ [**2**][10] and 8,9,10,12-$(OHCH_2CH_2CH_2)_4$-1,2-*closo*-$C_2B_{10}H_8$ [**6**][10] were synthesised as reported at the literature.

Elemental analyses were performed using a Carlo Erba EA1108 micro analyzer. IR spectra (ν, cm^{-1}; KBr pellets) were obtained on a Shimadzu FTIR-8300 spectrophotometer. The ^{1}H- and ^{1}H{^{11}B}-NMR (300.13 MHz), ^{13}C{^{1}H}-NMR (75.47 MHz) and ^{11}B- and ^{11}B{^{1}H}-NMR (96.29 MHz) spectra were recorded on a Bruker ARX 300 instrument equipped with the appropriate decoupling accessories. All NMR spectra were performed in deuterated acetone at 22ºC. The ^{11}B- and ^{11}B{^{1}H}-NMR shifts were referenced to external $BF_3{\cdot}OEt_2$, while the ^{1}H, ^{1}H{^{11}B}, and ^{13}C{^{1}H}-NMR shifts were referenced to $SiMe_4$. Chemical shifts are reported in units of parts per million downfield from reference, and all coupling constants in Hz. The mass spectra were recorded in the negative ion mode using a Bruker Biflex MALDI-TOF-MS [N_2 laser; λ_{exc} 337 nm (0.5 ns pulses); voltage ion source 20.00 kV (Uis1) and 17.50 kV (Uis2)], and using a FIA-ES/MS (Shimadzu AD VP/ API 150) instrument for neutral species.

Synthesis of 9,12-(Ph-CH=CHCH$_2$)$_2$-1,2-*closo*-C$_2$B$_{10}$H$_{10}$ [**3**]: To a stirring solution of 9,12-$(CH_2=CHCH_2)_2$-1,2-*closo*-$C_2B_{10}H_{10}$ (156 mg, 0.7 mmol) in dry DMF (5 mL) were added dropwise 0.3 mL of iodobenzene (2.8 mmol) and 0.19 mL of 2,6-lutidine (1.7 mmol). After stirring at room temperature for 30 minutes, *cis*-$[PdCl_2(PPh_3)_2]$ (19.5 mg, 4% equiv.) was added in a single portion, following which the reaction was heated to reflux (140ºC) for 24 hours. The solvent was removed and 10 mL of chloroform and 10 mL of an aqueous solution of HCl (0.25 M) were added to the residue. The organic layer was separated from the mixture, and the aqueous layer was extracted with chloroform (3 x 10 mL). The combined organic phase was dried over $MgSO_4$, filtered and the solvent removed under reduced pressure. The crude product was purified by flash column chromatography on silica gel with an hexane/chloroform mixture (3:2 by volume) as the eluent to give 170 mg of 9,12-(Ph-CH=CHCH$_2$)$_2$-1,2-*closo*-C$_2$B$_{10}$H$_{10}$ (65 %). IR (KBr): ν [cm^{-1}] =3065, 3023 (vs, ν_s($C_{cluster}$-H, =CH_2 and C_{phenyl}-H)), 2997, 2959, 2927, 2911, 2878, 2851, 2810 (m, ν_s(=CH and CH_2)), 2594 (vs, ν_s(B-H)), 1636 (vs, ν_s(C=C)), 1596, 1493, 1445 (vs, ν_s(C-C_{phenyl})), 1110, 1023 (s, ν_{as}(=CH_2)). ^{1}H NMN: δ [ppm]=7.36, 7.30, 7.27 (m, 10H, H_{phenyl}), 6.26 (m, 2H, Ph-CH=C*H*CH_2), 5.51 (m, 2H, Ph-C*H*=C*H*CH_2), 3.32 (s, 2H, $C_{cluster}$-*H*), 3.10–1.00 (m, 8H, B-$H_{terminal}$), 1.68 (s, 4H, Ph-CH=CH-CH_2). ^{1}H{^{11}B} NMR: δ [ppm] =7.36, 7.30, 7.27 (m, 10H, H_{phenyl}), 6.26 (m, 2H, Ph-CH=C*H*CH_2), 5.51 (m, 2H, Ph-C*H*=C*H*CH_2), 3.32 (s, 2H, $C_{cluster}$-*H*), 2.50, 2.39, 2.27, 2.10 (s, 8H, B-$H_{terminal}$), 1.68 (s, 4H, Ph-CH=CH-CH_2). ^{13}C{^{1}H} NMR: δ [ppm] =138.9 (s, Ph-CH=*C*H-CH_2), 132.7 (s, Ph-*C*H=CH-CH_2), 127.3 (m, *Ph*-CH=CH-CH_2) 48.5 (s, $C_{cluster}$), 18.5 (s, Ph-CH=CH-*C*H_2). ^{11}B NMR: δ [ppm]= 6.0 (s, 2B, B(9,12)), -8.4 (d, ^1J(B,H)=154 Hz, 2B, B(8,10)), -13.7 (d, ^1J(B,H)=182 Hz, 4B, B(4,5,7,11)), -15.4 (d, ^1J(B,H)=165 Hz, 2B, B(3,6)). MALDI-TOF MS: *m/z* (%)=375.83 (100) $[M-1]^-$.

Synthesis of 8,9,10,12-(PhCH=CHCH$_2$)$_2$-(CH$_2$=CHCH$_2$)$_2$-1,2-*closo*-C$_2$B$_{10}$H$_8$ [**4**]: To a stirring solution of 8,9,10,12-$(CH_2=CHCH_2)_4$-1,2-*closo*-$C_2B_{10}H_8$ (103 mg, 0.34 mmol) in dry DMF (5 mL) were added dropwise 0.3 mL of iodobenzene (2.7 mmol) and 0.18 mL of 2,6-lutidine (1.6 mmol). After stirring at room temperature for 30 minutes, *cis*-$[PdCl_2(PPh_3)_2]$ (9.5 mg, 4% equiv.) was added in a single portion, following which the reaction was heated to reflux (140ºC) for 24 hours. The solvent was removed and 10 mL of chloroform were added to the residue. The excess of Grignard reagent was destroyed by slow addition of dilute HCl (0.25 M). The organic layer was separated from the mixture, and the aqueous layer was extracted with chloroform (3 x 10 mL). The combined organic phase was dried over $MgSO_4$, filtered and the solvent removed under reduced pressure. The crude product was purified by flash column chromatography on silica gel with chloroform the eluent to give 83 mg of 8,9,10,12-

(PhCH=CHCH$_2$)$_2$-(CH$_2$=CHCH$_2$)$_2$-1,2-*closo*-$C_2B_{10}H_8$ (54 %). IR (KBr): ν [cm^{-1}] =3064, 3023 (vs, ν_s($C_{cluster}$-H i =CH$_2$)), 2996, 2958, 2927, 2910, 2876, 2851, 2721 (m, ν_s(=CH and CH$_2$)), 2613, 2591 (vs, ν_s(B-H)), 1635 (vs, ν_s(C=C)), 1597, 1493, 1447 (vs, ν_s(C-$C_{aromatic}$)), 1106, 1027, 980 (s, ν_{as}(=CH$_2$)).^{1}H NMR: δ [ppm] =7.28 (m, 10H, Ph), 6.28 (m, 2H, Ph-C*H*=CHCH$_2$), 5.81 (m, 2H, Ph-CH=C*H*CH$_2$), 5.51 (m, 2H, CH$_2$=C*H*-CH$_2$), 4.87 (m, 4H, C*H*$_2$=CH-CH$_2$), 3.40 (s, 1H, $C_{cluster}$-*H*), 3.34 (s, 1H, $C_{cluster}$-*H*), 3.10–1.00 (m, 6H, B-$H_{terminal}$), 1.77 (m, 8H, Ph-CH=CH-C*H*$_2$, CH$_2$=CH-C*H*$_2$). ^{1}H{^{11}B} NMR: δ [ppm] =7.28 (m, 10H, H_{phenyl}), 6.28 (m, 2H, Ph-C*H*=CHCH$_2$), 5.81 (m, 2H, Ph-CH=C*H*CH$_2$), 5.51 (m, 2H, CH$_2$=C*H*-CH$_2$), 4.87 (m, 4H, C*H*$_2$=CH-CH$_2$), 3.40 (s, 1H, $C_{cluster}$-*H*), 3.34 (s, 1H, $C_{cluster}$-*H*), 2.31, 2.20, 2.07 (s, 6H, B-$H_{terminal}$), 1.77 (m, 8H, Ph-CH=CH-C*H*$_2$, CH$_2$=CH-C*H*$_2$). ^{13}C{^{1}H} NMR: δ [ppm]=140.2 (s, CH$_2$=*C*H-CH$_2$), 138.6 (s, PhCH=*C*H-CH$_2$) 128.5 (m, *Ph*-CH=CH-CH$_2$), 127.5, 125.9 (s, PhC*H*=C*H*-CH$_2$), 112.2 (s, *C*H$_2$=CH-CH$_2$), 47.9 (s, $C_{cluster}$), 21.4 (s, Ph-CH=CH-*C*H$_2$, CH$_2$=CH-*C*H$_2$).^{11}B NMR: δ [ppm] =7.4, 5.9 (s, 2B, B(9,12)), 1.2, 0.3 (s, 2B, B(8,10)), -14.4 (d, ^{1}*J*(B,H)=120 Hz, 4B, B(4,5,7,11)), -18.2 (d, ^{1}*J*(B,H)=120 Hz, 2B, B(3,6)). MALDI-TOF MS: *m/z* (%)= 457.2 (100) [M-1]$^-$.

Synthesis of 9,12-(HOCH$_2$CH$_2$CH$_2$)$_2$-1,2-*closo*-$C_2B_{10}H_{10}$ [5]: To a stirring solution of 9,12-(CH$_2$=CHCH$_2$)$_2$-1,2-*closo*-$C_2B_{10}H_{10}$ (300 mg, 1.34 mmol) in THF (4 mL) at 0 ºC, was added, dropwise, a solution of BH_3·THF in THF (2.75 mL, 1M, 2.75 mmol). The resulting suspension was stirred at 0 ºC for 30 minutes and at room temperature for further 30 minutes. Then, the reaction mixture was cooled again to 0 ºC in an ice-water bath and water (4 mL) was slowly added. When gas evolution had stopped, an aqueous KOH solution (1.3 mL, 3M, 3.9 mmol) and subsequently, H_2O_2 in water (0.4 mL, 35%, 4.6 mmol), were added. Stirring was maintained at room temperature for 1.5 h, after which two liquid phases were observed. The upper organic layer was separated from the mixture and the aqueous layer and washed with THF (3 x 2 mL). The combined organic phase was dried over $MgSO_4$, filtered and the solvent removed *in vacuo* to give 9,12-(HOCH$_2$CH$_2$CH$_2$)$_2$-1,2-*closo*-$C_2B_{10}H_{10}$. Yield: 324 mg (93%). Elemental Analysis for $C_8B_{10}H_{24}O_2$: calc: C 36.92, H 9.23; found: C 37.21, H 9.21. IR (KBr): ν [cm^{-1}] =3366 (vs, ν_s(O-H)), 3074 (vs, ν_s($C_{cluster}$-H)), 2930, 2886, 2822 (vs, ν_s(C_{alkyl}-H)), 2617, 2589, 2556 (s, ν_s(B-H)), 1055, 1022, 998 (s, ν_s(C-O)). ^{1}H NMR: δ [ppm]=4.30 (s, 2H, $C_{cluster}$-*H*), 3.43 (m, ^{3}*J*(H,H)=6.8 Hz, 4H, HOC*H*$_2$CH$_2$CH$_2$), 3.33 (t, ^{3}*J*(H,H)=5.5 Hz, 2H, *H*OCH$_2$CH$_2$CH$_2$), 1.46 (m, 4H, HOCH$_2$C*H*$_2$CH$_2$), 0.69 (t, ^{3}*J*(H,H)=17.2 Hz, 4H, HOCH$_2$CH$_2$C*H*$_2$). ^{1}H{^{11}B} NMR: δ [ppm]=4.30 (s, 2H, $C_{cluster}$-*H*), 3.43 (m, ^{3}*J*(H,H)=6.8 Hz, 4H, HOC*H*$_2$CH$_2$CH$_2$), 3.33 (t, ^{3}*J*(H,H)=5.5 Hz, 2H, *H*OCH$_2$CH$_2$CH$_2$), 2.00 (s, 8H, B-$H_{terminal}$), 1.46 (m, 4H, HOCH$_2$C*H*$_2$CH$_2$), 0.69 (t, ^{3}*J*(H,H)=17.2 Hz, 4H, HOCH$_2$CH$_2$C*H*$_2$). ^{13}C{^{1}H} NMR: δ [ppm]=64.28 (s, HOC*H*$_2$CH$_2$CH$_2$), 49.17 (s, $C_{cluster}$), 32.01 (s, HOCH$_2$C*H*$_2$CH$_2$), 13.21 (s, HOCH$_2$CH$_2$C*H*$_2$). ^{11}B NMR: δ [ppm]=8.1 (s, 2B, B(9,12)), -8.8 (d, ^{1}*J*(B,H)=144 Hz, 2B, B(8,10)), -14.4 (d, ^{1}*J*(B,H)=156 Hz, 4B, B(4,5,7,11)), -16.1 (d, ^{1}*J*(B,H)=144 Hz, 2B, B(3,6)). MALDI-TOF MS: *m/z* (%)=259.2 (100) [M-1]$^-$.

Synthesis of 9,12-(ClCH$_2$CH$_2$CH$_2$)$_2$-1,2-*closo*-$C_2B_{10}H_{10}$ [7]: To a stirring solution of 9,12-(HOCH$_2$CH$_2$CH$_2$)$_2$-1,2-*closo*-$C_2B_{10}H_{10}$ (144 mg, 0.55 mmol) and (CH$_3$(CH$_2$)$_3$)$_4$NCl (63.8 mg, 0.23 mmol) in dry THF (5 mL) at 0 ºC, was added $SOCl_2$ dropwise (0.25 mL, 3.4 mmol). The resulting solution was stirred at 0 ºC for 30 minutes and at room temperature for further 6 hours. The solvent was removed under reduced pressure, and 5 mL of diethyl ether were added. A solution of Na_2CO_3 (5 mL, 2 M) was slowly added with stirring. The mixture was thoroughly shaken, and the two layers separated. The aqueous layer was extracted with diethyl ether (3 x 5 mL). Then, the combined organic phase was separated and a solution of HCl (5 mL, 0.1 M) was added, the mixture was thoroughly shaken again. The upper organic layer was separated from the mixture, and the aqueous layer was washed with diethyl ether (3 x 5 mL). Finally, the combined organic phase was dried over $MgSO_4$, filtered and the solvent removed *in vacuo* to give 9,12-(ClCH$_2$CH$_2$CH$_2$)$_2$-1,2-*closo*-$C_2B_{10}H_{10}$. Yield: 153 mg (93%). Elemental Analysis for $C_8B_{10}H_{22}Cl_2$: calc: C 32.32, H 7.40; found: C 32.73, H 7.43. IR (KBr): ν [cm^{-1}] =3070 (s, ν_s($C_{cluster}$-H)), 2989 2952, 2931, 2910, 2893, 2837 (s, ν_s(C_{alkyl}-H)), 2616, 2582 (s, ν_s(B-H)), 1310, 1281 (s, ν_{wag}(CH$_2$-Cl)), 725, 650 (s, ν_s(C-Cl)). ^{1}H NMR: δ [ppm] =4.37 (s, 2H, $C_{cluster}$-*H*), 3.52 (t, ^{3}*J*(H,H)=6.0 Hz, 4H, ClC*H*$_2$CH$_2$CH$_2$), 1.70 (m, 4H, ClCH$_2$C*H*$_2$CH$_2$), 0.78 (t, ^{3}*J*(H,H)=9.0 Hz, 4H, ClCH$_2$CH$_2$C*H*$_2$). ^{1}H{^{11}B} NMR: δ [ppm] =4.37 (s, 2H, $C_{cluster}$-*H*), 3.52 (t, ^{3}*J*(H,H)=6.0 Hz, 4H, ClC*H*$_2$CH$_2$CH$_2$), 2.24, 2.08, 1.98 (s, 8H, B-$H_{terminal}$), 1.70 (m, 4H, ClCH$_2$C*H*$_2$CH$_2$), 0.78 (t, ^{3}*J*(H,H)=9.0 Hz, 4H, ClCH$_2$CH$_2$C*H*$_2$). ^{13}C{^{1}H} NMR: δ [ppm] =49.69 (s, $C_{cluster}$), 47.16 (s, ClC*H*$_2$CH$_2$CH$_2$), 32.84 (s, ClCH$_2$C*H*$_2$CH$_2$), 13.33 (s, ClCH$_2$CH$_2$C*H*$_2$). ^{11}B NMR: δ [ppm]=8.1 (s, 2B, B(9,12)), -8.1 (d, ^{1}*J*(B,H)=147 Hz, 2B, B(8,10)), -12.7 (d, ^{1}*J*(B,H)=159 Hz, 4B, B(4,5,7,11)), -16.2 (d, ^{1}*J*(B,H)=182 Hz, 2B, B(3,6)).

Synthesis of 8,9,10,12-(ClCH$_2$CH$_2$CH$_2$)$_4$-1,2-*closo*-$C_2B_{10}H_8$ [8]: To a stirring solution of 8,9,10,12-(HOCH$_2$CH$_2$CH$_2$)$_4$-1,2-*closo*-$C_2B_{10}H_8$ (400 mg, 1.06 mmol) and (CH$_3$(CH$_2$)$_3$)$_4$NCl (238.6 mg, 0.86 mmol) in dry THF (10 mL) at 0 ºC, was added $SOCl_2$ dropwise (0.94 mL, 4.3 mmol). The resulting solution was stirred at 0 ºC for

30 minutes and at room temperature for further 6 hours. The solvent was removed under reduced pressure, and 10 mL of diethyl ether were added. A solution of Na_2CO_3 (10 mL, 2 M) was slowly added with stirring. The mixture was thoroughly shaken, and the two layers separated. The aqueous layer was extracted with diethyl ether (3 x 5 mL). Then, the combined organic phase was separated and a solution of HCl (5 mL, 0.1 M) was added, the mixture was thoroughly shaken again. The upper organic layer was separated from the mixture, and the aqueous layer was washed with diethyl ether (3 x 5 mL). Finally, the combined organic phase was dried over $MgSO_4$, filtered and the solvent removed *in vacuo* to give 8,9,10,12-($ClCH_2CH_2CH_2$)$_4$-1,2-*closo*-$C_2B_{10}H_8$. Yield: 438 mg (92%). Elemental Analysis for $C_{14}B_{10}H_{32}Cl_4$: calc: C 37.00, H 7.00; found: C 37.32, H 7.29. IR (KBr): ν [cm^{-1}] =3071 (s, ν_s($C_{cluster}$-H)), 2991, 2953, 2931, 2911, 2893, 2836 (s, ν_s(C_{alkyl}-H)), 2615, 2586 (s, ν_s(B-H)), 1310, 1281 (s, ν_{wag}(CH_2-Cl)), 728, 647 (s, ν_s(C-Cl)). ^{1}H NMR: δ [ppm] =4.30 (br s, 2H, $C_{cluster}$*H*), 3.60 (t, ^{3}*J*(H,H)=6.0 Hz, 4H, Cl*C*$H_2$$CH_2CH_2$), 3.53 (t, ^{3}*J*(H,H)=6.0 Hz, 4H, Cl*C*$H_2$$CH_2CH_2$), 2.4–0.8 (br m, 6H, B*H*), 1.89 (m, 4H, $ClCH_2C$$H_2$$CH_2$), 1.70 (m, 4H, $ClCH_2C$$H_2$$CH_2$), 0.82 (m, 4H, $ClCH_2CH_2C$$H_2$), 0.61 (m, 4H, $ClCH_2CH_2C$$H_2$). ^{1}H{^{11}B} NMR: δ [ppm] = 4.30 (br s, 2H, $C_{cluster}$*H*), 3.60 (t, ^{3}*J*(H,H)=6.0 Hz, 4H, Cl*C*$H_2$$CH_2CH_2$), 3.53 (t, ^{3}*J*(H,H)=6.0 Hz, 4H, Cl*C*$H_2$$CH_2CH_2$), 2.15, 1.94 (br s, 6H, B*H*), 1.89 (m, 4H, $ClCH_2C$$H_2$$CH_2$), 1.70 (m, 4H, $ClCH_2C$$H_2$$CH_2$), 0.82 (m, 4H, $ClCH_2CH_2C$$H_2$), 0.61 (m, 4H, $ClCH_2CH_2C$$H_2$). ^{13}C{^{1}H} NMR: δ [ppm] =47.9 (s, $C_{cluster}$), 47.3 (s, Cl*C*$H_2$$CH_2CH_2$), 33.1, 32.0 (s, $ClCH_2$*C*$H_2$$CH_2$), 10.8 (br s, $ClCH_2CH_2$*C*H_2). ^{11}B NMR: δ [ppm] =7.6 (s, 2B, B(9,12)), 1.5 (s, 2B, B(8,10)), -14.4 (d, ^{1}*J*(B,H)=153 Hz, 4B, B(4,5,7,11)), -18.2 (d, ^{1}*J*(B,H) =168 Hz, 2B, B(3,6)). ESI MS: *m*/*z* (%)=449.4 (70) [M-1]$^-$.

Synthesis of 9,12-($BrCH_2CH_2CH_2$)$_2$-1,2-*closo*-$C_2B_{10}H_{10}$ [9]: To a stirring solution of 9,12-($HOCH_2CH_2CH_2$)$_2$-1,2-*closo*-$C_2B_{10}H_{10}$ (400 mg, 1.54 mmol) and CBr_4 (1532 mg, 4.62 mmol) in dry CH_2Cl_2 (15 mL) at 0 ºC, was added dropwise a solution of PPh_3 (1372 mg, 5.24 mmol, in 10 mL of dry CH_2Cl_2). The resulting solution was stirred at room temperature for 3 hours. The solvent was removed under reduced pressure, and 10 mL of dry diethyl ether were added, after a filtration, the filtrate was concentrated to yield 445 mg (75%) of 9,12-($BrCH_2CH_2CH_2$)$_2$-1,2-*closo*-$C_2B_{10}H_{10}$. Elemental Analysis $C_8B_{10}H_{22}Br_2$: calc: C 24.87, H, 5.70; found: C 25.06, H 5.74. IR (KBr): ν [cm^{-1}] =3077 (s, ν_s($C_{cluster}$-H)), 2987, 2926 (s, ν_s(C_{alkyl}-H)), 2586, 2543 (s, ν_s(B-H)), 1192, 1119 (s, ν_{wag}(CH_2-Br)), 722, 695 (s, ν_s(C-Br)). ^{1}H NMR: δ [ppm]=4.44 (s, 2H, $C_{cluster}$-*H*), 3.43 (t, ^{3}*J*(H,H)=6.0 Hz, 4H, $BrC$$H_2$$CH_2CH_2$), 1.79 (m, 4H, $BrCH_2C$$H_2$$CH_2$), 0.79 (t, ^{3}*J*(H,H)=9.0 Hz, 4H, $BrCH_2CH_2C$$H_2$). ^{1}H{^{11}B} NMR: δ [ppm] =4.44 (s, 2H, $C_{cluster}$-*H*), 3.43 (t, ^{3}*J*(H,H)=6.0 Hz, 4H, $BrC$$H_2$$CH_2CH_2$), 2.23, 2.1 (s, 8H, B-$H_{terminal}$), 1.79 (m, 4H, $BrCH_2C$$H_2$$CH_2$), 0.79 (t, ^{3}*J*(H,H)=9.0 Hz, 4H, $BrCH_2CH_2C$$H_2$). ^{13}C{^{1}H} NMR: δ [ppm] =48.15 (s, $C_{cluster}$), 36.80 (s, $BrC$$H_2$$CH_2CH_2$), 33.34 (s, $BrCH_2C$$H_2$$CH_2$), 13.19 (s, $BrCH_2CH_2C$$H_2$). ^{11}B NMR: δ [ppm] =7.8 (s, 2B, B(9,12)), -8.3 (d, ^{1}*J*(B,H)=143 Hz, 2B, B(8,10)), -13.7 (d, ^{1}*J*(B,H)=152 Hz, 4B, B(4,5,7,11)), -15.3 (d, ^{1}*J*(B,H)=177 Hz, 2B, B(3,6)).

Synthesis of 8,9,10,12-($BrCH_2CH_2CH_2$)$_4$-1,2-*closo*-$C_2B_{10}H_8$ [10]: To a stirring solution of 8,9,10,12-($HOCH_2CH_2CH_2$)$_4$-1,2-*closo*-$C_2B_{10}H_8$ (300 mg, 0.8 mmol) and CBr_4 (1421 mg, 5.4 mmol) in dry CH_2Cl_2 (15 mL) at 0 ºC, was added dropwise a solution of PPh_3 (1590 mg, 4.8 mmol, in 10 mL of dry CH_2Cl_2). The resulting solution was stirred at room temperature for 3 hours. The solvent was removed under reduced pressure, and 10 mL of dry diethyl ether were added, after a filtration, the filtrate was concentrated to yield 360 mg (72%) of 8,9,10,12-($BrCH_2CH_2CH_2$)$_4$-1,2-*closo*-$C_2B_{10}H_8$. Elemental Analysis for $C_{14}B_{10}H_{28}Br_4$: calc: C 26.92, H 4.48; found: C 27.89, H 4.59. IR (KBr): ν [cm^{-1}] =3080 (s, ν_s($C_{cluster}$-H)), 2928 (s, ν_s(C_{alkyl}-H)), 2620, 2581 (s, ν_s(B-H)), 1194, 1120 (s, ν_{wag}(CH_2-Br)), 721, 695 (s, ν_s(C-Br)). ^{1}H NMR: δ [ppm] =4.40 (br s, 2H, $C_{cluster}$*H*), 3.52 (t, ^{3}*J*(H,H)=6.0 Hz, 4H, $BrC$$H_2$$CH_2CH_2$), 3.45 (t, ^{3}*J*(H,H)=6.0 Hz, 4H, $BrC$$H_2$$CH_2CH_2$), 2.4–0.8 (br m, 6H, B*H*), 1.94 (m, 4H, $BrCH_2C$$H_2$$CH_2$), 1.79 (m, 4H, $BrCH_2C$$H_2$$CH_2$), 0.85 (m, 4H, $BrCH_2CH_2C$$H_2$), 0.65 (m, 4H, $BrCH_2CH_2C$$H_2$). ^{1}H{^{11}B} NMR: δ [ppm] =4.40 (br s, 2H, $C_{cluster}$*H*), 3.52 (t, ^{3}*J*(H,H)=6.0 Hz, 4H, $BrC$$H_2$$CH_2CH_2$), 3.45 (t, ^{3}*J*(H,H)=6.0 Hz, 4H, $BrC$$H_2$$CH_2CH_2$), 2.10, 1.83 (br s, 6H, B*H*), 1.94 (m, 4H, $BrCH_2C$$H_2$$CH_2$), 1.79 (m, 4H, $BrCH_2C$$H_2$$CH_2$), 0.85 (m, 4H, $BrCH_2CH_2C$$H_2$), 0.65 (m, 4H, $BrCH_2CH_2C$$H_2$). ^{13}C{^{1}H} NMR: δ [ppm] =48.1 (s, $C_{cluster}$), 36.8 (s, $BrC$$H_2$$CH_2CH_2$), 33.3, 32.3 (s, $BrCH_2C$$H_2$$CH_2$), 13.2 (br s, $BrCH_2CH_2C$$H_2$). ^{11}B NMR: δ [ppm] =7.8 (s, 2B, B(9,12)), 1.6 (s, 2B, B(8,10)), -14.2 (d, ^{1}*J*(B,H)=150 Hz, 4B, B(4,5,7,11)), -18.2 (d, ^{1}*J*(B,H) =154 Hz, 2B, B(3,6)). ESI MS: *m*/*z* (%)=627.2 (20) [M-1]$^-$, 708.1 (100) [M+Br]$^-$.

Synthesis of 8,9,10,12-(CH_3-C_6H_4-$SO_3(CH_2)_3$)$_4$-1,2-$C_2B_{10}H_8$ [11]: To a stirring solution of 8,9,10,12-($HO(CH_2)_3$)$_4$-1,2-$C_2B_{10}H_8$ (175 mg, 0.46 mmol) and anhydrous $N(CH_3)_3HCl$ (17.8 mg, 0.19 mmol) in dry toluene (5 mL), were added 1.5 mL of $N(CH_2CH_3)_3$ (in excess). Then the mixture was cooled to 0 ºC in an ice-water bath and a solution of p-toluensulfonyl chloride in 3 mL of dry toluene (532 mg, 2.8 mmol) was added, following which the reaction was stirred overnight at room temperature. The solvent was removed and 10 mL of diethyl ether and 5 mL of water were added to the residue, and the organic layer was washed successively with 10 mL of brine

and with 10 mL of water. Then the combined organic phase was dried over $MgSO_4$, filtered and the solvent removed *in vacuo* to give 8,9,10,12-(CH_3-C_6H_4-$SO_3(CH_2)_3$)$_4$-1,2-$C_2B_{10}H_8$. Yield: 332 mg (72%). Elemental Analysis for $C_{42}B_{10}H_{60}O_{12}S_4$: calc: C 50.81, H 6.05, S 12.90; found: C 51.22, H 6.07, S 12.54. IR (KBr): ν [cm^{-1}] = 3072 (s, $\nu_s(C_{cluster}$-H)), 2957, 2930, 2894 (s, $\nu_s(C_{alkyl}$-H)), 2616, 2585 (s, ν_s(B-H)), 1357 (s, ν_s(S=O)), 1189, 1175 (s, ν_s(S-O)), 1097, 981, 954, 918 (s, ν_s(C-O)). ^{1}H NMR: δ [ppm]=7.79 (m, 8H, H_{meta}), 7.48 (m, 8H, H_{ortho}), 4.25 (br s, 2H, $C_{cluster}$-H), 4.02 (t, ^{3}J(H,H)=6 Hz, 4H, TsO-CH_2), 3.96 (t, ^{3}J(H,H)=6 Hz, 4H, TsO-CH_2), 3.00-1.50 (br m, 6H, BH), 2.44 (s, 12H, C$H_3C_6H_4$), 1.70 (m, 4H, TsOCH$_2$CH_2CH$_2$), 1.45 (m, 4H, TsOCH$_2$CH_2CH$_2$), 0.47 (m, 4H, TsOCH$_2$CH$_2$CH_2), 0.24 (m, 4H, TsOCH$_2$CH$_2$CH_2). ^{1}H{^{11}B} NMR: δ [ppm] =7.79 (m, 8H, H_{meta}), 7.48 (m, 8H, H_{ortho}), 4.25 (br s, 2H, $C_{cluster}$-H), 4.02 (t, ^{3}J(H,H)=6 Hz, 4H, TsO-CH_2), 3.96 (t, ^{3}J(H,H)=6 Hz, 4H, TsO-CH_2), 2.44 (s, 12H, C$H_3C_6H_4$), 1.75 (br s, 6H, BH), 1.70 (m, 4H, TsOCH$_2$CH_2CH$_2$), 1.45 (m, 4H, TsOCH$_2$CH_2CH$_2$), 0.47 (m, 4H, TsOCH$_2$CH$_2$CH_2), 0.24 (m, 4H, TsOCH$_2$CH$_2$CH_2). ^{13}C{^{1}H} NMR: δ [ppm] =129.94 (s, C_{meta}), 127.75 (s, C_{ortho}), 72.82 (s, TsOCH$_2$CH$_2$CH$_2$), 47.82 (s, $C_{cluster}$), 37.23 (s, TsOCH$_2$$CH_2CH_2$), 20.60 (s, C$H_3$-Ph), 8.88 (br s, TsOCH$_2CH_2$$CH_2$). ^{11}B NMR: δ [ppm] =7.4 (br s, 2B, B(9,12)), 1.3 (br s, 2B, B(8,10)), -14.4 (d, ^1J(B,H)=161 Hz, 4B, B(4,5,7,11)), -17.5 (d, ^1J(B,H)=120 Hz, 2B, B(3,6)). ESI MS: *m/z* (%)=1016.2 (100) $[M-1+Na]^+$.

Synthesis of 8,9,10,12-(HOCOCH$_2$CH$_2$)$_4$-1,2-*closo*-$C_2B_{10}H_8$ [12]: First, the Jones reagent was prepared dissolving CrO3 (2016 mg, 20 mmol) with 1.5 mL of distilled water, then cooled at 0ºC in an ice bath and 1.7 mL of concentrated H_2SO_4 were added slowly. A precipitate immediately formed which dissolved after the addition of 3.5 mL of distilled water, and while cool, acetone (6.0 mL) was then added to the mixture. Afterwards, a solution of 8,9,10,12-(HOCH$_2$CH$_2$CH$_2$)$_4$-1,2-*closo*-$C_2B_{10}H_8$ (270 mg, 0.72 mmol) in acetone (10 mL) was added dropwise to the cooled Jones reagent, and then was allowed to stir overnight at room temperature. The solvent was removed at reduced pressure by rotary evaporation and the dark residue was transferred to a separator/funnel and extracted with diethyl ether (3 x 10 mL). The combined ether layers were extracted with brine (3 x 10 mL) and then dried over anhydrous $MgSO_4$, filtered, and the solvent removed at reduced pressure by rotary evaporation. The remaining solid was recrystallized from boiling hexane to yield 232 mg (75%) of 8,9,10,12-(HOCOCH$_2$CH$_2$)$_4$-1,2-*closo*-$C_2B_{10}H_8$. Elemental Analysis for $C_{14}B_{10}H_{28}O_8$: calc: C 38.88, H, 6.48; found: C 38.97, H 6.50. IR (KBr): ν [cm^{-1}] = 3200 (b, ν_s(O-H)), 3074 (s, $\nu_s(C_{cluster}$-H)), 2965, 2921, 2853 (s, $\nu_s(C_{alkyl}$-H)), 2589 (s, ν_s(B-H)), 1705 (s, ν_s(C=O)), 1256 (s, ν_s(C-O)).^{1}H NMR: δ [ppm] = 6.20 (br s, 4H, HOCOCH_2CH$_2$), 4.33 (br s, 2H, $C_{cluster}H$), 2.4–0.8 (br m, 6H, BH), 2.41 (m, 4H, HOCOCH_2CH$_2$), 2.21 (m, 4H, HOCOCH_2CH$_2$), 1.02 (m, 4H, HOCOCH$_2$CH_2), 0.84 (m, 4H, HOCOCH$_2$CH_2). ^{1}H{^{11}B} NMR: δ [ppm] =6.20 (br s, 4H, HOCOCH_2CH$_2$), 4.33 (br s, 2H, $C_{cluster}H$), 2.10, 1.91 (br s, 6H, BH), 2.41 (m, 4H, HOCOCH_2CH$_2$), 2.21 (m, 4H, HOCOCH_2CH$_2$), 1.02 (m, 4H, HOCOCH$_2$CH_2), 0.84 (m, 4H, HOCOCH$_2$CH_2). ^{13}C{^{1}H} NMR: δ [ppm] =175.7 (s, HOCO), 48.2 (s, $C_{cluster}$), 33.4, 32.4 (s, HOCOCH$_2$CH$_2$), 8.8 (br s, HOCOCH$_2$$CH_2$). ^{11}B NMR: δ [ppm] = 7.9 (s, 2B, B(9,12)), 2.2 (s, 2B, B(8,10)), -13.9 (m, 6B, B(3,4,5,6,7,11)). ESI MS: *m/z* (%)=432.3 (100) $[M-1]^-$.

Synthesis of 9,12-(PhCOOCH$_2$CH$_2$CH$_2$)$_2$-1,2-*closo*-$C_2B_{10}H_{10}$ [13]: To a stirring solution of 9,12-(HOCH$_2$CH$_2$CH$_2$)$_2$-1,2-*closo*-$C_2B_{10}H_{10}$ (50 mg, 0.20 mmol), 4-N,N-dimethylaminopyridine (26 mg, 0.21 mmol), N,N'-dicyclohexylcarbodiimide (44 mg, 0.21 mmol) and benzoic acid (52 mg, 0.42 mmol) in dry CH_2Cl_2 (5 mL). The resulting solution was stirred at room temperature for 30 minutes. The white precipitate (dicyclohexylurea) is filtered and then 10 mL of HCl (1 M) were added to the residue. The aqueous layer was extracted with CH_2Cl_2 (3 x 10 mL). The combined organic phase was dried over $MgSO_4$, filtered and the solvent removed under reduced pressure. Yield: 63 mg (70%). Elemental Analysis for $C_{22}B_{10}H_{32}O_4$: calc: C 56.41, H 6.83; found: C 56.92, H 6.88. ^{1}H NMR: δ [ppm]= 8.03 (d, $^1J(H_{orto},H_{meta})$=6 Hz, 4H, $H_{phenyl\text{-}meta}$), 7.53 (t, $^1J(H_{para},H_{meta})$=9 Hz, 2H, $H_{phenyl\text{-}para}$), 7.41 (m, 4H, $H_{phenyl\text{-}meta}$), 4.24 (t, ^3J(H,H)=6.0 Hz, 4H, PhCOOCH_2CH$_2$CH$_2$), 3.52 (s, 2H, $C_{cluster}$-H), 3.50–1.50 (m, 8H, B-$H_{terminal}$), 1.73 (m, 4H, PhCOOCH$_2$CH_2CH$_2$), 0.81 (m, 4H, PhCOOCH$_2$CH$_2$CH_2).^{1}H{^{11}B} NMR: δ [ppm] =8.03 (d, $^1J(H_{orto},H_{meta})$=6 Hz, 4H, $H_{phenyl\text{-}meta}$), 7.53 (t, $^1J(H_{para},H_{meta})$=9 Hz, 2H, $H_{phenyl\text{-}para}$), 7.41 (m, 4H, $H_{phenyl\text{-}meta}$), 4.24 (t, ^3J(H,H)=6.0 Hz, 4H, PhCOOCH_2CH$_2$CH$_2$), 3.52 (s, 2H, $C_{cluster}$-H), 1.95 (m, 8H, B-$H_{terminal}$), 1.73 (m, 4H, PhCOOCH$_2$CH_2CH$_2$), 0.81 (m, 4H, PhCOOCH$_2$CH$_2$CH_2).^{13}C{^{1}H} NMR: δ [ppm] =166.0 (s, PhCOOCH$_2$CH$_2$CH$_2$), 132.8 (s, $C_{phenyl\text{-}para}$), 130.8 (s, $C_{phenyl\text{-}ipso}$), 129.2 (s, $C_{phenyl\text{-}meta}$), 128.5 (s, $C_{phenyl\text{-}orto}$), 66.8 (s, PhCOOCH$_2$CH$_2$CH$_2$), 49.7 (s, $C_{cluster}$), 25.8 (s, PhCOOCH$_2$$CH_2CH_2$), 12.4 (s, PhCOOCH$_2CH_2$$CH_2$). ^{11}B NMR: δ [ppm]=8.0 (s, 2B, B(9,12)), -8.9 (d, ^1J(B,H)=140 Hz, 2B, B(8,10)), -14.7 (m, 6B, B(3,4,5,6,7,11)). MALDI-TOF MS: *m/z* (%)=461.4 (100) $[M-1+Li]^-$.

Synthesis of 8,9,10,12-(PhCOOCH$_2$CH$_2$CH$_2$)$_4$-1,2-*closo*-$C_2B_{10}H_8$ [14]: To a stirring solution of 8,9,10,12-(HOCH$_2$CH$_2$CH$_2$)$_4$-1,2-*closo*-$C_2B_{10}H_{10}$ (50 mg, 0.13 mmol), 4-N,N-dimethylaminopyridine (71 mg, 0.58 mmol), N,N'-dicyclohexylcarbodiimide (121 mg,

0.58 mmol) and benzoic acid (71 mg, 0.58 mmol) in dry CH_2Cl_2 (5 mL). The resulting solution was stirred at room temperature for 30 minutes. The white precipitate (dicyclohexylurea) is filtered and then 10 mL of HCl (1 M) were added to the residue. The aqueous layer was extracted with CH_2Cl_2 (3 x 10 mL). The combined organic phase was dried over $MgSO_4$, filtered and the solvent removed under reduced pressure. Yield: 74 mg (62%). Elemental Analysis for $C_{42}B_{10}H_{52}O_8$: calc: C 63.63, H 6.57; found: C 64.28, H 6.61. ^{1}H NMR: δ [ppm] =7.90 (m, 8H, Ph_{meta}), 7.23 (m, 12H, $Ph_{orto,para}$), 4.11 (t, ^3J(H,H)=9.0 Hz, 4H, PhCOOCH_2CH$_2$CH$_2$), 4.17 (t, ^3J(H,H)=6.0 Hz, 4H, PhCOOCH_2CH$_2$CH$_2$), 3.37 (s, 2H, $C_{cluster}$-H), 3.50–1.50 (m, 8H, B-$H_{terminal}$), 1.77 (m, 4H, PhCOOCH$_2$CH_2CH$_2$), 1.56 (m, 4H, PhCOOCH$_2$CH_2CH$_2$), 0.72 (m, 4H, PhCOOCH$_2$CH$_2$CH_2), 0.49 (m, 4H, PhCOOCH$_2$CH$_2$CH_2). ^{1}H{^{11}B} NMR: δ [ppm] =7.90 (m, 8H, Ph_{meta}), 7.23 (m, 12H, $Ph_{orto,para}$), 4.11 (t, ^3J(H,H)=9.0 Hz, 4H, PhCOOCH_2CH$_2$CH$_2$), 4.17 (t, ^3J(H,H)=6.0 Hz, 4H, PhCOOCH_2CH$_2$CH$_2$), 3.37 (s, 2H, $C_{cluster}$-H), 1.94 (m, 6H, B-$H_{terminal}$), 1.77 (m, 4H, PhCOOCH$_2$CH_2CH$_2$), 1.56 (m, 4H, PhCOOCH$_2$CH_2CH$_2$), 0.72 (m, 4H, PhCOOCH$_2$CH$_2$CH_2), 0.49 (m, 4H, PhCOOCH$_2$CH$_2$CH_2).^{13}C{^{1}H} NMR: δ [ppm]= 166.0 (s, Ph*C*OOCH$_2$CH$_2$CH$_2$), 129.2 (m, Ph), 66.4 (s, PhCOO*C*H$_2$CH$_2$CH$_2$), 47.6 (s, $C_{cluster}$), 24.7 (s, PhCOOCH$_2$*C*H$_2$CH$_2$), 9.8 (s, PhCOOCH$_2$CH$_2$*C*H$_2$). ^{11}B NMR: δ [ppm] =7.5 (s, 2B, B(9,12)), 1.0 (s, 2B, B(8,10)), -15.6 (m, 6B, B(3,4,5,6,7,11)). ESI MS: *m/z* (%)=792 (100) $[M\text{-}1]^-$.

Synthesis of $[N(CH_3)_4]_2$[9,12-(3,3'-Co-{8-$(OCH_2CH_2)_2$-1,2-$C_2B_9H_{10}$-1',2'-$C_2B_9H_{11}$}-O$(CH_2)_3)_2$-1,2-$C_2B_{10}H_{10}$] [**15**]: To a stirring solution of 9,12-(HOCH$_2$CH$_2$CH$_2$)$_2$-1,2-*closo*-$C_2B_{10}H_{10}$ (130 mg, 0.5 mmol) in THF (10 mL) cooled to 0 ºC in an ice-water bath was added dropwise a solution of butyllithium in hexanes (0.65 mL, 1.6M, 1.02 mmol). After stirring at room temperature for 30 minutes, a solution of [8-{O(CH$_2$CH$_2$)$_2$O}-3,3'-Co(1,2-$C_2B_9H_{10}$)(1',2'-$C_2B_9H_{11}$)] (421 mg, 1.02 mmol) in THF (5mL) was added via a syringe, following which the reaction was heated to reflux for 2 hours. Afterwards the solvent was removed under reduced pressure, 5mL of diethyl ether and 5mL of a diluted solution of HCl (0.1M) were added, then the mixture was thoroughly shaken and the two layers separated. The organic layer was separated, and the aqueous layer was extracted with diethyl ether (3 x 10mL). The combined organic phase was dried over $MgSO_4$, filtered and the solvent removed under reduced pressure. Afterwards, an aqueous solution of $[NMe_4]$Cl was added until no more precipitate was formed. The orange solid was filtered and rinsed with water. Yield: 478 mg (78%). Elemental Analysis for $C_{30}B_{46}H_{104}Co_2N_2O_6$: calc: C 32.33, H 8.47, N 2.28; found: C 32.74, H 8.49, N 2.35. IR (KBr): ν [cm^{-1}]=3584 (s, ν_s(N-H)), 3068, 3040 (w, ν_s($C_{cluster}$-H)), 2926, 2873 (s, ν_s(C_{alkyl}-H)), 2564 (s, ν_s(B-H)), 1456 (s, ν_s(N-C)), 1155, 1122, 1098, 1081 (s, ν_s(C-O)). ^{1}H NMR: δ [ppm] =4.25 (br s, 8H, $C_{cluster}$*H*), 3.58 (br m, 18H, OCH_2CH_2O (16H), $C_{cluster}$*H* (2H)), 3.43 (br s, 24H, N(CH_3)), 3.00-1.50 (br m, 42H, B*H*), 2.60 (m, 4H, OCH_2CH$_2$CH$_2$), 1.47 (m, 4H, OCH$_2$CH_2CH$_2$), 0.66 (m, 4H, OCH$_2$CH$_2$CH_2). ^{1}H{^{11}B} NMR: δ [ppm] =4.25 (br s, 8H, $C_{cluster}$*H*), 3.58 (br m, 10H, OCH_2CH_2O (8H), $C_{cluster}$*H* (2H)), 3.43 (br s, 24H, N(CH_3)), 3.00-1.50 (br m, 42H, B*H*), 2.98, 2.19, 1.96, 1.75, 1.66, 1.54 (br s, 42H, B*H*), 2.60 (m, 4H, OCH_2CH$_2$CH$_2$), 1.47 (m, 4H, OCH$_2$CH_2CH$_2$), 0.66 (m, 4H, OCH$_2$CH$_2$CH_2). ^{13}C{^{1}H} NMR: δ [ppm] =71.68 (s, O*C*H$_2$CH$_2$O), 71.52 (s, O*C*H$_2$CH$_2$O), 69.17 (s, OCH$_2$*C*H$_2$O)), 68.25 (s, OCH$_2$*C*H$_2$O), 64.37 (s, OCH$_2$CH$_2$CH$_2$), 55.19 (s, N(*C*H$_3$)), 54.72 (*C*$_{cluster}$), 46.36 (s, *C*$_{cluster}$), 34.12 (s, *C*$_{cluster}$), 33.23 (s, OCH$_2$*C*H$_2$*C*H$_2$), 13.21 (s, OCH$_2$CH$_2$*C*H$_2$). ^{11}B NMR: δ [ppm] =22.5 (s, 2B, B(8)), 3.39 (d, ^{1}J(B,H)=129 Hz, 2B, B(8')), 0.19 (d, ^{1}J(B,H)=142 Hz, 2B, B(10')), -2.72 (d, ^{1}J(B,H)=132 Hz, 4B, B(9,12)), -4.40 (d, ^{1}J(B,H)=183 Hz, 4B, B(4,7)), -7.79 (d, ^{1}J(B,H)=140 Hz, 2B, B(10)), -8.53 (d, ^{1}J(B,H)=153 Hz, 8B, B(4',7',9',12')), -17.5 (d, ^{1}J(B,H)=160 Hz, 4B, B(5',11')), -20.73 (d, ^{1}J(B,H)=151 Hz, 4B, B(5,11)), -22.0 (d, ^{1}J(B,H)=149 Hz, 2B, B(6')), -28.8 (d, ^{1}J(B,H)=142 Hz, 2B, B(6)). ESI MS: *m/z* (%)=540 (100) $[M\text{-}1]^{2-}$

Synthesis of $[N(CH_3)_4]_4$[8,9,10,12-(3,3'-Co-{8-$(OCH_2CH_2)_2$-1,2-$C_2B_9H_{10}$-1',2'-$C_2B_9H_{11}$}-O$(CH_2)_3)_4$-1,2-$C_2B_{10}H_8$] [**16**]: To a stirring solution of 8,9,10,12-(HOCH$_2$CH$_2$CH$_2$)$_4$-1,2-*closo*-$C_2B_{10}H_8$ (100 mg, 0.26 mmol) in THF (10 mL) cooled to 0 ºC in an ice-water bath was added dropwise a solution of butyllithium in hexanes (0.68 mL, 1.6M, 1.09 mmol). After stirring at room temperature for 30 minutes, a solution of [8-{O(CH$_2$CH$_2$)$_2$O}-3,3'-Co(1,2-$C_2B_9H_{10}$)(1',2'-$C_2B_9H_{11}$)] (447 mg, 1.09 mmol) in THF (10mL) was added via a syringe, following which the reaction was heated to reflux for 2 hours. Afterwards the solvent was removed under reduced pressure, 10 mL of diethyl ether and 10 mL of a diluted solution of HCl (0.1M) were added. The mixture was throughly shaken, and the two layers separated. The organic layer was separated from the mixture, and the aqueous layer was extracted with diethyl ether (3 x 10mL). The combined organic phase was dried over $MgSO_4$, filtered and the solvent removed under reduced pressure. Afterwards, an aqueous solution of $[NMe_4]$Cl was added dropwise until no more precipitate was formed. The orange solid was filtered and rinsed with water. Yield: 430 mg (70%). Elemental Analysis for $C_{62}B_{82}H_{196}Co_4N_4O_{12}$: calc: C 32.73, H 8.48, N 2.42; found: C 32.98, H 8.49, N 2.47. IR (KBr): ν [cm^{-1}] =3433 (s, ν_s(N-H)), 3039 (w, ν_s($C_{cluster}$-H)), 2923, 2862 (s, ν_s(C_{alkyl}-H)), 2553 (s, ν_s(B-H)), 1481 (s, ν_s(N-C)), 1172, 1103 (s, ν_s(C-O)). ^{1}H NMR: δ [ppm] =4.27 (br s, 10H, $C_{cluster}$*H* (8H), $C_{cluster}$*H* (2H)), 3.51 (br m,

48H, OCH_2CH_2O (32H), OCH_2CH_2CH_2 (8H), $C_{cluster}$H (8H)), 3.45 (br s, 48H, N(CH_3)), 3.00-1.50 (br m, 78H, B*H*), 1.52 (m, 4H, OCH$_2$CH_2CH$_2$), 1.35 (m, 4H, OCH$_2$CH_2CH$_2$), 1.12 (m, 4H, OCH$_2$CH$_2$CH_2), 0.90 (m, 4H, OCH$_2$CH$_2$CH_2). ^{1}H{^{11}B} NMR: δ [ppm] =4.27 (br s, 10H, $C_{cluster}$*H* (8H), $C_{cluster}$*H* (2H)), 3.51 (br m, 48H, OCH_2CH_2O (32H), OCH_2CH_2CH_2 (8H), $C_{cluster}$*H* (8H)), 3.45 (br s, 48H, N(CH_3)), 3.00-1.50 (br m, 78H, B*H*), 2.91, 2.76, 2.69 (br m, 24H, B*H*), 2.45, 2.38 (br s, 4H, B*H*), 1.98 (br s, 10H, B*H*), 1.77 (br s, 40H, B*H*), 1.52 (m, 4H, OCH$_2$CH_2CH$_2$), 1.35 (m, 4H, OCH$_2$CH_2CH$_2$), 1.12 (m, 4H, OCH$_2$CH$_2$CH_2), 0.90 (m, 4H, OCH$_2$CH$_2$CH_2). ^{13}C{^{1}H} NMR: δ [ppm] =71.87, 70.32 (s, OCH_2CH$_2$O), 70.22, 70.50 (s, OCH_2CH_2CH$_2$), 69.98, 68.38 (s, OCH$_2$CH_2O), 55.18 (s, N(CH_3)), 54.59 ($C_{cluster}$), 46.36 ($C_{cluster}$), 34.10, 31.76 (s, OCH$_2$CH_2CH_2), 17.41 (s, OCH$_2$CH$_2$CH_2). ^{11}B NMR: δ [ppm] =23.6 (s, 4B, B(8)), 4.47 (d, ^{1}J(B,H)=137 Hz, 4B, B(8')), 1.14 (d, ^{1}J(B,H)=141 Hz, 4B, B(10')), -1.69 (d, ^{1}J(B,H)=142 Hz, 8B, B(9,12)), -3.45 (d, ^{1}J(B,H)=140 Hz, 8B, B(4,7)), -6.77 (d, ^{1}J(B,H)=142 Hz, 4B, B(10)), -7.50 (d, ^{1}J(B,H)=129 Hz, 16B, B(4',7',9',12')), -16.5 (d, ^{1}J(B,H)=153 Hz, 8B, B(5',11')), -19.7 (d, ^{1}J(B,H)=143 Hz, 8B, B(5,11)), -20.9 (d, ^{1}J(B,H)=187 Hz, 4B, B(6')), -27.7 (d, ^{1}J(B,H)=156 Hz, 4B, B(6)). ESI MS: *m/z* (%)=503.9 (100) [M-1]$^{4-}$.

X-ray structure analysis

X-ray crystal structure analyses were performed by using an Enraf Nonius CCD area detector diffractometer with MoK$_\alpha$ radiation (λ = 0.71073 Å) equipped with an Oxford Cryostream low-temperature unit. The data sets were corrected for abortion using SADABS program.[30] The structures were solved with the program SIR97,[31] full-least-squares refinements on F^2 were performed with SHELXL97[32] using anisotropic displacement parameters for most of the non-H atoms. The hydrogen atoms were treated as riding atoms using the SHELX97 default parameters or their positional parameters were refined isotropically according to the riding model. All calculations and graphics were done at WinGX [33] platform.

8,9,10,12-(ClCH$_2$CH$_2$CH$_2$)$_4$-1,2-*closo*-C$_2$B$_{10}$H$_8$ [**8**]: $C_{14}B_{10}H_{32}Cl_4$, M_r = 450.32, space group P2$_1$/c (No.14), a = 15.1769(3), b = 10.7294(2), c = 30.2110(6) Å; α = 90, β =104.1410(10), γ = 90 °, V = 4770.46 Å^3, Z = 8, T = 173(2), R-factor = 5.6 %.

Notes and References

[1] a) R. N. Grimes, *Angew. Chem., Int. Ed. Engl.* **1993**, *32*, 1289; b) T. J. Wedge and M. F. Hawthorne, *Coord. Chem. Rev.* **2003**, *240*, 111; c) M. A. Fox and A. K. Hughes, *Coord. Chem. Rev.* **2004**, *248*, 457; d) P. C. Andrews, M. J. Hardie and C. L. Raston, *Coord. Chem. Rev.* **1999**, 189, 169; e) B. H. Northrop, H. B. Yang and P. J. Stang, *Chem. Commun*. **2008**, 5896; f) A. V. Puga, F. Teixidor, R. Sillanpää , R. Kivekäs, M. Arca, G. Barberà and C. Viñas, *Chem.–Eur. J.* **2009**, *15*, 9755; g) A. V. Puga, F. Teixidor, R. Sillanpää , R. Kivekäs, M. Arca, G. Barberà and C. Viñas, *Chem.–Eur. J.* **2009**, *15*, 9764.

[2] a) M. F. Hawthorne, *Angew. Chem., Int. Ed. Engl.* **1993**, *32*, 950; b) A. H. Soloway, W. Tjarks, B. A. Barnum, F. G. Rong, R. F. Barth, I. M. Codogni and J. G. Wilson, *Chem. Rev.* **1998**, *98*, 1515; c) V. I. Bregadze, I. B. Sivaev, D. Gabel and D. Wöhrle, *J. Porphyrins Phthalocyanines* **2001**, *5*, 767; d) J. F. Valliant, K. J. Guenther, A. S. King, P. Morel, P. Schaffer, O. O. Sogbein and K. A. Stephenson, *Coord. Chem. Rev.* **2002**, *232*, 173; e) R. F. Barth, J. A. Coderre, M. G. H. Vicente and T. E. Blue, *Clin. Cancer Res.* **2005**, *11*, 3987; f) V. I. Bregadze and I. B. Sivaev, *Eur. J. Inorg. Chem.* **2009**, 1433, and references therein.

[3] a) B. P. Dash, R. Satapathy, E. R. Gaillard, J. A. Maguire and N. S. Hosmane, *J. Am. Chem. Soc.* **2010**, *132*, 6578; b) R. Núñez, A. González, C. Viñas, F. Teixidor, R. Sillanpää and R. Kivekäs, *Org. Lett.* **2005**, *7*, 231; c) A. González- Campo, E. J. Juárez- Pérez, C. Viñas, B. Boury, R. Sillanpää , R. Kivekäs and R. Núñez, *Macromolecules* **2008**, *41*, 8458; d) A. Mollard and I. Zharov, *Inorg. Chem.* **2006**, 45, 10172; e) G.Wu, R. F. Barth, W. L. Yang, M. Chatterjee, W. Tjarks, M. J. Ciesielski and R. A. Fenstermaker, *Bioconjugate Chem.* **2004**, 15, 185; f) D. Armspach, M. Cattalini, E. C. Constable, C. E. Housecroft and D. Phillips, *Chem. Commun.* **1996**, 1823; g) E. Hao, E. Friso, G. Miotto, G. Jori, M. Soncin, C. Fabris, M. Sibrian-Vazquez and M. G. H. Vicente, *Org. Biomol. Chem.* **2008**, *6*, 3732; h) H. J. Yao, R. N. Grimes, M. Corsini and P. Zanello, *Organometallics* **2003**, *22*, 4381.

[4] a) L. Ma, J. Hamdi, F. Wong and M. F. Hawthorne, *Inorg. Chem.* **2006**, *45*, 278; b) T. J. Li, S. S. Jalisatgi, M. J. Bayer, A. Maderna, S. I. Khanm and M. F. Hawthorne, *J. Am. Chem. Soc.* **2005**, *127*, 17832.

[5] R. Núñez, A. González-Campo, A. Laromaine, F. Teixidor, R. Sillanpää, R. Kivekäs and C. Viñas, *Org. Lett.* **2006**, *8*, 4549.

[6] a) F. Teixidor and C. Viñas, *in Science of Synthesis.* ed. D. E. Kaufmann and D. S. Matteson, Georg Thieme Verlag, Stuttgart, **2005**; b) V. I. Bregadze, *Chem. Rev.* **1992**, 92, 209; c) R. N. Grimes, *Carboranes*, Academic Press, New York, **1970**.

[7] H. D. Smith, T. A. Knowles and H. Schroeder, *Inorg. Chem.* **1965**, *4*, 107.

[8] J. A. Potenza, W. N. Lipscomb, G. D. Vickers and H. Schroeder, *J. Am. Chem. Soc.* **1966**, *88*, 628.

[9] a) G. Barberà, A. Vaca, F. Teixidor, R. Sillanpää, R. Kivekäs and C. Viñas, *Inorg. Chem.* **2008**, *47*, 7309; b) A. Vaca, F. Teixidor, R. Kivekäs, R. Sillanpää and C. Viñas, *Dalton Trans*., **2006**, 4884, and references therein.

[10] "Building Highly Dense Multibranched o-Carborane Derivatives by means of Kumada Cross Coupling Reaction". A. Pepiol, F. Teixidor, R. Silanpää, C. Viñas. In preparation.

[11] A. Vaca, F. Teixidor, R. Sillanpää , R. Kivekäs, C. Viñas, *Chem. Commun.* **2011**, *47*, 2252–2254.

[12] T. Mizoroki, K. Mori, A. Ozaki, *Bull. Chem. Soc. Jpn*., **1971**, 44, 581.

[13] R. F. Heck, J. P. Nolley, Jr., *J. Org. Chem*., **1972**, 37, 2320-2322.

[14] H. A. Dieck, R. F. Heck, *J. Am. Chem. Soc.*, **1974**, 96, 1133-1136.

[15] Y. Ben-David, M. Portnoy, M. Gozin, D. Milstein, *Organometallics*, **1992,** 11, 1995-1996.

[16] T. Jeffery, *J. Chem. Soc., Chem. Commun.*, **1984,** 1287-1289.

[17] R. Apple, *Angew. Chem. Int. Ed*., **1975**, 14, 801-811.

[18] Y. Yoshida, Y. Sakakura, N. Aso, S. Okada, Y. Tanabe, *Tetrahedron*, **1999**, 55, 2183-2192.

[19] K. Bowden, I. M. Heilbron, E. R. H. Jones, B. C. L. Weedon, *J. Chem. Soc.*, **1946**, 39-45.

[20] a) B. Neises, W. Steglich, *Organic Syntheses*, **1990**, 7, 93; b) B. Neises, W. Steglich, *Angew. Chem. Int. Ed*., **1978**, 7, 522-524; c) B. Neises, W. Steglich, *Organic Syntheses*, **1985**, 63, 183.

[21] a) J. Plešek, S. Heřmanek, K. Baše, L.J. Todd, W.F. Wright, *Collect. Czech. Chem. Commun.* **1976**, *41*, 3509; b) A. Petřina, V. Petříček, K. Malý , V. Šubrtova, A. Linek, L. Hummel, *Z. Kristallogr.* **1981**, *154*, 217; c) V. Šubrtova, V. Petříček, L. Hummel, *Acta Crystallogr., Sect. C* **1989**, *45*, 1964.

[22] J. Plešek, S. Heřmanek, A. Franken, I. Cisařova, C. Nachtigal, *Collect. Czech. Chem. Commun.* **1997**, *62*, 47.

[23] F. Teixidor, J. Pedrajas, I. Rojo, C. Vinas, R. Kivekas, R. Sillanpaa, I. Sivaev, V. Bregadze, S. Sjoberg, *Organometallics* **2003**, *22*, 3414.

[24] P. Farras, F. Teixidor, R. Kivekas, R. Sillanpaa, C. Viñas, B. Gruner, I. Cisarova, *Inorg. Chem.* **2008**, *47*, 9497.

[25] J. Llop, C. Vinas, F. Teixidor, Ll. Victori, *J. Chem. Soc., Dalton Trans.* **2002**, *8*,1559.

[26] a) B. Gruner, L. Mikulašek, J. Bacˇa, I. Cisarˇova, V. Bohmer, C. Danila, M.M. Resinoso-Garcia, W. Verboom, D.N. Reihoudt, A. Casnati, R. Ungaro, *Eur. J. Org. Chem.* **2005**, 2022–2039; b) L. Mikulašek, B. Gruner, C. Danila, V. Bohmer, J. Časlavský , P. Selucký , *Chem. Commun.* **2006**, 4001–4003; c) L. Mikulašek, B. Grüner, C. Dordea, V. Rudzevich, V. Böhmer, J. Haddaoui, V. Hubscher, F. Arnaud-Neu, J.Časlavsky´ , P. Selucký , *Eur. J. Org. Chem.* **2007**, *28*, 4772–4783.

[27] P. Selucký , J. Rais, M. Lučanikova, B. Gruner, M. Kvičalova, K. Fejfarova, I. Cisařova, *Radiochim. Acta 96* **2008**, *4–5*, 273–284, and the references therein.

[28] P. Cigler, M. Kožišek, P. Řezačova, J. Brynda, Z. Otwinowski, J. Pokorna, J. Plešek, B. Gruner, L. Dolecˇkova-Marešova, M. Maša, J. Sedlaček, J. Bodem, H.G. Krausslich, V. Kral, J. Konvalinka, *PNAS* **2005**, *102*, 15394.

[29] A. A. Semioshkin, I. B. Sivaev, V. I. Bregadze, *Dalton Trans.* **2008**, 977.

[30] G. M. Sheldrick *SADABS*, University of Göttingen, Germany, **2008**.

[31] A. Altomare, M. C. Burla, M. Camalli, G. L. Cascarano, C. Giacovazzo, A. Guagliardi, A.G. G. Moliterni, G. Polidori, R. Spagna, SIR 97: A new tool for crystal structure determination and refinement. *J. Appl. Cryst.* **1999**, *32*, 115-119.

[32] G. M. Sheldrick *Acta Crystallogr. , Sect. A: Found. Crystallogr.* **2008**, *A64*, 112-122.

[33] L. J. Farrugia, WinGX suite for small-molecule single-crystal crystallography. *J. Appl.Cryst.* **1999**, *32*, 837-838.

SCHEME 1. Kumada cross coupling reaction on [2] using cis-$[Pd(PPh_3)_2Cl_2]$ and CuI as a catalysts, in THF refluxing overnight. To synthesize [1] same procedure was used.

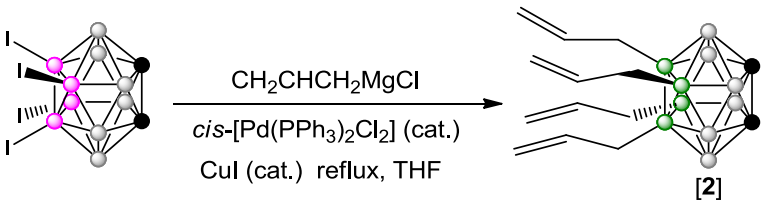

SCHEME 2. Heck cross coupling reaction on [**1**] using *cis*-$[Pd(PPh_3)_2Cl_2]$ as a catalysts, 2,6-litidine as a base in DMF refluxing 24h.

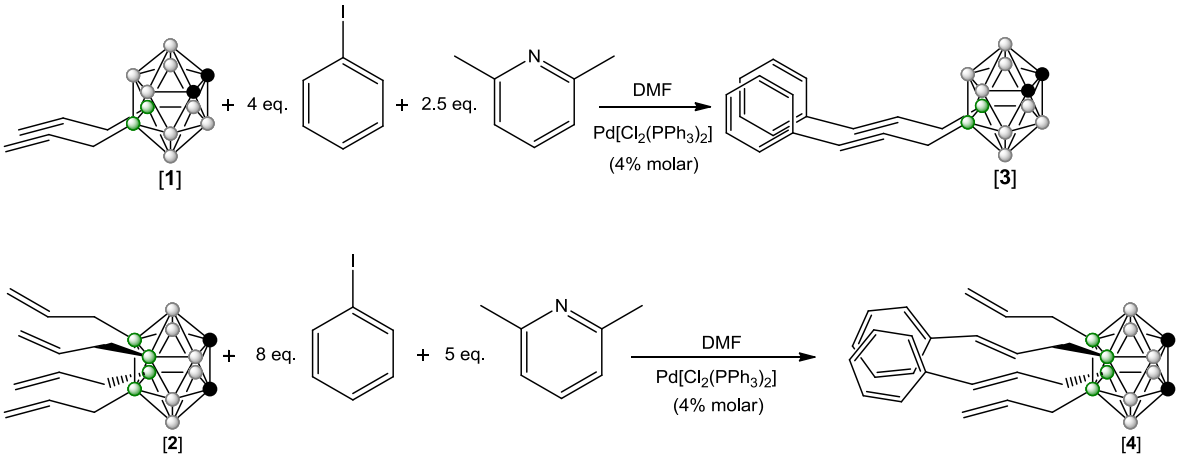

SCHEME 3. Hydroboration/oxidation process on terminal olefinic groups of [**1**] and [**2**] using BH_3·THF, H_2O_2 in basic aqueous solution (KOH) to obtain [**5**] and [**6**] in good to high yield.

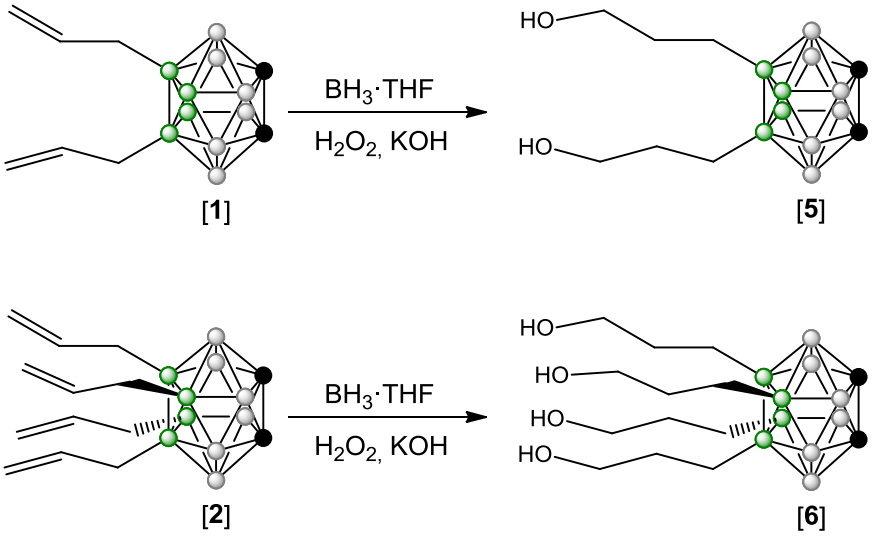

B-H C-H B-I B

SCHEME 4. Derivatization reactions on [**5**]: (i) chlorination using $SOCl_2$ and $N(CH_2)_3CH_3)_4]Cl$, (ii) Appel bromination using PPh_3 and CBr_4, (iii) Steglich esterification with benzoic acid, DCC and DMAP.

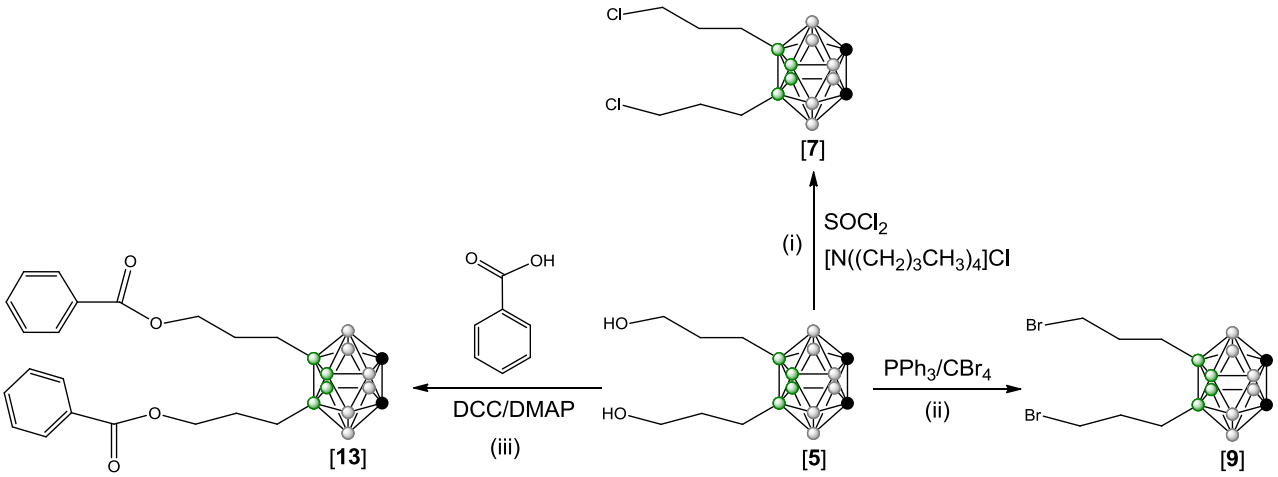

SCHEME 5. Derivatization reactions on [**6**]: (i) chlorination using $SOCl_2$ and $N(CH_2)_3CH_3)_4]$ Cl, (ii) Appel bromination using PPh_3 and CBr_4, (iii) tosylation using TsCl, NEt_3 $[NH(CH_3)_3]Cl$, (iv) oxidation into carboxylic acid with CrO_3 and H_2SO_4 in acetone (v) Steglich esterification with benzoic acid, DCC and DMAP.

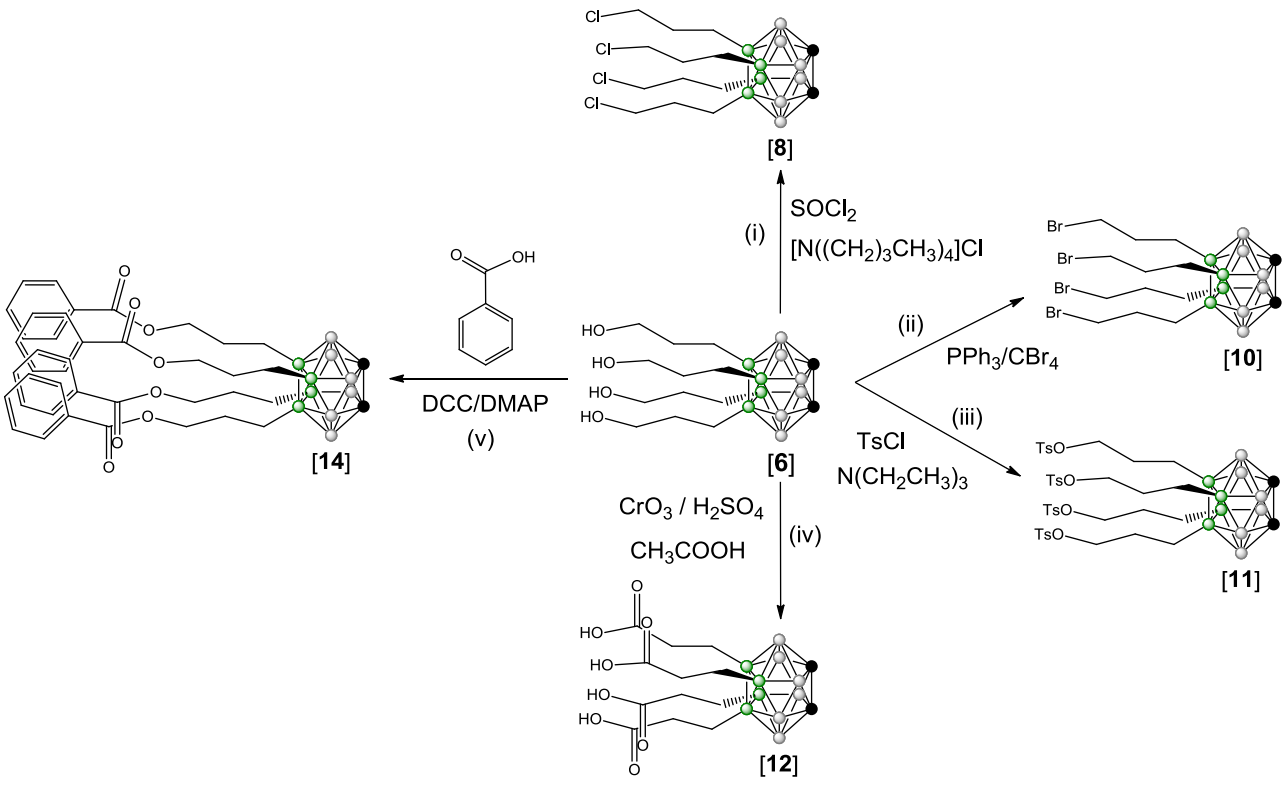

B-H C-H B

SCHEME 6. Nucleophilic oxonium ring-opening reaction on zwiterionic compound [3,3′-Co(8-$C_4H_8O_2$-1,2-$C_2B_9H_{10}$)(1′,2′-C_2B_9-H_{11})] by deprotonated hydroxyl derivatives [**5**] and [**6**] to obtain $[N(CH_3)_4]_2$[9,12-(3,3'-Co-{8-($C_4H_8O_2$-1,2-$C_2B_9H_{10}$-1',2'-$C_2B_9H_{11}$}-$O(CH_2)_3)_2$-1,2-$C_2B_{10}H_{10}$] [**15**] and $[N(CH_3)_4]_4$[8,9,10,12-(3,3'-Co-{8-($C_4H_8O_2$-1,2-$C_2B_9H_{10}$-1',2'-$C_2B_9H_{11}$}-$O(CH_2)_3)_4$-1,2-$C_2B_{10}H_8$] [**16**].

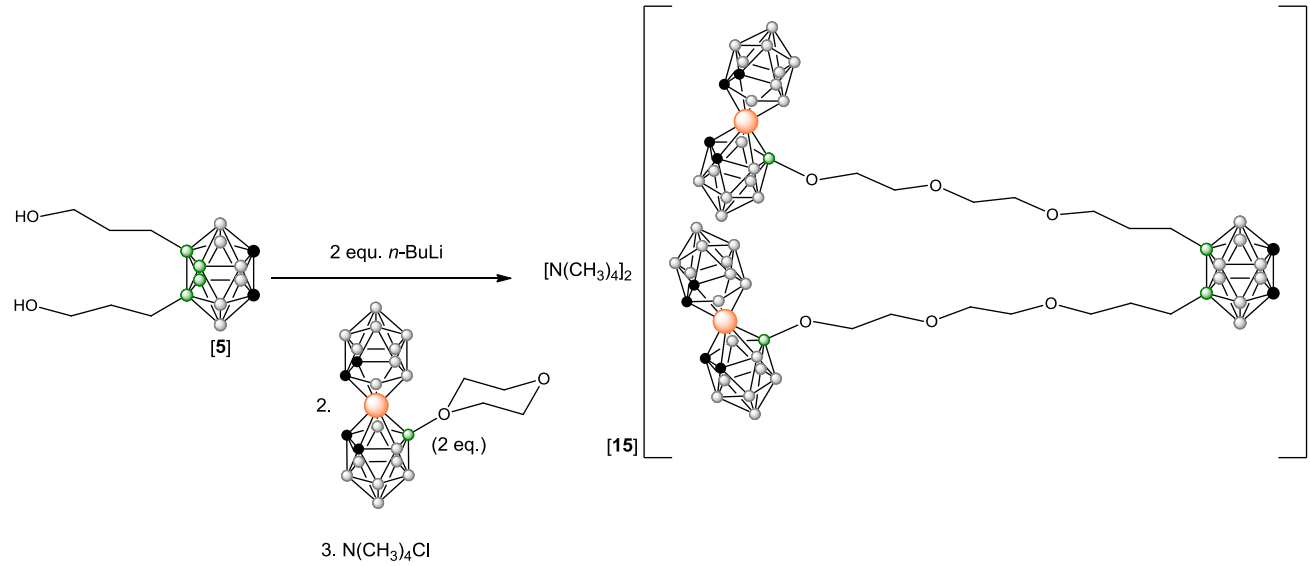

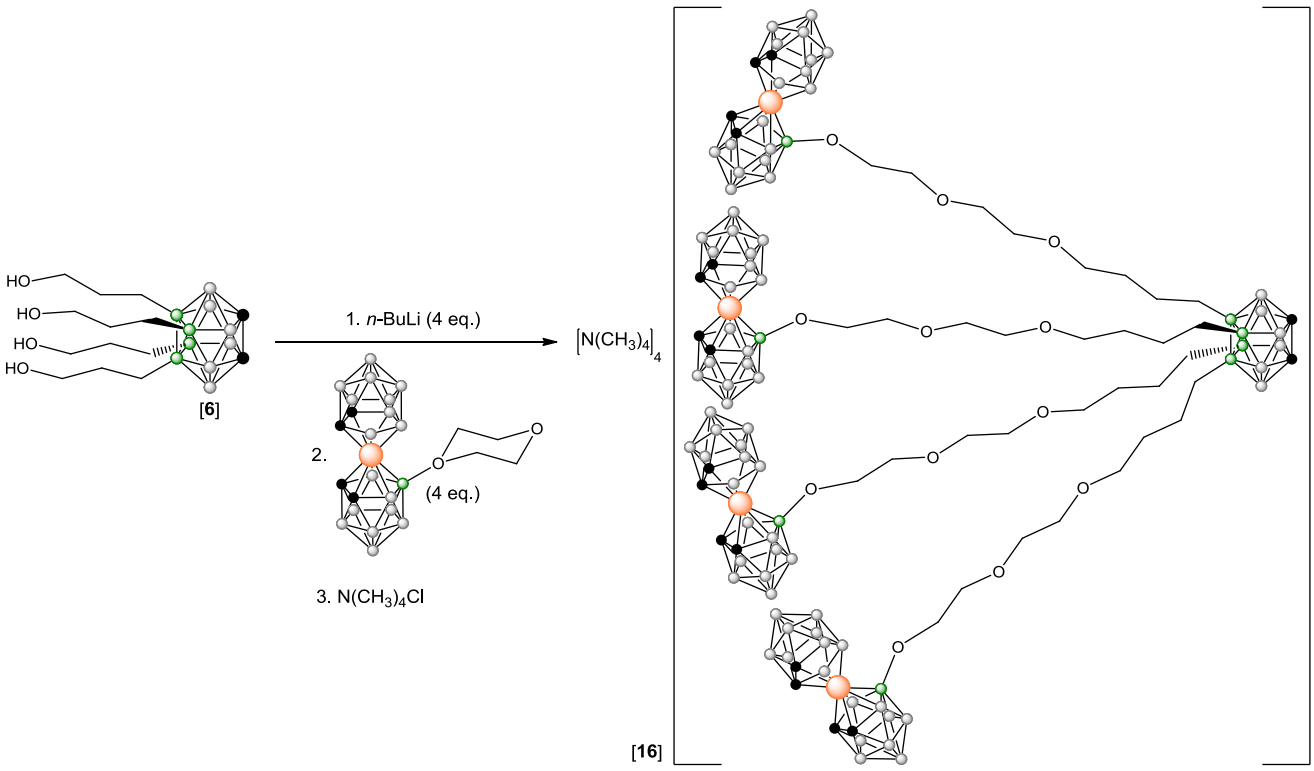

B-H C-H B Co

FIGURE 1. MALDI-TOF spectrum of 9,12-$(PhCH_2CHCH_2)_2$1,2-*closo*-$C_2B_{10}H_{10}$ [**3**] and 8,9,10,12-$(PhCH_2CHCH_2)_2(CH_2CHCH_2)_2$-1,2-*closo*-$C_2B_{10}H_8$ [**4**].

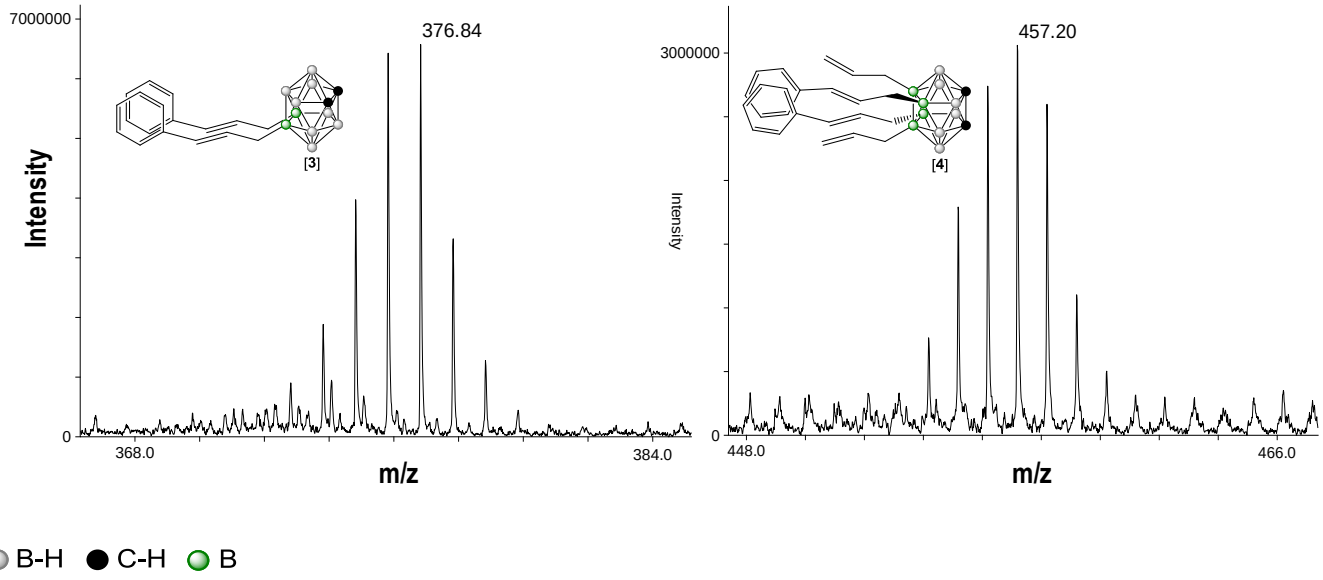

B-H C-H B

FIGURE 2. Crystal packing of [**8**] showing the periodical $C_{cluster}$-H···Cl-C interactions, view down crystallographic *c* axis. White = H, pink = B, grey = C). Contacts shorter than the sum of Van der Waals radii are plotted as dashed dark lines.

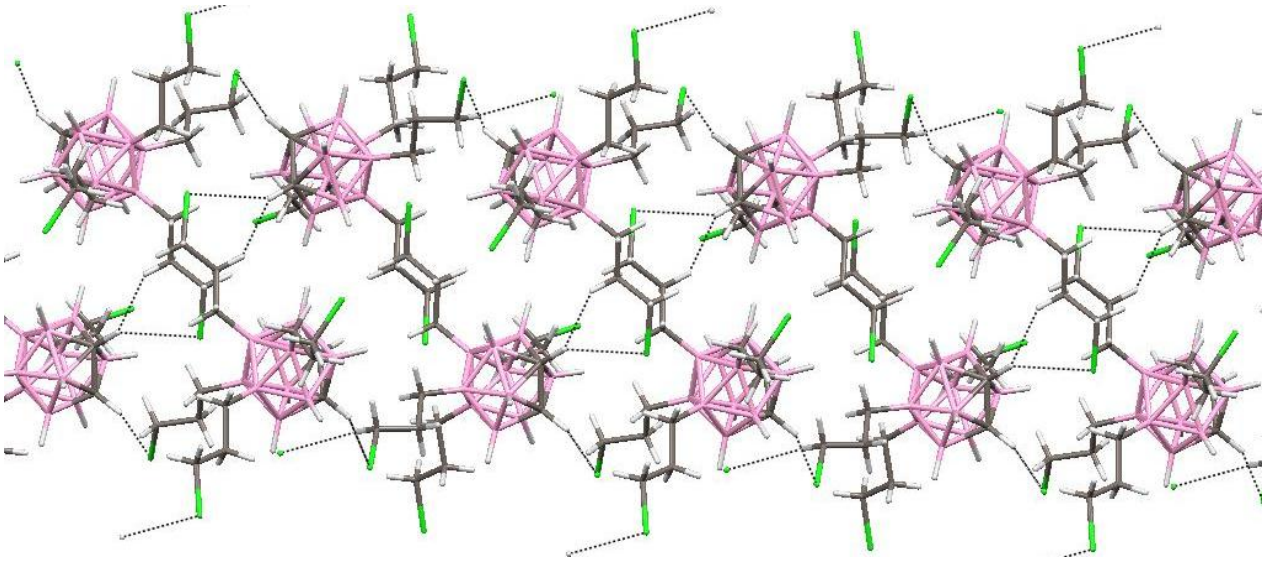

FIGURE 3. $^{13}C\{^{1}H\}$-NMR spectra comparison of [**6**], [**8**], [**10**] and [**11**].

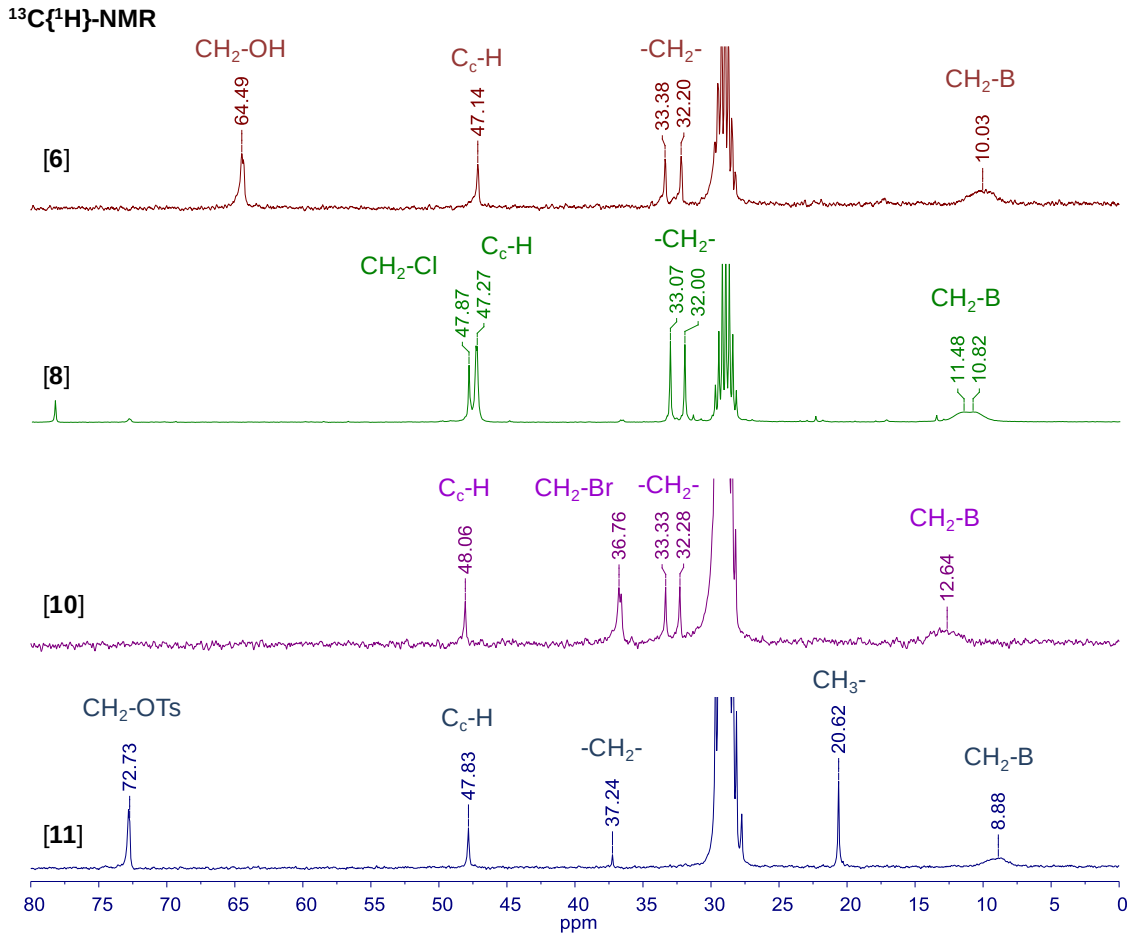

FIGURE 4. MALDI-TOF-MS spectra of $[N(CH_3)_4]_2[9,12\text{-}(3,3'\text{-}Co\text{-}\{8\text{-}(C_4H_8O_2\text{-}1,2\text{-}C_2B_9H_{10}\text{-}1',2'\text{-}C_2B_9H_{11}\}\text{-}O(CH_2)_3)_4\text{-}1,2\text{-}C_2B_{10}H_{10}]$ [**15**].

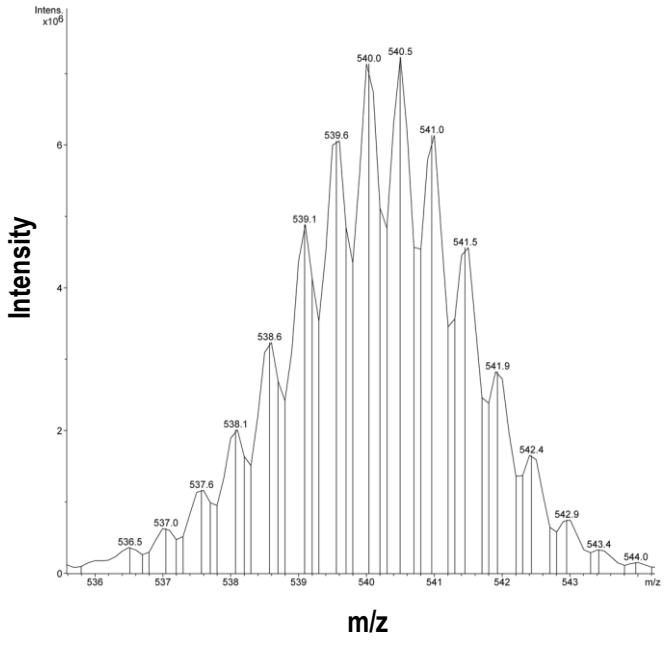

FIGURE 5. MALDI-TOF-MS spectra of $[N(CH_3)_4]_4[8,9,10,12\text{-}(3,3'\text{-}Co\text{-}\{8\text{-}(C_4H_8O_2\text{-}1,2\text{-}C_2B_9H_{10}\text{-}1',2'\text{-}C_2B_9H_{11}\}\text{-}O(CH_2)_3)_4\text{-}1,2\text{-}C_2B_{10}H_8]$ [**16**].

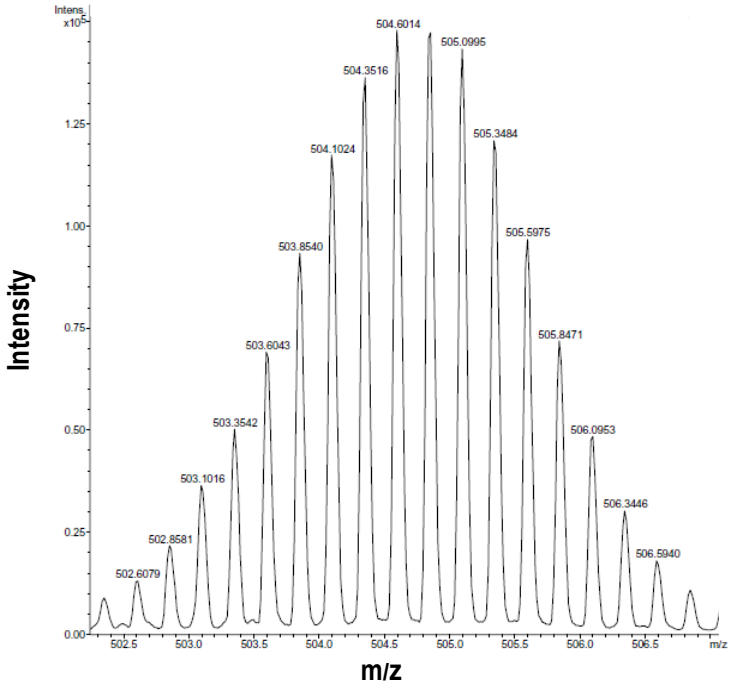

Towards the Synthesis of High Boron Content Neutral and Polyanionic Multicluster Macromolecules via *B,C*-Substituted Icosahedral o-Carboranes

Ariadna Pepiol[a], Francesc Teixidor[a], Clara Viñas[a*]

[a] *Institut de Ciencia de Materials de Barcelona (CSIC) Campus UAB, 08193 Bellaterra, Spain. e-Mail clara@icmab.es*

The use of nucleophilic and electrophilic processes have allowed the synthesis of a number of *C*- and *B*-derivatives of *o*-carborane. Because the utility of carborane units is dependent upon their functionalization,[1] the introduction of functional groups at the boron and carbon atoms is an important target.

The substitution of the carbon hydrogen in carborane clusters is easy because the C-H vertices may be deprotonated with strong bases. Conversely, the chemistry of boron-substituted carboranes is less developed than that of the carbon-substituted analogues because of the higher difficulty of introducing functional groups at the boron atoms of the carborane cage.

Following a reported method for the functionalization of *o*-carboranes through their boron atoms by Kumada cross-coupling reaction, which allows the substitution of iodine atoms for organic moieties, we synthesize 9,12-$(CH_2CHCH_2)_2$-1,2-*closo*-$C_2B_{10}H_{10}$ [**1**][2] and 8,9,10,12-$(CH_2CHCH_2)_4$-1,2-*closo*-$C_2B_{10}H_8$ [**2**].[3] In this work we report the carbon cluster vertexes functionalization of these two compounds [**1**] and [**2**] through nucleophilic substitution with allyl bromide. Terminal olefinic groups are free to perform further reactions on them, enabling the *ortho*-carborane cluster to become the core for the design of a new type of globular dendrimers, having a rigid head with four and six branches appending from it.

Dendrimers are known for their well-defined globular hyperbranched structures and low polydispersity that combined with the high number of functional groups and metal fragments, that can be localized at the core or at the periphery, provides a wide range of macromolecules with interesting catalytic, redox, magnetic, photo-optical and biomedical properties. [4], [5]

In the course of our research on high boron-content molecules, we recently developed different synthetic strategies for the preparation of anionic dendrimeric systems, by using *B*-functionalized carborane nucleolus as scaffold in which anionic metallacarborane clusters were placed at the periphery.[6]

Following our studies on developing boron-rich anionic dendrimers, we considered appropriate to use [3,3′-Co(8-$C_4H_8O_2$-1,2-$C_2B_9H_{10}$)(1′,2′-C_2B_9-H_{11})] to be peripherally attached to dendrimers. This metallacarborane is an electron-deficient sandwich with 18 boron atoms, which is characterized by its extraordinary chemical and thermal stability.[7] This compound is hydrophobic,[8] a weakly coordinating and low nucleophilic anion,[9], [10] which made it suitable for a wide range of applications. [11]

Cobaltabisdicarbollide derivatives have also been considered promising agents as boron rich carriers for cancer treatment and diagnosis in Boron Neutron Capture Therapy (BNCT).[12] These boron compounds can be delivered into tumor cells using different

strategies for tumor targeting or can be used as building blocks for the synthesis of boron-containing biomolecules. For that reason, this metallacarborane has been attached to different organic groups and biomolecules, such as nucleosides and porphyrins. [13]

The design of water soluble boron-rich dendritic or macromolecular systems is of interest for boron neutron capture therapy (BNCT) or for drug delivery systems. The *closo*-carboranes have been tested for boron delivery into tumors; however, their extreme lipophilicity often produces water-insoluble structures with limited bioavailability, precluding thus effective application of such compounds in BNCT. One solution to the problem of the water solubility of BNCT agents could be to replace a neutral carborane with an anionic metallacarborane.

The generation of diverse macromolecules and supramolecular assemblies constitutes a main focus for our current research. To achieve this proposal, the insertion of organic moieties on carbon cluster vertexes was required, in order to construct a globular like dendron nucleolus.

First, deprotonation of the two hydrogen bonded to carbon atoms of 9,12-$(CH_2CHCH_2)_2$-1,2-*closo*-$C_2B_{10}H_{10}$ [**1**] and 8,9,10,12-$(CH_2CHCH_2)_4$-1,2-*closo*-$C_2B_{10}H_8$ [**2**] was carried out with 2 equivalents of *n*-butillitium at low temperature. Afterwards, allyl bromide was added in order to perform a nucleophilic substitution on carbon cluster vertexes and achieve 1,2-$(CH_2CHCH_2)_2$-9,12-$(CH_2CHCH_2)_2$-1,2-*closo*-$C_2B_{10}H_8$ [**3**] and 1,2-$(CH_2CHCH_2)_2$-8,9,10,12-$(CH_2CHCH_2)_4$-1,2-*closo*-$C_2B_{10}H_6$ [**4**] in good to high yield, 89 and 86%, respectively (Scheme 1).

As a first approach to the development of dendritic precursors a hydroboration/oxidation reaction has been carried out to transform the terminal double bonds to hydroxyl groups of [**3**] and [**4**]. BH_3·THF was used as the hydroborating agent. Subsequent oxidation was performed by treatment with H_2O_2 in a basic aqueous solution. No hindered hydroboranes were thus needed for the control of the regioselectivity. This anticipates a versatile chemistry for dendritic growth, given the availability of the four and six terminal hydroxyl groups for further elongation of the chains. Compounds 1,2-$(OHCH_2CH_2CH_2)_2$-9,12-$(OHCH_2CH_2CH_2)_2$-1,2-*closo*-$C_2B_{10}H_8$ [**5**] and 1,2-$(OHCH_2CH_2CH_2)_2$-8,9,10,12-$(OHCH_2CH_2CH_2)_4$-1,2-*closo*-$C_2B_{10}H_6$ [**6**] were isolated in good yields 87 and 80%, respectively (Scheme 2, (i)).

On the other hand, Apple reaction[14] has been carried out in order to exchange terminal hydroxyl groups of [**5**] and [**6**] by bromide atoms, using PPh_3 and CBr_4 to achieve 1,2-$(BrCH_2CH_2CH_2)_2$-9,12-$(BrCH_2CH_2CH_2)_2$-1,2-*closo*-$C_2B_{10}H_8$ [**7**] and 1,2-$(BrCH_2CH_2CH_2)_2$-8,9,10,12-$(BrCH_2CH_2CH_2)_4$-1,2-*closo*-$C_2B_{10}H_6$ [**8**] (Scheme 2, (ii)).

Since the discovery of nucleophilic oxonium ring-opening (ORO) reactions in the carborane and metallacarborane series by Plešek et al.,[15] has elapsed more than 30 years. These reactions represent an important feature of substitution boron chemistry and many examples can be found in the literature.[16-22] Moreover, a recent exhaustive review by Semioshkin et al. [23] has been published on this field.

In this paper, we extend this viable structural feature by our results on the isolation of di- and tetranions combining both the [3,3′-Co(8-$C_4H_8O_2$-1,2-$C_2B_9H_{10}$)(1′,2′-C_2B_9-H_{11})] and *o*-carborane derivatives structural motifs. We were interested in exploring the possibility of using both known and new types of nucleophiles to get high-boron-content compounds. In order to enchance the nucleophilic character of the terminal hydroxyl groups of [**6**] we used *n*-BuLi to deprotonate the nucleophile. The addition of the base was done dropwise at low temperatures, and it was left stirring for 1 h. Afterwards, the reaction was cooled down again to 0 °C, followed by the addition of [3,3′-

$Co(8\text{-}C_4H_8O_2\text{-}1,2\text{-}C_2B_9H_{10})(1',2'\text{-}C_2B_9\text{-}H_{11})]$. After stirring at room temperature for 30 minutes, compounds $[N(CH_3)_4]_6[1,2,8,9,10,12\text{-}(3,3'\text{-}Co\text{-}\{8\text{-}(C_4H_8O_2\text{-}1,2\text{-}C_2B_9H_{10}\text{-}1',2'\text{-}C_2B_9H_{11}\}\text{-}O(CH_2)_3)_6\text{-}1,2\text{-}C_2B_{10}H_6]$ [**9**] was isolated by a cationic metathesis to tetramethylammonium salt, getting an orange solid as the final product (Scheme 2, (iii)). This nucleophilic oxonium ring-opening reaction leads to hexa-anionic compound that contain both metallabisdicarbaborane and carborane structural motifs in one molecule.

All the synthesized compounds have been corroborated by elemental analysis, matrix-assisted laser desorption/ionization-time of flight mass spectrometry (MALDI-TOF-MS), IR and ^1H, $^1H\{^{11}B\}$, $^{13}C\{^1H\}$, ^{11}B, and $^{11}B\{^1H\}$ NMR spectroscopies.

Figure 1 shows MALDI-TOF-MS spectrum of compound [**9**] in which the molecular ion peak of $[N(CH_3)_4]_4[1,2,8,9,10,12\text{-}(3,3'\text{-}Co\text{-}\{8\text{-}(C_4H_8O_2\text{-}1,2\text{-}C_2B_9H_{10}\text{-}1',2'\text{-}C_2B_9H_{11}\}\text{-}O(CH_2)_3)_6\text{-}1,2\text{-}C_2B_{10}H_6]^{4-}$ is observed at m/z = 775. It should be noticed the separation between isotopic peaks distribution is of m/z 0.25 unites corresponding to the tetra-anion fragment.

Figure 2 shows a comparison of ^{11}B NMR diagram spectra for 9,12-$(CH_2CHCH_2)_2$-1,2-*closo*-$C_2B_{10}H_{10}$ [**1**], 8,9,10,12-$(CH_2CHCH_2)_4$-1,2-*closo*-$C_2B_{10}H_8$ [**2**], 1,2-$(CH_2CHCH_2)_2$-9,12-$(CH_2CHCH_2)_2$-1,2-*closo*-$C_2B_{10}H_8$ [**3**] and 1,2-$(CH_2CHCH_2)_2$-8,9,10,12-$(CH_2CHCH_2)_4$-1,2-*closo*-$C_2B_{10}H_6$ [4].

Table 1 shows the ^{11}B-NMR chemical shifts (in ppm) for several 9,12-R_2-1,2-*closo*-$C_2B_{10}H_{10}$, 8,9,10,12-R_4-1,2-*closo*-$C_2B_{10}H_8$, 1,2,9,12-R_4-1,2-*closo*-$C_2B_{10}H_8$ and 1,2,8,9,10,12-R_6-1,2-*closo*-$C_2B_{10}H_6$.

Table 2 shows the $^{13}C\{^1H\}$-NMR chemical shifts (in ppm) for several 9,12-R_2-1,2-*closo*-$C_2B_{10}H_{10}$, 8,9,10,12-R_4-1,2-*closo*-$C_2B_{10}H_8$, 1,2,9,12-R_4-1,2-*closo*-$C_2B_{10}H_8$ and 1,2,8,9,10,12-R_6-1,2-*closo*-$C_2B_{10}H_6$.

The *o*-carborane cluster then provides a unique platform for the construction of highly dense multibranched molecules with a wide range of possibilities for derivatization. Derivatives of *o*-carborane with precise patterns of substitution can be prepared by judicious choice of the synthetic procedure. We have coupled hydroxyl terminated arms onto a specific, compact area of the cluster occupied by adjacent carbon and boron vertices, ultimately leading to a tetra and hexa-branched structure which might serve as a versatile dendritic precursor.

Furthermore, compound [**9**] can be used as a core to make a new class of dendrimers that contain multiple carborane or metallacarborane clusters at their periphery. Further work to synthesize potential new classes of BNCT compounds is now underway.

Experimental Section

Materials and instrumentation: All *o*-carboranes prepared are air and moisture stable. All manipulations were carried out under inert atmosphere. THF was distilled from sodium benzophenone prior to use. Reagents were obtained commercially and used as purchased. 1,2-*closo*-$C_2B_{10}H_{12}$ was obtained from Katchem., 9,12-$(CH_2CHCH_2)_2$-1,2-*closo*-$C_2B_{10}H_{10}$ [**1**], [2] 8,9,10,12-$(CH_2CHCH_2)_4$-1,2-*closo*-$C_2B_{10}H_8$ [**2**] [3] and 8,9,10,12-$(OHCH_2CH_2CH_2)_4$-1,2-*closo*-$C_2B_{10}H_8$ [**6**] [3] were synthesised as reported at the literature.

Elemental analyses were performed using a Carlo Erba EA1108 micro analyzer. IR spectra (ν, cm^{-1}; KBr pellets) were obtained on a Shimadzu FTIR-8300 spectrophotometer. The ^1H- and $^1H\{^{11}B\}$-NMR (300.13 MHz), $^{13}C\{^1H\}$-NMR (75.47 MHz) and ^{11}B- and $^{11}B\{^1H\}$-NMR (96.29 MHz) spectra were recorded on a Bruker ARX 300 instrument equipped with the appropriate decoupling accessories. All NMR spectra were performed in deuterated acetone at 22ºC. The ^{11}B- and $^{11}B\{^1H\}$-NMR shifts were referenced to external $BF_3{\cdot}OEt_2$, while the ^1H, $^1H\{^{11}B\}$, and $^{13}C\{^1H\}$-NMR shifts were referenced to $SiMe_4$. Chemical shifts are reported in units of parts per million downfield from reference, and all coupling constants in Hz. The mass spectra were recorded in the negative ion mode using a Bruker Biflex MALDI-TOF-MS [N_2 laser; λ_{exc} 337 nm (0.5 ns pulses); voltage ion source 20.00 kV (Uis1) and 17.50 kV (Uis2)], and using a FIA-ES/MS (Shimadzu AD VP/ API 150) instrument for neutral species.

Synthesis of 9,12-$(CH_2{=}CHCH_2)_2$-1,2-$(CH_2{=}CHCH_2)_2$-*closo*-$C_2B_{10}H_8$ [**3**]: To a stirring solution of 9,12-$(CH_2{=}CHCH_2)_2$-1,2-

closo-$C_2B_{10}H_{10}$ (40 mg, 0.18 mmol) in dry THF (3 mL) at 0ºC were added dropwise butyllithium in hexanes (0.24 mL, 1.6M, 0.37 mmol), the resulting solution was stirred at 0 ºC for 30 minutes. Then the mixture was cooled at -78ºC to add dropwise a solution of CH_2=$CHCH_2Br$ in dry THF (0.39 mL, 1M, 0.39 mmol), and allowed to stir overnight at room temperature. Afterwards, the solvent was removed and 10 mL of diethyl ether and 10 mL of dilute HCl (0.25 M) were added to the residue. The organic layer was separated from the mixture, and the aqueous layer was extracted with diethyl ether (3 x 10 mL). The combined organic phase was dried over $MgSO_4$, filtered and the solvent removed under reduced pressure. The remaining solid was recrystallized from boiling hexane to yield 48 mg of 9,12-(CH_2=$CHCH_2$)$_2$-1,2-(CH_2=$CHCH_2$)$_2$-*closo*-$C_2B_{10}H_8$ (89 %). Elemental Analysis for $C_{14}B_{10}H_{28}$: calc: C 55.26, H 9.21; found C 55.22, H, 9.29. IR (KBr): ν=3074 (s, ν_s(=CH_2)), 2971, 2923, 2877, 2854 (s, ν_s(=CH and CH_2)), 2593 (vs, ν_s(B-H)), 1634 (vs, ν_s(C=C)), 1095, 994 cm^{-1} (s, ν_{as}(=CH_2)). ^{1}H NMR (300 MHz, CD_3COCD_3): δ=5.80 (m, 4H, CH_2=C*H*-CH_2-B(9,12), CH_2=C*H*-CH_2-C(1,2)), 5.20 (m, 4H, *C*H_2=CH-*C*H_2-C(1,2)), 4.72 (m, 4H, *C*H_2=CH-*C*H_2-B(9,12)), 3.10–1.00 (m, 8H, B-$H_{terminal}$), 3.11 (d, ^3J(H,H)=6 Hz, 4H, CH_2=CH-CH_2-C(1,2)), 1.65 (br s, 4H, CH_2=CH-CH_2-B(9,12)), ^{1}H{^{11}B} NMR (300 MHz, CD_3COCD_3): δ=5.80 (m, 4H, CH_2=C*H*-CH_2-B(9,12), CH_2=C*H*-CH_2-C(1,2)), 5.20 (m, 4H, *C*H_2=CH-*C*H_2-C(1,2)), 4.72 (m, 4H, *C*H_2=CH-*C*H_2-B(9,12)), 3.11 (d, ^3J(H,H)=6 Hz, 4H, CH_2=CH-CH_2-C(1,2)), 2.18, 2.0 (br s, 8H, B-*H*), 1.64 (d, ^3J(H,H)=9 Hz, 4H, CH_2=CH-CH_2-B(9,12)). ^{13}C{^{1}H} NMR (75 MHz, CD_3COCD_3): δ=140.1 (s, CH_2=*C*H-CH_2-B(9,12)), 133.2 (s, CH_2=*C*H-CH_2-C(1,2)), 118.9 (s, *C*H_2=CH-CH_2-B(9,12)), 111.1 (s, *C*H_2=CH-CH_2-C(1,2)), 72.2 (s, $C_{cluster}$), 37.9 (s, CH_2=CH-*C*H_2-C(1,2)), 22.3 ppm (m, CH_2=CH-*C*H_2-B(9,12)). ^{11}B NMR (96 MHz, CD_3COCD_3): δ=5.9 (s, 2B, B(9,12)), -8.9 (d, ^1J(B,H)=152 Hz, 2B, B(8,10)), -10.5 (d, ^1J(B,H)=160 Hz, 4B, B(4,5,7,11)), -12.9 ppm (d, ^1J(B,H)=173 Hz, 2B, B(3,6)). ESI MS: *m/z* (%)= 303.3 (60) $[M-1]^-$.

Synthesis of 8,9,10,12-(CH_2=$CHCH_2$)$_4$-1,2-(CH_2=$CHCH_2$)$_2$-*closo*-$C_2B_{10}H_6$ [4]: To a stirring solution of 8,9,10,12-(CH_2=$CHCH_2$)$_4$-1,2-*closo*-$C_2B_{10}H_{10}$ (400 mg, 1.3 mmol) in dry THF (5 mL) at 0ºC were added dropwise butyllithium in hexanes (1.72 mL, 1.6M, 2.76 mmol), the resulting solution was stirred at 0 ºC for 30 minutes. Then the mixture was cooled at -78ºC to add dropwise a solution of CH_2=$CHCH_2Br$ in dry THF (0.23 mL, 1M, 2.88 mmol), and allowed to stir overnight at room temperature. Afterwards, the solvent was removed and 10 mL of diethyl ether and 10 mL of dilute HCl (0.25 M) were added to the residue. The organic layer was separated from the mixture, and the aqueous layer was extracted with diethyl ether (3 x 10 mL). The combined organic phase was dried over $MgSO_4$, filtered and the solvent removed under reduced pressure. The remaining solid was recrystallized from boiling hexane to yield 435 mg of 8,9,10,12-(CH_2=$CHCH_2$)$_4$-1,2-(CH_2=$CHCH_2$)$_2$-*closo*-$C_2B_{10}H_8$ (86 %). Elemental Analysis for $C_{20}B_{10}H_{36}$: calc: C 62.50, H 9.37; found: C 61.98, H 9.22. IR (KBr): ν=3074 (s, ν_s(=CH_2)), 2995, 2972, 2912, 2882, 2813, 2797 (s, ν_s(=CH and CH_2)), 2592 (vs, ν_s(B-H)), 1634 (vs, ν_s(C=C)), 1102, 994 cm^{-1} (s, ν_{as}(=CH_2)). ^{1}H NMR (300 MHz, CD_3COCD_3): δ=5.83 (m, 6H, CH_2=C*H*-CH_2-B(8,9,10,12), CH_2=C*H*-CH_2-C(1,2)), 5.20 (m, 4H, *C*H_2=CH-*C*H_2-C(1,2)), 4.84 (m, 8H, *C*H_2=CH-*C*H_2-B(8,9,10,12)), 3.10–1.00 (m, 6H, B-$H_{terminal}$), 3.12 (d, ^3J(H,H)=6 Hz, 4H, CH_2=CH-CH_2-C(1,2)), 1.65 (br s, 4H, CH_2=CH-CH_2-B(9,12)), 1.50 (br s, 4H, CH_2=CH-CH_2-B(8,10)). ^{1}H{^{11}B} NMR (300 MHz, CD_3COCD_3): δ=5.83 (m, 6H, CH_2=C*H*-CH_2-B(8,9,10,12), CH_2=C*H*-CH_2-C(1,2)), 5.20 (m, 4H, *C*H_2=CH-*C*H_2-C(1,2)), 4.84 (m, 8H, *C*H_2=CH-*C*H_2-B(8,9,10,12)), 3.12 (d, ^3J(H,H)=6 Hz, 4H, CH_2=CH-CH_2-C(1,2)), 2.13 (br s, 4H, 1.65 (br s, 4H, B(4,5,7,11)-$H_{terminal}$), 2.07 (br s, 2H, B(3,6)-$H_{terminal}$), 1.65 (d, ^3J(H,H)=6 Hz, 4H, CH_2=CH-CH_2-B(9,12)),1.50 (d, ^3J(H,H)=9 Hz, 4H, CH_2=CH-CH_2-B(8,10)). ^{13}C{^{1}H} NMR (75 MHz, CD_3COCD_3): δ=140.1,139.6 (s, CH_2=*C*H-CH_2-B(8,9,10,12)), 132.9 (s, CH_2=*C*H-CH_2-C(1,2)), 118.7 (s, *C*H_2=CH-CH_2-B(8,9,10,12)), 112.1 (s, *C*H_2=CH-CH_2-C(1,2)), 69.2 (s, $C_{cluster}$), 38.6 (s, CH_2=CH-*C*H_2-C(1,2)), 20.4 ppm (m, CH_2=CH-*C*H_2-B(8,9,10,12)). ^{11}B NMR (96 MHz, CD_3COCD_3): δ=4.1 (s, 2B, B(9,12)), -0.8 (s, 2B, B(8,10)), -12.1 (d, ^1J(B,H)=163 Hz, 4B, B(4,5,7,11)), -14.2 ppm (d, ^1J(B,H)=150 Hz, 2B, B(3,6)). ESI MS: *m/z* (%)= 407.4 (100) $[M-1+Na]^+$.

Synthesis of 9,12-($HOCH_2CH_2CH_2$)$_2$-1,2-($HOCH_2CH_2CH_2$)$_2$-*closo*-$C_2B_{10}H_8$ [5]: To a stirring solution of 9,12-(CH_2=$CHCH_2$)$_2$-1,2-(CH_2=$CHCH_2$)$_2$-*closo*-$C_2B_{10}H$ (190 mg, 0.61 mmol) in dry THF (5 mL) at 0 ºC, was added, dropwise, a solution of BH_3·THF in THF (2.52 mL, 1M, 2.52 mmol). The resulting suspension was stirred at 0 ºC for 30 minutes and at room temperature for further 30 minutes. Then, the reaction mixture was cooled again to 0 ºC in an ice-water bath and water (1 mL) was slowly added. When gas evolution had stopped, an aqueous KOH solution (0.84 mL, 3M, 2.5 mmol) and subsequently, H_2O_2 in water (0.22 mL, 35%, 2.5 mmol), were added. Stirring was maintained at room temperature for 1.5 h, after which two liquid phases were observed. The upper organic layer was separated from the mixture, and the aqueous layer and washed with THF (3 x 2 mL). The combined organic phase was dried over $MgSO_4$, filtered and the solvent removed *in vacuo* to give 9,12-($HOCH_2CH_2CH_2$)$_2$-1,2-($HOCH_2CH_2CH_2$)$_2$-*closo*-$C_2B_{10}H_8$. Yield: 205 mg (87%). Elemental Analysis for $C_{14}B_{10}H_{36}O_4$: calc: C 44.68,

H 9.57; found: C 45.03, H 9.61. IR (KBr): ν=3339 (vs, ν_s(O-H), ν_s($C_{cluster}$-H)), 2929, 2882 (s, ν_s(C_{alkyl}-H)), 2591 (s, ν_s(B-H)), 1057, 1004 cm^{-1} (s, ν_s(C-O)). ^{1}H NMR (300 MHz, CD_3SOCD_3): δ=4.70 (m, 1H, *H*OCH$_2$CH$_2$CH$_2$), 4.55 (m, 1H, *H*OCH$_2$CH$_2$CH$_2$), 4.25 (m, 2H, *H*OCH$_2$CH$_2$CH$_2$-B(9,12)), 3.10–1.00 (m, 8H, B-$H_{terminal}$), 2.28 (m, 4H, HOCH$_2$CH$_2$C*H*$_2$-C_c(1,2)), 1.61, 1.35, 1.23, 1.16, 1.05 (m, 8H, HOCH$_2$C*H*$_2$CH$_2$-B(9,12), HOCH$_2$C*H*$_2$CH$_2$-C_c(1,2)), 0.55 ppm (m, 4H, HOCH$_2$CH$_2$C*H*$_2$-B(9,12)). ^{1}H{^{11}B} NMR (300 MHz, CD_3SOCD_3): δ=4.75 (m, 1H, *H*OCH$_2$CH$_2$CH$_2$), 4.55 (m, 1H, *H*OCH$_2$CH$_2$CH$_2$), 4.24 (m, 2H, *H*OCH$_2$CH$_2$CH$_2$-B(9,12)), 2.28 (m, 4H, HOCH$_2$CH$_2$C*H*$_2$-C_c(1,2)), 1.89 (m, 8H, B-$H_{terminal}$), 1.61, 1.35, 1.23, 1.16, 1.05 (m, 8H, HOCH$_2$C*H*$_2$CH$_2$-B(9,12), HOCH$_2$C*H*$_2$CH$_2$-C_c(1,2)), 0.53 ppm (m, 4H, HOCH$_2$CH$_2$C*H*$_2$-B(9,12)). ^{13}C{^{1}H} NMR (75 MHz, CD_3SOCD_3): δ=65.96 (s, HO*C*H$_2$CH$_2$CH$_2$-C_c(1,2)), 64.24 (s, HO*C*H$_2$CH$_2$CH$_2$-B(9,12)), 61.0 (s, $C_{cluster}$), 34.61, 33.36 (s, HOCH$_2$*C*H$_2$CH$_2$-B(9,12)), 29.95 (s, HOCH$_2$*C*H$_2$CH$_2$-C_c(1,2)), 24.72 (s, HOCH$_2$CH$_2$*C*H$_2$-C_c(1,2)), 12.31 ppm (s, HOCH$_2$CH$_2$*C*H$_2$-B(9,12)). ^{11}B NMR (96 MHz, CD_3SOCD_3): δ=7.3 (br s, 2B, B(9,12)), -8.9 ppm (br s, 8B, B(3,4,5,6,7,8,10,11)). ESI MS: *m*/*z* (%)= 400.4 (100) $[M+Na]^+$.

Synthesis of 8,9,10,12-(HOCH$_2$CH$_2$CH$_2$)$_4$-1,2-(HOCH$_2$CH$_2$CH$_2$)$_2$-*closo*-C$_2$B$_{10}$H$_6$ [6]: To a stirring solution of 8,9,10,12-(CH$_2$=CHCH$_2$)$_4$-1,2-(CH$_2$=CHCH$_2$)$_2$-*closo*-$C_2B_{10}H_6$ (200 mg, 0.52 mmol) in dry THF (5 mL) at 0 ºC, was added, dropwise, a solution of BH_3·THF in THF (3.2 mL, 1M, 3.2 mmol). The resulting suspension was stirred at 0 ºC for 30 minutes and at room temperature for further 30 minutes. Then, the reaction mixture was cooled again to 0 ºC in an ice-water bath and water (1 mL) was slowly added. When gas evolution had stopped, an aqueous KOH solution (1.05 mL, 3M, 3.1 mmol) and subsequently, H_2O_2 in water (0.27 mL, 35%, 3 mmol), were added. Stirring was maintained at room temperature for 1.5 h, after which two liquid phases were observed. The upper organic layer was separated from the mixture, and the aqueous layer and washed with THF (3 x 2 mL). The combined organic phase was dried over $MgSO_4$, filtered and the solvent removed *in vacuo* to give 8,9,10,12-(HOCH$_2$CH$_2$CH$_2$)$_4$-1,2-(HOCH$_2$CH$_2$CH$_2$)$_2$-*closo*-$C_2B_{10}H_6$. Yield: 162 mg (80%). Elemental Analysis for $C_{20}B_{10}H_{48}O_6$: calc: C 48.78, H 9.75; found: C 49.44, H 9.78. IR (KBr): ν=3338 (vs, ν_s(O-H)), 2929, 2881 (s, ν_s(C_{alkyl}-H)), 2589 (s, ν_s(B-H)), 1057, 1005 cm^{-1} (s, ν_s(C-O)). ^{1}H NMR (300 MHz, CD_3SOCD_3): δ=4.68 (m, 1H, *H*OCH$_2$CH$_2$CH$_2$), 4.53 (m, 1H, *H*OCH$_2$CH$_2$CH$_2$), 4.30, 424 (m, 2H, *H*OCH$_2$CH$_2$CH$_2$-B(9,12)), 3.10–1.00 (m, 6H, B-$H_{terminal}$), 2.31, 2.28 (m, 12H, HOC*H*$_2$CH$_2$CH$_2$-B(9,12), HOC*H*$_2$CH$_2$CH$_2$-C_c(1,2)), 1.60, 1.49, 1.34, 1.11 (m, 16H, HOCH$_2$C*H*$_2$CH$_2$-B(9,12), HOCH$_2$C*H*$_2$C*H*$_2$-C_c(1,2)), 0.53, 0.31 ppm (m, 8H, HOCH$_2$CH$_2$C*H*$_2$-B(9,12)). ^{1}H{^{11}B} NMR (300 MHz, CD_3SOCD_3): δ=4.68 (m, 1H, *H*OCH$_2$CH$_2$CH$_2$), 4.53 (m, 1H, *H*OCH$_2$CH$_2$CH$_2$), 4.30, 424 (m, 2H, *H*OCH$_2$CH$_2$CH$_2$-B(9,12)), 2.01 (m, 6H, B-$H_{terminal}$), 2.31, 2.28 (m, 12H, HOC*H*$_2$CH$_2$CH$_2$-B(9,12), HOC*H*$_2$CH$_2$CH$_2$-C_c(1,2)), 1.60, 1.49, 1.34, 1.11 (m, 16H, HOCH$_2$C*H*$_2$CH$_2$-B(9,12), HOCH$_2$C*H*$_2$C*H*$_2$-C_c(1,2)), 0.53, 0.31 ppm (m, 8H, HOCH$_2$CH$_2$C*H*$_2$-B(9,12)). ^{13}C{^{1}H} NMR (75 MHz, CD_3SOCD_3): δ=65.98, 60.13 (s, HO*C*H$_2$CH$_2$CH$_2$-C_c(1,2)), 64.64 (s, HO*C*H$_2$CH$_2$CH$_2$-B(8,9,10,12)), 64.6 (s, $C_{cluster}$), 33.45, 32.27 (s, HOCH$_2$*C*H$_2$CH$_2$-B(8,9,10,12)), 31.27 (s, HOCH$_2$*C*H$_2$CH$_2$-C_c(1,2)), 25.2 (s, HOCH$_2$CH$_2$*C*H$_2$-C_c(1,2)), 10.24 ppm (s, HOCH$_2$CH$_2$*C*H$_2$-B(8,9,10,12)). ^{11}B NMR (96 MHz, CD_3SOCD_3): δ=5.9 (br s, 2B, B(9,12)), 1.3 (br s, 2B, B(8,10)), -9.9 ppm (br s, 6B, B(3,4,5,6,7,11)). ESI MS: *m*/*z* (%)= 515.5 (100) $[M+Na]^+$.

Synthesis of 9,12-(BrCH$_2$CH$_2$CH$_2$)$_2$-1,2-(BrCH$_2$CH$_2$CH$_2$)$_2$-*closo*-C$_2$B$_{10}$H$_8$ [7]: To a stirring solution of 9,12-(HOCH$_2$CH$_2$CH$_2$)$_2$-1,2-(HOCH$_2$CH$_2$CH$_2$)$_2$-*closo*-$C_2B_{10}H_8$ (100 mg, 0.26 mmol) and CBr_4 (474 mg, 1.8 mmol) in dry THF (15 mL) at 0 ºC, was added dropwise a solution of PPh_3 (530 mg, 1.6 mmol, in 5 mL of dry THF). The resulting solution was stirred at room temperature for 3 hours. The solvent was removed under reduced pressure, and 10 mL of dry diethyl ether were added, after a filtration, the filtrate was concentrated. The crude product was purified by flash column chromatography on silica gel with chloroform as the eluent to give 9,12-(BrCH$_2$CH$_2$CH$_2$)$_2$-1,2-(BrCH$_2$CH$_2$CH$_2$)$_2$-*closo*-$C_2B_{10}H_8$. Yield: 125 mg (75%). Elemental Analysis for $C_{14}B_{10}H_{36}Br_4$: calc: C 26.75, H 5.73; found: C 27.22, H 5.78. IR (KBr): ν=2955, 2925, 2854 (s, ν_s(C_{alkyl}-H)), 2589 (s, ν_s(B-H)), 1259 cm^{-1} (s, ν_{wag}(CH_2-Br)). ^{1}H NMR (300 MHz, CD_3COCD_3): δ=3.58 (m, 4H, BrC*H*$_2$CH$_2$CH$_2$-C_c(1,2)), 3.45 (m, 4H, BrC*H*$_2$CH$_2$CH$_2$-B(9,12)), 3.10–1.00 (m, 8H, B-$H_{terminal}$), 1.84,1.80 (m, 8H, BrCH$_2$C*H*$_2$CH$_2$-B(9,12), BrCH$_2$C*H*$_2$CH$_2$-C_c(1,2)), 0.89 ppm (m, 8H, BrCH$_2$CH$_2$C*H*$_2$-B(9,12), BrCH$_2$CH$_2$C*H*$_2$-C_c(1,2)). ^{1}H{^{11}B} NMR (300 MHz, CD_3COCD_3): δ=3.58 (m, 4H, BrC*H*$_2$CH$_2$CH$_2$-C_c(1,2)), 3.45 (m, 4H, BrC*H*$_2$CH$_2$CH$_2$-B(9,12)), 2.23 (m, 8H, B-$H_{terminal}$), 1.84,1.80 (m, 8H, BrCH$_2$C*H*$_2$CH$_2$-B(9,12), BrCH$_2$C*H*$_2$CH$_2$-C_c(1,2)), 0.89 ppm (m, 8H, BrCH$_2$CH$_2$C*H*$_2$-B(9,12), BrCH$_2$CH$_2$C*H*$_2$-C_c(1,2)). ^{13}C{^{1}H} NMR (75 MHz, CD_3COCD_3): δ= 69.3 (s, $C_{cluster}$), 44.31 (s, BrCH$_2$CH$_2$*C*H$_2$-C_c(1,2)), 37.12 (m, Br*C*H$_2$CH$_2$CH$_2$-C_c(1,2), Br*C*H$_2$CH$_2$CH$_2$-B(9,12)), 32.72 (m, BrCH$_2$*C*H$_2$CH$_2$-C_c(1,2), BrCH$_2$*C*H$_2$CH$_2$-B(9,12)), 13.43 ppm (s, BrCH$_2$CH$_2$*C*H$_2$-B(9,12)). ^{11}B NMR (96 MHz, CD_3COCD_3): δ=6.3 (br s, 2B, B(9,12)), -8.2 (br s, 8B, B(8,10), -10.6 (br s, 4B, B(4,5,7,11), -12.9 ppm (br s, 2B, B(3,6). ESI MS: *m*/*z* (%)= 645.2 (100) $[M-1+H_2O]^-$.

Synthesis of 8,9,10,12-($BrCH_2CH_2CH_2)_4$-1,2-($BrCH_2CH_2CH_2)_2$-*closo*-$C_2B_{10}H_6$ [**8**]: To a stirring solution of 8,9,10,12-($HOCH_2CH_2CH_2)_4$-1,2-($HOCH_2CH_2CH_2)_2$-*closo*-$C_2B_{10}H_6$ (100 mg, 0.20 mmol) and CBr_4 (606 mg, 1.8 mmol) in dry THF (10 mL) at 0 ºC, was added dropwise a solution of PPh_3 (543 mg, 2.1 mmol, in 5 mL of dry THF). The resulting solution was stirred at room temperature for 3 hours. The solvent was removed under reduced pressure, and 10 mL of dry diethyl ether were added, after a filtration, the filtrate was concentrated. The crude product was purified by flash column chromatography on silica gel with chloroform as the eluent to give 8,9,10,12-($BrCH_2CH_2CH_2)_4$-1,2-($BrCH_2CH_2CH_2)_2$-*closo*-$C_2B_{10}H_6$. Yield: 118 mg (67%). Elemental Analysis for $C_{20}B_{10}H_{42}Br_6$: calc: C 27.58, H 4.82; found: C 28.54, H 4.80. IR (KBr): ν=2957, 2927, 2904, 2895, 2857, 2828 (s, $\nu_s(C_{alkyl}$-H)), 2591 (s, ν_s(B-H)), 1258, 1244 cm^{-1} (s, $\nu_{wag}(CH_2$-Br)). ^{1}H NMR (300 MHz, CD_3COCD_3): δ=3.48 (m, 12H, Br*C*$H_2CH_2CH_2$-B(8,9,10,12), Br*C*$H_2CH_2CH_2$-C_c(1,2)), 2.85 (m, 4H, $BrCH_2CH_2C$*H*$_2$-C_c(1,2)), 3.10–1.00 (m, 6H, B-*H*$_{terminal}$), 1.83,1.63 (m, 12H, $BrCH_2C$*H*$_2CH_2$-B(9,12), $BrCH_2C$*H*$_2CH_2$-C_c(1,2)), 0.88, 0.68 ppm (m, 8H, $BrCH_2CH_2C$*H*$_2$-B(9,12)). ^{1}H{^{11}B} NMR (300 MHz, CD_3COCD_3): δ=3.48 (m, 12H, Br*C*$H_2CH_2CH_2$-B(8,9,10,12), Br*C*$H_2CH_2CH_2$-C_c(1,2)), 2.85 (m, 4H, $BrCH_2CH_2C$*H*$_2$-C_c(1,2)), 2.18 (m, 6H, B-*H*$_{terminal}$), 1.83,1.63 (m, 12H, $BrCH_2C$*H*$_2CH_2$-B(9,12), $BrCH_2C$*H*$_2CH_2$-C_c(1,2)), 0.88, 0.68 ppm (m, 8H, $BrCH_2CH_2C$*H*$_2$-B(9,12)). ^{13}C{^{1}H} NMR (75 MHz, CD_3COCD_3): δ= 71.6 (s, $C_{cluster}$), 46.8 (s, $BrCH_2CH_2$*C*H_2-C_c(1,2)), 36.85-36.66 (m, Br*C*$H_2CH_2CH_2$-C_c(1,2), Br*C*$H_2CH_2CH_2$-B(8,9,10,12)), 33.30-32.36 (m, $BrCH_2$*C*H_2CH_2-C_c(1,2), $BrCH_2$*C*H_2CH_2-B(8,9,10,12)), 12.41 ppm (s, $BrCH_2CH_2$*C*H_2-B(8,9,10,12)). ^{11}B NMR (96 MHz, CD_3COCD_3): δ=6.6 (br s, 2B, B(9,12)), 1.1 (br s, 8B, B(8,10), -11.2 ppm (br s, 6B, B(3,4,5,6,7,11). ESI MS: *m*/*z* (%)= 950.0 (100) $[M\text{-}Br]^-$, 870.0 (75) $[M]^-$

Synthesis of $[N(CH_3)_4]_6$[8,9,10,12-(3,3'-Co-{8-($OCH_2CH_2)_2$-1,2-$C_2B_9H_6$-1',2'-$C_2B_9H_7$}-$O(CH_2)_3)_4$-1,2-(3,3'-Co-{8-($OCH_2CH_2)_2$-1,2-$C_2B_9H_6$-1',2'-$C_2B_9H_7$}-$O(CH_2)_3)_2$-$C_2B_{10}H_6$] [**9**]: To a stirring solution of 8,9,10,12-($HOCH_2CH_2CH_2)_4$-1,2-($HOCH_2CH_2CH_2)_2$-*closo*-$C_2B_{10}H_6$ (43 mg, 0.09 mmol) in DME (5 mL) cooled to 0 ºC in an ice-water bath was added dropwise a solution of butyllithium in hexanes (0.35 mL, 1.53M, 0.53 mmol). After stirring at room temperature for 30 minutes, a solution of [8-{$O(CH_2CH_2)_2O$}-3,3'-Co(1,2-$C_2B_9H_{10}$)(1',2'-$C_2B_9H_{11}$)] (218 mg, 0.53 mmol) in THF (5mL) was added via a syringe, following which the reaction was heated to reflux overnight. Afterwards the solvent was removed under reduced pressure, 10 mL of diethyl ether and 10 mL of a diluted solution of HCl (0.1M) were added. The mixture was throughly shaken, and the two layers separated. The organic layer was separated from the mixture, and the aqueous layer was extracted with diethyl ether (3 x 10mL). The combined organic phase was dried over $MgSO_4$, filtered and the solvent removed under reduced pressure. Afterwards, an aqueous solution of $[NMe_4]Cl$ was added dropwise until no more precipitate was formed. The orange solid was filtered and rinsed with water. Yield: 104 mg (35%). IR (KBr): ν=3433 (s, ν_s(N-H)), 3039 (w, $\nu_s(C_{cluster}$-H)), 2923, 2862 (s, $\nu_s(C_{alkyl}$-H)), 2553 (s, ν_s(B-H)), 1481 (s, ν_s(N-C)), 1172, 1103 cm^{-1} (s, ν_s(C-O)). ^{1}H NMR (300 MHz, $CDCl_3$): δ=4.28 (br s, 24H, $C_{cluster}$*H*), 3.58 (br m, 60H, O*C*H_2*C*H_2O (48H), O*C*$H_2CH_2CH_2$--B (12H)), 3.45 (br s, 72H, N(*C*H_3)), 3.00-1.50 (br m, 108H, B*H*), 2.43 (m, 4H, Cc-*C*$H_2CH_2CH_2O$-), 1.70, 1.53 (m, 12H, Cc-CH_2*C*H_2CH_2O- (4H), OCH_2*C*H_2CH_2-B (8H)), 0.68, 0.47 ppm (m, 8H, OCH_2CH_2*C*H_2-B). ^{1}H{^{11}B} NMR (300 MHz, $CDCl_3$): δ=4.28 (br s, 24H, $C_{cluster}$*H*), 3.58 (br m, 60H, O*C*H_2*C*H_2O (48H), O*C*$H_2CH_2CH_2$--B (12H)), 3.45 (br s, 72H, N(*C*H_3)), 2.91, 2.76, 2.70 (br m, 32H, B*H*), 2.43 (m, 4H, Cc-*C*$H_2CH_2CH_2O$-), 1.97 (br s, 16H, B*H*), 1.78, 1.67, 1.56, 1.48 (br s, 60H, B*H*), 1.70, 1.53 (m, 12H, Cc-CH_2*C*H_2CH_2O- (4H), OCH_2*C*H_2CH_2-B (8H)), 0.68, 0.47 ppm (m, 8H, OCH_2CH_2*C*H_2-B). ^{13}C{^{1}H} NMR (75 MHz, $CDCl_3$): δ=73.7, 71.6, 70.2, 68.1 (s, O*C*H_2), 55.18 (s, N(*C*H_3)), 55.1 ($C_{cluster}$), 47.0 ($C_{cluster}$), 38.7 (s, Cc-*C*$H_2CH_2CH_2O$-), 32.3 (s, OCH_2*C*H_2CH_2-B), 23.4 (s, Cc-CH_2*C*H_2CH_2O-), 13.6 ppm (s, OCH_2CH_2*C*H_2-B). ^{11}B NMR (96 MHz, $CDCl_3$): δ=23.9 (s, 6B, B(8)), 4.64 (d, ^{1}J(B,H)=117 Hz, 6B, B(8')), 1.18 (d, ^{1}J(B,H)=127 Hz, 6B, B(10')), -1.67 (d, ^{1}J(B,H)=129 Hz, 12B, B(9,12)), -3.42 (d, ^{1}J(B,H)=165 Hz, 12B, B(4,7)), -6.75 (d, ^{1}J(B,H)=138 Hz, 6B, B(10)), -7.40 (d, ^{1}J(B,H)=127 Hz, 24B, B(4',7',9',12')), -16.51 (d, ^{1}J(B,H)=154 Hz, 12B, B(5',11')), -19.7 (d, ^{1}J(B,H)=149 Hz, 12B, B(5,11)), -21.1 (d, ^{1}J(B,H)=192 Hz, 6B, B(6')), -27.7 ppm (d, ^{1}J(B,H)=144 Hz, 6B, B(6)). ESI MS: *m*/*z* (%)=775 (40) $[M+2(NCH_3)_4]^{4-}$

Notes and references

[1] a) R. N. Grimes, R. N. *Carboranes*, Academic Press: New York, **1970**; b) S. C. Mehta, D. R. Lu, *Pharm. Res.* **1996**, *13*, 344; c) R. F. Barth, A. H. Soloway, R. M. Brugger, *Cancer InVest.* **1996**, *14*, 534; d) R. N. Grimes, *J. Chem. Educ.* **2004**, *81*, 658; e) J. Plešek, *Chem. Rev.* **1992**, *92*, 269.

[2] "Building Highly Dense Multibranched o-Carborane Derivatives by means of Kumada Cross Coupling Reaction". A Pepiol, F. Teixidor, R. Silanpää, C. Viñas. In preparation.

[3] A. Vaca, F. Teixidor, R. Sillanpää , R. Kivekäs, C. Viñas, *Chem. Commun.* **2011**, *47*, 2252–2254.

[4] a) *Dendrimers and other dendritic polymers* J. M. Fréchet, D. A. Tomalia, Eds.; Wiley Series in Polymer Science, John

Wiley & sons, Ltd., UK, **2001**; b) D. Astruc, F. Chardac, *Chem. Rev.* **2001**, 101, 2991; c) R. M. Crooks, M. Zhao, L. Sun, V. Chechik, L. K. Yeung, *Acc. Chem. Res.* **2001**, *34*, 181, d) G. R. Newkome, C. N. Moorefield, F. Vötgle, *Dendrimers and Dendrons: Concepts, Synthesis, Applications*; Wiley: New York, **2002**; e) U. Boas, P. Heegarard, *Chem. Soc. Rev.* **2004**, *33*, 43; f) A. M. Caminade, J. P. Majoral, *Acc. Chem. Res.* **2004**, *37*, 341; g) C. Liang, J. M. Fréchet, *Prog. Polym. Sci.* **2005**, *30*, 385; h) D. Jiang, T. Aida, *Prog. Polym. Sci.* **2005**, *30*, 403; i) D. Astruc, C. Ornelas, J. Ruiz, *Acc. Chem. Res.* **2008**, *41*, 841; j) A .M Caminade, P. Servin, R. Laurent, J. P. Majoral, *Chem. Soc. Rev.* **2008**, *37*, 56.

[5] a) B. Qualmann, M. M. Kessels, H. J. Musiol, W. D. Sierralta, P. W. Jungblut, L. Moroder, *Angew. Chem.-Int. Edit. Engl.* **1996**, *35*, 909; (c) D. Armspach, M. Cattalini, E. C. Constable, C. E. Housecroft, D. Phillips, *Chem. Commun.* **1996**, 1823; b) K. Yamamoto, M. Higuchi, S. Shiki, M. Tsuruta, H. Chiba, *Nature* **2002**, *415*, 509; (c) H. Frey, R. Haag, *Rev. Mol. Biotechnol.* **2002**, *90*, 257.

[6] a) R. Núñez, A. González, C. Viñas, F. Teixidor, R. Sillanpää, R. Kivekäs, *R. Org. Letters* **2005**, *7*, 231, b) R. Núñez, A. González-Campo, C. Viñas, F. Teixidor, R. Sillanpää, R. Kivekäs, *Organometallics* **2005**, *24*, 6351; c) R. Núñez, A. González-Campo, A. Laromaine, F. Teixidor, R. Sillanpää, R. Kivekäs, C. Viñas, *Org. Letters* **2006**, 8, 4549; d) F. Lerouge, C. Viñas, F. Teixidor, R. Núñez, A. Abreu, E. Xochitiotzi, R. Santillan, N. Farfán, *Dalton Trans.* **2007**, 1898.

[7] I. B. Sivaev, V. I. Bregadze, *Collect. Czech. Chem. Commun.* **1999**, *64*, 783.

[8] a) L. Ma, J. Hamdi, M. F. Hawthorne, *Inorg. Chem.* **2005**, *44*, 7249; b) P. Matejicek, P. Cigler, K. Procházka, K.; V. Kral, *Langmuir* **2006**, *22*, 575; c) G. Chevrot, R. Schurhammer, G. Wipff, *J. Phys. Chem. B* **2006**, *110*, 9488.

[9] a) S. H. Strauss, *Chem. Rev.* **1993**, *93*, 927; b) C. Reed, *Acc. Chem. Res.* **1998**, *31*, 133.

[10] C. Masalles, J. Llop, C. Viñas, F. Teixidor, *Adv. Mater.* **2002**, *14*, 826.

[11] J. Plešek, *Chem. Rev.* **1992**, *92*, 269.

[12] a) M .F. Hawthorne, A. Maderna, *Chem. Rev.* **1999**, *99*, 3421, b) E. Hao, M. G. H. Vicente, *Chem. Commun.* **2005**, 1306, c) R. F. Barth, J. A. Coderre, M. G. H. Vicente, T. E. Blue, *Clin. Cancer Res.* **2005**, *11*, 3987, d) V. Gottumukkala, O. Ongayi, D. G. Baker, L. G. Lomax, M. .G. H. Vicente, *Bioorg. Med. Chem.* **2006**, *14*, 1871; e) J. Q. Wang, C. X. Ren, L. H. Weng, G. H. Jin, *Chem. Commun.* **2006**, 162; f) V. I. Bregadze, I. B. Sivaev, S. A. Glazun, *Anti-Cancer Agents Med. Chem.* **2006**, *6*, 75.

[13] E. Hao, M. Sibrian-Vazquez, W. Serem, J. Garno, F. Fronczek, M. Vicente, *Chem. Eur. J.*, **2007**, 13, 9035-9042.

[14] R. Apple, *Angew. Chem. Int. Ed*., **1975**, 14, 801-811.

[15] a) J. Plešek, S. Heřmanek, K. Baše, L.J. Todd, W.F. Wright, *Collect. Czech. Chem. Commun.* **1976**, *41*, 3509; b) A. Petřina, V. Petříček, K. Malý , V. Šubrtova, A. Linek, L. Hummel, *Z. Kristallogr.* **1981**, *154*, 217; c) V. Šubrtova, V. Petříček, L. Hummel, *Acta Crystallogr., Sect. C* **1989**, *45*, 1964.

[16] J. Plešek, S. Heřmanek, A. Franken, I. Cisařova, C. Nachtigal, *Collect. Czech. Chem. Commun.* **1997**, *62*, 47.

[17] F. Teixidor, J. Pedrajas, I. Rojo, C. Vinas, R. Kivekas, R. Sillanpaa, I. Sivaev, V. Bregadze, S. Sjoberg, *Organometallics* **2003**, *22*, 3414.

[18] P. Farras, F. Teixidor, R. Kivekas, R. Sillanpaa, C. Vinas, B. Gruner, I. Cisarova, *Inorg. Chem.* **2008**, *47*, 9497.

[19] J. Llop, C. Vinas, F. Teixidor, Ll. Victori, *J. Chem. Soc., Dalton Trans.* **2002**, *8*,1559.

[20] a) B. Gruner, L. Mikulašek, J. Bacˇa, I. Cisarˇova, V. Bohmer, C. Danila, M.M. Resinoso-Garcia, W. Verboom, D.N. Reihoudt, A. Casnati, R. Ungaro, *Eur. J. Org. Chem.* **2005**, 2022–2039; b) L. Mikulašek, B. Gruner, C. Danila, V. Bohmer, J. Časlavský , P. Selucký , *Chem. Commun.* **2006**, 4001–4003; c) L. Mikulašek, B. Grüner, C. Dordea, V. Rudzevich, V. Böhmer, J. Haddaoui, V. Hubscher, F. Arnaud-Neu, J.Časlavsky´ , P. Selucký , *Eur. J. Org. Chem.* **2007**, *28*, 4772–4783.

[21] P. Selucký , J. Rais, M. Lučanikova, B. Gruner, M. Kvičalova, K. Fejfarova, I. Cisařova, *Radiochim. Acta 96* **2008**, *4–5*, 273–284, and the references therein.

[22] P. Cigler, M. Kožišek, P. Řezačova, J. Brynda, Z. Otwinowski, J. Pokorna, J. Plešek, B. Gruner, L. Dolecˇkova-Marešova, M. Maša, J. Sedlaček, J. Bodem, H.G. Krausslich, V. Kral, J. Konvalinka, *PNAS* **2005**, *102*, 15394.

[23] A. A. Semioshkin, I. B. Sivaev, V. I. Bregadze, *Dalton Trans.* **2008**, 977.

Scheme 1. Deprotonation reaction on C_c-H of *B*-substituted *o*-carborane derivatives [**1**] and [**2**] with *n*-butillitium. Nucleophilic substitution with allyl bromide to obtain [**3**] and [**4**].

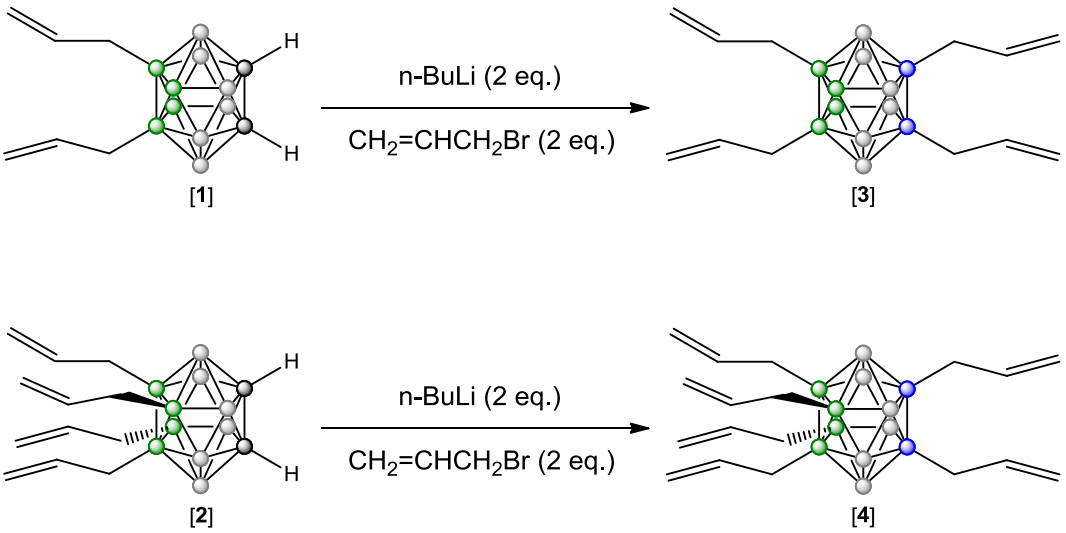

B-H C-H C B

Scheme 2. (i) Hydroboration and oxidation reaction on the olefinic terminal groups of [**3**] and [**4**] to achieve 1,2-$(OHCH_2CH_2CH_2)_2$-9,12-$(OHCH_2CH_2CH_2)_2$-1,2-*closo*-$C_2B_{10}H_8$ [**5**] and 1,2-$(OHCH_2CH_2CH_2)_2$-8,9,10,12-$(OHCH_2CH_2CH_2)_4$-1,2-*closo*-$C_2B_{10}H_6$ [**6**]. (ii) Apple bromination reaction on hydroxyl groups using PPh_3 and CBr_4 to obtain 1,2-$(BrCH_2CH_2CH_2)_2$-9,12-$(BrCH_2CH_2CH_2)_2$-1,2-*closo*-$C_2B_{10}H_8$ [**7**] and 1,2-$(BrCH_2CH_2CH_2)_2$-8,9,10,12-$(BrCH_2CH_2CH_2)_4$-1,2-*closo*-$C_2B_{10}H_6$ [**8**]. (iii) Nucleophilic oxonium ring-opening reaction on zwiterionic compound [3,3′-Co(8-$C_4H_8O_2$-1,2-$C_2B_9H_{10}$)(1′,2′-C_2B_9-H_{11})] by deprotonated hydroxyl derivative [**6**] to obtain $[N(CH_3)_4]_6$[1,2,8,9,10,12-(3,3'-Co-{8-($C_4H_8O_2$-1,2-$C_2B_9H_{10}$-1',2'-$C_2B_9H_{11}$}-$O(CH_2)_3)_6$-1,2-$C_2B_{10}H_6$] [**9**].

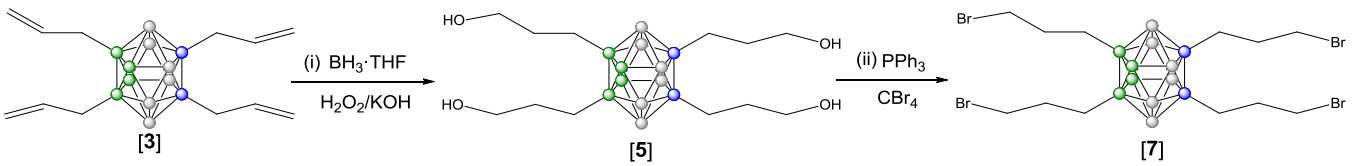

B-H C-H C B

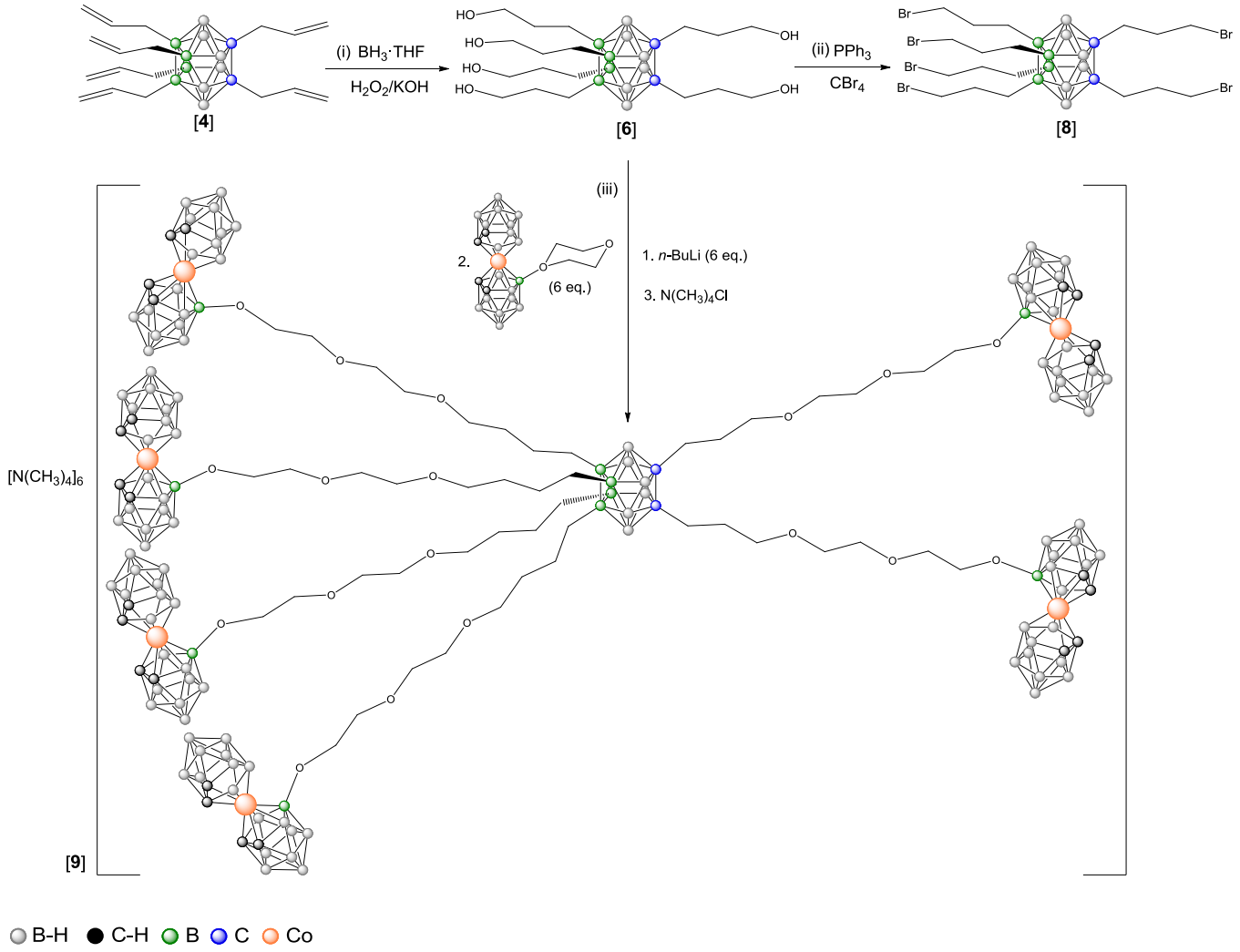

Figure 1. MALDI-TOF spectrum of $[N(CH_3)_4]_4[1,2,8,9,10,12\text{-}(3,3'\text{-}Co\text{-}\{8\text{-}(C_4H_8O_2\text{-}1,2\text{-}C_2B_9H_{10}\text{-}1',2'\text{-}C_2B_9H_{11}\}\text{-}O(CH_2)_3)_6\text{-}1,2\text{-}C_2B_{10}H_6]^{4-}$ fragment.

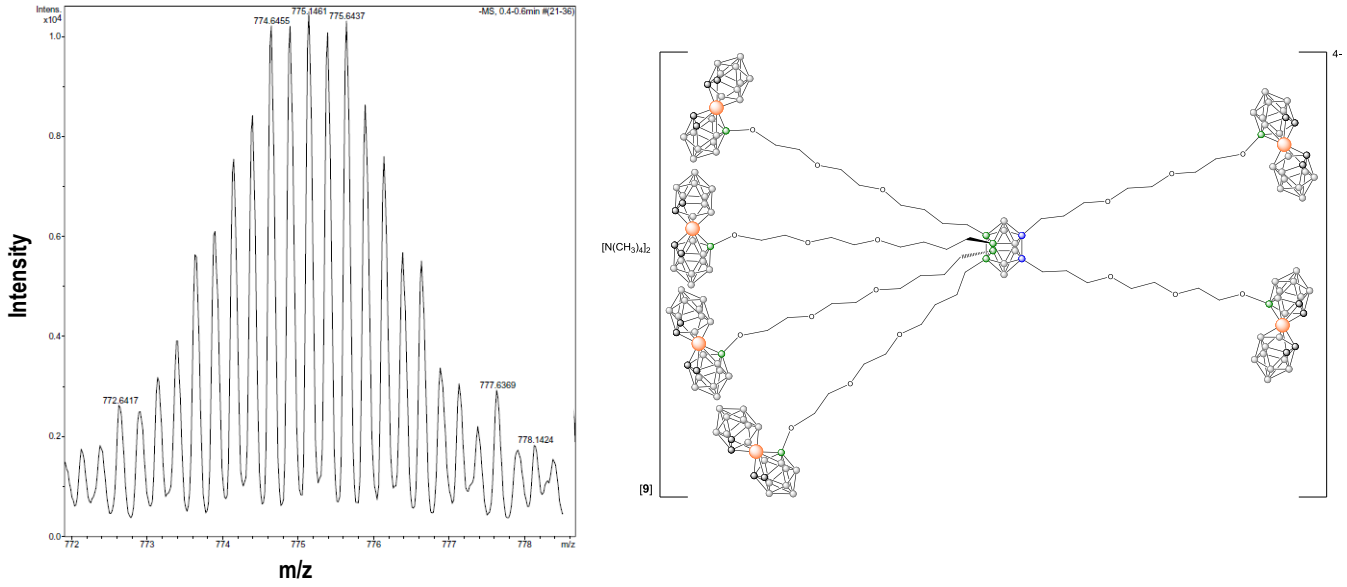

Figure 2. Diagram $^{11}B\{^{1}H\}$-NMR spectra with the peak assignments for the 9,12-$(CH_2CHCH_2)_2$-1,2-*closo*-$C_2B_{10}H_{10}$ [**1**], 8,9,10,12-$(CH_2CHCH_2)_4$-1,2-*closo*-$C_2B_{10}H_8$ [**2**], 1,2-$(CH_2CHCH_2)_2$-9,12-$(CH_2CHCH_2)_2$-1,2-*closo*-$C_2B_{10}H_8$ [**3**] and 1,2-$(CH_2CHCH_2)_2$-8,9,10,12-$(CH_2CHCH_2)_4$-1,2-*closo*-$C_2B_{10}H_6$ [**4**].

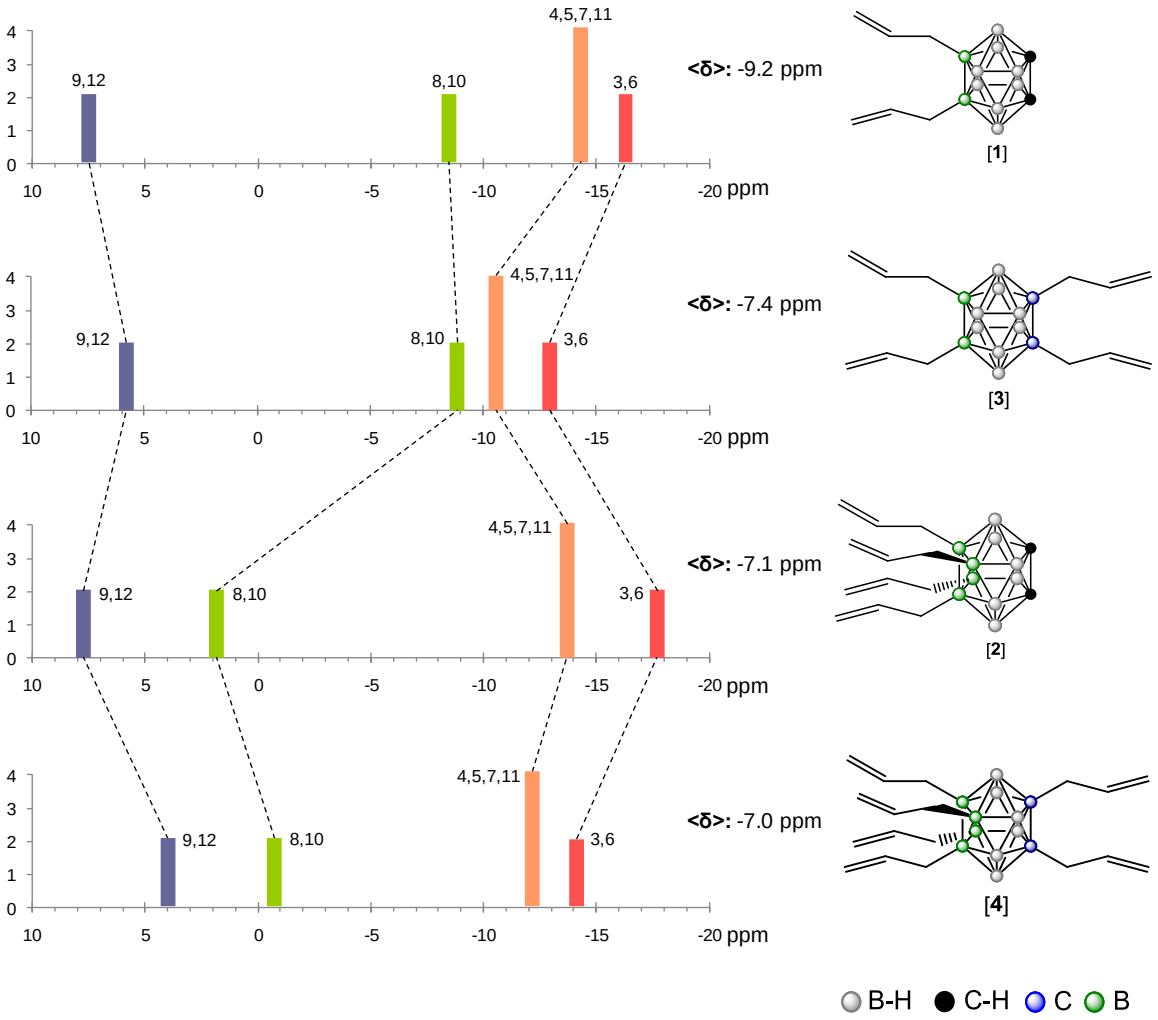

Table 1. ^{11}B- NMR chemical shifts (in ppm) for several 9,12-R_2-1,2-*closo*-$C_2B_{10}H_{10}$, 8,9,10,12-R_4-1,2-*closo*-$C_2B_{10}H_8$, 1,2,9,12-R_4-1,2-*closo*-$C_2B_{10}H_8$ and 1,2,8,9,10,12-R_6-1,2-*closo*-$C_2B_{10}H_6$. Spectra were run in acetone-d_6 solutions.

Compost	Substituents	B(3,6)	B(4,5,7,11)	B(8,10)	B(9,12)	<δ>
[**1**]	9,12-$(CH_2=CHCH_2)_2$	-16.3	-14.3	-8.6	7.5	-9.2
[**2**]	8,9,10,12-$(CH_2=CHCH_2)_4$	-17.8	-13.7	1.9	7.8	-7.1
[**3**]	1,2.9,12-$(CH_2=CHCH_2)_4$	-12.9	-10.5	-8.9	5.9	-7.4
[**4**]	1,2,8,9,10,12-$(CH_2=CHCH_2)_6$	-14.2	-12.1	-0.8	4.1	-7.0
[**5**]	1,2,9,12-$(OH(CH_2)_3)_4$	-8.9	-8.9	-8.9	7.3	-5.7
[**6**]	1,2,8,9,10,12-$(OH(CH_2)_3)_6$	-9.9	-9.9	1.3	5.9	-4.5
[**7**]	1,2,9,12-$(Br(CH_2)_3)_4$	-12.9	-10.6	-8.2	6.3	-7.2
[**8**]	1,2,8,9,10,12-$(Br(CH_2)_3)_6$	-11.2	-11.2	1.1	6.6	-5.2

Table 2. $^{13}C\{^1H\}$- NMR and in acetone-d_6 (ppm) and stretching frequencies in (cm^{-1}) for several 9,12-R_2-1,2-*closo*-$C_2B_{10}H_{10}$, 8,9,10,12-R_4-1,2-*closo*-$C_2B_{10}H_8$, 1,2,9,12-R_4-1,2-*closo*-$C_2B_{10}H_8$ and 1,2,8,9,10,12-R_6-1,2-*closo*-$C_2B_{10}H_6$. Spectra were run in acetone-d_6 solutions. *Spectra run in $CDCl_3$ solutions.

		δ ($^{13}C\{^1H\}$) ppm	**υ (cm^{-1})**
Compost	**Substituents**	$C_{clúster}$	υ (B-H)
[**1**]	9,12-$(CH_2=CHCH_2)_2$	48.3*	2594
[**2**]	8,9,10,12-$(CH_2=CHCH_2)_4$	46.5*	2617, 2596
[**3**]	1,2.9,12-$(CH_2=CHCH_2)_4$	72.2	2593
[**4**]	1,2,8,9,10,12-$(CH_2=CHCH_2)_6$	69.2	2592
[**5**]	1,2,9,12-$(OH(CH_2)_3)_4$	61.0	2591
[**6**]	1,2,8,9,10,12-$(OH(CH_2)_3)_6$	64.6	2589
[**7**]	1,2,9,12-$(Br(CH_2)_3)_4$	69.3	2589
[**8**]	1,2,8,9,10,12-$(Br(CH_2)_3)_6$	71.6	2591

Synthesis of Regioselective *B*-Organosubstituted *Nido* and Cobaltabisdicarbollide Derivatives

Ariadna Pepiol[a], Francesc Teixidor[a], Clara Viñas[a*]

[a] *Institut de Ciencia de Materials de Barcelona (CSIC) Campus UAB, 08193 Bellaterra, Spain. e-Mail clara@icmab.es*

It has been reported that 1,2-dicarba-*closo*-dodecaborane is readily partially degraded, one boron atom removal, by bases under controlled conditions to $[7,8\text{-}C_2B_9H_{12}]^-$. The deprotonation of this monoanion generates alkali metal salt of the carborane dianion a $[7,8\text{-}C_2B_9H_{11}]^{2-}$ which are easily protonated by moisture.

Boron removal from the cluster takes place via nucleophilic attack to most positive boron atoms B(3) or B(6), which are adjacent to both cluster carbon atoms. *nido*-Carborane derivatives are key compounds for the coordination of boron clusters to metal ions for the formation of complexes.[1-4] With few exceptions,[5] the metal complexation or metal insertion in the cluster can be viewed as the substitution of one or more bridging hydrogen atoms by the metal. Therefore, a necessary requirement for the complexation is the deprotonation of the *nido* cluster to generate a coordination site for that metal (Scheme 1).

The derivativatization of the most intensively studied anionic borate cluster, the cobaltabisdicarbollide $[3,3'\text{-}Co(1,2\text{-}C_2B_9H_{11})_2]^-$, remains very much unexplored. Two basic substitutions may occur on $[3,3'\text{-}Co(1,2\text{-}C_2B_9H_{11})_2]^-$, either on carbon or on boron. With few exceptions,[6] substitutions on carbon have been achieved only at an early stage of the synthetic process, that is, on the starting *o*-carborane,[7] but not by direct reaction with the $[3,3'\text{-}Co(1,2\text{-}C_2B_9H_{11})_2]^-$ cage. Substitution at boron has been achieved under Friedel-Crafts conditions[8] or with strong alkylating agents.[9] Consequently, regioselective substitutions were not possible, and specific derivatives were obtained only after careful separations of complex mixtures.

Up to today, the usual *via* to attach this metallacarborane to the different groups is through the boron atom in position 8', by the reaction of the dioxane-metallacarborane derivative, $[3,3'\text{-}Co(8\text{-}C_4H_8O_2\text{-}1,2\text{-}C_2B_9H_{10})(1',2'\text{-}C_2B_9\text{-}H_{11})]$ [10] with the corresponding nucleophiles.[11-14]

Recently, the construction of high-boron content molecules has received considerable interest.[15] At the same time, the introduction of carboranes into different types of dendrimeric structures, at the inner region or at the surface of the molecules, is also being explored.[16] The design of boron-rich dendritic or macromolecular systems is of interest for boron neutron capture therapy (BNCT) or for drug delivery systems.

For this purpose, BNCT, bio-active functionalized *nido*-carboranes and metallacarboranes have been characterized,[11] and cobaltabisdicarbollide derivatives have been attached to different organic groups and biomolecules.[12], [13] Furthermore, the carborane subunits can be easily modified by attaching variable substituents onto the carbon and boron vertex, making out of these structurally flexible compounds potential

candidates for BNCT of cancer and HIV Protease inhibition. [17]

Although the *closo* carborane clusters are structures showing high stability with respect to strong acids they react with Lewis bases yielding more opened structures, known as *nido*, by a partial deboronation process that implies the loss of a clusters' vertex. Several nucleophiles such as alkoxides, [18] amines, [19] fluorides, [20] phosphanes[21] have been used. The nucleophilic attack takes place at the boron atoms directly bounded to both carbon atoms, the B(3) or its equivalent B(6), since they both present electronic deficiency.

Following our studies on developing anionic dendritic cores, here we report the preparation of *nido* and metallacarboranes anionic clusters di- and tetrasubstituted on boron vertexes, by using a deboronation of starting *B*-functionalized *closo o*-carborane derivatives.

Regioselective removal of one BH vertex from the *B*-disubstituted *closo o*-carborane derivatives, 9,12-$(CH_2CHCH_2)_2$-1,2-*closo*-$C_2B_{10}H_{10}$ [**1**] and 9,12-$(PhC{\equiv}C)_2$-1,2-*closo*-$C_2B_{10}H_{10}$ [**3**],[22] by heating with ethanolic KOH (5 eq.) for 3h and followed by a precipitation with $[N(CH_3)_4]Cl$ which leads to the formation of $[N(CH_3)_4]$[5,6-$(CH_2CHCH_2)_2$-7,8-*nido*-$C_2B_9H_{10}$] [**2**] and $[N(CH_3)_4]$[5,6-$(PhC{\equiv}C)_2$-7,8-*nido*-$C_2B_9H_{10}$] [**4**] in good to high yield, 87 and 78%, respectively (Scheme 2).

Same procedure was followed to deboronate tetrasubstituted *closo* o-carborane compounds 8,9,10,12-$(CH_2CHCH_2)_4$-1,2-*closo*-$C_2B_{10}H_8$ [**5**] and 8,9,10,12-$(OHCH_2CH_2CH_2)_4$-1,2-*closo*-$C_2B_{10}H_8$ [**7**], which were synthesized as previously reported. [23] In this case, the organic substituent on B(10) entailed a greater amount of nucleophilic agent EtOK (20 eq.) in order to remove the B(3). The two *nido* compounds were successfully isolated in good yield, $[N(CH_3)_4]$[1,5,6,10-$(CH_2CHCH_2)_4$-7,8-*nido*-$C_2B_9H_8$] [**6**] (70%) and $[N(CH_3)_4]$[1,5,6,10-$(OHCH_2CH_2CH_2)_4$-7,8-*nido*-$C_2B_9H_8$] [**8**] (73%) as $[N(CH_3)_4]^+$ salts by precipitation with $[N(CH_3)_4]Cl$ (Scheme 3).

Afterwards, a complexation reaction with cobalt was performed on $[N(CH_3)_4]$[5,6-$(CH_2CHCH_2)_2$-7,8-*nido*-$C_2B_9H_{10}$] [**2**] by extracting the bridging proton with *n*-butillitium. After the addition of $CoCl_2$ the reaction was stirred at room temperature for 1 hour and precipitated with $[N(Me)_4]Cl$ to obtain $[N(Me)_4]$[3,3'-Co-(9,12-$(CH_2CHCH_2)_2$-1,2-*closo*-$C_2B_9H_9)_2$] [**9**] in good to high yield, 83% (Scheme 4).

All the synthesized compounds have been fully characterized using ^{1}H-, ^{11}B-, ^{13}C-NMR and MS spectroscopy. As an example, the ESI-MS spectrum of $[N(CH_3)_4]$[1,5,6,10-$(CH_2CHCH_2)_4$-7,8-*nido*-$C_2B_9H_8$] [**6**] is displayed in Figure 1, showing a peak with isotopic distribution at m/z 294.3 corresponding to $[C_{14}B_9H_{28}]^-$.

Influence of B-C vertexes on the bridging proton of *nido* species: The bridging proton in [7,8-nido-$C_2B_9H_{12}]^-$ derivatives [**2**], [**4**], [**6**], [**8**] is relatively acidic and can be removed by the addition of strong bases. Comparing the chemical shift of this bridging proton in unsubstituted [7,8-nido-$C_2B_9H_{12}]^-$ with di- and tetra-substituted *nido* compounds, we observe that the presence of organic groups on boron vertexes move the δ to higher fields (Table 1). The substitution on the open face boron vertex of *nido* compounds, B(10), with an organic branch produces even a larger effect on the bridging proton chemical shift to higher fields compared to the disubstituted counterparts.

NMR Spectral Considerations ^{11}B NMR. $^{11}B\{^1H\}$-NMR spectra of $[N(CH_3)_4]$[5,6-$(CH_2CHCH_2)_2$-7,8-*nido*-$C_2B_9H_{10}$] [**2**] is in the range -7 to -38 ppm**,** characteristic of *o*-carborane *nido* species. [24] The spectrum displays a 2:2:1:2:1:1 pattern (low to high field), and metallacarborane [**9**] shows a pattern 2:4:2:4:4:2 (low to

high field) (Figure 2).

In Figure 2 can be noticed that deboronation cause the ^{11}B resonance of *nido* [**2**] to appear at higher field in comparison to *closo* cluster [**1**] (<δ> = -15.8 and <δ> = -9.2 ppm, respectively), whereas the complexation cause the ^{11}B resonance of metallacarborane [**9**] to appear at lower field (<δ> = -6.6 ppm).

The $^{11}B\{^1H\}$-NMR spectrum of $[N(CH_3)_4][5,6\text{-}(PhC{\equiv}C)_2\text{-}7,8\text{-}nido\text{-}C_2B_9H_{10}]$ [**4**] displays a 2:2:1:2:1:1 pattern (low field to high field) with the resonances sufficiently separated enough to allow their unambiguous assignment by means of $^{11}B\{^1H\}$-$^{11}B\{^1H\}$ COSY. Figure 3 shows ^{11}B (in orange) and $^{11}B\{^1H\}$-NMR (in blue) spectra of [**4**]. The peak at -29 ppm is easily assigned to B(10) since it appears as a broad doublet in the ^{11}B-NMR spectrum due to the coupling with the H bridge as well as the *exo*-H. The peak at -34.4 ppm, at highest field, corresponds to B(1), the position antipodal to the open face. The spectrum also exhibits a singlet at -14.53 ppm corresponding to the B(5,6) substituted with phenylethynyl branches. The doublet at -17.5 ppm corresponds to B(3) since integrates the one. With the resonances due to B(1), B(3), B(5,6) and B(10) thus established, analysis of the cross peak easily allowed the assignment of the 2:2:1:2:1:1 pattern to B(9,11): B(5,6): B(3): B(2,4): B(10): B(1), respectively

Experimental Section

Materials and instrumentation: All prepared compounds are air and moisture stable. All manipulations were carried out under inert atmosphere. THF was distilled from sodium benzophenone prior to use. Reagents were obtained commercially and used as purchased. 1,2-*closo*-$C_2B_{10}H_{12}$ was obtained from Katchem. 9,12-$(CH_2CHCH_2)_2$-1,2-*closo*-$C_2B_{10}H_{10}$ [**1**],[22] 9,12-$(PhC{\equiv}C)_2$-1,2-*closo*-$C_2B_{10}H_{10}$ [**3**],[22] 8,9,10,12-$(CH_2CHCH_2)_4$-1,2-*closo*-$C_2B_{10}H_8$ [**5**][23] and 8,9,10,12-$(OHCH_2CH_2CH_2)_4$-1,2-*closo*-$C_2B_{10}H_8$ [**7**][23] were synthesised as reported at the literature.

Elemental analyses were performed using a Carlo Erba EA1108 micro analyzer. IR spectra (ν, cm^{-1}; KBr pellets) were obtained on a Shimadzu FTIR-8300 spectrophotometer. The ^{1}H- and $^1H\{^{11}B\}$-NMR (300.13 MHz), $^{13}C\{^1H\}$-NMR (75.47 MHz) and ^{11}B- and $^{11}B\{^1H\}$-NMR (96.29 MHz) spectra were recorded on a Bruker ARX 300 instrument equipped with the appropriate decoupling accessories. All NMR spectra were performed in deuterated acetone at 22ºC. The ^{11}B- and $^{11}B\{^1H\}$-NMR shifts were referenced to external $BF_3{\cdot}OEt_2$, while the ^{1}H, $^1H\{^{11}B\}$, and $^{13}C\{^1H\}$-NMR shifts were referenced to $SiMe_4$. Chemical shifts are reported in units of parts per million downfield from reference, and all coupling constants in Hz. The mass spectra were recorded in the negative ion mode using a Bruker Biflex MALDI-TOF-MS [N_2 laser; λ_{exc} 337 nm (0.5 ns pulses); voltage ion source 20.00 kV (Uis1) and 17.50 kV (Uis2)].

Synthesis of $[N(CH_3)_4][5,6\text{-}CH_2{=}CHCH_2)_2\text{-}7,8\text{-}nido\text{-}C_2B_9H_{10}]$ [2]: To a solution of KOH (127 mg, 2.27mmol) in degassed EtOH (4 mL) was added 9,12- $(CH_2{=}CHCH_2)_2$-1,2-*closo*-$C_2B_{10}H_{10}$ (100 mg, 0.44 mmol). The solution was refluxed for 3 h. After cooling to room temperature, the solvent was removed under reduced pressure and the solid residue was dissolved in 10 mL of water. The solution was neutralized with 0.25M HCl. Afterwards, an aqueous solution of $[N(CH_3)_4]Cl$ was added dropwise until no more precipitate was formed. The white solid was filtered and rinsed with water obtaining $[N(CH_3)_4][5,6\text{-}CH_2{=}CHCH_2)_2\text{-}7,8\text{-}nido\text{-}C_2B_9H_{10}]$. Yield: 112 mg (87%). Elemental Analysis for $C_{12}B_9H_{32}N$: calc: C 50.14, H 11.14, N 4.87; found: C 50.80, H 11.15, N 4.77. IR (KBr): ν=3032 (s, $\nu_s(C_c\text{-}H)$, 2983, 2955, 2899, 2863 (s, $\nu_s(C_{alkyl}\text{-}H)$, 2507 (s, ν_s(B-H)), 1481 cm^{-1} (s, ν_s(N-CH3)), 945 cm^{-1} (s, $\nu_{as}(CH_3)$). ^{1}H NMR (300 MHz, CD_3COCD_3): δ=5.90 (m, 2H, $CH_2{=}CH\text{-}CH_2$), 4.67-4.44 (m, 4H, $CH_2{=}CH\text{-}CH_2$), 3.47 (s, 12H, $N(CH_3)_4$), 3.10–1.00 (m, 7H, B-$H_{terminal}$), 2.05 (br s, 2H, $C_{cluster}H$), 1.58 ppm (m, 2H, $CH_2{=}CH\text{-}CH_2$), 1.46 ppm (m, 2H, $CH_2{=}CH\text{-}CH_2$), -2.40--2.60 ppm (s, 1H, B-H_{bridge}). $^1H\{^{11}B\}$ NMR (300 MHz, CD_3COCD_3): δ=5.90 (m, 2H, $CH_2{=}CH\text{-}CH_2$), 4.67-4.44 (m, 4H, $CH_2{=}CH\text{-}CH_2$), 3.47 (s, 12H, $N(CH_3)_4$), 2.05 (br s, 2H, $C_{cluster}H$), 1.98, 1.67, 1.28, 0.45, 0.06 (br s, 7H, B-$H_{terminal}$), 1.58 ppm (m, 2H, $CH_2{=}CH\text{-}CH_2$), 1.46 ppm (m, 2H, $CH_2{=}CH\text{-}CH_2$), -2.57 ppm (d, $^1J(H_{bridge},H_{terminal})$=12 Hz 1H, B-$H_{bridge}$). $^{13}C\{^1H\}$ NMR (75 MHz, CD_3COCD_3): δ=145.2 (s, $CH_2{=}CH\text{-}CH_2$), 107.2 (s, $CH_2{=}CH\text{-}CH_2$), 55.2 (s, $N(CH_3)_4$), 24.7 ppm (m, $CH_2{=}CH\text{-}CH_2$). ^{11}B NMR (96 MHz, $CDCl_3$): δ=-6.4 (s, 2B, B(5,6)), -10.0 (d, ^1J(B,H)=134 Hz, 2B, B(9,11)), -17.9 (d, ^1J(B,H)=157 Hz, 1B, B(3)), -21.2 (d, ^1J(B,H)=146 Hz, 2B, B(2,4)), -29.6 (br d, ^1J(B,H)=115 Hz, 1B, B(10)), -35.1 ppm (d, ^1J(B,H)=137 Hz, 1B, B(1)). MALDI-TOF MS: *m/z* (%)= 213.2 (100) $[M\text{-}1]^-$.

Synthesis of [N(CH$_3$)$_4$][5,6-PhC≡C)$_2$-7,8-*nido*-C$_2$B$_9$H$_{10}$] [**4**]:To a solution of KOH (142 mg, 2.5 mmol) in degassed EtOH (4 mL) was added 9,12-(PhC≡C)$_2$-1,2-*closo*-C$_2$B$_9$H$_{10}$ (100 mg, 0.25 mmol). The solution was refluxed for 3 h. After cooling to room temperature, the solvent was removed under reduced pressure and the solid residue was dissolved in 10 mL of water. The solution was neutralized with 0.25M HCl. Afterwards, an aqueous solution of [N(CH$_3$)$_4$]Cl was added dropwise until no more precipitate was formed. The white solid was filtered and rinsed with water obtaining NMe$_4$[5,6-PhC≡C)$_2$-7,8-*nido*-C$_2$B$_9$H$_{10}$]. Yield: 92.3 mg (78%). Elemental Analysis for C$_{22}$B$_9$H$_{32}$N: calc: C 64.86, H 7.86, N 3.43; found: C 65.12, H 7.84, N 3.45. IR (KBr): ν=3211 (m, ν$_s$(C$_{aromatic}$-H)), 3028 (s, ν$_s$(C$_c$-H), 2927, 2855 (s, ν$_s$(C$_{alkyl}$-H), 2537 (s, ν$_s$(B-H)), 1487 cm^{-1} (s, ν$_s$(N-CH3)). ^{1}H NMR (300 MHz, CD$_3$COCD$_3$): δ=7.30 (s, 2H, Ph$_{para}$), 7.21 (s, 8H, Ph$_{ortho}$, Ph$_{meta}$), 3.43 (s, 12H, N(C*H*$_3$)$_4$), 3.50–1.50 ppm (m, 7H, B-*H*$_{terminal}$), 1.81 (br s, 2H, C$_{cluster}$*H*), -2.10--2.40 ppm (s, 1H, B-*H*$_{bridge}$). ^{1}H{^{11}B} NMR (300 MHz, CD$_3$COCD$_3$): δ=7.30 (s, 2H, Ph$_{para}$), 7.21 (s, 8H, Ph$_{ortho}$, Ph$_{meta}$), 3.43 (s, 12H, N(C*H*$_3$)$_4$), 2.22 (br s, 2H, B(9,11)-*H*$_{terminal}$), 1.81 (br s, 2H, C$_{cluster}$*H*), 1.77 (br s, 1H, B(3)-*H*$_{terminal}$), 1.57 (br s, 2H, B(2,4)-*H*$_{terminal}$), 0.98 (br s, 1H, B(10)-*H*$_{terminal}$), 0.59 (d, ^{1}*J*(B,H)=9 Hz, 1H, B(1)-*H*$_{terminal}$), -2.31 (d, ^{1}*J*(B,H)=9 Hz, 1H, B(10)-*H*$_{bridge}$). ^{13}C{^{1}H} NMR (75 MHz, CD$_3$COCD$_3$): δ=132.1 (s, Ph$_{meta}$), 128.8 (s, Ph$_{ortho}$), 128.1 (s, Ph$_{para}$), 126.9 (s, Ph$_{ipso}$), 56.2 (s, N(*C*H$_3$)$_4$), 41.4 ppm (s, *C*$_{cluster}$). ^{11}B RMN (96 MHz, CD$_3$COCD$_3$): δ=-9.8 (d, ^{1}*J*(B,H)=133 Hz, 2B, B(9,11)), -14.5 (br s, 2B, B(5,6)), -17.6 (d, ^{1}*J*(B,H)=165 Hz, 1B, B(3), -20.6 (d, ^{1}*J*(B,H)=150 Hz, 2B, B(2,4)), -29.0 (d, ^{1}*J*(B,H)=104 Hz, 1B, B(10), -34.4 ppm (d, ^{1}*J*(B,H)=143 Hz, 1B, B(1)). MALDI-TOF MS: *m/z* (%)=335 (100) [M-1]$^-$.

Synthesis of [N(CH$_3$)$_4$][1,5,6,10-CH$_2$=CHCH$_2$)$_4$-7,8-*nido*-C$_2$B$_9$H$_8$] [**6**]: To a solution of KOH (225 mg, 4 mmol) in degassed EtOH (5 mL) was added 8,9,10,12-(CH$_2$=CHCH$_2$)$_4$-1,2-*closo*-C$_2$B$_{10}$H$_8$ (60 mg, 0.20 mmol). The solution was refluxed for 3 h. After cooling to room temperature, the solvent was removed under reduced pressure and the solid residue was dissolved in 10 mL of water. The solution was neutralized with 0.25M HCl. Afterwards, an aqueous solution of [N(CH$_3$)$_4$]Cl was added dropwise until no more precipitate was formed. The white solid was filtered and rinsed with water obtaining [N(CH$_3$)$_4$][1,5,6,10-CH$_2$=CHCH$_2$)$_4$-7,8-*nido*-C$_2$B$_9$H$_8$]. Yield: 50.7 mg (70%). Elemental Analysis for C$_{18}$B$_9$H$_{40}$N: calc: C 58.82, H 10.89, N 3.81; found: C 59.31, H 10.08, N 3.72. IR (KBr): ν=3033 (s, ν$_s$(C$_c$-H), 2982, 2955, 2898, 2863 (s, ν$_s$(C$_{alkyl}$-H), 2508 (s, ν$_s$(B-H)), 1481 cm^{-1} (s, ν$_s$(N-CH3)), 945 cm^{-1} (s, ν$_{as}$(CH$_3$)). ^{1}H NMR (300 MHz, CD$_3$COCD$_3$): δ=6.05 (m, 4H, CH$_2$=C*H*-CH$_2$), 4.70-4.55 (m, 8H, C*H*$_2$=CH-CH$_2$), 3.45 (s, 12H, N(C*H*$_3$)$_4$), 3.10–1.00 (m, 7H, B-*H*$_{terminal}$), 2.07 (br s, 2H, C$_{cluster}$*H*), 1.61 ppm (m, 4H, CH$_2$=CH-C*H*$_2$), 1.17 ppm (m, 4H, CH$_2$=CH-C*H*$_2$), -2.00--2.20 ppm (s, 1H, B-*H*$_{bridge}$). ^{1}H{^{11}B} NMR (300 MHz, CD$_3$COCD$_3$): δ=6.05 (m, 4H, CH$_2$=C*H*-CH$_2$), 4.70-4.55 (m, 8H, C*H*$_2$=CH-CH$_2$), 3.45 (s, 12H, N(C*H*$_3$)$_4$), 2.07 (br s, 2H, C$_{cluster}$*H*), 1.92 (s, 2H, B-*H*$_{terminal}$), 1.68 (s, 2H, B-*H*$_{terminal}$), 1.51 (s, 1H, B-*H*$_{terminal}$), 1.61 ppm (m, 4H, CH$_2$=CH-C*H*$_2$), 1.17 ppm (m, 4H, CH$_2$=CH-C*H*$_2$), -1.97 ppm (s, 1H, B-*H*$_{bridge}$). ^{13}C{^{1}H} NMR (75 MHz, CD$_3$COCD$_3$): δ=144.4 (s, CH$_2$=*C*H-CH$_2$), 108.2 (s, *C*H$_2$=CH-CH$_2$), 54.8 (s, N(*C*H$_3$)$_4$), 22.8 ppm (m, CH$_2$=CH-*C*H$_2$).^{11}B NMR (96 MHz, CDCl$_3$): δ=-7.7 (s, 2B, B(5,6)), -11.0 (d, ^{1}*J*(B,H)=133 Hz, 2B, B(9,11)), -19.4 (d, ^{1}*J*(B,H)=148 Hz, 1B, B(3)), -21.7 (br s, 1B, B(10)), -21.7 (d, ^{1}*J*(B,H)=160 Hz, 2B, B(2,4)), -26.4 ppm (br s, 1B, B(1)). ESI MS: *m/z* (%)=294.3 (100) [M-1]$^-$.

Synthesis of [N(CH$_3$)$_4$][1,5,6,10-HOCH$_2$CH$_2$CH$_2$)$_4$-7,8-*nido*-C$_2$B$_9$H$_8$] [**8**]:To a solution of KOH (595 mg, 10.6 mmol) in degassed EtOH (5 mL) was added 8,9,10,12-(HOCH$_2$CH$_2$CH$_2$)$_4$-1,2-*closo*-C$_2$B$_{10}$H$_8$ (200 mg, 0.53 mmol). The solution was refluxed for 3 h. After cooling to room temperature, the solvent was removed under reduced pressure and the solid residue was dissolved in 10 mL of water. The solution was neutralized with 0.25M HCl. Afterwards, an aqueous solution of [N(CH$_3$)$_4$]Cl was added dropwise until no more precipitate was formed. The white solid was filtered and rinsed with water obtaining [N(CH$_3$)$_4$][1,5,6,10- HOCH$_2$CH$_2$CH$_2$)$_4$-7,8-*nido*-C$_2$B$_9$H$_8$]. Yield: 171 mg (73%). Elemental Analysis for C$_{18}$B$_9$H$_{48}$O$_4$N: calc: C 49.18, H 10.92, N, 4.00; found: C 47.64, H 10.03, N 3.79. IR (KBr): ν=3379 (vs, ν$_s$(O-H)), 3028 (vs, ν$_s$(C$_{cluster}$-H)), 2962, 2935, 2871 (vs, ν$_s$(C$_{alkyl}$-H)), 2540, 2511 (s, ν$_s$(B-H)), 1069, 1022, 901 (s, ν$_s$(C-O)), 1449 cm^{-1} (s, ν$_s$(N-CH3)). ^{1}H NMR (300 MHz, CD$_3$COCD$_3$): δ=3.52 (m, 8H, HOC*H*$_2$CH$_2$CH$_2$), 3.47 (s, 12H, N(C*H*$_3$)$_4$), 1.62-1.53 (m, 8H, HOCH$_2$C*H*$_2$-CH$_2$), 3.10–1.00 (m, 5H, B-*H*$_{terminal}$), 2.10 (br s, 2H, C$_{cluster}$*H*), 0.87-0.57 (m, 8H, HOCH$_2$CH$_2$-C*H*$_2$), -2.00--2.20 ppm (s, 1H, B-*H*$_{bridge}$). ^{1}H{^{11}B} NMR (300 MHz, CD$_3$COCD$_3$): δ=3.52 (m, 8H, HOC*H*$_2$CH$_2$CH$_2$), 3.47 (s, 12H, N(C*H*$_3$)$_4$), 2.10 (br s, 2H, C$_{cluster}$*H*), 1.62-1.53 (m, 8H, HOCH$_2$C*H*$_2$CH$_2$), 1.90,1.50,1.20 (br s, 5H, B-*H*$_{terminal}$), 0.87-0.57 (m, 8H, HOCH$_2$CH$_2$-C*H*$_2$), -2.02 ppm (br s, 1H, B-*H*$_{bridge}$). ^{13}C{^{1}H} NMR (75 MHz, CD$_3$COCD$_3$): δ=73.0 (s, HOCH$_2$C*H*$_2$CH$_2$), , 68.0 (s, N(*C*H$_3$)$_4$), 29.4 (s, HOCH$_2$C*H*$_2$CH$_2$), 14.6 ppm (m, HOCH$_2$C*H*$_2$CH$_2$). ^{11}B NMR (96 MHz, CDCl$_3$): δ=-6.3 (s, 2B, B(5,6)), -11.1 (d, ^{1}*J*(B,H)=111 Hz, 2B, B(9,11)), -20.0 (d, ^{1}*J*(B,H)=148 Hz, 1B, B(3)), -21.0 (br s, 1B, B(10)), -21.8 (d, ^{1}*J*(B,H)=157 Hz, 2B, B(2,4)), -25.7 ppm (br s, 1B, B(1)). MALDI-TOF MS: *m/z* (%)=367.2 (100) [M-1]$^-$.

Synthesis of [N(CH$_3$)$_4$][3,3'-Co-(9,12-(CH$_2$=CHCH$_2$)$_2$-1,2-*closo*-C$_2$B$_9$H$_9$)$_2$] [**9**]: To a stirring solution of [N(CH$_3$)$_4$][5,6-

CH_2=$CHCH_2$-7,8-$C_2B_9H_{10}$] (30 mg, 0.1 mmol) in THF (2mL) cooled to 0 ºC in an ice-water bath was added, dropwise, a solution of butyllithium in hexanes (0.1mL, 1.6M, 0.11mmol). The suspension was stirred for 1 hour at 0ºC at room temperature. Volatiles were removed under reduced pressure. The resulting solution was then transferred via a syringe onto solid $CoCl_2$ anhydrous (42mg, 0.33mmol), following which the reaction was heated to reflux for 15 minutes. After stirring for 1 hour, the solvent was removed under reduced pressure. Then, 10mL of diethyl ether and 10mL of water were added to the residue. The mixture was thoroughly shaken, and the two layers separated. The organic layer was separated from the mixture, and the aqueous layer was extracted with diethyl ether (3 x 10mL). The combined organic phase was dried over $MgSO_4$, filtered and the solvent removed under reduced pressure. Afterwards, an aqueous solution of [NMe_4]Cl was added dropwise until no more precipitate was formed. The orange solid was filtered and rinsed with water obtaining [$N(CH_3)_4$][3,3'-Co-(9,12-CH_2=$CHCH_2$-1,2-*closo*-$C_2B_9H_9)_2$]. Yield: 25 mg (83%). Elemental Analysis for $C_{20}B_{18}H_{50}NCo$: calc: C 43.06, H 8.97, N 2.51; found: C 45.12, H 9.01, N 2.30. IR (KBr): ν=3020 (s, $\nu_s(C_{cluster}$-H)), 2958, 2924, 2857 (s, $\nu_s(C_{alkyl}$-H), 2557 (vs, ν_s(B-H)), 1459 (ν_s(N-CH3)), 945 cm^{-1} (s, $\nu_{as}(CH_3)$). ^{1}H NMR (300 MHz, CD_3COCD_3): δ=5.86 (m, 4H, CH_2=C*H*-CH_2), 4.68-4.57 (m, 8H, CH_2=CH-CH_2), 3.83 (br s, 4H, $C_{cluster}$*H*), 3.65 (s, 12H, N(CH_3)$_4$), 3.10–1.00 (m, 18H, B-$H_{terminal}$), 1.62 ppm (m, 4H, CH_2=CH-CH_2), 1.54 ppm (m, 4H, CH_2=CH-CH_2). ^{1}H{^{11}B} NMR (300 MHz, CD_3COCD_3): δ=5.86 (m, 4H, CH_2=C*H*-CH_2), 4.68-4.57 (m, 8H, CH_2=CH-CH_2), 3.82 (br s, 4H, $C_{cluster}$*H*), 3.65 (s, 12H, N(CH_3)$_4$), 3.14, 2.98, 2.68, 1.55 (br s, 18H, B-$H_{terminal}$), 1.62 ppm (m, 4H, CH_2=CH-CH_2), 1.53 ppm (m, 4H, CH_2=CH-CH_2). ^{13}C{^{1}H} NMR (75 MHz, CD_3COCD_3): δ=131.0 (s, CH_2=*C*H-CH_2), 128.9 (s, *C*H_2=CH-CH_2), 67.3 (s, $C_{cluster}$), 10.2 ppm (m, CH_2=CH-*C*H_2). ^{11}B NMR (96 MHz, CD_3COCD_3): δ=8.9 (d, ^1J(B,H)=135 Hz, 2B, B(8,8'), 3.7 (s, 4B, B(9,9',12,12'), 2.4 (d, ^1J(B,H)=113 Hz, 2B, B(10,10'), -4.9 (d, 4B, ^1J(B,H)=144 Hz, B(4,4',7,7'), -17.0 (d, 4B, ^1J(B,H)=139 Hz, B(5,5',11,11')), -22.7 ppm (d, ^1J(B,H)=166 Hz, 2B, B(6,6')). ESI MS: *m*/*z* (%)= 501.7 (100) [M+Na]$^-$.

Notes and references

[1] M. F. Hawthorne, D. C. Young, P. A. Wegner, *J. Am. Chem. Soc.* **1965**, *87*, 1818.

[2] A. Zalkin, D. H. Templeton, M. F. Hawthorne, *J. Am. Chem. Soc.* **1965**, *87*, 3988.

[3] J. Llop, C. Viñas, F. Teixidor, R. Sillanpää, R. Kivekäs, *Chem. Eur. J.* **2005**, *11*, 1939.

[4] R. Núñez, O. Tutusaus, F. Teixidor, C. Viñas, R. Sillanpää, R. Kivekäs, *Chem. Eur. J.* **2005**, *11*, 5637.

[5] a) O. Tutusaus, C. Viñas, R. Kivekäs, R. Sillanpää, F. Teixidor, *Chem. Commun.* **2003**, *19*, 2458; *b)* F. Teixidor, M . A. Flores, C. Viñas, R. Sillanpää, R. Kiveka¨s, *J. Am. Chem. Soc.* **2000**, *122*, 1963.

[6] a) R. M. Chamberlin, B. L. Scott, M. M. Melo, *Inorg. Chem.* **1997**, *36*, 809; b) I. Rojo, F. Teixidor, C. Viñas, R. Kivekäs, R. Sillanpää, *Chem. Eur. J.* **2004**, *10*, 5376; c) E. J. Juárez-Pérez, C. Viñas, A. González-Campo, F. Teixidor, R. Kivekäs, R. Sillanpää, R. Núñez, *Chem. Eur. J.* **2008**, *14*, 4924.

[7] a) C. Viñas, J. Pedrajas, J. Bertran, F. Teixidor, R. Kivekäs, R. Sillanpää, *Inorg. Chem.* **1997**, *36*, 2482; b) C. Viñas, S. Gomez, J. Bertran, T. Teixidor, J. F. Dozol, H. Rouquette, *Chem. Commun.* **1998**, 191; c) C. Viñas, S. Gomez, J. Bertran, F. Teixidor, J. F. Dozol, H. Rouquette, *Inorg. Chem.* **1998**, *37*, 3640; d) C. Viñas, J. Bertran, S. Gomez, F. Teixidor, J. F. Dozol, H. Rouquette, R. Kivekäs, R. Sillanpää, *Chem. Soc., Dalton Trans.* **1998**, 2849. e) C. Viñas, J. Pedrajas, F. Teixidor, R. Kivekäs, R. Sillanpää, A. J. Welch, *Inorg. Chem.* **1997**, *36*, 2988.

[8] J. N. Francis, M. F. Hawthorne, *Inorg. Chem.* **1971**, *10*, 594.

[9] a) J. Plesek, S. Heřmánek, K. Base, L. J. Todd, W. F. Wright, *Collect. Czech. Chem. Commun.* **1976**, *41*, 3509, b) Z. Janousek, J. Plesek, S. Heřmánek, K. Base, L. J. Todd, W. F. Wright, *Collect. Czech. Chem. Commun.* **1981**, *46*, 2818. c) I. Rojo, F. Teixidor, C. Viñas, R. Kivekäs, R. Sillanpää, *Chem Eur. J.* **2003**, *9*, 4311.

[10] J. Plesek, S. Hermanek, A. Franken, I. Cisarova, C. Nachtigal, *Collect. Czech. Chem. Commun.* **1997**, *62*, 47.

[11] J. F. Valliant, K. J. Guenther, A. S. King, P. Morel, O. O. Schaffer, K. A. Sogbein, K. A. Stephenson, *Coord. Chem. Rev.* **2002**, *232*, 173.

[12] a) A. B. Olejniczak, J. Plesek, O. Kriz, Z. Lesnikowski, *Angew. Chem. Int. Ed.* **2003**, *42*, 5720; b) Z. Lesnikowski, E. Paradowska, A. B. Olejniczak, M. Studzinska, P. Seekamp, U. Schüfler, D. Gabel, R. Schinazi, J. Plesek, *Bioorg. Med. Chem.* **2005**, *13*, 4168. c) A. B. Olejniczak, J. Plesek, Z. J. Lesnikowski, *Chem. Eur. J.* **2007**, *13*, 311.

[13] a) M. Sibrian-Vazquez, E. Hao, T. J. Jenssen, M. G. H. Vicente, *Biocong. Chem.* **2006**, *17*, 928. b) E. Hao, M. Sibrian-Vazquez, W. Serem, J. C. Garno, F. R. Fronczek M. G. H. Vicente, *Chem. Eur. J.* **2007**, *13*, 9035. c) F. Li, F. R. Fronczek, M. G. H. Vicente, *Tetrah. Lett.*, **2008**, *49*, 4828.

[14] J. Llop, C. Masalles, C. Viñas, F. Teixidor, R. Sillanpää, R. Kivekäs, *Dalton Trans.* **2003**, 556.

[15] a) J. Thomas, M. F. Hawthorne, *Chem Commun.* **2001**, 1884; b) Y. Azev, I. Slepukhina, D. Gabel, *Appl. Radiat. Isot.* **2004**, *61*, 1107; c) L. Ma, J. Hamdi, F. Wong, M. F. Hawthorne, *Inorg. Chem.* **2006**, *45*, 278; d) A. R. Genady, M. E. El-Zaria, D. J. Gabel, *Organomet. Chem.* **2004**, *689*, 3242; e) R. Luguya, F. R. Fronczek, K. M. Smith, M. G. H. Vicente, *Appl.*

Radiat. Isot. **2004**, *61*, 1117; f) J. C. Clark, F. R. Fronczek, M. G. H. Vicente, *Tetrahedron Lett*. **2005**, *46*, 2365.

[16] a) G. R. Newkome, C. N. Moorefield, J. M. Keith, G. R. Baker, G. H. Escamilla, *Angew. Chem., Int. Ed. Engl.* **1994**, *33*, 666; b) R. F. Barth, D. M. Adamns, A. H. Solovay, F. Alam, M. V. Darby, *Bioconjugate Chem.* **1994**, *5*, 58; c) D. Armspach, M. Cattalini, E. C. Constable, C. E. Housecroft, D. Phillips, *Chem. Commun.* **1996**, 1823; d) B. Qualman, M. M. Kessels, H. J. Musiol, W. D. Sierralta, P. W. Jungblut, L. Moroder, *Angew. Chem., Int. Ed. Engl.* **1996**, *35*, 909; e) M. C. Parrott, E. B Marchington, J. F. Valliant, A. Adronov, *J. Am. Chem. Soc.* **2005**, *127*, 12081; f) R. Nuñez, A. Gonzaález, C. Viñas, F. Teixidor, R. Sillanpää, R. Kivekäs, *Org. Lett.* **2005**, *7*, 231; g) R. Núñez, A. González, C. Viñas, F. Teixidor, R. Sillanpää, R. Kivekäs, *Organometallics* **2005**, *24*, 6351.

[17] a) M. F. Hawthorne, *Angew. Chem. Int. Ed.*, **1993**, *32*, 950; b) A. H. Soloway, W. Tjarks, B. A. Barnum, F. G. Rong, R. F. Barth, L. M. Codogni, J. G. Wilson, *Chem. Rev.*, **1998**, *98*, 1515; c) I. B. Sivaev, V. Bregadze, S. Sjöberg, in *Research and Development in Neutron Capture Therapy*, ed. W. Sauerwein, R. Moss and A. Wittig, Monduzzi Editore S.p.A., Bologna, **2002**, pp. 19–23.

[18] a) R. A. Wiesboeck, M. F. Hawthorne, *J. Am. Chem. Soc*., **1964**, *86*, 1642; b) P. M. Garret, F. N. Tebbe, M. F. Hawthorne, *J. Am. Chem. Soc*., **1964**, *86*, 5016; c) M. F. Hawthorne, D. C. Young, P. M. Garret, D. A. Owen, S. G. Schwerin, F. N. Tebbe, P. M. Wegner, *J. Am. Chem. Soc.*, **1968**, *90*, 862.

[19] L. I. Zakharkin, U. N. Kalinin, *Tetrah. Letters*, **1965**, 407; b) L. I. Zakharkin, V. S. Kirillova, *Izv. Akad. Nauk SSSR, Ser. Khim*., **1975**, 2596; c) Y. Taoda, T. Sawabe, Y. Endo, K. Yamaguchi, S. Fujii, H. Kagechika, *Chem. Commun.*, **2008**, 2049.

[20] a) M. A. Fox, W. R. Gill, P. L. Herbertson, J. A. H. MacBride, K. Wade, *Polyhedron*, **1996**, *16*, 565; b) M. A. Fox, J. A. H. MacBride, K. Wade, *Polyhedron*, **1997**, *16*, 2499; c) M. A. Fox, K. Wade, *Polyhedron*, **1997**, *16*, 2517; d) J. Yoo, J. W. Hwang, Y. Do, *Inorg. Chem.*, **2001**, *40*, 568.

[21] M. G. Davidson, M. A. Fox, T. G. Hibbert, J. A. K. Howard, A. Mackinnon, I. S. Neretin, K. Wade, *Chem. Commun*., **1999**, 1649.

[22] "Building Highly Dense Multibranched o-Carborane Derivatives by means of Kumada Cross Coupling Reaction". A Pepiol, F. Teixidor, R. Silanpää, C. Viñas. In preparation.

[23] A. Vaca, F. Teixidor, R. Sillanpää , R. Kivekäs, C. Viñas, *Chem. Commun.*, **2011**, 47, 2252–2254.

[24] J. Buchanan, E. M. Hamilton, D. Reed, A. J. Welch, *J. Chem. Soc., Dalton Trans*. **1990**, 677.

SCHEME 1. Partial degradation of *o*-carborane by a nucleophilic attack to generate a *nido* cluster and complexation reaction with Co(II) to obtain cobaltabisdicarbollide anion.

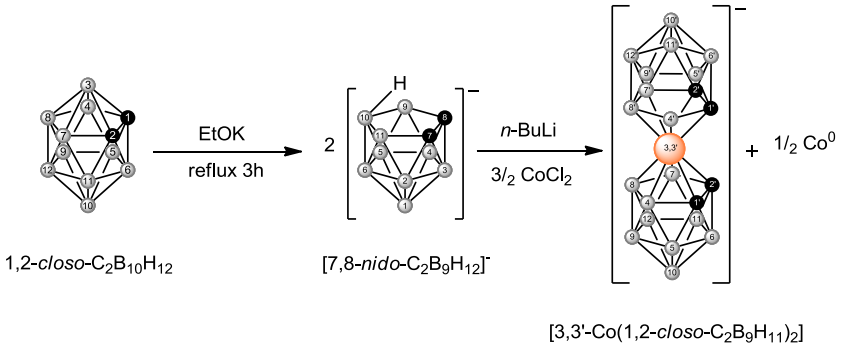

SCHEME 2. Removal of B(3) by EtOK nucleophilic attack on *B*-disubstituted *closo* o-carborane counterparts [**1**] and [**3**].

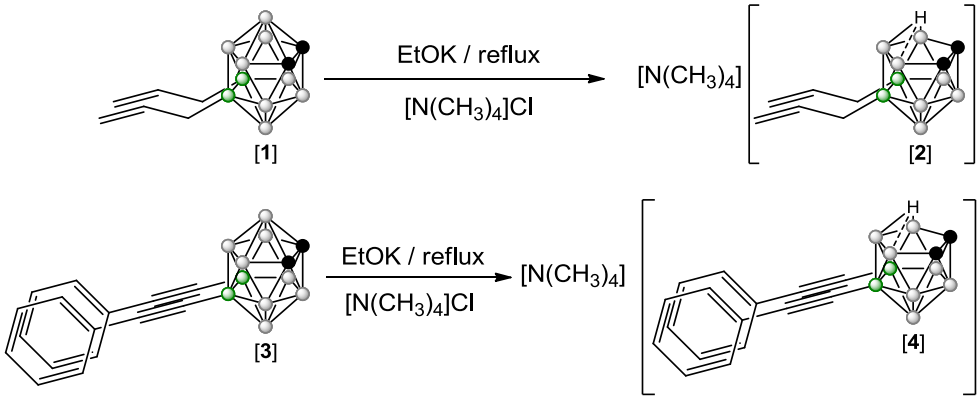

SCHEME 3. Removal of B(3) by EtOK nucleophilic attack on *B*-disubstituted *closo* o-carborane counterparts [**1**] and [**3**].

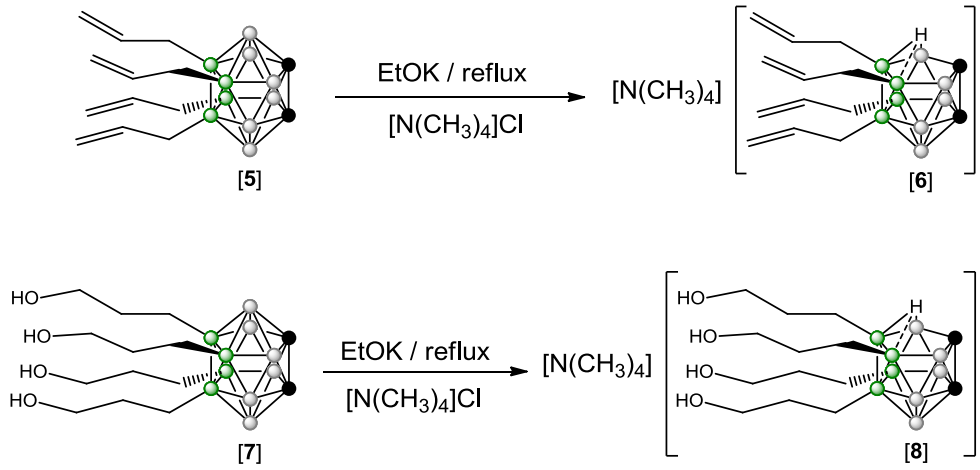

B-H C-H B Co

SCHEME 4. Complexation reaction of *nido* cluster [**2**] to metallacarboranes of Co(III) to obtain [N(Me)$_4$][3,3'-Co-(9,12-(CH$_2$CHCH$_2$)$_2$-1,2-*closo*-C$_2$B$_9$H$_9$)$_2$] [**9**].

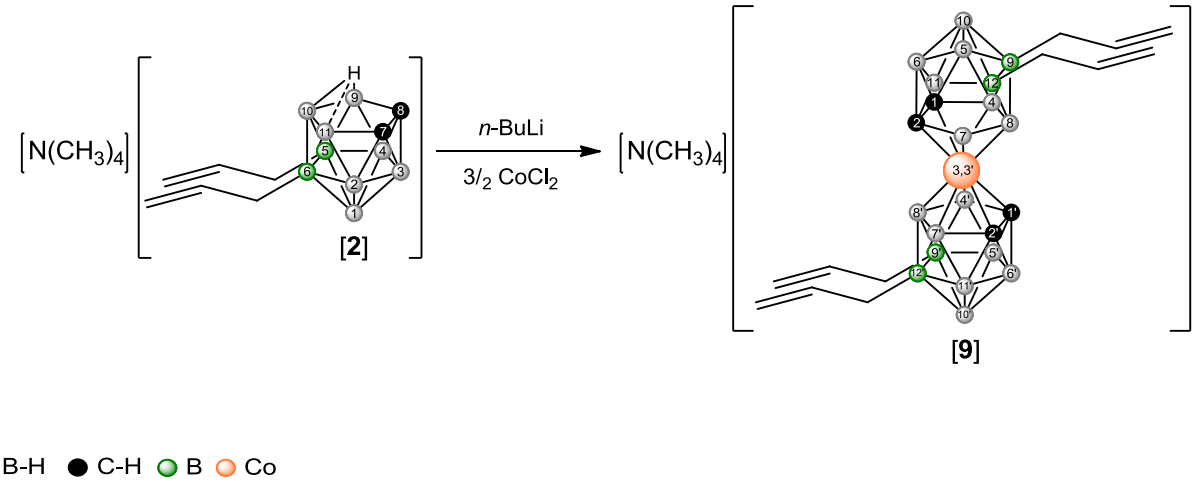

FIGURE 1. ESI-MS spectrum of [N(CH$_3$)$_4$][1,5,6,10-(CH$_2$CHCH$_2$)$_4$-7,8-*nido*-C$_2$B$_9$H$_8$] [**6**].

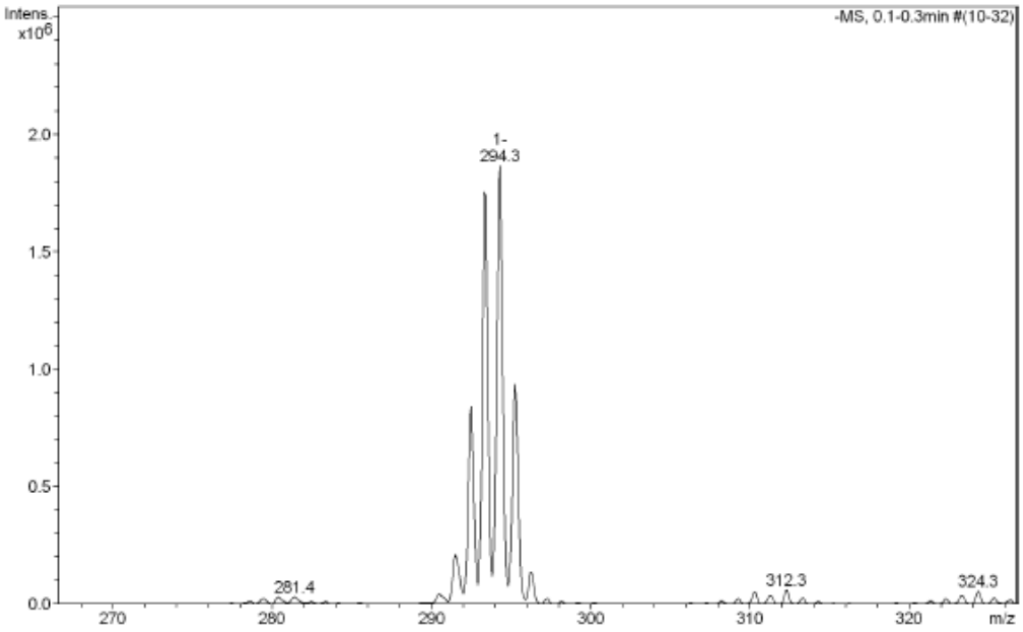

FIGURE 2. Diagram $^{11}B\{^{1}H\}$-NMR spectra with the peak assignments for the compounds [**1**], [**2**] and [**9**].

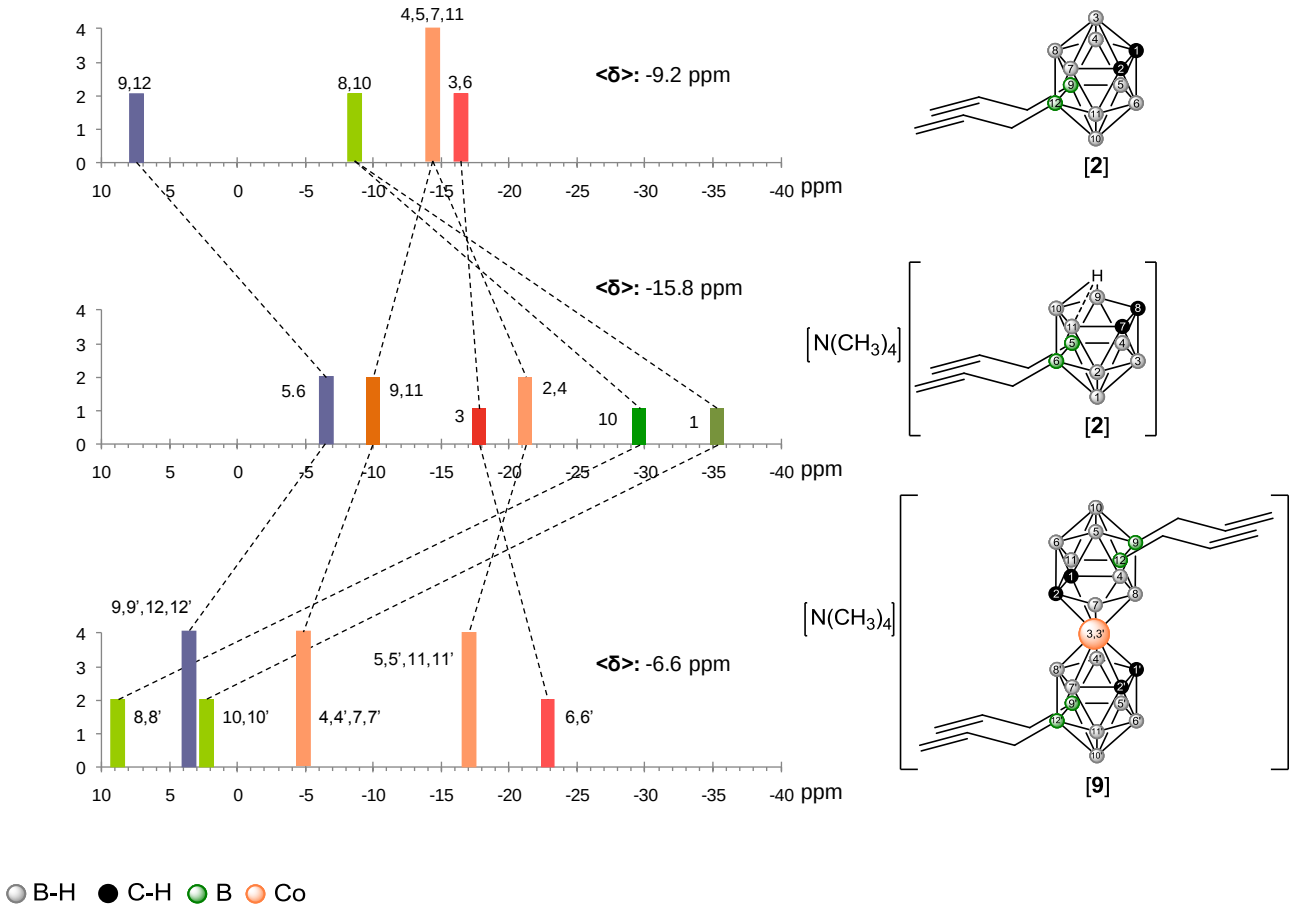

FIGURE 3. ^{11}B and $^{11}B\{^{1}H\}$-NMR spectra comparison of compound [**4**].

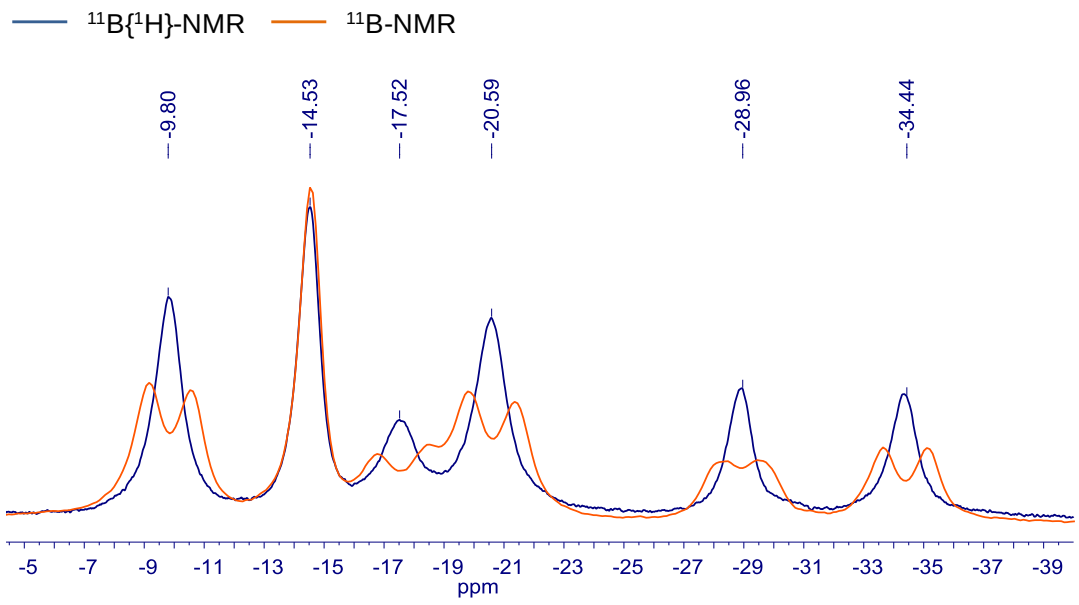

TABLE 1. Chemical shift of bridge BHB protons in *nido*-carboranes [**2**], [**4**], [**6**] and [**8**].

Compounds	Chemical shift of bridge BHB protons (ppm)
$[7,8\text{-nido-}C_2B_9H_{12}]^-$	-2.90
$[5,6\text{-}(CH_2CHCH_2)_2\text{-}7,8\text{-}nido\text{-}C_2B_9H_{10}]^-$	-2.57
$[5,6\text{-}(PhC{\equiv}C)_2\text{-}7,8\text{-}nido\text{-}C_2B_9H_{10}]^-$	-2.31
$[1,5,6,10\text{-}(CH_2CHCH_2)_4\text{-}7,8\text{-}nido\text{-}C_2B_9H_8]^-$	-1.97
$[1,5,6,10\text{-}(OHCH_2CH_2CH_2)_4\text{-}7,8\text{-}nido\text{-}C_2B_9H_8]^-$	-2.02